Cyclocybe aegerita as a model organism for the elucidation of volatile organic compound biosynthesis pathways in fungi.

Cumulative Dissertation

Presented by

M.Sc. Axel Martin Orban

Submitted to the

Faculty of Biology and Chemistry

Prepared in the

Institute of Food Chemistry and Food Biotechnology

For the degree of

Doctor Rerum Naturalium (*Dr. rer. nat.*)

Justus Liebig University Giessen, Germany

Giessen 2021

Members of the thesis committee: Prof. Dr. Martin Rühl

Prof. Dr. Sylvia Schnell

Prof. Dr. Bernhard Spengler

apl. Prof. Dr. Thomas Degenkolb

1. Referee:

Prof. Dr. Martin Rühl
Institute of Food Chemistry and Food Biotechnology, Justus-Liebig-University Giessen, 35392 Giessen

2. Referee:

Prof. Dr. Sylvia Schnell
Institute of Applied Microbiology, IFZ, Justus-Liebig-University Giessen, 35392 Giessen

I declare that I have completed this dissertation single-handedly without the unauthorized help of a second party and only with the assistance acknowledged therein. I have appropriately acknowledged and cited all text passages that are derived verbatim from or are based on the content of published work of others, and all information relating to verbal communications. I consent to the use of an anti-plagiarism software to check my thesis. I have abided by the principles of good scientific conduct laid down in the charter of the Justus Liebig University Giessen "Satzung der Justus-Liebig-Universität Gießen zur Sicherung guter wissenschaftlicher Praxis" in carrying out the investigations described in the dissertation.

_____

Date, Place Signature

The practical work for my dissertation could only be realized due to the contribution and support of many people whom I like to thank. First of all, I want to express profound gratitude to Prof. Dr. Martin Rühl for supervising me during my doctoral time. I really appreciate the guidance he offered me and I am thankful for the trust and support I received from him. Besides his professional expertise, I especially value his qualities as a person with a healthy portion of empathy. All these aspects highly contributed to a pleasant working atmosphere enabling me to carry out my research in a successful way.

I highly appreciate the willingness of Prof. Dr. Sylvia Schnell to be the second supervisor and I am very grateful for her thesis review. I am also very thankful to Prof. Dr. Bernhard Spengler and apl. Prof. Dr. Thomas Degenkolb for their contribution in the thesis committee.

Furthermore, I would like to thank my colleagues (including former ones) of the Institute of Food Chemistry and Food Biotechnology cordially for their help, advice and the efforts they made to help me. I am more than thankful to be part of such an innovative and joyful research group. In this context, I would namely like to thank Fabio Bresca, Jenny Ahlborn, Bernhard Hellmann, Andreas Hammer, Tobias Trapp, Friederike Bürger, Friederike Hahne, Ilya Galperin, Victoria Klis, Wendell Albuquerque, Garima Maheshwari, Julia Büttner, Suzan Yalman, Nadine Sella, Patrick Klüber, Philipp Honold, Dr. Judith Delius, Dr. Miriam Sowa, Dr. Daniel Bakonyi, Dr. Tetiana Zhuk and Dr. Alejandra Omarini. I would especially like to thank Marcus Schulze, Florian Prell, Florian Birk, Svenja Sommer, Carolin Mewe, Nikolas Hoberg, Dominik Karrer, Christopher Back and Janin Pfeiffer for their support and all the good times we shared.

Additionally, I want to sincerely thank Bianka Dauberthäuser and Peter Seum for their small and great efforts to keep the institute going.

Special thanks go to Dr. Marco Alexander Fraatz for his unremitting efforts and his scientific guidance, especially regarding everything related to gas chromatography and IT issues.

I would also like to thank Florian Hennicke for the good cooperation and his valuable contribution to my work.

Furthermore, I like to acknowledge the scientific Input I obtained from Prof. Dr. Holger Zorn and Dr. habil. Astrid Spielmeyer.

Many thanks also to Joline Bergel and Stella Nagy for their support and help with all administrative tasks.

During my doctoral work I had the chance to supervise several students through their degree theses and internships. I want to thank Jonathan Schüler for his good work in context of his B.Sc. thesis as well as Simon Arzt and Jeanny Jaline Jerschow for their outstanding jobs during their B.Sc. theses and the following internships. To Lisa Schwab, Deniz Tay, Annsophie Weber, Vanessa Weigel and again Simon Arzt I like to express my gratitude for the great efforts they made during their M.Sc. theses.

I gratefully acknowledge the financial support of my PhD thesis by the Deutsche Forschungsgemeinschaft (DFG, German Research Foundation, Grant Number: RU 2137/1-1).

Last but not least, I would like to express sincerest gratitude for my family who always believes in me, supports me and comforts me even in tough times.

Mushrooms are part of the human diet since time immemorial, appreciated for their nutritional value and especially for their delicious flavors. Hundreds of volatile organic compounds (VOCs) have been identified in fungi contributing to the unique aroma of each species. Generally, studies on mushroom VOCs are carried out with chopped fruiting bodies of more or less one developmental stage. For determine fungal aromas for assessment of the food quality this procedure might be adequate. Nonetheless, for analysis of the biological role of fungal VOCs in context of *inter alia* VOC biosynthesis or fungal communication this approach can suffer from drawbacks. First of all, damaging fruiting bodies can lead to VOC artefacts due to cell disruption and the occurrence of unnatural enzymatic reactions. Furthermore, fungal VOC profiles are dynamic, changing with ongoing development. For better understanding of the biological function of fungal VOCs it is therefore helpful to know which volatile patterns are characteristic for a certain developmental stage.

Against this background, an approach was developed enabling on one hand the cultivation of fungi during different developmental stages, including the growth of fruiting bodies, and on the other hand the non-invasive analysis of VOCs in the headspace (HS) of fungal cultures. These requirements were complied with modified crystallizing dishes for culture purposes and a HS-SPME-GC-MS approach to analyze the VOCs. This method was applied to analyze the volatilomes of the dikaryotic strain *C. aegerita* AAE-3 and four monokaryotic offspring siblings with different fruiting phenotypes throughout ten life stages. At early stages, in the HS of all tested strains alcohols and ketones, such as oct-1-en-3-ol, 2-methylbutan-1-ol and cyclopentanone, were the most prominent VOCs. Particularly counting for the dikaryon, the volatilome altered with continued fruiting body development exhibiting remarkable changes during sporulation. Here, sesquiterpenes, especially Δ^6-protoilludene, α-cubebene and δ-cadinene, were the most abundant VOCs in the HS of *C. aegerita* AAE-3. After sporulation, the amount of sesquiterpenes decreased along with the appearance of other VOCs including octan-3-one. In contrast, less VOCs were present in the HS of the monokaryotic strains of which all were as well detectable in the HS of the dikaryon. The changes of the volatilome were the fundament for a subsequent transcriptome analysis aiming to identify enzymes involved in fungal VOC biosynthesis, especially regarding C_8 VOC formation, which is, despite the fact that these substances are ubiquitous found in fungi, still barely understood. The transcriptomic study was carried out

with seven developmental stages of *C. aegerita* AAE-3, which during the volatilome study exhibited interesting volatile patterns. Additionally, fruiting bodies (five stages) and mycelia (seven stages) samples were harvested separately to get further insights about the putative origin of the VOCs observed in the HS of *C. aegerita*. Combining transcriptome and volatilome data, enzymes putatively involved in the biosynthesis of C_8 oxylipins in *C. aegerita* including lipoxygenases (LOXs), dioxygenases (DOXs), hydroperoxide lyases (HPLs), alcohol dehydrogenases (ADHs) and ene-reductases could be identified. Especially the putative DOX AAE3_13098, the putative HPLs AAE3_05330 and AAE3_09203, the putative ADHs AAE3_00054 and AAE3_06559 as well as the putative ene-reductase AAE3_15349 exhibit remarkable transcriptomic patterns making these enzymes highly interesting for future characterization studies. Furthermore, the study showed that the mycelium is probably the main source for sesquiterpenes observed during sporulation in the HS of *C. aegerita* AAE-3 cultures whereas changes in the C_8 profile detected in late stages of development are probably due to the activity of enzymes located in the fruiting bodies.

Reviewed book chapters:

1 Orban, A., Fraatz, M.A., and Rühl, M. (2019). Aroma Profile Analyses of Filamentous Fungi Cultivated on Solid Substrates. In Solid State Fermentation: Research and Industrial Applications, S. Steudler, A. Werner, and J.J. Cheng, eds. Adv Biochem Eng Biotechnol. *169,* 85–107.

Peer-reviewed publications:

1 Orban, A., Hennicke, F., and Rühl, M. (2020). Volatilomes of *Cyclocybe aegerita* during different stages of monokaryotic and dikaryotic fruiting. Biol. Chem. *401*, 995–1004.

2 Zhang, C., Chen, X., Orban, A., Shukal, S., Birk, F., Too, H.-P., and Rühl, M. (2020). *Agrocybe aegerita* Serves As a Gateway for Identifying Sesquiterpene Biosynthetic Enzymes in Higher Fungi. ACS Chem. Biol. *15*, 1268–1277.

3 Orban, A., Weber, A., Herzog, R., Hennicke, F., and Rühl, M. (2021). Transcriptome of different fruiting stages in the cultivated mushroom *Cyclocybe aegerita* suggests a complex regulation of fruiting and reveals enzymes putatively involved in fungal oxylipin biosynthesis. BMC Genomics *22*, 324.

Conference contributions:

Presentations:

1 Orban, A. and Rühl, M. (2018). Volatilome of the mushroom *Agrocybe aegerita* during different developmental stages. VAAM conference, Wolfsburg, Germany, April 2018.

2 Orban, A. and Rühl, M. (2019). Volatilom und Transkriptom des Speisepilzes *Agrocybe aegerita*. Regionalverbandstagung Südwest, Hohenheim, Germany, March 2019.

3 Orban, A. and Rühl, M. (2019). *Agrocybe aegerita* – ein Modellorganismus zur Aufklärung von Biosynthesewegen flüchtiger organischer Substanzen in Speisepilzen. Deutscher Lebensmittelchemikertag, Dresden, Germany, September 2019.

4 Orban, A. and Rühl, M. (2021). Volatile organic compounds of the mushroom *Cyclocybe aegerita* – an example of altering volatilomes during fungal developmental stages, DGfM conference, Blaubeuren, Germany, October 2021.

Posters:

1 Orban, A., Hennicke, F., and Rühl, M. (2019). Analysis of volatilomes and transcriptomes of *Agrocybe aegerita* during different stages of monokaryotic and dikaryotic fruiting. Fungal Genetics Conference, Pacific Grove, California, USA, March 2019.

ADHs	alcohol dehydrogenases
AOS	allene oxide synthase
CYPs	cytochromes P450
DOXs	dioxygenases
EAS	epoxy alcohol synthase
GC	gas chromatography
HPLs	hydroperoxide lyases
HS	headspace
LDS	linoleate diol synthase
LOXs	lipoxygenases
MS	mass spectrometry
NGS	next-generation sequencing
O	olfactometry
PCR	polymerase chain reaction
SPME	solid-phase microextraction
STSs	sesquiterpene synthases
VOCs	volatile organic compounds

1 Introduction

For more than 200 years, mycologists argue about which characteristics are essential for organisms to be counted as fungi (Blackwell, 2011). Criteria used to recognize fungal species such as phenotypic/genetic cohesion, reproductive biology or ecological cohesion have a remarkable impact on the outcome of the question what a fungal species is (Steenkamp et al., 2018). The appearance of teleomorphic and anamorphic stages, occurring polyphyly as well as various phenotypes in the fungal kingdom, including yeasts, molds, rusts, smuts, lichens and mushrooms, further impede the clear identification and phylogenetic placement of fungi (Fell et al., 2000). In this regard, the invention of the polymerase chain reaction (PCR) in the 1980s by Kary B. Mullis and his coworkers was a milestone for fungal taxonomy (Saiki et al., 1985). In fact, the first universal primers for categorizing organisms were designed for fungi in the early 1990s, being complementary to conserved regions of the 18S, 5.8S and 28S rRNA genes and able to amplify the noncoding and variable regions between them known as Internal Transcribed Spacers (ITS) (White et al., 1990). These original ITS primers are still in wide use even though new ones with improved coverage across diverse taxonomic groups of fungi have been developed (Toju et al., 2012). However, taxonomic classification on basis of solely ITS sequences as molecular marker is not adequate in general. Especially at the species level ITS sequences can lack a clear identification. Additional molecular markers, such as hypervariable regions within the Large Subunit (LSU) of the 28S rRNA gene (Arbefeville et al., 2017) or the β-tubulin gene (Visagie et al., 2014), have therefore been established. Furthermore, for certain fungal groups additional DNA barcodes, including elongation factor1 alpha (*TEF-1α*) of *Fusarium* and *Trichoderma* spp., the small subunit (nuSSU) and the large subunit (nuLSU) of the nuclear ribosomal RNA operon in arbuscular mycorrhizal (AM) and in rust fungi as well as the mitochondrial cytochrome oxidase c subunits (*COX1* and *COX2*) for *Oomycota*, were successfully applied (Lücking et al., 2020, 2021). Over the last two decades, next-generation sequencing (NGS) has proven to be a powerful tool for the identification of new species, especially for microscopic fungi (Wu et al., 2019). However, even with modern DNA sequencing approaches the distinction between fungal species is not trivial because the question remains what differences in DNA are adequate to account for the classification of an organism as a new species (Hyde et al., 2020). Today, there are around 120,000 described fungal species (Hawksworth and Lücking, 2017). The estimated number of fungal

species worldwide differ strongly, ranging between 0.72 and 13.2 million (Schmit and Mueller, 2007; Wu et al., 2019) with an amount of 2.2 to 3.8 million species being accepted as an quite realistic assumption (Hawksworth and Lücking, 2017; Hyde et al., 2020). Nonetheless, the prediction of the accurate number of fungal species is more than challenging since all extrapolations are lacking sufficient information *inter alia* about populations in unstudied habitats such as rainforests, caves and deep-sea oceans or about the ratio host to fungal species, on which many calculations are based (Hyde et al., 2020).

Closely related to the question which features are essential for a species to be called fungus are changes during the fungal life cycle. For example, varying morphotypes, differences in metabolome (volatile) profiles and alternations in gene expression patterns are aspects that should also be considered for a taxonomic classification. These developmental processes are highly complex and the mechanisms and the biological functions are hitherto barely understood.

1.1 Life cycle of Basidiomycota (Agaricomycetes)

The fungal kingdom comprises a highly diverse clade of heterotrophic eukaryotes, all showing unique genetic, metabolic and morphological characteristics (Naranjo-Ortiz and Gabaldón, 2019). To tap all these properties would go beyond the scope of this work. Therefore, the focus will be on the phylum Basidiomycota especially on the class Agaricomycetes to which most mushrooms, including the black poplar mushroom *Cyclocybe aegerita* (V. Brig.) Vizzini (syn. *Agrocybe aegerita, Agrocybe cylindracea and Pholiota aegerita*), belong (James, 2015). Today, there are about 36,000 described Agaricomycete species with fruiting bodies showing various shapes and features (Figure 1) (Sánchez-García et al., 2020).

The typical Agaricomycete life cycle starts with the germination of basidiospores and the subsequent development of monokaryotic mycelium (primary mycelium, monokaryons) from the appearing hyphal cells and the resulting hyphae, respectively (Kües, 2000; de Mattos-Shipley et al., 2016). Generally, monokaryons contain only one haploid nucleus per hyphal cell, nonetheless in the primary mycelium of *Coprinopsis cinerea* cells with two or even three nuclei were observed (Kües, 2000; de Mattos-Shipley et al., 2016). Basidiospores from an individual fungal specimen can show genetic variation, leading to different growth rates and phenotypes of the emerging monokaryons (Omarini et al., 2014;

Herzog et al., 2016). In some cases, as shown for different monokaryotic *C. aegerita* strains, the monokaryotic mycelium is able to produce fruiting bodies that, however, generally differ from fruiting bodies developing from dikaryotic mycelium (secondary mycelium, dikaryons) (Uno and Ishikawa, 1971; Stahl and Esser, 1976; Esser et al., 1979; Herzog et al., 2016).

Fungi do not have sexes in a common sense. Instead, most Agaricomycetes, including *C. aegerita*, possess a tetrapolar mating-type system consisting of the two unlinked genetic loci *A* and *B*, resulting in various mating types (e.g. *Schizophylum commune* (Figure 1F) has about 18,000 distinct mating types) (Meinhardt and Leslie, 1982; Kües, 2015; Raudaskoski, 2015). A dikaryon is formed by hyphal fusion (called plasmogamy) of two monokaryons with compatible mating types (Raudaskoski, 2015; de Mattos-Shipley et al., 2016). In contrast to plants and animals, cell fusion is in most cases not accompanied by karyogamy (fusion of the two nuclei) leading to the dikaryotic state with two distinct haploid nuclei per cell. Normally, this state is maintained by clamp and septa formation during cell division and ends with basidia formation in fruiting bodies (Raudaskoski, 2015; de Mattos-Shipley et al., 2016). Under certain conditions, dikaryotic mycelium can differentiate into fruiting bodies (Dias and Brito, 2017). The formation of fruiting bodies in Agaricomycetes is one of the most complex developmental processes in the fungal life cycle. (Sánchez-García et al., 2020). As a first step, hyphae aggregate to form mycelial cords, developing on local spots of the mycelium into hyphal knots due to intense branching. The hyphal knots develop successively into fruiting body initials (secondary hyphal knots) with a size of about 1–2 mm (Kües and Liu, 2000; Kües et al., 2018). Cell differentiation results in the formation of bipolar primordia basically comprising the various tissues being characteristic for mature fruiting bodies. Subsequently, differentiated primordia develop into fruiting bodies primarily due to cell elongation rather than cell differentiation (Kües, 2000). In mature fruiting bodies of Basidiomycota, karyogamy and meiosis take place in the basidium, leading to the formation of basidiospores that are released during sporulation and marking the beginning of a new life cycle (Oberwinkler, 1982).

Figure 1: Examples of fruiting bodies of different Agaricomycetes. A: *Pleurotus ostreatus*, B: *Craterellus tubaeformis*, C: *Flammulina velutipes*, D: *Sparassis crispa*, E: *Amanita muscaria*, F: *Schizophyllum commune*, G: *Stropharia aeruginosa*, H: *Laetiporus sulphureus*, I: *Boletus edulis*; Photos: Axel Orban.

The fruiting process is regulated by environmental factors, e.g. light induction and low concentrations of CO_2 have been proven to be necessary for proper fruiting body development (Turner, 1977; Wessels, 1993; Kinugawa et al., 1994; Kües and Navarro-González, 2015). Additionally, several gene deletion studies on *inter alia C. cinerea* and *S. commune* have proven that certain genes are essential for the fruiting process (Fernandez Espinar and Labarère, 1997; Muraguchi and Kamada, 1998; Murata et al., 1998; Santos and Labarère, 1999; Sirand-Pugnet and Labarère, 2002; Sirand-Pugnet et al., 2003; Arima et al., 2004; Terashima et al., 2005; Liu et al., 2006; Muraguchi et al., 2008; Kamada et al., 2010; Kuratani et al., 2010; Ohm et al., 2011; Knabe et al., 2013; Ohm et al., 2013; Pelkmans et al., 2017). For instance, the deletion of the transcriptional factor the deletion of *HOM1* and *GAT1* results in the development of several small fruiting bodies with an odd shape compared to the wild type (Ohm et al., 2011; Pelkmans et al., 2017). Besides

morphological changes during fruiting body development, the odor as a result of released volatile organic compounds (VOCs) is an important characteristic of different fungal species.

1.2 Volatile organic compounds (VOCs) of fungi

Since ancient times, mushrooms are viewed as a worthwhile food favored for their health and nutritional benefits as well as for their unique and delicious flavors. More than 300 distinct fungal VOCs have been identified so far, many being aroma active compounds (reviewed in (Dickschat, 2017)). The investigation of the diverse fungal VOCs requires different approaches often including the analysis by means of gas chromatography coupled with mass spectrometry and olfactometry (GC-MS-O) and extraction methods such as solvent extraction or solid-phase microextraction (SPME) (reviewed in (Orban et al., 2019)). Even today, odorants are frequently used for mushroom species identification and play a role in fungal chemotaxonomy (Malheiro et al., 2013; Müller et al., 2013). In fact, for some mushrooms the characteristic odor impression dictated the naming of the species. For example, the intense, anise-like flavor of the aniseed toadstool is not only reflected by its common name but is also expressed in the Latin name *Clitocybe odora* (Rapior et al., 2002). Furthermore, *Mycetinis alliaceus* (Latin: *allium* = garlic; *aceous* = like) reveals a pronounced garlic smell (Rapior et al., 1997) and the Latin name *Lactarius deliciosus* given to the saffron milk cap indicates the pleasant taste of this mushroom.

Although the flavor for each fungal species is unique, mushrooms can be classified in four groups accordingly to which VOCs contributes most to the aroma profile. The first group consists of fungi with flavors dominated by C_8 oxylipins such as oct-1-en-3-ol, octan-3-one, oct-1-en-3-one, octan-3-ol and octanal. In the button mushroom *Agaricus bisporus*, oct-1-en-3-ol is the most abundant C_8 VOC contributing to a flavor perceived as 'typical' for mushrooms (Cruz et al., 1997; Venkateshwarlu et al., 1999), whereas fruiting bodies of *C. aegerita* contain octan-3-one as the most dominant C_8 derivate (Rapior et al., 1998; Costa et al., 2015). A second group harbors fungi with high volatile terpenoid content. The cedarwood waxcap *Hygrophorus russocoriaceus* belongs to this cohort with fruiting bodies emitting a woody and cedar-like odor due to the presence of sesquiterpenes including α-longipinene, β-chamigrene and β-himachalene (Ouzouni et al., 2009). A third class consists of fungi with volatilomes dominated by sulfur containing VOCs. A famous member

of this group is the shiitake mushroom *Lentinula edodes*, which is highly appreciated for its intense aroma in China and Japan. Especially in dried form, the characteristic sulfurous odor develops, caused by *inter alia* lenthionine (1,2,3,5,6-pentathiepane), 1,2,4-trithiolane, 1,2,4,6-tetrathiepane, 1,2,3,4,5,6-hexathiepane, methanethiol, dimethyl disulfide and dimethyl trisulfide (Morita and Kobayashi, 1967; Chen and Ho, 1986). Fungi emitting an anise- or bitter almond-like odor can be classified as a fourth group. Some *Agaricus* species such as *A. essetti* and *A. augustus* as well as other fungi including *C. odora*, *Lentinellus cochleatus* and *Gloeophyllum odoratum* are part of this latter group owing their aroma VOCs like *p*-anisaldehyde, methyl *p*-anisate, benzaldehyde and benzyl alcohol (Wood et al., 1990; Rösecke and König, 2000; Rapior et al., 2002).

Not only is the species of particular importance regarding the flavor composition of fungi. Different fungal morphological structures such as mycelia and fruiting bodies or various parts of a structure e.g. pileus, gills and stipe of mushrooms might also differ in their VOC composition. For example, in stipes and the pileus of the pine-mushroom *Tricholoma matsutake* VOCs like hexanal, linalool and 3-octanol contribute differently to the overall odor impression (Cho et al., 2008). Furthermore, in stipes of *A. bisporus* oct-1-en-3-one was detected whereas in gills and skin of the fruiting bodies this VOC was not found (Combet et al., 2009). Additionally, recent volatilome and transcriptome studies on *C. aegerita* revealed that the mycelium rather than fruiting bodies might be the source of various sesquiterpenes observed in the HS of *C. aegerita* during sporulation (Orban et al., 2021). This indicates a so far barely understood communication between fruiting bodies and the mycelium and explains why sesquiterpenes were not found in fruiting bodies of *C. aegerita* (Rapior et al., 1998; Kleofas et al., 2014; Costa et al., 2015).

Beside variances of VOC composition in different parts of the fungus, biosynthesis of VOCs seems to be time dependent and volatile profiles of fungi alters with different developmental stages. For *C. aegerita*, C_8 volatile and sesquiterpene profiles changed during development, fruiting body formation and sporulation (Orban et al., 2020). Interestingly, certain VOC patterns noticed in the HS of *C. aegerita*, *inter alia* the release of sesquiterpenes during sporulation, was also confirmed for other fungal species. Studies on VOCs produced by *C. cinerea* cultures during development from mycelium stage until autolysis showed a tight connection between the appearance of sesquiterpenes and

fruiting body development (Chaisaena, 2009; Thakeow, 2008). The concentration of sesquiterpenes such as β-himachalene and cuparene increased along with stipe elongation and autolysis, during which most spores are released (Kües, 2000). In an early study, Fäldt et al. (1999) investigated VOCs emitted by the bracket fungi *Fomitopsis pinicola* and *Fomes fomentarius*. Therefore, they enclosed fruiting bodies growing on trunks with plastic bags and used a dynamic HS approach as well as SPME-GC-MS to analyze VOCs produced by these fungi. During sporulation, an increase of sesquiterpenes, *inter alia* Δ^6-protoilludene, in the HS of both species was observed.

Additionally, alternations of the C_8 profile during fungal maturation have been investigated for several species. Wu et al. (2005) analyzed the VOCs in young and matured fruiting bodies of *Laetiporus sulphureus*. Young fruiting bodies offered a pleasant fungal odor with five key aroma compounds, among them oct-1-en-3-one and oct-1-en-3-ol. Aged specimens on the other hand revealed four characteristic odorous compounds, *inter alia* 2-methylpropanoic acid, contributing to a repelling scent and only traces of oct-1-en-3-ol were detected. Cho et al. (2006) investigated the differences in VOCs of *T. matsutake* according to four different grades. Young fruiting bodies displayed lower amounts of C_8 VOCs, including oct-1-en-3-ol and octan-3-one, compared to older specimens. Comparable results for the oct-1-en-3-ol content were found in the straw mushroom *Volvariella volvacea* (Mau et al., 1997). Tasaki et al. (2019) studied the changes of the oct-1-en-3-ol content in the oyster mushroom *Pleurotus ostreatus* (Figure 1A) during different developmental stages. Similar to *C. aegerita* (Orban et al., 2020), the oct-1-en-3-ol content decreased from the mycelium stage to primordium stage and increased thereafter. The highest amount was determined in mature fruiting bodies and decreased with further aging. Cruz et al. (1997) reported comparable results for the oct-1-en-3-ol concentration in two strains of *A. bisporus*. In fruiting bodies of both strains, the oct-1-en-3-ol as well as the octan-3-one content increased from the button stage, peaked at the medium stage and decreased remarkable at the last mature stage. These three stages were designated 2, 3, and 7, respectively, in the classification of Hammond and Nichols (1975). Combet et al. (2009) also investigated the VOCs of fruiting bodies of *A. bisporus* using SPME-GC-MS to compare the stages 1–7 (Hammond and Nichols (1975) classification). The highest amounts of oct-1-en-3-ol and octan-3-one were found in stage 1, which drastically decreased at

stage 2 and thereafter showed a development similar to the one described by Cruz et al. (1997).

Overall, the examples above illustrate that fungal volatilomes are species-dependent and dynamic, showing interesting changes during different developmental stages. However, the question remains which biological role VOCs play in fungi and why VOCs profiles alter.

1.3 Biological function of fungal VOCs

In contrast to several animals, fungi are lacking the ability to communicate by sound. Instead, VOCs in fungi seems to play an important role as infochemicals, meaning substances that are involved in intra- or interspecific biological communication (reviewed in (Holighaus and Rohlfs, 2019; Kües et al., 2018)). As mentioned above, C_8 VOCs are typical compounds found in fungi and, therefore, it is not surprising that these substances might be involved in fungal communication. Several studies demonstrated that C_8 VOCs have an influence on the behavior of invertebrates and might have an important function as infochemicals (reviewed in (Holighaus and Rohlfs, 2019)). Generally, invertebrates show two different types of behavioral responses regarding C_8 VOCs and other volatile infochemicals: attracting/arresting and repelling/avoiding. Invertebrates being attracted to fungi can be grouped in specialists with a focus on one or a few fungal species or in generalists drawn to various species. Fungi are attractive for invertebrates for several reasons. Fruiting bodies offer a valuable source for direct feeding or can be perfect places for oviposition, providing stable conditions, protection and food for the brood (Kües et al., 2018). A repelling effect might protect the fungus of unwanted damage from fungivore insects. However, fungi might also benefit from attracting invertebrates using them as spore distributors or from luring predatory insects feeding on fungivore invertebrates (Holighaus and Rohlfs, 2019).

Interestingly, despite being ubiquitously found in fungi, it seems that C_8 VOCs are not only signals for invertebrates living on diverse fungal species but also for specialized ones. There are several reasons why C_8 VOCs may have a function as specific signals. An important precondition is of course that invertebrates perceive these substances. In this context, a study conducted by Hallem and Carlson (2006) is of special interest, dealing with odorant receptor responses of *Drosophila* to over 100 substances including the C_8 VOCs oct-1-en-3-ol and octan-1-ol. Of the 24 receptors present in *Drosophila*, twelve were

triggered by oct-1-en-3-ol and ten by octan-1-ol, partially showing a distinctive pattern regarding the type of response (excitatory or inhibitory) or the signal strength. This combinatorial coding could be one of the keys giving invertebrates the ability to distinguish between various C_8 VOCs and leading to individual responses (Hallem and Carlson, 2006). Furthermore, the effect of a substance on invertebrate behavior might be concentration dependent. Low concentrations of oct-1-en-3-ol have proven to be an attractant for the grain beetle *Cryptolestes ferrugineus*, whereas high amounts showed a repellent effect (Pierce et al., 1991). However, these kind of behavioral studies have the tendency to use unnatural high concentrations of VOCs, questioning the actual relevance of such results for natural systems (Kües et al., 2018). Invertebrates have developed several additional strategies to discriminate between C_8 VOCs maybe enabling them to select the preferred fungal species. This includes the ability of some species to distinguish C_8 enantiomers, having different preferences depending on sex (Fäldt et al., 1999) and life stage (Holighaus and Rohlfs, 2019). In this context, a study on the beetle *Cis boleti* preferring fungi from the genus *Trametes* including *Trametes gibbosa* as hosts is of special interest. In behavioral tests, female beetles were attracted to the (*S*)-enantiomer of oct-1-en-3-ol at ten time lower concentrations than male beetles (Thakeow et al., 2008). Oct-1-en-3-ol is the most dominant VOC in the HS of *T. gibbosa*, showing a ratio of the *(R*)- and (*S*)-enantiomers of 93:7, respectively, indicating that the female beetles play a major role in the fruiting body colonization of *T. gibbosa* (Thakeow et al., 2008). This might also count for other beetle and fungi species. In fact, field experiments showed that females of the beetles *Malthodes fuscus*, *Anaspis marginicollis* and *A. rufilabris* were, in contrast to their male counterparts, attracted to traps loaded with oct-1-en-3-ol (Fäldt et al., 1999). Additionally to the mechanisms displayed by invertebrates to distinguish between C_8 VOCs mentioned above, it seems that in some cases responses are only triggered by a combination of substances. Fäldt et al. (1999) observed in their field studies that the beetle *Lordithon lunulatus*, a generalist predator on fungivore insects, was only attracted to a mix of oct-1-en-3-ol and octan-3-one and not to the single substances.

Most studies investigating C_8 VOCs and there potential as infochemicals use only a few substances, mainly oct-1-en-3-ol. Taking into account that more than thirty C_8 VOCs have been found in fungi, this group of substances is highly interesting as fungal infochemicals (Holighaus and Rohlfs, 2019). Furthermore, other fungal VOCs have proven to function as

putative infochemicals. Electroantennographic and behavioral experiments revealed that several insects are able to perceive and distinguish various terpenes (de Bruyne and Baker, 2008; Thakeow et al., 2008; Drilling and Dettner, 2009; Balakrishnan K. et al., 2017; Kües et al., 2018). Other ways of fungi to use non-C_8 VOCs for communication are outstandingly exemplified by the fungal family Phallaceae, also known as stinkhorns. Mature stinkhorns produce gelatinous gleba, which contains the spores and offers a foolish, fecal or carrion-like odor. Responsible for this scent are *inter alia* butanoic acid, phenol, 4-methylphenol, indole, dimethyl disulfide and dimethyl trisulfide (Chen et al., 2014; Pudil et al., 2014)., Invertebrates, especially flies, are attracted by these substances, feed on the gleba and disperse the spores (Sleeman et al., 1997; Tuno, 1998; Chen et al., 2014). Interestingly, the reproduction mechanisms of some stinkhorns involving the interaction with invertebrates seems to be more complex than a simple spreading of spores. Certain flies feed on gleba defecate faster than feed on dung or sucrose resulting in a rapid deposition of high amounts of spores (Sleeman et al., 1997). Additionally, *Lysurus mokusin* spores passing the digestive system of *Anisolabis maritima* earwigs displayed significantly higher germination rates than spores directly obtained from gleba (Chen et al., 2014).

Overall, considering the various different fungal VOCs and the several ways they can be perceived by invertebrates the potential of volatile substances for communication purposes is almost endless.

The question remains why volatilomes of fungi alters during different developmental stages and, in this context, what role VOCs as infochemicals play. A hint is given by a study of Holighaus et al. (2014), which investigated the changes in the C_8 VOC composition of four different fruiting body stages of the tinder fungus *F. fomentarius* and monitored the occurrence of fungivorous beetles simultaneously. The study showed changes in the C_8 VOC profile during development accompanied by a clear alternation of the fungal beetle community with specialized fungivores favoring earlier stages compared to generalists. The specialist fungivore *Bolitophagus reticulatus* seemed to prefer the second of four tested fungal stages with octan-3-one being the most prominent C_8 compounds and avoided the first stage with comparable high amounts of oct-1-en-3-ol. The ability of *B. reticulatus* to distinguish between different C_8 VOCs was further confirmed by a behavioral study consisting of walking olfactometer preference tests revealing that *B. reticulatus* is attracted by octan-3-one and repelled by oct-1-en-3-ol (Holighaus et al., 2014). The colonization of

the fungus by different beetle species at different developmental stages might be part of complex survival strategies coordinated by the time-dependent release of VOCs and probably benefits the fungus and/or the insects.

Besides their role as infochemicals in interspecific communication, C_8 VOCs have proven to have an influence on biological processes in fungi. Chitarra et al. (2005) reported inhibition of conidia germination by 4 mM oct-1-en-3-ol in *Penicillium paneum* whereas octan-3-one and, less pronounced, also octan-3-ol and oct-1-en-3-ol stimulated the conidiation of *Trichoderma* ssp. up to a concentration of 500 μM and 100 μM, respectively (Nemčovič et al., 2008). Furthermore, Eastwood et al. (2013) showed that a low concentration of oct-1-en-3-ol in the HS of *A. bisporus* enables the formation of hyphal knots whereas higher concentrations (350 ppm) have an inhibitory effect. Besides the regulatory functions of C_8 VOCs, other VOCs might play important biological roles. For example, sesquiterpenes have shown antimicrobial activity and could therefore protect fungi against other fungi or bacteria (Ishikawa et al., 2001; Scher et al., 2004; Solís et al., 2004; Sterner et al., 1985).

Altogether, VOCs seems to be an important part of fungal communication and regulators of developmental processes in fungi. Changes in the fungal volatilome are probably due to the adaption of the organisms to the altering requirements coming along with varying life stages. Nonetheless, hitherto little is known about the mode of action, the biological role and the biosynthesis of fungal VOCs.

1.4 Biosynthesis of fungal VOCs

The various VOCs originating from fungi can be connected to several biosynthetic pathways. Nonetheless, the formation processes are in many cases still barely understood (Dickschat, 2017). Even for the ubiquitously present C_8 VOCs, profound knowledge is still missing. It is widely accepted that fungal (volatile) oxylipins, including C_8 VOCs, are derived from linoleic acid. However, a resilient connection of further steps in the formation process involving lipoxygenases (LOXs), dioxygenases (DOXs), hydroperoxide lyases (HPLs), alcohol dehydrogenases (ADHs) and ene-reductases representing the complete C_8-pathways is still missing (Chen and Wu, 1984; Wurzenberger and Grosch, 1984a, 1984b; Wanner and Tressl, 1998; Tasaki et al., 2019) (Figure 2). LOXs are present in animals, plants, fungi and bacteria. They are non-heme dioxygenases generally harboring iron in the active site (Oliw, 2002). LOXs catalyze the insertion of molecular oxygen into polyunsaturated fatty acids

comprising (*Z*),(*Z*)-1,4-pentadiene motives, including linoleic acid, linolenic acid and arachidonic acid, resulting in fatty acid hydroperoxides with (*Z*),(*E*)-diene configuration (Sugio et al., 2018) (Figure 2).

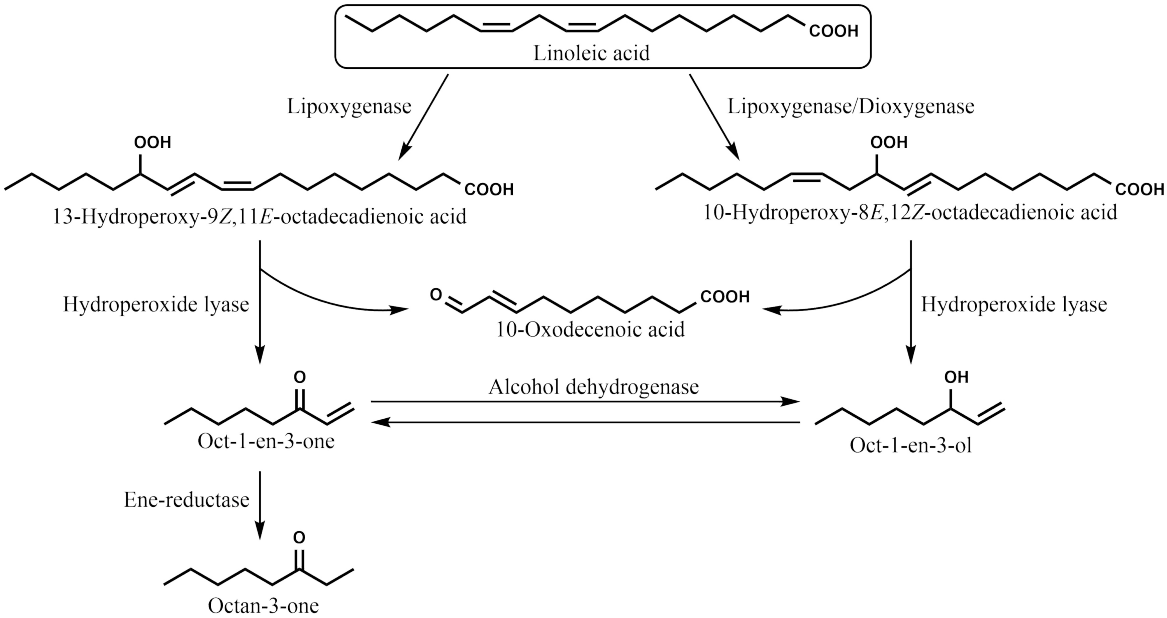

Figure 2: Putative biosynthesis pathways of chosen oxylipins derived from linoleic acid (Orban et al., 2021).

Compared to mammalian and plant LOXs, fungal LOXs have been scarcely studied (Stolterfoht et al., 2019). Furthermore, investigation of fungal LOXs is mainly focused on the phylum Ascomycota with well-studied LOXs from various species such as *Terfezia claveryi* (Pérez-Gilabert et al., 2005), *Thermomyces lanoginosus* (Li et al., 2001), *Fusarium oxysporum* (Brodhun et al., 2013), *Penicillium cammemberti, Penicillium roqueforti* (Perraud and Kermasha, 2000), *Fusarium proliferatum* (Bisakowski et al., 1998) and *Morchella esculenta* (Bisakowski et al., 2000). In addition, Mn-LOXs with manganese as catalytic metal have been characterized from the Ascomycota *Gaeumannomyces graminis* (Su and Oliw, 1998), *Magnaporthe salvinii* (Wennman and Oliw, 2013; Sugio et al., 2018), *Aspergillus fumigatus* (Heshof et al., 2014), *Fusarium oxysporum* and *Colletotrichum gloeosporioides* (Wennman et al., 2015). In contrast, only three LOXs from Basidiomycota are functionally characterized so far (Kuribayashi et al., 2002; Plagemann et al., 2013; Karrer and Rühl, 2019). The *C. aegerita* Lox4 is a 13-LOX exclusively producing 13-hydroperoxy-9,11-octadecadienoic acid (13-HPOD) (Karrer and Rühl, 2019). In contrast, LOXs from *Pleurotus ostreatus* (Kuribayashi et al., 2002) and *Pleurotus sapidus* (Plagemann et al., 2013) are able, apart from the main product 13-HPOD, to produce small amounts of 9-hydroperoxy-10,12-octadecadienoic acid

(9-HPOD). The role of 13-HPOD in the biosynthesis of fungal VOCs is still barely known. Various studies excluded 13-HPOD from being a precursor of oct-1-en-3-ol (Assaf et al., 1997; Matsui et al., 2003; Wurzenberger and Grosch, 1984b), but it seems that 13-HPOD is a precursor of n-hexanal (Matsui et al., 2003). Nonetheless, 13-HPOD might be involved in the synthesis of oct-1-en-3-one, which can be subsequently reduced to oct-1-en-3-ol or octan-3-one by so far unknown ADHs or ene-reductases, respectively (Figure 2) (Chen and Wu, 1984; Wanner and Tressl, 1998; Tasaki et al., 2019). These conversions of C_8 VOCs are a so far scarcely tapped topic with nearly no information available about regulation processes or biological functions. Additionally, several studies linked 10-hydroperoxy-8,12-octadecadienoic acid (10-HPOD) to the formation of oct-1-en-3-ol in fungi (Figure 2) (Wurzenberger and Grosch, 1984a, 1984b; Matsui et al., 2003; Akakabe et al., 2005).However, no fungal 10-LOX has been found so far. Therefore, DOXs might be involved in the biosynthesis of oct-1-en-3-ol. The fungal linoleate diol synthase (LDS) family harbors 8-, 9- and 10-DOXs, often fused to catalytically active cytochrome P450s (CYPs). Over twenty DOX fusion proteins from Ascomycota have been characterized so far that can be grouped into 5,8- and 7,8-LDS, 10*R*-DOX-EAS (epoxy alcohol synthase), 9*S*- and 9*R*-DOX-AOS (allene oxide synthase), 8*S*- and 8*R*-DOX-AOS and 10*R*-DOX-CYP enzymes (Brodhun et al., 2010; Oliw, 2018, 2020). All DOX fusion proteins contain the dioxygenase domain at the N-terminus, whereas the P450 domain, responsible for the rearrangement of the N-terminally formed hydroperoxide fatty acid, is located at the C-terminus (Hoffmann and Oliw, 2013). Especially 10*R*-DOX-CYPs are interesting for C_8 VOCs formation, proven to produce mainly 10-HPOD. Moreover, addition of linoleic acid to an extract of *E. coli* containing a recombinant 10*R*-DOX-CYP from *A. nidulans* resulted in the production of oct-1-en-3-ol, oct-2-en-1-ol, oct-2-enal and octan-3-one (Brodhun et al., 2010). Interestingly, no DOXs from Basidiomycota have been characterized yet. This lack of information on the biosynthetic pathway in fungi is also true for the subsequent cleavage of fatty acid hydroperoxides. Contradictory in plants, HPLs, being responsible especially for the formation of C6- and C9-aldehydes, have been extensively studied (Hassan et al., 2015; Stolterfoht et al., 2019). In fungi, the role of HPLs in the biosynthesis of C_8 VOCs derived from HPODs has been proposed (Figure 2), but nothing is known about their distinct function in fungi. However, pioneering work on the enzymatic cleavage was conducted by Wurzenberger and Grosch (1984b) adding 9-, 10-, 12- and 13-HPOD to a protein fraction

isolated from an extract gained from *A. bisporus*. Interestingly, only incubation with 10-HPOD leaded to the formation of oct-1-en-3-ol and 10-oxo-trans-8-decenoic acid probably due to the catalytic activity of a 10-HPOD specific HPL. Other studies also suggest an involvement of fungal HPLs in the biosynthesis of C_8 VOCs (Assaf et al., 1997; Matsui et al., 2003), but so far no fungal HPLs have been isolated and characterized. Recently, Lee et al. (2020) attempted to elucidate fungal oct-1-en-3-ol biosynthesis using the baker's yeast *Saccharomyces cerevisiae* as an expression host for putative LOXs and a putative HPL from *T. matsutake*. Addition of linoleic acid to crude protein extracts or whole cells of *S. cerevisiae* transformands containing various combinations of putative LOXs and the putative HPL resulted in the formation of different amounts of oct-1-en-3-ol, varying between 0.27 and 0.66 mg L^{-1}. However, no information about the standard variation of oct-1-en-3-ol concentrations was given and no control experiments with non-transformed *S. cerevisiae* were done. Furthermore, no tests with the purified enzymes were carried out. Therefore, observed oct-1-en-3-ol production might originate, at least partly, from endogenous pathways of *S. cerevisiae*, which itself harbors LOXs and other enzymes putatively involved in C_8 volatile formation (Bisakowski et al., 1995; Wanner and Tressl, 1998). Accordingly, it is difficult to make statements about the role of the chosen enzymes from *T. matsutake* for the oct-1-en-3-ol biosynthesis. Altogether, detailed information about C_8 VOCs biosynthesis in fungi is still missing, especially for regulation processes leading to the alternation of C_8 VOCs profiles during different fungal developmental stages.

Terpenes are ubiquitous present in fungi and contribute to the unique flavor of numerous species (reviewed in (Kramer and Abraham, 2012; Quin et al., 2014; Dickschat, 2017)). The large diversity of terpenes is derived from only two precursors, dimethylallyl diphosphate and isopentenyl diphosphate, which in fungi are produced from acetyl-CoA by the mevalonate pathway (Miziorko, 2011). Condensation of these two isomers results in linear molecules with different chain length: C10 geranyl diphosphate, C15 farnesyl diphosphate, C20 geranylgeranyl diphosphate, C25 geranylfarnesyl diphosphate. Dephosphorylation and cyclization reactions of these hydrocarbons, catalyzed by terpene synthases, are the origin of the wide range of terpenes (Christianson, 2006). Additionally, modifications of terpenes catalyzed by cytochrome P450 monooxygenases, oxidoreductases and different transferases contribute also to the high diversity of terpenes in fungi (Quin et al., 2014). Of these, especially monoterpenes (C10) and sesquiterpenes (C15) contribute to the

volatilome of fungi due to the fact that diterpenes (C20) and higher terpenes exhibit a remarkably less pronounced volatility (Dickschat, 2017). Several monoterpenes have been identified in fungi including naturally often occurring ones like α-pinene in *C. aegerita* or linalool in *Lepista nuda*, but also comparable rare substances like dill ether and wine lactone from *Pleurotus sapidus* (Breheret et al., 1997; Trapp et al., 2019). The formation processes of fungal sesquiterpenes are well known compared to the C_8 VOC synthesis. Sesquiterpene synthases (STSs) bind farnesyl pyrophosphate at the active site using an Mg^{2+} cluster consisting of three ions (Schmidt-Dannert, 2015). The metal ligands are coordinated by an NSE/DTE and an aspartate–rich motif. The latter [D(D/E/N)XX(D/E)] can slightly differ from the [DDXX(D/E)] motif usually found in plants (Cane and Kang, 2000; Ashour et al., 2010; López-Gallego et al., 2010; Miller and Allemann, 2011). Heterolytic cleavage of the diphosphate group results in the formation of a carbocation being initiator of diverse cyclization and rearrangement reactions (Schmidt-Dannert, 2015). STSs from fungi have proven to have often a high catalytic promiscuity, leading to diverse numbers of sesquiterpenes despite low variety of enzymes (Agger et al., 2009; Lopez-Gallego et al., 2010; Wawrzyn et al., 2012; Quin et al., 2013; Zhang et al., 2020). Recently, Zhang et al. (2020) showed that fungal STSs with shared conserved sequences also have common products. For this, amino acid sequence data from over thousand putative fungal STSs were combined with data of characterized STSs proving that bioinformatics can be a powerful tool for the functional prediction of STSs. However, most putative STSs are still not analyzed or do not cluster in a group with already characterized STSs. Thus, these enzymes harbor high potential for being new STSs with hitherto unknown products (Zhang et al., 2020).

Several fungal VOCs are derived from amino acids. The Ehrlich pathway is a source of these substances and is well studied in *S. cerevisiae*. In a first step, the amino group of an amino acid, such as valine, leucine, isoleucine, tryptophan, tyrosine, phenylalanine and methionine, is transferred to α-ketoglutarate leading to the formation of glutamate and the corresponding α-keto acid of the amino acid. This reaction is catalyzed by different aminotransferases. In *S. cerevisiae*, the transaminases Aro8 and Aro9 have proven to accept aromatic amino acids as well as methionine and leucine as substrates, whereas Twt1/Bat1 and Twt2/Bat2 shows activity regarding branched chain amino acids (Eden et al., 1996; Kispal et al., 1996; Iraqui et al., 1998; Urrestarazu et al., 1998; Hazelwood et al., 2008). Decarboxylation results in the formation of fusel aldehydes. Depending on the

structure of the precursor, the reaction is catalyzed by different decarboxylases, with Aro10 being a key player showing a broad-substrate-specificity (Vuralhan et al., 2003, 2005). The fusel aldehydes can be oxidized to fusel acids by aldehyde dehydrogenases or reduced to fusel alcohols via alcohol dehydrogenases, including Adh1, Adh2, Adh3, Adh4 and Adh5 (Dickinson et al., 2003). These reactions are the origin of several VOCs found in Ascomycota, e.g. 2-methylpropanal derived from valine or 2-phenylethanol with phenylalanine as precursor. Additionally, VOCs stemmed from amino acids have also been reported for Basidiomycota. Using ^{13}C labelled amino acids, Lanfermann et al. (2014) showed that *L. sulphureus* is able to convert isoleucine into the corresponding α-keto acid and further to 4-hydroxy-3-methyl-2-oxopentanoic acid and finally to 3-hydroxy-4,5-dimethyl-2(5*H*)-furanone (sotolon), the latter being a potent aroma compound also known to contribute to the typical aroma of lovage (Blank and Schieberle, 1993). Furthermore, the basidiomycete *Bjerkandera adusta* is able to convert phenylalanine into aroma compounds such as benzaldehyde and benzyl alcohol with a phenylalanine ammonia lyase being important for the initial reaction (Lapadatescu et al., 2000). Recently, Zhang et al. (2018) demonstrated that *L. edodes* uses isoleucine as precursor for methyl 2-methylbutanoat, with different intermediates including 2-oxo-3-methylpentanoic acid, 2-methylbutanoyl-CoA, 2-methylbutanal and 2-methylbutanoic acid being involved in the formation process. In *L. edodes* might be the Ehrlich pathway¸ beside the postulated 'standard' pathway, also functional during biosynthesis of methyl 2-methylbutanoat (Zhang et al., 2018). Additionally, the typical sulfurous compounds from *L. edodes*, including lenthionine, are derived from lentinic acid, involving a glutamyl transpeptidase and a cysteine sulfoxide lyase in the formation process (reviewed in (Fraatz and Zorn, 2011)). Lentinic acid itself is a sulfur-containing peptide consisting *inter alia* of glutamate and modified cysteine (Yasumoto et al., 1971). Kleofas et al. (2015) observed the presence of aroma compounds derived from amino acids, such as 3-methylbutanoic acid, in dried fruiting bodies of *Calocybe gambosa* being not detectable in the fresh specimens. Analysis of the amino acid and glucose content revealed that the origin of these VOCs is probably the Ehrlich pathway.However, the source of aldehydes present in fruiting bodies processed at high temperature might alternatively be the Strecker degradation of corresponding amino acids (Kleofas et al., 2015).

Overall, VOC formation in fungi involves many substances and enzymes, intertwining several biosynthetic pathways altogether resulting in a multitude of compounds. Identification of enzymes contributing to these processes is a challenging task and the subsequent functional characterization of enzymes often turns out to be a time-consuming process. In this context, *de novo* sequencing methods in combination with sophisticated bioinformatics, which includes amino acid sequence alignments of putative enzymes with characterized ones, have been used within the experimental work of this thesis to identify enzymes putatively involved in different VOC pathways.

1.5 Transcriptomic analysis of fungi

Functional genomics is a field of molecular biology aiming to provide knowledge about the functions and interactions of genes and proteins (Bunnik and Le Roch, 2013). In the last two decades, data obtained from omics approaches have given valuable insights to illuminate these complex coherences including the analysis and interspecific comparison of genes (comparative genomics), the expression profiles of genes (transcriptomic) and proteins (proteomic) as well as analysis of (volatile) metabolites (metabolome/volatilome) of organisms under certain conditions (Téllez-Téllez and Diaz-Godinez, 2019). The availability of a sequenced and annotated genome of the analyzed species can be seen as a valuable fundament to these approaches. For fungi, the 1.000 fungal genome project, a collaboration of international researchers with the JGI (Joint Genome Institute), is such a beneficial source for genetic data providing more than 1.700 fungal genomes (https://mycocosm.jgi.doe.gov/fungi/fungi.info.html) (Grigoriev et al., 2014). NGS has highly contributed to this large number of sequenced fungal genomes making sequencing affordable also for smaller research groups. Most commercial NGS platforms fall under the concept of sequencing by synthesis (SBS). SBS approaches are based on the elongation of a DNA strand using a DNA-polymerase and the detection of the nucleotide incorporation by fluorescence or sensing of the reaction products (Goodwin et al., 2016). Other shared features of SBS methods for NGS approaches are (1) the fragmentation of DNA/RNA strands prior to sequencing, (2) in case of RNA samples, the reverse transcription of RNA fragments into cDNA, (3) the ligation of common adaptors (synthesized oligonucleotides of known sequence) to the fragments, (4) attachment of the DNA templates to a surface using covalently bonded oligonucleotides complementary to the adaptors and (5) amplification of the DNA templates. The resulting multiple copies of a DNA fragment in a defined area is

necessary for an adequate signal to noise ratio during sequencing (Goodwin et al., 2016; Martin and Wang, 2011; McCombie et al., 2019). A main difference between the SBS approaches used for NGS is the detection of the nucleotide incorporation. There are basically two ways, (1) the direct sensing of fluorescence using cyclic reversible termination or (2) indirect detection of reaction products resulting from nucleotide incorporation after single nucleotide addition (Goodwin et al., 2016; McCombie et al., 2019). The first method is closely related to the original Sanger approach using individually fluorophore labeled nucleotides where the ribose 3′-OH group is blocked. During each cycle, a mixture of all four nucleotides is added. The complementary nucleotide is incorporated to the elongating strand and the fluorescence signal is detected after removal of the unbound nucleotides. After each cycle, the fluorophore and the blocking group are cleaved off and the cycle can be repeated. The Illumina CRT system, accounting for the largest market share of sequencing platforms, belongs to this sequencing type (Goodwin et al., 2016; McCombie et al., 2019). The second method uses unlabeled nucleotides and identification of the incorporated nucleotide takes place via the occurring byproducts. Two types of this indirect post-incorporation method are applied: (1) detection of light emitted as a result of an enzyme cascade involving ATP sulfurylase and luciferase reacting with pyrophosphate (released during nucleotide incorporation), APS and luciferin (applied by e.g. Roche 454) or (2) detection of pH change due to hydrogen ions released during nucleotide incorporation (e.g. Ion Torrent) (McCombie et al., 2019). Furthermore, variations of the NGS methods, such as the QuantSeq 3’ mRNA approach, can be powerful tools for transcriptome analysis of organisms with sequenced and annotated genomes. Focusing on the 3’ end of polyadenylated mRNA, this method generates for each transcript only one fragment so the number of reads can be linked directly to the number of transcripts and is therefore proportional to the gene expression avoiding complicated coverage-based quantification (Moll et al., 2014). Despite being cost-effective, accurate, and well established for a wide range of analysis tools and pipelines, NGS technologies suffer from the drawback to be limited regarding the read length, normally not exceeding 600 bp, which can cause problems during gene assembly especially when repetitive regions are present in the DNA sample (Amarasinghe et al., 2020; Kanwar et al., 2021). Long-read sequencing, also called third-generation sequencing can be helpful to overcome this disadvantage. Prominent examples for third-generation sequencing are PacBio single-molecule real-time (SMRT)

sequencing and Oxford Nanopore Technologies' nanopore sequencing. SMRT is a SBS based approach using a DNA polymerase attached to the bottom of a nanoscale observation chamber. The polymerase incorporate fluorescently labelled nucleotides and a sensor detects in real-time fluorescence events that correspond to the addition of one specific nucleotide enabling the sequencing of the DNA strand (Ardui et al., 2018). In contrast to NGS, the read length is usually not limited by the size of the nucleotide fragments but depends on the activity of the polymerase (Ardui et al., 2018). For nanopore sequencing, the DNA is guided through biological nanopores, which are embedded in a membrane separating two compartments, with help of an enzyme (Jain et al., 2016). An electric potential is applied over the membrane, causing an ion current and transfer of DNA through the pore. As the DNA passes through the pore, sensors measure changes in the ion current, with different nucleotides causing specific patterns of current variation. The distinct current signals can be used to infer the DNA sequence (Amarasinghe et al., 2020; Rang et al., 2018). Long-read sequencing can commonly achieve a read length of 30 kbp or higher offering remarkable advantages for *de novo* genome assembly applications (Amarasinghe et al., 2020; Goodwin et al., 2016). Nonetheless, these techniques offer lower per read accuracy than NGS approaches. Therefore, the combination of long-read sequencing with the accuracy of additional short-read data can be used (Amarasinghe et al., 2020). This hybrid assembly approach was also applied for the genome sequencing of *C. aegerita* using Illumina and PacBio data (Gupta et al., 2018).

NGS enabled a multitude of (fungal) transcriptomic studies in recent years. Comparative transcriptomic analysis can help to identify genes coding for enzymes that might play distinctive roles under certain conditions by comparing two or more states with each other. For fungi of the phylum Basidiomycota, several studies have been conducted, focusing on gene expression during *inter alia* fruiting body development (Chum et al., 2008; Cheng et al., 2013; Plaza et al., 2014; Muraguchi et al., 2015; Zhang et al., 2015; León-Ramírez et al., 2017; Song et al., 2018; Wang et al., 2018; Tong et al., 2020), mating (Erdmann et al., 2012; Freihorst et al., 2018), mycorrhiza development (Larsen et al., 2010) and lignocellulose degradation (Chen et al., 2016; Vasina et al., 2017). Transcriptomic analysis of four developmental stages of *Hypsizygus marmoreus*, namely mycelial knot, mycelial pigmentation, primordium and fruiting body, showed that the transition from the mycelial knot stage to the mycelium pigmentation stage was associated with the upregulation of

genes encoding for a blue light receptor, a phytochrome-like protein and a phytochrome-related signal transduction histidine kinase (Zhang et al., 2015). In this context it is worth mentioning that light is an important trigger for fungal development and blue light sensing is essential for fruiting body formation (Kuratani et al., 2010; Ohm et al., 2013; Pelkmans et al., 2017; Terashima et al., 2005; Sakamoto, 2018). Furthermore, Kyoto Encyclopedia of Genes and Genomes (KEGG) analysis showed that genes involved in fatty acid metabolism were upregulated in fruiting bodies compared to primordia, which is interesting because linoleic acid serves as a precursor for C_8 VOCs and changes regarding fatty acid content or composition might also affect the fungal volatilome (Zhang et al., 2015). Recently, Song et al. (2018) investigated the transcriptomes of a mycelium stage and mature fruiting bodies of the dikaryotic *L. edodes* strain Sanjo701 using a Illumina HiSeq platform. Fiftyone genes were designated as fruiting body-specific by comparison of transcripts from the two developmental stages. LE_004420, coding for the isopentenyl diphosphate isomerase, was exclusively expressed in fruiting bodies, being an important enzyme for terpene biosynthesis including volatile terpenes. Besides looking into transcriptomic changes of one species, it can be helpful to compare gene expression patterns among several species to find common patterns and, therefore, getting insights about genes (proteins) of general functionality. Recently, Krizsán et al. (2019) showed that fungi have conserved transcriptomic signatures of fruiting body development by comparing six different developmental stages of six Agaricomycetes. Interestingly, genes related to fungal cell wall synthesis, oxidoreductase activity and carbohydrate metabolism were upregulated among all species along with fruiting initiation, indicating that cell wall remodeling is a shared feature of mushrooms during fruiting body development. Moreover, commonly upregulated genes were associated with DNA replication, transmembrane sugar transport and ribosome as well as lipid biosynthesis, the latter category, as mentioned above, interestingly regarding C_8 Oxylipin formation (Krizsán et al., 2019). However, many types of genes were expressed only by certain species, harboring the potential to identify individually regulated biosynthesis pathways. In this context of special interest is the combination of transcriptomic data with other omics approaches such as metabolomics. Freihorst et al. (2018) investigated changes regarding the transcriptome, proteome and volatilome after mating of *S. commune* giving hints about enzymes that might be involved in the formation of C_8 VOCs. Nonetheless, a profound analysis of this subject was not

conducted (Freihorst et al., 2018). In fact, despite harboring great potential to obtain in-depth knowledge about VOC biosynthesis, combined transcriptomic and metabolomics studies in fungi were barely carried out so far.

1.6 Objectives

Generally, sample preparation in studies analyzing fungal VOCs is a problematic issue. Prior to extraction of VOCs, fruiting bodies are normally chopped or elsewise impaired, inducing unwanted enzymatic reactions naturally not occurring in the fungus. Thus, one purpose of this work was to establish a non-invasive method to analyze VOCs in the HS of fungal cultures to monitor volatile profiles under nearly natural circumstances. Applying this system, the VOCs of different developmental stages of the fungus *C. aegerita* AAE-3 should be analyzed. However, triggering the fungus to form fruiting bodies and to sporulate under laboratory conditions is not trivial. Therefore, the cultivation system should, besides enabling an adequate extraction of VOCs, offer the right conditions, like aeration, humidity and light, for fruiting body development. Volatilome data obtained in this non-invasive way during different developmental stages can be a powerful tool for analyzing the formation processes of VOCs in fungi and their biological function as e.g. infochemicals.

As described above, the biosynthetic pathways of many fungal VOCs, especially regarding C_8 VOCs, are hitherto insufficiently elucidated. To tap this neglected topic, volatilome data should be combined with transcriptome data during different developmental stages of *C. aegerita* AAE-3 to identify matching patterns between VOC profiles and gene expression of enzymes putatively involved in the biosynthesis of the volatiles. Overall, the outcome of this work should serve as a fundament for subsequent enzyme characterization studies and as a guideline for a general procedure of analyzing VOC formation in fungi.

1.7 References

Agger, S., Lopez-Gallego, F., and Schmidt-Dannert, C. (2009). Diversity of sesquiterpene synthases in the basidiomycete *Coprinus cinereus*. Mol. Microbiol. *72*, 1181–1195.

Akakabe, Y., Matsui, K., and Kajiwara, T. (2005). Stereochemical correlation between 10-hydroperoxyoctadecadienoic acid and 1-octen-3-ol in *Lentinula edodes* and *Tricholoma matsutake* mushrooms. Biosci. Biotechnol. Biochem. *69*, 1539–1544.

Amarasinghe, S.L., Su, S., Dong, X., Zappia, L., Ritchie, M.E., and Gouil, Q. (2020). Opportunities and challenges in long-read sequencing data analysis. Genome Biol. *21*, 30.

Arbefeville, S., Harris, A., and Ferrieri, P. (2017). Comparison of sequencing the D2 region of the large subunit ribosomal RNA gene (MicroSEQ®) versus the internal transcribed spacer (ITS) regions using two public databases for identification of common and uncommon clinically relevant fungal species. J. Microbiol. Methods *140*, 40–46.

Ardui, S., Ameur, A., Vermeesch, J.R., and Hestand, M.S. (2018). Single molecule real-time (SMRT) sequencing comes of age: applications and utilities for medical diagnostics. Nucleic Acids Res. *46*, 2159–2168.

Arima, T., Yamamoto, M., Hirata, A., Kawano, S., and Kamada, T. (2004). The eln3 gene involved in fruiting body morphogenesis of *Coprinus cinereus* encodes a putative membrane protein with a general glycosyltransferase domain. Fungal Genet. Biol. *41*, 805–812.

Ashour, M., Wink, M., and Gershenzon, J. (2010). Biochemistry of Terpenoids: Monoterpenes, Sesquiterpenes and Diterpenes. In Annual Plant Reviews Volume 40: Biochemistry of Plant Secondary Metabolism, (John Wiley & Sons, Ltd), pp. 258–303.

Assaf, S., Hadar, Y., and Dosoretz, C.G. (1997). 1-Octen-3-ol and 13-hydroperoxylinoleate are products of distinct pathways in the oxidative breakdown of linoleic acid by *Pleurotus pulmonarius*. Enzyme Microb. Technol. *21*, 484–490.

Balakrishnan K., Holighaus G., Weißbecker B., and Schütz S. (2017). Electroantennographic responses of red flour beetle *Tribolium castaneum* Herbst (Coleoptera: Tenebrionidae) to volatile organic compounds. J. Appl. Entomol. *141*, 477–486.

Bisakowski, B., Kermasha, S., and Schuepp, C. (1995). Partial purification and some properties of lipoxygenase from *Saccharomyces cerevisiae*. World J. Microbiol. Biotechnol. *11*, 494–496.

Bisakowski, B., Kermasha, S., and Spinnler, E. (1998). Characterization of Purified Lipoxygenase Extracts from *Fusarium proliferatum*. J. Agric. Food Chem. *46*, 2382–2388.

Bisakowski, B., Atwal, A.S., and Kermasha, S. (2000). Characterization of lipoxygenase activity from a partially purified enzymic extract from *Morchella esculenta*. Process Biochem. *36*, 1–7.

Blackwell, M. (2011). The Fungi: 1, 2, 3 … 5.1 million species? Am. J. Bot. *98*, 426–438.

Blank, I., and Schieberle, P. (1993). Analysis of the seasoning-like flavour substances of a commercial lovage extract (*Levisticum officinale* Koch.). Flavour Fragr. J. *8*, 191–195.

Breheret, S., Talou, T., Rapior, S., and Bessière, J.-M. (1997). Monoterpenes in the Aromas of Fresh Wild Mushrooms (Basidiomycetes). J. Agric. Food Chem. *45*, 831–836.

Brodhun, F., Schneider, S., Göbel, C., Hornung, E., and Feussner, I. (2010). PpoC from *Aspergillus nidulans* is a fusion protein with only one active haem. Biochem. J. *425*, 553–565.

Brodhun, F., Cristobal-Sarramian, A., Zabel, S., Newie, J., Hamberg, M., and Feussner, I. (2013). An Iron 13S-Lipoxygenase with an α-Linolenic Acid Specific Hydroperoxidase Activity from *Fusarium oxysporum*. PLOS ONE *8*, e64919.

de Bruyne, M., and Baker, T.C. (2008). Odor Detection in Insects: Volatile Codes. J. Chem. Ecol. *34*, 882–897.

Bunnik, E.M., and Le Roch, K.G. (2013). An Introduction to Functional Genomics and Systems Biology. Adv. Wound Care *2*, 490–498.

Cane, D.E., and Kang, I. (2000). Aristolochene Synthase: Purification, Molecular Cloning, High-Level Expression in Escherichia coli, and Characterization of the *Aspergillus terreus* Cyclase. Arch. Biochem. Biophys. *376*, 354–364.

Chaisaena, W. (2009). Light effects on fruiting body development of wildtype in comparison to light-insensitive mutant strains of the basidiomycete *Coprinopsis cinerea*, grazing of mites (*Tyrophagus putrescentiae*) on the strains and production of volatile organic compounds during fruiting body development. PhD thesis, University of Göttingen, Göttingen, Germany. https://ediss.uni-goettingen.de/handle/11858/00-1735-0000-0006-B11E-F

Chen, C.C., and Ho, C.T. (1986). Identification of sulfurous compounds of Shiitake mushroom (*Lentinus edodes* Sing.). J. Agric. Food Chem. *34*, 830–833.

Chen, C.C., and Wu, C.M. (1984). Studies on the enzymic reduction of 1-octen-3-one in mushroom (*Agaricus bisporus*). J. Agric. Food Chem. *32*, 1342–1344.

Chen, G., Zhang, R.-R., Liu, Y., and Sun, W.-B. (2014). Spore Dispersal of Fetid *Lysurus mokusin* by Feces of Mycophagous Insects. J. Chem. Ecol. *40*, 893–899.

Chen, L., Gong, Y., Cai, Y., Liu, W., Zhou, Y., Xiao, Y., Xu, Z., Liu, Y., Lei, X., Wang, G., et al. (2016). Genome Sequence of the Edible Cultivated Mushroom *Lentinula edodes* (Shiitake) Reveals Insights into Lignocellulose Degradation. PLOS ONE *11*, e0160336.

Cheng, C.K., Au, C.H., Wilke, S.K., Stajich, J.E., Zolan, M.E., Pukkila, P.J., and Kwan, H.S. (2013). 5'-Serial Analysis of Gene Expression studies reveal a transcriptomic switch during fruiting body development in *Coprinopsis cinerea*. BMC Genomics *14*, 195.

Chitarra, G.S., Abee, T., Rombouts, F.M., and Dijksterhuis, J. (2005). 1-Octen-3-ol inhibits conidia germination of *Penicillium paneum* despite of mild effects on membrane permeability, respiration, intracellular pH, and changes the protein composition. FEMS Microbiol. Ecol. *54*, 67–75.

Cho, I.H., Choi, H.-K., and Kim, Y.-S. (2006). Difference in the Volatile Composition of Pine-Mushrooms (*Tricholoma matsutake* Sing.) According to Their Grades. J. Agric. Food Chem. *54*, 4820–4825.

Cho, I.H., Namgung, H.-J., Choi, H.-K., and Kim, Y.-S. (2008). Volatiles and key odorants in the pileus and stipe of pine-mushroom (*Tricholoma matsutake* Sing.). Food Chem. *106*, 71–76.

Christianson, D.W. (2006). Structural Biology and Chemistry of the Terpenoid Cyclases. Chem. Rev. *106*, 3412–3442.

Chum, W.W.Y., Ng, K.T.P., Shih, R.S.M., Au, C.H., and Kwan, H.S. (2008). Gene expression studies of the dikaryotic mycelium and primordium of *Lentinula edodes* by serial analysis of gene expression. Mycol. Res. *112*, 950–964.

Combet, E., Henderson, J., Eastwood, D.C., and Burton, K.S. (2009). Influence of Sporophore Development, Damage, Storage, and Tissue Specificity on the Enzymic Formation of Volatiles in Mushrooms (*Agaricus bisporus*). J. Agric. Food Chem. *57*, 3709–3717.

Costa, R., De Grazia, S., Grasso, E., and Trozzi, A. (2015). Headspace-Solid-Phase Microextraction-Gas Chromatography as Analytical Methodology for the Determination of Volatiles in Wild Mushrooms and Evaluation of Modifications Occurring during Storage. J. Anal. Methods Chem. *2015*, 951748.

Cruz, C., Noël-Suberville, C., and Montury, M. (1997). Fatty Acid Content and Some Flavor Compound Release in Two Strains of *Agaricus bisporus*, According to Three Stages of Development. J. Agric. Food Chem. *45*, 64–67.

Dias, E.S., and Brito, M.R. de (2017). Mushrooms: Biology and Life Cycle. In Edible and Medicinal Mushrooms, (John Wiley & Sons, Ltd), pp. 15–33.

Dickinson, J.R., Salgado, L.E.J., and Hewlins, M.J.E. (2003). The catabolism of amino acids to long chain and complex alcohols in *Saccharomyces cerevisiae*. J. Biol. Chem. *278*, 8028–8034.

Dickschat, J.S. (2017). Fungal volatiles – a survey from edible mushrooms to moulds. Nat. Prod. Rep. *34*, 310–328.

Drilling, K., and Dettner, K. (2009). Electrophysiological responses of four fungivorous coleoptera to volatiles of *Trametes versicolor*: implications for host selection. Chemoecology *19*, 109.

Eastwood, D.C., Herman, B., Noble, R., Dobrovin-Pennington, A., Sreenivasaprasad, S., and Burton, K.S. (2013). Environmental regulation of reproductive phase change in *Agaricus bisporus* by 1-octen-3-ol, temperature and CO2. Fungal Genet. Biol. *55*, 54–66.

Eden, A., Simchen, G., and Benvenisty, N. (1996). Two yeast homologs of ECA39, a target for c-Myc regulation, code for cytosolic and mitochondrial branched-chain amino acid aminotransferases. J. Biol. Chem. *271*, 20242–20245.

Erdmann, S., Freihorst, D., Raudaskoski, M., Schmidt-Heck, W., Jung, E.-M., Senftleben, D., and Kothe, E. (2012). Transcriptome and Functional Analysis of Mating in the Basidiomycete *Schizophyllum commune*. Eukaryot. Cell *11*, 571–589.

Esser, K., Saleh, F., and Meinhardt, F. (1979). Genetics of fruit body production in higher basidiomycetes II. Monokaryotic and dikaryotic fruiting in *Schizophyllum commune*. Curr. Genet. *1*, 85–88.

Fäldt, J., Jonsell, M., Nordlander, G., and Borg-Karlson, A.-K. (1999). Volatiles of Bracket Fungi *Fomitopsis pinicola* and *Fomes fomentarius* and Their Functions as Insect Attractants. J. Chem. Ecol. *25*, 567–590.

Fell, J.W., Boekhout, T., Fonseca, A., Scorzetti, G., and Statzell-Tallman, A. (2000). Biodiversity and systematics of basidiomycetous yeasts as determined by large-subunit rDNA D1/D2 domain sequence analysis. Int. J. Syst. Evol. Microbiol. *50*, 1351–1371.

Fernandez Espinar, M.-T., and Labarère, J. (1997). Cloning and sequencing of the Aa-Pri1 gene specifically expressed during fruiting initiation in the edible mushroom *Agrocybe aegerita*, and analysis of the predicted amino-acid sequence. Curr. Genet. *32*, 420–424.

Fraatz, M.A., and Zorn, H. (2011). Fungal Flavours. In Industrial Applications, M. Hofrichter, ed. (Berlin, Heidelberg: Springer Berlin Heidelberg), pp. 249–268.

Freihorst, D., Brunsch, M., Wirth, S., Krause, K., Kniemeyer, O., Linde, J., Kunert, M., Boland, W., and Kothe, E. (2018). Smelling the difference: Transcriptome, proteome and volatilome changes after mating. Fungal Genet. Biol. *112*, 2–11.

Goodwin, S., McPherson, J.D., and McCombie, W.R. (2016). Coming of age: ten years of next-generation sequencing technologies. Nat. Rev. Genet. *17*, 333–351.

Grigoriev, I.V., Nikitin, R., Haridas, S., Kuo, A., Ohm, R., Otillar, R., Riley, R., Salamov, A., Zhao, X., Korzeniewski, F., et al. (2014). MycoCosm portal: gearing up for 1000 fungal genomes. Nucleic Acids Res. *42*, D699–D704.

Gupta, D.K., Rühl, M., Mishra, B., Kleofas, V., Hofrichter, M., Herzog, R., Pecyna, M.J., Sharma, R., Kellner, H., Hennicke, F., et al. (2018). The genome sequence of the commercially cultivated mushroom *Agrocybe aegerita* reveals a conserved repertoire of fruiting-related genes and a versatile suite of biopolymer-degrading enzymes. BMC Genomics *19*, 48.

Hallem, E.A., and Carlson, J.R. (2006). Coding of Odors by a Receptor Repertoire. Cell *125*, 143–160.

Hammond, J.B.W., and Nichols, R. (1975). Changes in respiration and soluble carbohydrates during the post-harvest storage of mushrooms (*Agaricus bisporus*). J. Sci. Food Agric. *26*, 835–842.

Hassan, M.N. ul, Zainal, Z., and Ismail, I. (2015). Green leaf volatiles: biosynthesis, biological functions and their applications in biotechnology. Plant Biotechnol. J. *13*, 727–739.

Hawksworth, D.L., and Lücking, R. (2017). Fungal Diversity Revisited: 2.2 to 3.8 Million Species. Microbiol. Spectr. *5*.

Hazelwood, L.A., Daran, J.-M., Maris, A.J.A. van, Pronk, J.T., and Dickinson, J.R. (2008). The Ehrlich Pathway for Fusel Alcohol Production: a Century of Research on *Saccharomyces cerevisiae* Metabolism. Appl. Environ. Microbiol. *74*, 2259–2266.

Herzog, R., Solovyeva, I., Rühl, M., Thines, M., and Hennicke, F. (2016). Dikaryotic fruiting body development in a single dikaryon of *Agrocybe aegerita* and the spectrum of monokaryotic fruiting types in its monokaryotic progeny. Mycol. Prog. *15*, 947–957.

Heshof, R., Jylhä, S., Haarmann, T., Jørgensen, A.L.W., Dalsgaard, T.K., and de Graaff, L.H. (2014). A novel class of fungal lipoxygenases. Appl. Microbiol. Biotechnol. *98*, 1261–1270.

Hoffmann, I., and Oliw, E.H. (2013). Discovery of a linoleate 9S-dioxygenase and an allene oxide synthase in a fusion protein of *Fusarium oxysporum*. J. Lipid Res. *54*, 3471–3480.

Holighaus, G., and Rohlfs, M. (2019). Volatile and non-volatile fungal oxylipins in fungus-invertebrate interactions. Fungal Ecol. *38*, 28–36.

Holighaus, G., Weißbecker, B., Fragstein, M. von, and Schütz, S. (2014). Ubiquitous eight-carbon volatiles of fungi are infochemicals for a specialist fungivore. Chemoecology *24*, 57–66.

Hyde, K.D., Jeewon, R., Chen, Y.-J., Bhunjun, C.S., Calabon, M.S., Jiang, H.-B., Lin, C.-G., Norphanphoun, C., Sysouphanthong, P., Pem, D., et al. (2020). The numbers of fungi: is the descriptive curve flattening? Fungal Divers. *103*, 219–271.

Iraqui, I., Vissers, S., Cartiaux, M., and Urrestarazu, A. (1998). Characterisation of *Saccharomyces cerevisiae* ARO8 and ARO9 genes encoding aromatic aminotransferases I and II reveals a new aminotransferase subfamily. Mol. Gen. Genet. MGG *257*, 238–248.

Ishikawa, N.K., Fukushi, Y., Yamaji, K., Tahara, S., and Takahashi, K. (2001). Antimicrobial Cuparene-Type Sesquiterpenes, Enokipodins C and D, from a Mycelial Culture of *Flammulina velutipes*. J. Nat. Prod. *64*, 932–934.

Jain, M., Olsen, H.E., Paten, B., and Akeson, M. (2016). The Oxford Nanopore MinION: delivery of nanopore sequencing to the genomics community. Genome Biol. *17*, 239.

James, T.Y. (2015). Why mushrooms have evolved to be so promiscuous: Insights from evolutionary and ecological patterns. Fungal Biol. Rev. *29*, 167–178.

Kamada, T., Sano, H., Nakazawa, T., and Nakahori, K. (2010). Regulation of fruiting body photomorphogenesis in *Coprinopsis cinerea*. Fungal Genet. Biol. *47*, 917–921.

Kanwar, N., Blanco, C., Chen, I.A., and Seelig, B. (2021). PacBio sequencing output increased through uniform and directional fivefold concatenation. Sci. Rep. *11*, 18065.

Karrer, D., and Rühl, M. (2019). A new lipoxygenase from the agaric fungus *Agrocybe aegerita*: Biochemical characterization and kinetic properties. PLOS ONE *14*, e0218625.

Kinugawa, K., Suzuki, A., Takamatsu, Y., Kato, M., and Tanaka, K. (1994). Effects of concentrated carbon dioxide on the fruiting of several cultivated basidiomycetes (II). Mycoscience *35*, 345–352.

Kispal, G., Steiner, H., Court, D.A., Rolinski, B., and Lill, R. (1996). Mitochondrial and cytosolic branched-chain amino acid transaminases from yeast, homologs of the myc oncogene-regulated Eca39 protein. J. Biol. Chem. *271*, 24458–24464.

Kleofas, V., Sommer, L., Fraatz, M.A., Zorn, H., and Rühl, M. (2014). Fruiting Body Production and Aroma Profile Analysis of *Agrocybe aegerita* Cultivated on Different Substrates. Nat. Resour. *05*, 233.

Kleofas, V., Popa, F., Niedenthal, E., Rühl, M., Kost, G., and Zorn, H. (2015). Analysis of the volatilome of *Calocybe gambosa*. Mycol. Prog. *14*, 93.

Knabe, N., Jung, E.-M., Freihorst, D., Hennicke, F., Horton, J.S., and Kothe, E. (2013). A Central Role for Ras1 in Morphogenesis of the Basidiomycete *Schizophyllum commune*. Eukaryot. Cell *12*, 941–952.

Kramer, R., and Abraham, W.-R. (2012). Volatile sesquiterpenes from fungi: what are they good for? Phytochem. Rev. *11*, 15–37.

Krizsán, K., Almási, É., Merényi, Z., Sahu, N., Virágh, M., Kószó, T., Mondo, S., Kiss, B., Bálint, B., Kües, U., et al. (2019). Transcriptomic atlas of mushroom development reveals conserved genes behind complex multicellularity in fungi. Proc. Natl. Acad. Sci. *116*, 7409–7418.

Kües, U. (2000). Life history and developmental processes in the basidiomycete *Coprinus cinereus*. Microbiol. Mol. Biol. Rev. MMBR *64*, 316–353.

Kües, U. (2015). From two to many: Multiple mating types in Basidiomycetes. Fungal Biol. Rev. *29*, 126–166.

Kües, U., and Liu, Y. (2000). Fruiting body production in basidiomycetes. Appl. Microbiol. Biotechnol. *54*, 141–152.

Kües, U., and Navarro-González, M. (2015). How do Agaricomycetes shape their fruiting bodies? 1. Morphological aspects of development. Fungal Biol. Rev. *29*, 63–97.

Kües, U., Khonsuntia, W., Subba, S., and Dörnte, B. (2018). Volatiles in Communication of Agaricomycetes. In Physiology and Genetics: Selected Basic and Applied Aspects, T. Anke, and A. Schüffler, eds. (Cham: Springer International Publishing), pp. 149–212.

Kuratani, M., Tanaka, K., Terashima, K., Muraguchi, H., Nakazawa, T., Nakahori, K., and Kamada, T. (2010). The dst2 gene essential for photomorphogenesis of *Coprinopsis cinerea* encodes a protein with a putative FAD-binding-4 domain. Fungal Genet. Biol. *47*, 152–158.

Kuribayashi, T., Kaise, H., Uno, C., Hara, T., Hayakawa, T., and Joh, T. (2002). Purification and Characterization of Lipoxygenase from *Pleurotus ostreatus*. J. Agric. Food Chem. *50*, 1247–1253.

Lanfermann, I., Krings, U., Schopp, S., and Berger, R.G. (2014). Isotope labelling experiments on the formation pathway of 3-hydroxy-4,5-dimethyl-2(5H)-furanone from l-isoleucine in cultures of *Laetiporus sulphureus*. Flavour Fragr. J. *29*, 233–239.

Lapadatescu, C., Giniès, C., Quéré, J.-L.L., and Bonnarme, P. (2000). Novel Scheme for Biosynthesis of Aryl Metabolites from l-Phenylalanine in the Fungus *Bjerkandera adusta*. Appl. Environ. Microbiol. *66*, 1517–1522.

Larsen, P.E., Trivedi, G., Sreedasyam, A., Lu, V., Podila, G.K., and Collart, F.R. (2010). Using Deep RNA Sequencing for the Structural Annotation of the *Laccaria bicolor* Mycorrhizal Transcriptome. PLOS ONE *5*, e9780.

Lee, N.-Y., Choi, D.-H., Kim, M.-G., Jeong, M.-J., Kwon, H.-J., Kim, D.-H., Kim, Y.-G., Luccio, E., Arioka, M., Yoon, H.-J., et al. (2020). Biosynthesis of (R)-(-)-1-Octen-3-ol in Recombinant *Saccharomyces cerevisiae* with Lipoxygenase-1 and Hydroperoxide Lyase Genes from *Tricholoma matsutake*. J. Microbiol. Biotechnol. *30*, 296–305.

León-Ramírez, C.G., Cabrera-Ponce, J.L., Martínez-Soto, D., Sánchez-Arreguin, A., Aréchiga-Carvajal, E.T., and Ruiz-Herrera, J. (2017). Transcriptomic analysis of basidiocarp development in *Ustilago maydis* (DC) Cda. Fungal Genet. Biol. *101*, 34–45.

Li, D.-C., Lui, Z.-W., and Lu, J. (2001). Purification and characterization of lipoxygenase from the thermophilic fungus *Thermomyces lanuginosus*. Mycol. Res. *105*, 190–194.

Liu, Y., Srivilai, P., Loos, S., Aebi, M., and Kües, U. (2006). An Essential Gene for Fruiting Body Initiation in the Basidiomycete *Coprinopsis cinerea* Is Homologous to Bacterial Cyclopropane Fatty Acid Synthase Genes. Genetics *172*, 873–884.

López-Gallego, F., Wawrzyn, G., and Schmidt-Dannert, C. (2010). Selectivity of Fungal Sesquiterpene Synthases: Role of the Active Site's H-1α Loop in Catalysis. Appl. Environ. Microbiol. *76*, 7723–7733.

Lopez-Gallego, F., Agger, S.A., Pella, D.A., Distefano, M.D., and Schmidt-Dannert, C. (2010). Sesquiterpene synthases Cop4 and Cop6 from *Coprinus cinereus*: Catalytic promiscuity and cyclization of farnesyl pyrophosphate geometrical isomers. Chembiochem Eur. J. Chem. Biol. *11*, 1093–1106.

Lücking, R., Aime, M.C., Robbertse, B., Miller, A.N., Ariyawansa, H.A., Aoki, T., Cardinali, G., Crous, P.W., Druzhinina, I.S., Geiser, D.M., et al. (2020). Unambiguous identification of fungi: where do we stand and how accurate and precise is fungal DNA barcoding? IMA Fungus *11*, 14.

Lücking, R., Aime, M.C., Robbertse, B., Miller, A.N., Aoki, T., Ariyawansa, H.A., Cardinali, G., Crous, P.W., Druzhinina, I.S., Geiser, D.M., et al. (2021). Fungal taxonomy and sequence-based nomenclature. Nat. Microbiol. *6*, 540–548.

Malheiro, R., Guedes de Pinho, P., Soares, S., César da Silva Ferreira, A., and Baptista, P. (2013). Volatile biomarkers for wild mushrooms species discrimination. Food Res. Int. *54*, 186–194.

Martin, J.A., and Wang, Z. (2011). Next-generation transcriptome assembly. Nat. Rev. Genet. *12*, 671–682.

Matsui, K., SASAHARA, S., AKAKABE, Y., and KAJIWARA, T. (2003). Linoleic Acid 10-Hydroperoxide as an Intermediate during Formation of 1-Octen-3-ol from Linoleic Acid in *Lentinus decadetes*. Biosci. Biotechnol. Biochem. *67*, 2280–2282.

de Mattos-Shipley, K.M.J., Ford, K.L., Alberti, F., Banks, A.M., Bailey, A.M., and Foster, G.D. (2016). The good, the bad and the tasty: The many roles of mushrooms. Stud. Mycol. *85*, 125–157.

Mau, J.-L., Chyau, C.-C., Li, J.-Y., and Tseng, Y.-H. (1997). Flavor Compounds in Straw Mushrooms *Volvariella volvacea* Harvested at Different Stages of Maturity. J. Agric. Food Chem. *45*, 4726–4729.

McCombie, W.R., McPherson, J.D., and Mardis, E.R. (2019). Next-Generation Sequencing Technologies. Cold Spring Harb. Perspect. Med. *9*, a036798.

Meinhardt, F., and Leslie, J.F. (1982). Mating types of *Agrocybe aegerita*. Curr. Genet. *5*, 65–68.

Miller, D.J., and Allemann, R.K. (2011). Sesquiterpene synthases: Passive catalysts or active players? Nat. Prod. Rep. *29*, 60–71.

Miziorko, H.M. (2011). ENZYMES OF THE MEVALONATE PATHWAY OF ISOPRENOID BIOSYNTHESIS. Arch. Biochem. Biophys. *505*, 131–143.

Moll, P., Ante, M., Seitz, A., and Reda, T. (2014). QuantSeq 3′ mRNA sequencing for RNA quantification. Nat. Methods *11*, i–iii.

Morita, K., and Kobayashi, S. (1967). Isolation, structure, and synthesis of lenthionine and its analogs. Chem. Pharm. Bull. (Tokyo) *15*, 988–993.

Müller, A., Faubert, P., Hagen, M., Castell, W., Polle, A., Schnitzler, J.-P., and Rosenkranz, M. (2013). Volatile profiles of fungi – Chemotyping of species and ecological functions. Fungal Genet. Biol. FG B *54*.

Muraguchi, H., and Kamada, T. (1998). The ich1 gene of the mushroom *Coprinus cinereus* is essential for pileus formation in fruiting. Development *125*, 3133–3141.

Muraguchi, H., Fujita, T., Kishibe, Y., Konno, K., Ueda, N., Nakahori, K., Yanagi, S.O., and Kamada, T. (2008). The exp1 gene essential for pileus expansion and autolysis of the inky cap mushroom *Coprinopsis cinerea* (*Coprinus cinereus*) encodes an HMG protein. Fungal Genet. Biol. *45*, 890–896.

Muraguchi, H., Umezawa, K., Niikura, M., Yoshida, M., Kozaki, T., Ishii, K., Sakai, K., Shimizu, M., Nakahori, K., Sakamoto, Y., et al. (2015). Strand-Specific RNA-Seq Analyses of Fruiting Body Development in *Coprinopsis cinerea*. PLOS ONE *10*, e0141586.

Murata, Y., Fujii, M., Zolan, M.E., and Kamada, T. (1998). Molecular analysis of pcc1, a gene that leads to A-regulated sexual morphogenesis in *Coprinus cinereus*. Genetics *149*, 1753–1761.

Naranjo-Ortiz, M.A., and Gabaldón, T. (2019). Fungal evolution: diversity, taxonomy and phylogeny of the Fungi. Biol. Rev. *94*, 2101–2137.

Nemčovič, M., Jakubíková, L., Víden, I., and Farkaš, V. (2008). Induction of conidiation by endogenous volatile compounds in *Trichoderma* spp. FEMS Microbiol. Lett. *284*, 231–236.

Oberwinkler, F. (1982). The Significance of the Morphology of the Basidium in the Phylogeny of Basidiomycetes. In Basidium and Basidiocarp: Evolution, Cytology, Function, and Development, K. Wells, and E.K. Wells, eds. (New York, NY: Springer), pp. 9–35.

Ohm, R.A., de Jong, J.F., de Bekker, C., Wösten, H.A.B., and Lugones, L.G. (2011). Transcription factor genes of *Schizophyllum commune* involved in regulation of mushroom formation. Mol. Microbiol. *81*, 1433–1445.

Ohm, R.A., Aerts, D., Wösten, H.A.B., and Lugones, L.G. (2013). The blue light receptor complex WC-1/2 of *Schizophyllum commune* is involved in mushroom formation and protection against phototoxicity. Environ. Microbiol. *15*, 943–955.

Oliw, E.H. (2002). Plant and fungal lipoxygenases. Prostaglandins Other Lipid Mediat. *68–69*, 313–323.

Oliw, E.H. (2018). Polyunsaturated C-18 fatty acids derivatized with Gly and Ile as an additional tool for studies of the catalytic evolution of fungal 8-and 9-dioxygenases. Biochim. Biophys. Acta-Mol. Cell Biol. Lipids *1863*, 1378–1387.

Oliw, E.H. (2020). Linoleate diol synthase related enzymes of the human pathogens *Histoplasma capsulatum* and *Blastomyces dermatitidis*. Arch. Biochem. Biophys. *696*, 108669.

Omarini, A.B., Plagemann, I., Schimanski, S., Krings, U., and Berger, R.G. (2014). Crosses between monokaryons of *Pleurotus sapidus* or P*leurotus florida* show an improved biotransformation of (+)-valencene to (+)-nootkatone. Bioresour. Technol. *171*, 113–119.

Orban, A., Fraatz, M.A., and Rühl, M. (2019). Aroma Profile Analyses of Filamentous Fungi Cultivated on Solid Substrates. In Solid State Fermentation: Research and Industrial Applications, S. Steudler, A. Werner, and J.J. Cheng, eds. (Cham: Springer International Publishing), pp. 85–107.

Orban, A., Hennicke, F., and Rühl, M. (2020). Volatilomes of *Cyclocybe aegerita* during different stages of monokaryotic and dikaryotic fruiting. Biol. Chem. *401*, 995–1004.

Orban, A., Weber, A., Herzog, R., Hennicke, F., and Rühl, M. (2021). Transcriptome of different fruiting stages in the cultivated mushroom *Cyclocybe aegerita* suggests a complex regulation of fruiting and reveals enzymes putatively involved in fungal oxylipin biosynthesis. BMC Genomics *22*, 324.

Ouzouni, P.K., Koller, W.-D., Badeka, A.V., and Riganakos, K.A. (2009). Volatile compounds from the fruiting bodies of three Hygrophorus mushroom species from Northern Greece. Int. J. Food Sci. Technol. *44*, 854–859.

Pelkmans, J.F., Patil, M.B., Gehrmann, T., Reinders, M.J.T., Wösten, H.A.B., and Lugones, L.G. (2017). Transcription factors of *Schizophyllum commune* involved in mushroom formation and modulation of vegetative growth. Sci. Rep. *7*, 310.

Pérez-Gilabert, M., Sánchez-Felipe, I., and García-Carmona, F. (2005). Purification and Partial Characterization of Lipoxygenase from Desert Truffle (*Terfezia claveryi* Chatin) Ascocarps. J. Agric. Food Chem. *53*, 3666–3671.

Perraud, X., and Kermasha, S. (2000). Characterization of lipoxygenase extracts from *Penicillum* sp. J. Am. Oil Chem. Soc. *77*, 335–342.

Pierce, A.M., Pierce, H.D., Borden, J.H., and Oehlschlager, A.C. (1991). Fungal volatiles: Semiochemicals for stored-product beetles (Coleoptera: Cucujidae). J. Chem. Ecol. *17*, 581–597.

Plagemann, I., Zelena, K., Arendt, P., Ringel, P.D., Krings, U., and Berger, R.G. (2013). LOXPsa1, the first recombinant lipoxygenase from a basidiomycete fungus. J. Mol. Catal. B Enzym. *87*, 99–104.

Plaza, D.F., Lin, C.-W., van der Velden, N.S.J., Aebi, M., and Künzler, M. (2014). Comparative transcriptomics of the model mushroom *Coprinopsis cinerea* reveals tissue-specific armories and a conserved circuitry for sexual development. BMC Genomics *15*, 492.

Pudil, F., Uvira, R., and Janda, V. (2014). VOLATILE COMPOUNDS IN STINKHORN (*PHALLUS IMPUDICUS* L. EX PERS.) AT DIFFERENT STAGES OF GROWTH. Eur. Sci. J. ESJ *10*.

Quin, M.B., Flynn, C.M., Wawrzyn, G.T., Choudhary, S., and Schmidt-Dannert, C. (2013). Mushroom hunting using bioinformatics: Application of a predictive framework facilitates the selective identification of sesquiterpene synthases in Basidiomycota. Chembiochem Eur. J. Chem. Biol. *14*, 2480–2491.

Quin, M.B., Flynn, C.M., and Schmidt-Dannert, C. (2014). Traversing the fungal terpenome. Nat. Prod. Rep. *31*, 1449–1473.

Rang, F.J., Kloosterman, W.P., and de Ridder, J. (2018). From squiggle to basepair: computational approaches for improving nanopore sequencing read accuracy. Genome Biol. *19*, 90.

Rapior, S., Breheret, S., Talou, T., and Bessière, J.-M. (1997). Volatile Flavor Constituents of Fresh *Marasmius alliaceus* (Garlic Marasmius). J. Agric. Food Chem. *45*, 820–825.

Rapior, S., Breheret, S., Talou, T., Pelissier, Y., Milhau, M., and Bessiere, J.M. (1998). Volatile components of fresh *Agrocybe aegerita* and *Tricholoma sulfureum*. Cryptogam. Mycol. *19*, 15–23.

Rapior, S., Breheret, S., Talou, T., Pélissier, Y., and Bessière, J.-M. (2002). The anise-like odor of *Clitocybe odora*, *Lentinellus cochleatus* and *Agaricus essettei*. Mycologia *94*, 373–376.

Raudaskoski, M. (2015). Mating-type genes and hyphal fusions in filamentous basidiomycetes. Fungal Biol. Rev. *29*, 179–193.

Rösecke, J., and König, W.A. (2000). Odorous compounds from the fungus *Gloeophyllum odoratum*. Flavour Fragr. J. *15*, 315–319.

Saiki, R.K., Scharf, S., Faloona, F., Mullis, K.B., Horn, G.T., Erlich, H.A., and Arnheim, N. (1985). Enzymatic amplification of beta-globin genomic sequences and restriction site analysis for diagnosis of sickle cell anemia. Science *230*, 1350–1354.

Sakamoto, Y. (2018). Influences of environmental factors on fruiting body induction, development and maturation in mushroom-forming fungi. Fungal Biol. Rev. *32*, 236–248.

Sánchez-García, M., Ryberg, M., Khan, F.K., Varga, T., Nagy, L.G., and Hibbett, D.S. (2020). Fruiting body form, not nutritional mode, is the major driver of diversification in mushroom-forming fungi. Proc. Natl. Acad. Sci. *117*, 32528–32534.

Santos, C., and Labarère, J. (1999). Aa-Pri2, a single-copy gene from *Agrocybe aegerita*, specifically expressed during fruiting initiation, encodes a hydrophobin with a leucine-zipper domain. Curr. Genet. *35*, 564–570.

Scher, J.M., Speakman, J.-B., Zapp, J., and Becker, H. (2004). Bioactivity guided isolation of antifungal compounds from the liverwort *Bazzania trilobata* (L.) S.F. Gray. Phytochemistry *65*, 2583–2588.

Schmidt-Dannert, C. (2015). Biosynthesis of Terpenoid Natural Products in Fungi. In Biotechnology of Isoprenoids, J. Schrader, and J. Bohlmann, eds. (Cham: Springer International Publishing), pp. 19–61.

Schmit, J.P., and Mueller, G.M. (2007). An estimate of the lower limit of global fungal diversity. Biodivers. Conserv. *16*, 99–111.

Sirand-Pugnet, P., and Labarère, J. (2002). Molecular characterization of the Pri3 gene encoding a cysteine-rich protein, specifically expressed during fruiting initiation within the *Agrocybe aegerita* complex. Curr. Genet. *41*, 31–42.

Sirand-Pugnet, P., Santos, C., and Labarère, J. (2003). The Aa-Pri4 gene, specifically expressed during fruiting initiation in the *Agrocybe aegerita* complex, contains an unusual CT-rich leader intron within the 5′ uncoding region. Curr. Genet. *44*, 124–131.

Sleeman, D.P., Jones, P., and Cronin, J.N. (1997). Investigations of an association between the stinkhorn fungus and badger setts. J. Nat. Hist. *31*, 983–992.

Solís, C., Becerra, J., Flores, C., Robledo, J., and Silva, M. (2004). ANTIBACTERIAL AND ANTIFUNGAL TERPENES FROM *Pilgerodendron uviferum* (D. DON) FLORIN. J. Chil. Chem. Soc. *49*, 157–161.

Song, H.-Y., Kim, D.-H., and Kim, J.-M. (2018). Comparative transcriptome analysis of dikaryotic mycelia and mature fruiting bodies in the edible mushroom *Lentinula edodes*. Sci. Rep. *8*, 1–15.

Stahl, U., and Esser, K. (1976). Genetics of fruit body production in higher basidiomycetes. Mol. Gen. Genet. MGG *148*, 183–197.

Steenkamp, E.T., Wingfield, M.J., McTaggart, A.R., and Wingfield, B.D. (2018). Fungal species and their boundaries matter – Definitions, mechanisms and practical implications. Fungal Biol. Rev. *32*, 104–116.

Sterner, O., Bergman, R., Kihlberg, J., and Wickberg, B. (1985). The Sesquiterpenes of *Lactarius vellereus* and Their Role in a Proposed Chemical Defense System. J. Nat. Prod. *48*, 279–288.

Stolterfoht, H., Rinnofner, C., Winkler, M., and Pichler, H. (2019). Recombinant Lipoxygenases and Hydroperoxide Lyases for the Synthesis of Green Leaf Volatiles. J. Agric. Food Chem. *67*, 13367–13392.

Su, C., and Oliw, E.H. (1998). Manganese Lipoxygenase: PURIFICATION AND CHARACTERIZATION*. J. Biol. Chem. *273*, 13072–13079.

Sugio, A., Østergaard, L.H., Matsui, K., and Takagi, S. (2018). Characterization of two fungal lipoxygenases expressed in *Aspergillus oryzae*. J. Biosci. Bioeng. *126*, 436–444.

Tasaki, Y., Kobayashi, D., Sato, R., Hayashi, S., and Joh, T. (2019). Variations in 1-octen-3-ol and lipoxygenase gene expression in the oyster mushroom *Pleurotus ostreatus* according to fruiting body development, tissue specificity, maturity, and postharvest storage. Mycoscience *60*, 170–176.

Téllez-Téllez, M., and Diaz-Godinez, G. (2019). Omic Tools to Study Enzyme Production from Fungi in the *Pleurotus* genus. BioResources *14*, 2420–2457.

Terashima, K., Yuki, K., Muraguchi, H., Akiyama, M., and Kamada, T. (2005). The dst1 Gene Involved in Mushroom Photomorphogenesis of *Coprinus cinereus* Encodes a Putative Photoreceptor for Blue Light. Genetics *171*, 101–108.

Thakeow, P. (2008). Development of a Basic Biosensor System for Wood Degradation using Volatile Organic Compounds. PhD thesis, University of Göttingen, Göttingen, Germany. https://ediss.uni-goettingen.de/handle/11858/00-1735-0000-0006-B11D-2

Thakeow, P., Angeli, S., Weißbecker, B., and Schütz, S. (2008). Antennal and Behavioral Responses of Cis boleti to Fungal Odor of *Trametes gibbosa*. Chem. Senses *33*, 379–387.

Toju, H., Tanabe, A.S., Yamamoto, S., and Sato, H. (2012). High-Coverage ITS Primers for the DNA-Based Identification of Ascomycetes and Basidiomycetes in Environmental Samples. PLoS ONE *7*, e40863.

Tong, X., Zhang, H., Wang, F., Xue, Z., Cao, J., Peng, C., and Guo, J. (2020). Comparative transcriptome analysis revealed genes involved in the fruiting body development of *Ophiocordyceps sinensis*. PeerJ *8*, e8379.

Trapp, T., Kirchner, T., Birk, F., Fraatz, M.A., and Zorn, H. (2019). Biosynthesis of Stereoisomers of Dill Ether and Wine Lactone by *Pleurotus sapidus*. J. Agric. Food Chem. *67*, 13400–13411.

Tuno, N. (1998). Spore dispersal of *Dictyophora* fungi (Phallaceae) by flies. Ecol. Res. *13*, 7–15.

Turner, E.M. (1977). Development of excised sporocarps of *Agaricus bisporus* and its control by CO2. Trans. Br. Mycol. Soc. *69*, 183–186.

Uno, I., and Ishikawa, T. (1971). Chemical and genetical control of induction of monokaryotic fruiting bodies in *Coprinus macrorhizus*. Mol. Gen. Genet. MGG *113*, 228–239.

Urrestarazu, A., Vissers, S., Iraqui, I., and Grenson, M. (1998). Phenylalanine- and tyrosine-auxotrophic mutants of *Saccharomyces cerevisiae* impaired in transamination. Mol. Gen. Genet. MGG *257*, 230–237.

Vasina, D.V., Moiseenko, K.V., Fedorova, T.V., and Tyazhelova, T.V. (2017). Lignin-degrading peroxidases in white-rot fungus *Trametes hirsuta* 072. Absolute expression quantification of full multigene family. PLOS ONE *12*, e0173813.

Venkateshwarlu, G., Chandravadana, M.V., and Tewari, R.P. (1999). Volatile flavour components of some edible mushrooms (Basidiomycetes). Flavour Fragr. J. *14*, 191–194.

Visagie, C.M., Houbraken, J., Frisvad, J.C., Hong, S.-B., Klaassen, C.H.W., Perrone, G., Seifert, K.A., Varga, J., Yaguchi, T., and Samson, R.A. (2014). Identification and nomenclature of the genus *Penicillium*. Stud. Mycol. *78*, 343–371.

Vuralhan, Z., Morais, M.A., Tai, S.-L., Piper, M.D.W., and Pronk, J.T. (2003). Identification and Characterization of Phenylpyruvate Decarboxylase Genes in *Saccharomyces cerevisiae*. Appl. Environ. Microbiol. *69*, 4534–4541.

Vuralhan, Z., Luttik, M.A.H., Tai, S.L., Boer, V.M., Morais, M.A., Schipper, D., Almering, M.J.H., Kötter, P., Dickinson, J.R., Daran, J.-M., et al. (2005). Physiological characterization of the ARO10-dependent, broad-substrate-specificity 2-oxo acid decarboxylase activity of *Saccharomyces cerevisiae*. Appl. Environ. Microbiol. *71*, 3276–3284.

Wang, Y., Zeng, X., and Liu, W. (2018). De novo transcriptomic analysis during *Lentinula edodes* fruiting body growth. Gene *641*, 326–334.

Wanner, P., and Tressl, R. (1998). Purification and characterization of two enone reductases from *Saccharomyces cerevisiae*. Eur. J. Biochem. *255*, 271–278.

Wawrzyn, G.T., Quin, M.B., Choudhary, S., López-Gallego, F., and Schmidt-Dannert, C. (2012). Draft genome of *Omphalotus olearius* provides a predictive framework for sesquiterpenoid natural product biosynthesis in Basidiomycota. Chem. Biol. *19*, 772–783.

Wennman, A., and Oliw, E.H. (2013). Secretion of two novel enzymes, manganese 9S-lipoxygenase and epoxy alcohol synthase, by the rice pathogen *Magnaporthe salvinii*. J. Lipid Res. *54*, 762–775.

Wennman, A., Magnuson, A., Hamberg, M., and Oliw, E.H. (2015). Manganese lipoxygenase of *F. oxysporum* and the structural basis for biosynthesis of distinct 11-hydroperoxy stereoisomers. J. Lipid Res. *56*, 1606–1615.

Wessels, J.G.H. (1993). Fruiting in the Higher Fungi. In Advances in Microbial Physiology, A.H. Rose, ed. (Academic Press), pp. 147–202.

White, T.J., Bruns, T., Lee, S., and Taylor, J. (1990). AMPLIFICATION AND DIRECT SEQUENCING OF FUNGAL RIBOSOMAL RNA GENES FOR PHYLOGENETICS. In PCR Protocols, (Elsevier), pp. 315–322.

Wood, W.F., Watson, R.L., and Largent, D.L. (1990). The Odor of *Agaricus Augustus*. Mycologia *82*, 276–278.

Wu, B., Hussain, M., Zhang, W., Stadler, M., Liu, X., and Xiang, M. (2019). Current insights into fungal species diversity and perspective on naming the environmental DNA sequences of fungi. Mycology *10*, 127–140.

Wu, S., Zorn, H., Krings, U., and Berger, R.G. (2005). Characteristic Volatiles from Young and Aged Fruiting Bodies of Wild *Polyporus sulfureus* (Bull.:Fr.) Fr. J. Agric. Food Chem. *53*, 4524–4528.

Wurzenberger, M., and Grosch, W. (1984a). Stereochemistry of the cleavage of the 10-hydroperoxide isomer of linoleic acid to 1-octen-3-ol by a hydroperoxide lyase from mushrooms (*Psalliota bispora)*. Biochim. Biophys. Acta BBA - Lipids Lipid Metab. *795*, 163–165.

Wurzenberger, M., and Grosch, W. (1984b). The formation of 1-octen-3-ol from the 10-hydroperoxide isomer of linoleic acid by a hydroperoxide lyase in mushrooms (*Psalliota bispora*). Biochim. Biophys. Acta BBA - Lipids Lipid Metab. *794*, 25–30.

Yasumoto, K., Iwami, K., and Mitsuda, H. (1971). A New Sulfur-containing Peptide from *Lentinus edodes* Acting as a Precursor for Lenthionine. Agric. Biol. Chem. *35*, 2059–2069.

Zhang, C., Chen, X., Orban, A., Shukal, S., Birk, F., Too, H.-P., and Rühl, M. (2020). *Agrocybe aegerita* Serves As a Gateway for Identifying Sesquiterpene Biosynthetic Enzymes in Higher Fungi. ACS Chem. Biol. *15*, 1268–1277.

Zhang, J., Ren, A., Chen, H., Zhao, M., Shi, L., Chen, M., Wang, H., and Feng, Z. (2015). Transcriptome Analysis and Its Application in Identifying Genes Associated with Fruiting Body Development in Basidiomycete *Hypsizygus marmoreus*. PLOS ONE *10*, e0123025.

Zhang, Y., Fraatz, M.A., Birk, F., Rigling, M., Hammer, A., and Zorn, H. (2018). Enantiomeric ratios of 2-methylbutanoic acid and its methyl ester: Elucidation of novel biogenetic pathways towards (R)-methyl 2-methylbutanoate in a beverage fermented with shiitake. Food Chem. *266*, 475–482.

Aroma Profile Analyses of Filamentous Fungi Cultivated on Solid Substrates.

Orban, A., Fraatz, M.A., and Rühl, M.

Adv Biochem Eng Biotechnol. 2019, *169,* 85–107.

DOI: 10.1007/10_2019_87

Adv Biochem Eng Biotechnol
DOI: 10.1007/10_2019_87

Aroma Profile Analyses of Filamentous Fungi Cultivated on Solid Substrates

Axel Orban, Marco A. Fraatz, and Martin Rühl

Contents

Abstract Filamentous fungi have been used since centuries in the production of food by means of solid substrate fermentation (SSF). The most applied SSF involving fungi is the cultivation of mushrooms, e.g., on tree stumps or sawdust, for human consumption. However, filamentous fungi are also key players during manufacturing of several processed foods, like mold cheese, tempeh, soy sauce, and sake. In addition to their nutritive values, these foods are widely consumed due to their pleasant flavors. Based on the potentials of filamentous fungi to grow on solid substrates and to produce valuable aroma compounds, in recent decades, several studies concentrated on the production of aroma compounds with SSF, turning

A. Orban and M. A. Fraatz
Justus Liebig University Giessen, Institute of Food Chemistry and Food Biotechnology, Giessen, Germany

M. Rühl (✉)
Justus Liebig University Giessen, Institute of Food Chemistry and Food Biotechnology, Giessen, Germany

Fraunhofer Institute for Molecular Biology and Applied Ecology IME, Project Group "Bioresources", Giessen, Germany
e-mail: martin.ruehl@uni-giessen.de

cheap agricultural wastes into valuable flavors. In this review, we focus on the presentation of common analytical methods for volatile substances and highlight various applications of SSF of filamentous fungi dealing with the production of aroma compounds.

Graphical Abstract

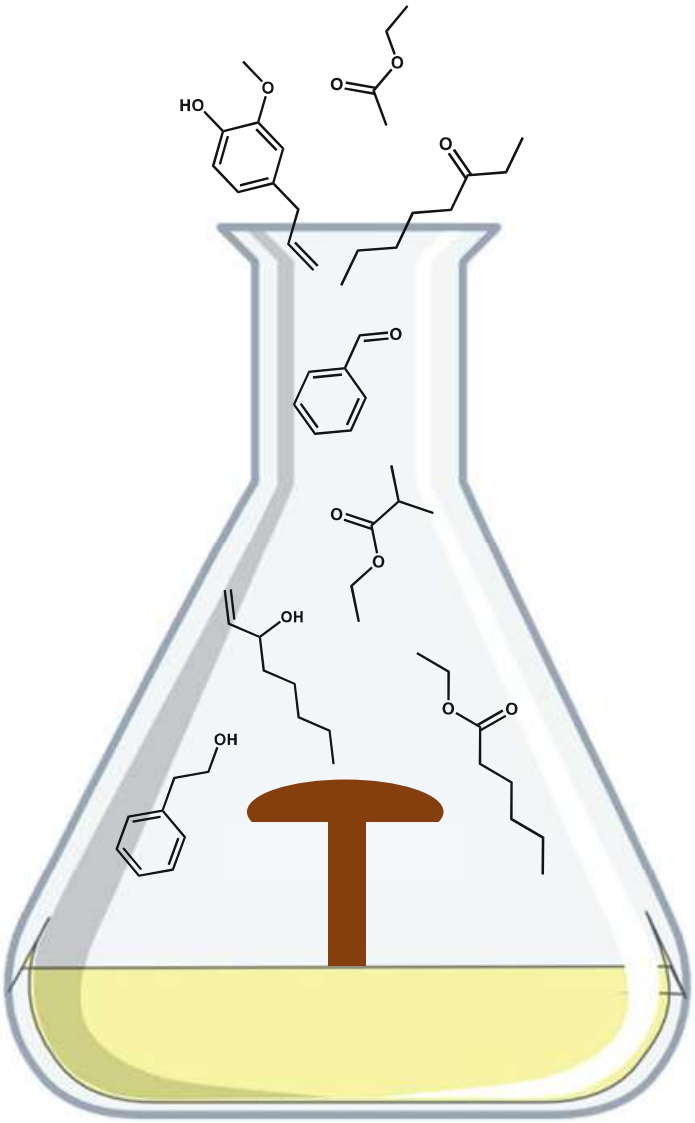

Keywords Ascomycetes, Basidiomycetes, Fermented food, SSF, Volatile organic compounds

Abbreviations

6-PP	6-Pentyl-α-pyrone
AAO	Aryl alcohol oxidase(s)
ADA	Aroma dilution analysis
AEDA	Aroma extract dilution analysis
CAR	Carboxen
DHS	Dynamic headspace
DM	Dry matter
DVB	Divinylbenzene
FD	Flavor dilution factor
FID	Flame ionization detector
GC	Gas chromatography
HS	Headspace
LLE	Liquid-liquid extraction
MS	Mass spectrometer
O	Olfactometry
OAV	Odor activity value
ODP	Olfactory detection port
PA	Polyacrylate
PDMS	Polydimethylsiloxane
PEG	Polyethylene glycol
SAFE	Solvent-assisted flavor evaporation
SBSE	Stir bar sorptive extraction
SmF	Submerged fermentation
SPME	Solid-phase microextraction
SSF	Solid substrate fermentation
TD	Thermal desorption
VOC	Volatile organic compound(s)

1 Aroma Profile Analysis

The analysis of aroma active compounds in food started in the 1960s with the possibility to separate complex aroma mixtures by means of capillary gas chromatography (GC) (reviewed in [1]). With this analytical method, new possibilities arose to determine the volatile composition of a sample. Nevertheless, the impact of each volatile organic compound (VOC) on the human nose still remained unknown until GC-olfactometry (GC-O) entered the aroma research. GC-O enables the correlation between a VOC and its perception using the human nose as a detector [1–3]. In most cases, the outlet of the GC capillary column is installed into a column flow splitter. The column flow splitter possesses two outlets directing the gas flow into a destructive detector (e.g., flame ionization detector

Fig. 1 GC-MS-O equipped with an autosampler and an ODP (highlighted)

(FID) or mass spectrometer (MS)) and into a nondestructive olfactory detection port (ODP) (Fig. 1). With this equipment, it is possible to directly assign an odor impression to an MS spectrum or FID peak, respectively [3, 4].

1.1 Methods for Volatile Organic Compound Extraction

Prior to the GC analysis, VOC have to be extracted from the analyte's matrix. Among others, this can be food, a plant, or a microbial culture, and the method of extraction depends on the matrix as well as on the VOC to be analyzed.

1.1.1 Solvent Extraction

Several extraction methods for aroma analysis exist, each having different pros and cons. This makes the decision for an optimal analytical method difficult. Continuous extraction of volatile organic compounds from a solid matrix using a Soxhlet extractor followed by a concentration of the extract is a basic method for

gaining an aroma extract. In 1964, Likens and Nickerson improved this method by inventing an apparatus for simultaneous solvent extraction and distillation, reducing the thermal load on the sample [5]. Nevertheless, elevated temperatures during distillation and extraction may lead to artefact formation. Thermal stress during extraction can be overcome by using a liquid-liquid extraction (LLE). Generally, the solid matrix is dispersed in an aqueous phase and extracted exhaustively using an organic solvent. For an efficient extraction and the subsequent analysis, different properties of the solvent including polarity, density, solubility, and potential reactivity regarding the analytes have to be taken into account [5]. The disadvantage of LLE is the often occurring concurrent extraction of nonvolatile compounds resulting in difficulties during GC analysis. This disadvantage as well as thermal stress can be reduced to a minimum by applying the solvent-assisted flavor evaporation (SAFE) method. The core part of this procedure is the SAFE distillation unit [6], which is evacuated by a high vacuum pump. The distillation starts by dropping the sample extract into the evaporation flask. The immediately formed vapor is transported into the distillation head, where nonvolatile compounds are trapped. Volatile compounds condense in a sample collection flask, which is cooled in a Dewar using liquid nitrogen [6]. Nonetheless, the demand for environment-friendly as well as more easy and fast extraction methods led to the development of solvent-free procedures.

1.1.2 Dynamic Headspace

One of the first dynamic headspace (DHS) systems was developed in the 1970s to establish a routine procedure for volatile extraction and analysis by means of GC [7]. DHS involves passing a defined flow of (inert) gas through a container holding the sample. The VOC inside the container are carried by the steady gas flow into a sorbent, a cryogenic container, or a solvent, where they are trapped [8]. When the gas flow is led through a liquid sample, the method is also referred to as “purge and trap” [9]. DHS can be conducted in a circular system by using a closed-looped stripping apparatus, where the extraction gas flows in a closed circuit [10, 11]. The sample might be heated, stirred, or supplemented with salts to increase the volatility of the analytes [9, 12]. With DHS, exhaustive extraction of the sample is possible, since the analytes are permanently removed from the headspace (HS), and therefore no equilibrium between the matrix and the gas phase is established [13]. In addition to the necessity to elicit the right gas flowrate, the extraction time and temperature as well as the type of sorbent in the trap are crucial parameters. Various trapping materials are commercially available, including activated charcoal, poly(2,6-diphenyl-*p*-phenylene oxide) (Tenax®), silica-based materials (Chromosorb®), carbon molecular sieves (Carboxen®), and graphitized carbon (Carbotrap®). Traps containing different types of sorbents are used frequently in order to achieve the extraction of a wider range of substances [14]. Depending on the sorbent applied, desorption of the VOC can be performed with a solvent or thermally in the GC [15]. For thermal desorption (TD) applications, Tenax® is often used due

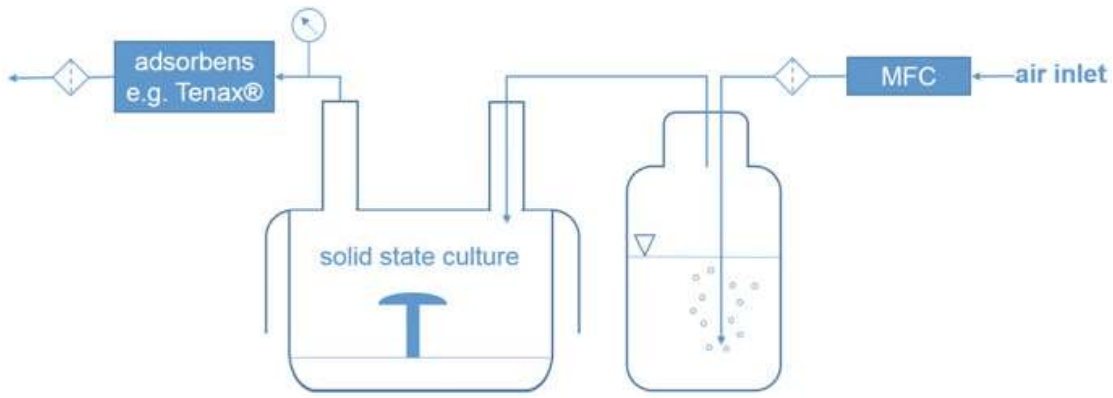

Fig. 2 Scheme of a laboratory installation for DHS during SSF of a fungus. *MFC* mass flow controller

to its high thermostability, its low water adsorption capacity, and its low bleed characteristic [8, 15, 16]. Nonetheless, Tenax® has some disadvantages: e.g., it has only a small surface area, resulting in a low adsorption capacity, and it is limited to the extraction of more nonpolar analytes because of its low affinity for polar compounds [17].

Generally, DHS is an important extraction method for volatile compounds since it reduces or even eliminates the need of solvents. It offers the possibility of multiple trapping approaches as well as the usage of various sorbent materials [18]. During solid substrate fermentation (SSF), DHS is applied in our laboratory to extract VOC produced during the cultivation of filamentous fungi (Fig. 2).

1.1.3 Microextraction Methods SPME and SBSE

Further options for the extraction of volatile compounds comprise solid-phase microextraction (SPME) and stir bar sorptive extraction (SBSE) [19]. SPME was presented to the scientific world in the early 1990s as a new possibility to perform sample extractions in a more environment-friendly way [20]. SPME is a non-exhaustive extraction technique in which a fiber coated with sorbent materials is exposed to the sample [20, 21]. Commercial SPME fibers often consist of fused-silica as a carrier modified with different absorbent or adsorbent materials, including polydimethylsiloxane (PDMS), polyethylene glycol (PEG), polyacrylate (PA), divinylbenzene (DVB), carboxen (CAR), as well as combinations thereof [22–24]. This diversity of available coatings makes SPME the method of choice in a broad range of applications, such as in the food [25], aroma [26], medical [27], environmental [28], or bioanalytical [29] sector. Extraction can be performed in the HS by incubating the fiber in the vapor phase above the sample (Fig. 3) or by direct immersion of the fiber into the matrix [30].

The benefits of SPME compared to LLE are the absence of solvents, the higher sensitivity, the demand for less sample material, and a faster and convenient handling [19, 20]. Furthermore, the entire extraction process at a specific

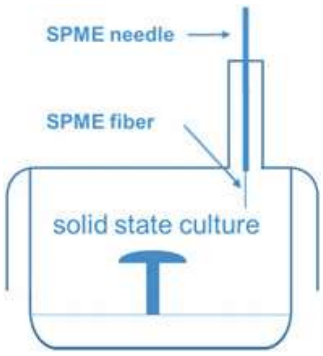

Fig. 3 SPME applied during SSF of a fungus

temperature for a given period can be conducted automatically by using GC systems equipped with multipurpose autosamplers (Fig. 4). Nonetheless, SPME suffers from drawbacks regarding the stability of the fiber and coating, the capacity for analytes, and the durability in organic solvents [23, 31]. It is worth mentioning that new materials for SPME fibers and coatings are on the rise, reducing the aforesaid problems [22, 32].

SBSE was developed around 20 years ago as a new microextraction method [33]. For SBSE, a magnetic stir bar, covered with a layer of sorbent material, usually PDMS [34], is used. In contrast to SPME, the coating is 50–250 times thicker, resulting in a higher capacity and sensitivity [35]. Extraction can be performed in the HS above a sample or, more common, in an aqueous sample by stirring the sample under controlled conditions [36]. The extraction process is followed by the desorption of the analytes which can be accomplished thermally or by rinsing the stir bar with a solvent [37]. In most SBSE GC applications, the TD is preferred due to easier handling. TD is usually conducted at a temperature range of 150–300°C. Compared to SPME, desorption time can be quite long, up to 15 min, due to the thicker coating of the stir bar. In this case, compounds might desorb too slowly, leading to insufficient chromatographic separation of the analytes. To ensure an adequate analysis, cryofocusing of the substances in the GC inlet is necessary [37]. Cryotrapping enables quantitative transfer of the analytes (with considerable increase in sensitivity) and minimizes chromatographic peak width [38]. Besides the need for special equipment, during the early days of SBSE, one drawback was that only PDMS as a coating material was commercially available. This made the analysis less suitable for more polar compounds. In recent years, new PEG- and PA-containing sorbents for SBSE were developed, thus making this method attractive for a broader range of applications [39]. Besides SPME and SBSE, further microextraction techniques like single-drop microextraction and microextraction by packed sorbent offer solutions for a wide-spread field of analytical problems [28, 40]. It is important to keep in mind that every method leads to a unique aroma profile and that there is no universal extraction technique available [41].

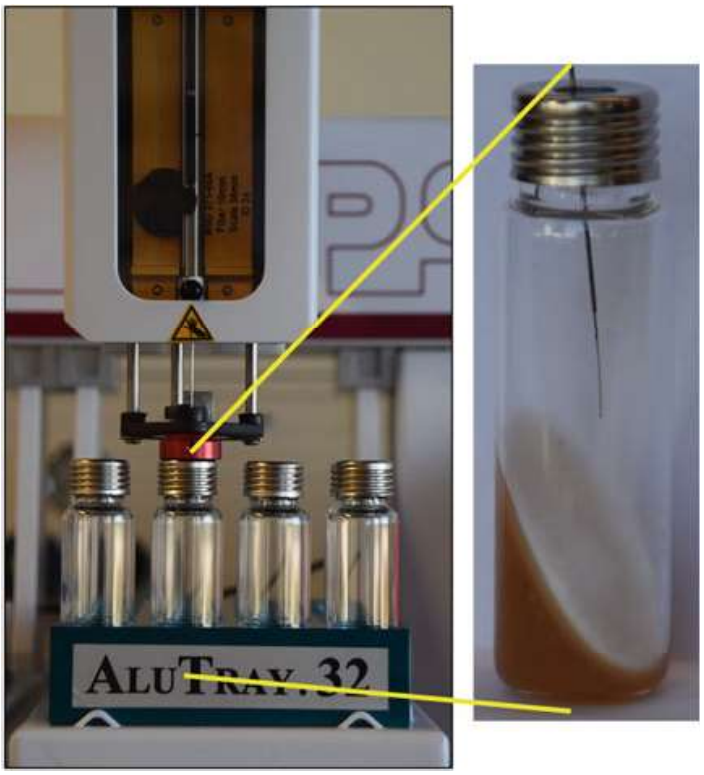

Fig. 4 Automatically performed SPME GC-MS analysis of SSF with filamentous fungi in 20 mL vials (height 7.5 cm; width 2 cm)

1.2 Detection of Volatile Compounds

Generally, the identification of volatile compounds is based on retention indices (RIs) and mass spectral analysis. RIs of the analytes obtained on two columns of different polarity have to be compared with those of the corresponding authentic reference compounds. In addition, the mass spectra of the analytes have to correspond to the mass spectra of the standard substances [42, 43]. Linear RIs modified after Kováts [44] should be calculated according to the retention times of homologous *n*-alkanes by linear interpolation. Additionally, it is common to compare the odor quality of the analyte with that of the authentic standard by olfactory detection at comparable concentration levels [43]. Although single compounds can be identified with this approach, the impact of each VOC on the overall aroma profile is still unknown. Especially in fermented products, several hundreds of VOC are present, i.e., more than 800 in coffee [1, 45]. To determine the compounds representing the sample, the so-called character impact compounds, an aroma extract dilution analysis (AEDA) using GC-O is carried out [45]. A stepwise dilution (generally 2^n) of an extract is performed, and each dilution is analyzed by means of GC-O until no compound is perceived at the ODP [45]. The highest dilution at which a flavor compound can still be perceived is defined as the so-called flavor dilution factor (FD) [45]. Thus, it is assumed that aroma compounds with the highest FD factors mainly contribute to the overall aroma. By focusing on these substances, the key odor compounds can be identified [4, 46]. In recent studies as an alternative to AEDA, an aroma dilution analysis (ADA) is performed without the need of

preparing an extract due to the usage of SPME or SBSE. The stepwise dilution is achieved by adjusting the split ratio of the carrier gas flow [47, 48].

Generally, the FD factor of a VOC is meaningless concerning the impact of this compound on the overall olfaction. For this purpose, the odor activity value (OAV) can be determined [43]. Besides the concentration of a specific compound, the odor threshold of a standard substance of this volatile compound has to be determined by several panelists. The OAV is then calculated by dividing the concentration of the volatile compound in the sample with the determined threshold of the specific substance. Only VOC with an OAV >1 are taken into account.

2 Fungal Volatile Organic Compounds

Higher fungi are a remarkable source of aroma compounds highly valued by humans since ancient times: (1) mushrooms are an esteemed repository for nutrition, appreciated for their medical benefits and their unique as well as delicious flavors, and (2) ascomycetes, like *Saccharomyces cerevisiae*, are essential in food processing, ensuring the quality and taste, e.g., in bread or beer. This review focuses on the aroma compounds produced by filamentous fungi during SSF within various applications. Besides the discussion on different VOC produced, the various extraction methods used within the works listed below should depict the possibilities of aroma analysis during SSF.

2.1 Fungal VOC in Food Manufacturing

Ascomycetes such as *Aspergillus oryzae* and *Aspergillus sojae* have been applied to ferment soy bean, rice, and wheat to hydrolyze starch and proteins. The product of this SSF is called *koji* and is used as a starter culture for subsequent fermentation of the material into soy sauce, miso, or sake [49]. Ito et al. investigated the volatile compounds during the production of *koji* for the sake manufacturing process, which is rice fermented with *A. oryzae* [50]. Husked rice grains were soaked in water for 2 h, steamed for 30 min, cooled, and drained. The rice was inoculated with conidia (asexual spores), and incubation was performed at 36°C with a relative humidity of 95%. Volatiles were extracted using a DHS system equipped with a Tenax® trap, desorbed via TD, and analyzed by means of GC-FID and GC-MS. In total, 17 compounds were identified, including alcohols (e.g., ethanol, 3-methyl-1-butanol, butanol, oct-1-en-3-ol, and octan-1-ol), aldehydes (e.g., acetaldehyde), ketones (e.g., acetone, butanone, and octan-3-one), and the ester ethyl acetate. Their presence within the headspace of the active *koji* culture varied during cultivation. After 22 h in the mid-log phase of the SSF, a grassy impression was dominant, whereas after 38 h, the grassy fragrances decreased, and oct-1-en-3-ol increased resulting in the mushroom-like odor in the stationary phase of *koji* making. The dependence of

Fig. 5 Surface of a 3-day-old *Rhizopus oligosporus* culture on soy beans (left) and cross section of the tempeh (right); photos kindly provided by Andrea Sabbatini

VOC on the stage of *koji* production enables process control of SSF on the basis of VOC analysis. This is depicted in the work of Kum et al. [51], where a soybean-based *koji* paste named *doenjang* is produced by means of SSF over a period of 8 weeks. The authors conducted a principal component analysis of the analyzed VOC, which revealed a distinct clustering of the calculated VOC components in relation to the cultivation period. Another soybean-based food is the traditional East Asian *tempeh*. Generally, for *tempeh* production, soybeans are soaked in water, cooked, and used as solid substrate for fungal colonization by the filamentous zygomycete *Rhizopus oligosporus*. After fermentation a structured matrix is formed, known as *tempeh* (Fig. 5). The aroma of fresh *tempeh* is specified by mainly moldy, mushroom-like, earthy, and boiled potato-like aroma compounds, such as 2-methylpropanal, oct-1-en-3-one, and 3-methylsulfanylpropanal (methional) [52, 53]. LLE of VOC from *tempeh* with subsequent SAFE and GC-MS analysis, followed by the determination of the corresponding OAV, revealed 2-methylpropanal and oct-1-en-3-one as main aroma compounds after 1 day of fermentation. After 5 days of fermentation, the boiled potato odor methional ensued [53]. In a HS analysis of *tempeh* with Tenax® as adsorbent [54], it was not possible to detect methional nor the typical mushroom odor oct-1-en-3-one found in liquid extracts, but other C8 volatiles were present. Interestingly, the key aroma compound 2-methlypropanal was detected in the fermented soybeans as well as in the non-fermented control, although in the latter only in small concentrations [54].

An SSF for food manufacturing with filamentous fungi adapted in Europe is the production of soft cheese including camembert and blue cheese, e.g., Roquefort and Gorgonzola. Filamentous fungi play an important role in the maturation of these cheeses, contributing to the unique flavor, texture, and product composition [55]. Camembert, a mold-ripened cheese originating from France, is traditionally manufactured from raw cow milk [56]. During production, the curd is molded with *Penicillium camemberti* on the surface, imparting the cheese its pronounced flavor. Analysis of the camembert aroma was performed using solvent and static HS extraction by means of GC-MS followed by AEDA and calculation of FD values [57] or OAV [58]. In both works, 42 VOC were identified of which dimethyl sulfide, methional, and especially methanethiol were key odorants of the sulfurous, garlic note. The C8 volatiles oct-1-en-3-one and oct-1-en-3-ol contributed to the

mushroom-like odor, whereas 3-methylbutanal could be linked to the malty scent of the camembert, and 2-phenylethyl acetate was related to a floral bouquet of the cheese. In contrast to the cultivation on curd, no sulfur-containing volatiles were detected when *P. camemberti* was cultivated on potato dextrose agar or Czapek's agar [59]. Similar to the curd fermentation, C8 compounds, including oct-1-en-3-ol, octan-3-ol, and octan-3-one, have been extracted with a DHS device equipped with Tenax® traps and identified in agar plate cultures. Another *Penicillium* species used for blue cheese manufacturing is *P. roqueforti*. Similar to Camembert fabrication, fungal conidia are either directly added to the milk or sprayed on the curd during blue cheese production. Usually, ripening is performed for about 90 days at 10°C and a relative humidity of at least 90% [60, 61]. *P. roqueforti* has a high tolerance regarding physical parameters. It can even grow in an oxygen-poor environment and in a broad pH range of 3–10. This enables, by adjusting suitable conditions, a selective growth of the fungus inside the cheese [62]. During maturation, several peptidases and lipases are expressed by *P. roqueforti*, leading to extensive degradation of proteins (up to 35%) and fats [60, 63, 64]. Portions of the released fatty acids are converted to 2-methyl ketones via oxidation to β-keto acids and a decarboxylation step [65]. 2-Methyl ketones have a strong impact on the characteristic aroma of blue cheese, contributing with fruity, floral, and musty notes [66, 67]. A comparative study of 55 *P. roqueforti* strains, using a DHS system with a Tenax® trap and analysis via GS-MS, resulted in the identification of 52 VOC. Several substances known from Camembert, like sulfur compounds (e.g., methanethiol) and alcohols (e.g., oct-1-en-3-ol), were detected. With 50–75% of the total volatiles, 2-methyl ketones were the most abundant analytes [61]. It is notable that the composition of the 2-methyl ketones in the cheese depends strongly on the stage of ripening [68], which again illustrates the growth phase-dependent VOC production.

2.2 VOC Produced During Non-food SSF of Ascomycetes

Biotransformation of industrial side streams into valuable products, such as volatile organic compounds, by means of fungal solid-state, respectively, solid-substrate fermentation, is done since ages. In most cases, filamentous fungi are used for SSF, but even yeasts have been applied on solid substrates. Rossi et al. [69] analyzed the aroma profile of the plant pathogen *Ceratocystis fimbriata* cultured in SSF on citric pulp, a residue of the citrus juice-producing industry. Citric pulp as substrate was tested solely or supplemented with soya molasses, sugarcane molasses, soya bran, or urea and different concentrations of saline solution (KH_2PO_4, $CaCl_2$, and $MgSO_4$). HS analysis was performed by means of GC-FID to identify VOC produced by the fungus. Acetaldehyde, ethanol, ethyl acetate, propyl acetate, ethyl isobutyrate, hexan-2-one, hexan-2-ol, and 3-methylbutyl acetate were identified. The addition of soya bran as N-source, sugarcane molasses as C-source, as well as saline solution to the citric pulp resulted in the highest production of total volatiles.

The amount of 3-methylbutyl acetate, a valuable banana aroma, increased 5.5-fold compared to the citrus culture without supplementation. SSF of *C. fimbriata* on cassava bagasse supplemented with either leucine or valine resulted in strong banana aroma, which was probably due to the presence of 3-methylbutyl acetate [70]. In contrast, SSF of cassava bagasse supplemented with urea showed a similar growth rate, but only a slight production of VOC. The high 3-methylbutyl acetate concentration in cultures supplemented with leucine might derive from an active Ehrlich pathway, yet not known for *C. fimbriata* but described for the ascomycete *S. cerevisiae* [71]. Here, leucine would be transformed into 3-methylbutanol, which can be converted into 3-methylbutyl acetate by an alcohol acyltransferase [72]. Contradictory to this assumption, valine would react via 2-methylpropanol into 2-methylpropyl ethanoate (isobutyl acetate) not detected by the authors [70]. On coffee residues, *C. fimbriata* showed a different VOC pattern during SSF [73]. Coffee pulp and coffee husk supplemented with glucose were used as substrates. After inoculation with spores, the volatiles in the HS were analyzed by means of GC-FID over a time period of 10 days. After 48 h, the highest amounts of volatile compounds were detected. The dominant volatiles in the HS of the coffee husk and coffee pulp samples were ethyl acetate (84.7 and 69.6%), ethanol (7.6 and 20.0%), and acetaldehyde (2.0 and 2.1%). Esters including ethyl propionate, propyl acetate, isobutyl acetate, ethyl isobutyrate, and ethyl butyrate contributed to the fruity odor of the culture, but no 3-methylbutyl acetate was detected.

In addition to the impact of substrates on the composition of VOC, the cultivation type, SSF or submerged fermentation (SmF), respectively, shaken or static cultures, has an effect on the overall productivity of VOC, e.g., for the coconut-like aroma compound 6-pentyl-α-pyrone (6-PP) in cultures of *Trichoderma* species. Kalyani et al. compared the production of 6-PP in potato extract medium supplemented with glucose in shaken and static cultures [74]. Over a period of 5 days, samples were harvested every day. Aliquots of the culture supernatant were extracted with dichloromethane, dried over sodium sulfate, concentrated, and 6-PP was quantified with GC-FID. After 96 h, the highest 6-PP concentration of 455 mg L^{-1} was obtained in the static cultures, whereas in the shaken cultures, the maximum amount of 187 mg L^{-1} was already reached after 48 h. In SSF cultures of *T. harzianum* on sugarcane bagasse, the 6-PP concentration was even higher with 933 mg L^{-1} at the end of cultivation after 10 days [75]. The productivity of 6-PP by *T. harzianum* was almost 14 times higher in SSF (171 mg L^{-1} day^{-1}) than in SmF cultures (12.5 mg L^{-1} day^{-1}) [75]. Sugarcane bagasse was also used in several other studies for 6-PP production. Araujo et al. screened 95 fungal isolates for the occurrence of 6-PP [76]. One *Trichoderma* species showed the highest product concentration with 3 mg 6-PP g^{-1} dry matter (DM) after 5 days of cultivation, accounting for approximately 940 mg 6-PP L^{-1} of supernatant [76]. Another *Trichoderma* species, *T. viride*, was cultivated on sugarcane bagasse for a period of 12 days. The highest 6-PP concentration (3.6 mg g^{-1} DM) was also achieved at day 5 [77]. It is worth mentioning that the usage of 6 g sugarcane bagasse instead of 4.5 g resulted in a significant decrease in 6-PP production (1.7 mg g^{-1} DM). Improvement of the cultivation conditions for 6-PP production by SSF of

T. harzianum on green coir powder was performed by Souza Ramos et al. [78] by altering the culture conditions regarding the composition of the supplements, the moisture content, the amount of spores for inoculation, and the temperature. After 7 days of fermentation, the HS was analyzed with SPME (PDMS) and GC-FID. The highest amount of 6-PP was achieved at 28°C by using per 100 g coir: 3 g sucrose, 0.24 g $NaNO_3$, 0.18 g $(NH_4)_2SO_4$, 0.1 g KH_2PO_4, an inoculum of 2.2×10^6 spores, and water to reach a final moisture level of 55%. The fermentation under the selected conditions led to a six times higher 6-PP production (5.0 mg g^{-1} DM) than the initial one (0.8 mg g^{-1} DM).

Another interesting fruity flavor is the pineapple odor ethyl hexanoate. Yamauchi et al. compared the production of ethyl hexanoate in SSF of *Neurospora* sp. on pregelatinized rice, wheat bran (*fusuma*), corn grits, and spent grain, supplemented with different additives [79]. Cultivation on pregelatinized rice with 5% malt broth resulted after 2 weeks in 180 mg kg^{-1} ethyl hexanoate, whereas cultures with *fusuma*, corn grits, and spent grain only reached 10 mg kg^{-1} or less. This SSF of pregelatinized rice with *Neurospora* sp. led to a *koji* used for the sake production and resulted in a fruity perception of the sake. Ethyl hexanoate is also a substantial flavor compound in traditional Chinese liquor, obtained by distilling SSF of grains fermented with *daqu*, which is a starter culture consisting of a diverse microbiome, including inter alia *Lactobacillus*, *Bacillus*, *Aspergillus*, and *Saccharomycopsis*. Zhang et al. [80] analyzed volatiles appearing during the fermentation process of *daqu* on a mixture of sorghum, corn, wheat, and rice. Cultivation was conducted at 30°C, and samples were harvested on days 1, 10, 23, 34, 48, 59, and 70. Aromatic esters were extracted with ethanol and quantified by GC-FID. Ethyl hexanoate firstly appeared on day 59 (93.3 μg g^{-1}) and only slightly increased until day 70 (96.1 μg g^{-1}). Such combinations of microorganisms can result in a diverse pattern of VOC. A mixture of orange pulp molasses, potato pulp, whey, brewer's spent grain, and malt spent rootlets was fermented by a kefir community consisting of symbiotic consortia of fungi and bacteria [81]. Volatiles in the HS of these cultures were extracted with SPME and identified using GC-MS. In the HS of kefir cultures, the highest total VOC concentrations have been determined with ε-pinene being the most abundant aroma compound (4,208 mg kg^{-1}).

2.3 VOC Produced During SSF of Basidiomycetes

Members of the phylum *Basidiomycota*, which most mushrooms belong to and referred to as basidiomycetes, have been cultivated since centuries by humans for the purpose of food production. The origin of mushroom production is in China, with the first handwritten instruction for mushroom cultivation dating back to the seventh century [82]. Generally, mushroom cultivation, which is probably the largest industrial SSF sector, is performed on agroforestry wastes, like straw, sawdust, reed grass, banana and bamboo leaves, tree bark and stems, husks, and scrubs [82–84].

In addition, side streams of the food-producing industry, like wheat straw, citrus peels, and cocoa shells, can be a valuable substrate source [85]. Worldwide, 950 different mushrooms are consumed and 50 different species are cultivated. China is the biggest commercial producer with an annual production of 7 million tons in 2013, which accounts for more than 70% of the worldwide production [86]. Several articles already reviewed the variety of aroma compounds present in fruiting bodies of fungi of the phylum Basidiomycota [87–89]. In the following, the focus is on the aroma compounds produced by the vegetative mycelium. The influence of different cultivation parameters, including substrate preparation, inoculation, and incubation time on the production of different aroma compounds, is highlighted. Moreover, also the genotype of the cultivated mushroom can have an impact on the production process and yield [90]. In addition, recent results on VOC production during the process of fructification are presented.

2.3.1 Volatiles Produced During Vegetative Growth

The fruiting bodies of the oyster mushroom *Pleurotus ostreatus* are known as a delicate food with a pleasant aroma and derive from SSF on lignocellulosic residues. When cultivated in liquid media or on an artificial solid substrate, the aroma composition of *P. ostreatus* cultures alters [91]. Kabbaj et al. compared VOC derived from *P. ostreatus* liquid cultures, agar plate cultures, and SSF on sugarcane bagasse with its fruiting bodies produced on wheat straw [91]. VOC were extracted with a DHS system equipped with a Tenax® trap. Afterward, volatiles were thermally desorbed, cryofocused, and analyzed via GC-MS. The volatile profile of the mycelium varied significantly between the different cultivation conditions. In fruiting bodies, octan-3-one contributed to 80% of the integrated peak areas, followed by octan-3-ol with about 14%. During SSF with sugarcane bagasse or on agar surface cultures, mainly octan-3-one (72.5% and 67.4%, respectively) was detected, with similar concentrations as in the fruiting bodies, whereas in liquid culture, it only contributed with 36.2% to the detected volatiles. In liquid cultures, oct-1-en-3-ol (38.5%) was the dominant compound but only found in small amounts in the SSF with sugarcane bagasse (0.3%) and agar medium (1%). It is worth mentioning that the approach with liquid medium contained relatively high quantities (16.2%) of 2-methylbutanol, resulting in a spicy and repellent note of the culture. This illustrates the impact of the culture conditions on the volatile composition. In addition to the culture conditions, the substrate itself has an effect on the VOC produced. When *P. ostreatus* was cultivated on spent leaves of *Eucalyptus cinerea* derived from the production of essential oils, the spectrum of VOC was influenced by the substrates [92]. Cultivation of *P. ostreatus* on spent *E. cinerea* leaves was carried out in propylene bags in darkness at 25°C for 30 days to completely colonize the substrate. Afterward, the bags were removed, and the substrate block was further cultivated for approximately 1 month at 20 ± 2°C and 86–90% relative humidity as well as day and night shifts to induce fructification. The volatiles of the substrate blocks after colonization and after fructification were extracted by hydrodistillation in a

Clevenger-type apparatus, a distillation method used for the extraction of essential oils. Analysis was performed with GC-FID and GC-MS. The amounts of various volatiles including eugenol, globulol, α-cadinol, longifolene, and *p*-cymene decreased during the fermentation of *P. ostreatus* on the spent leaves, whereas the quantities of 1,8-cineole and β-caryophyllene increased significantly, and sabinene hydrate appeared. The increase of the monoterpenes and β-caryophyllene might be due to an active release of these compounds by *P. ostreatus*. 1,8-Cineole was hydroxylated by the fungus to 1,3,3-trimethyl-2-oxabicyclo[2.2.2]octan-6-ol and further oxidized to 1,3,3-trimethyl-2-oxabicyclo[2.2.2]octan-6-one.

Wu et al. [93] analyzed the volatile biotransformation products of vine tea, a product derived from the vine species *Ampelopsis grossedentata*, during SSF with the medical mushroom *Wolfiporia cocos* (synonym: *Poria cocos*). The fungus was cultivated on moistened tea leaves at 28°C for 15 days. Unfermented vine tea inhered a strange taste, whereas fermented tea exhibited a pleasant aroma. Every third day, cultures were harvested for LLE with water and dichloromethane. The extracts were distilled for 5 h, subsequently concentrated, and analyzed by means of GC-MS. During the fermentation remarkable amounts of methyl 2-methylpentanoate were produced, resulting in the fruity note of the processed vine tea. Aroma compound production of the medically valuable mushroom *Antrodia camphorata* was observed during cultivation on millet for 25 days at 28°C [94]. On days 10, 15, 20, and 25 volatiles in the HS were analyzed by means of SPME (CAR/PDMS) and GC-MS. In total, 124 compounds were detected not present in the unfermented millet. The VOC profile varied remarkably during fermentation. In early stages, C8 compounds, such as oct-1-en-3-ol, octan-3-one, and octan-1-ol, accounted for approximately 50% of all detected VOC. In later stages, octan-3-one (32–38%) was the most abundant substance, followed by methyl 2-phenylacetate (13.1–16.6%). The relative amount of oct-1-en-3-ol decreased rapidly over the time (down to 0.9%), whereas the quantity of sesquiterpenes and lactones, including 5-butyloxolan-2-one, 5-heptyloxolan-2-one, and 6-heptyloxan-2-on, increasingly contributed to a fruit-like flavor with herbal fresh notes.

As already shown, basidiomycetes are mainly cultivated on residues from industrial or agricultural processes for human consumption. In general, the substrate used consists of lignocellulose, which can be metabolized by all commercially cultivated mushrooms using their diverse enzymatic system to a certain extent. This so-called lignocellulolytic system can also generate some volatile side products and thus might be an unexploited source for aroma compounds. The major class of lignin degrading enzymes are class II fungal peroxidases, which require H_2O_2 as a cofactor. The H_2O_2 is provided by different alcohol and glucose oxidases, such as the aryl alcohol oxidases (AAO) [95]. As a substrate, AAO demand aryl alcohols, such as benzyl alcohol, which are converted by the AAO into the almond flavor benzaldehyde [96]. Bonnarme and coworkers had a closer look into this system comparing cultivation conditions and their impact on VOC production and enzymatic activity [97, 98]. They used the white rot fungus *Bjerkandera adusta* for SSF and SmF for the production of benzaldehyde, benzyl alcohol, and benzoic

acid [97, 98]. When SmF cultures of *B. adusta* were supplemented with polyurethane foam cubes, the benzaldehyde concentration increased significantly (8.3-fold) as did the AAO activity (4.3-fold). On the other hand, the maximum benzyl alcohol concentration was higher in non-immobilized SmF cultures (1.5-fold). This emphasizes the possible usage of lignocellulolytic enzymes for the aroma biosynthesis. In a similar study, the effect of different solid supports was investigated concerning the production of aryl metabolites. In comparison to the inert carrier perlite, the utilization of lignocellulosic wheat bran for SSF of *B. adusta* resulted in a remarkable production increase of benzyl alcohol and benzaldehyde (up to tenfold). Similar to the SmF, the AAO activity was only detected in SSF on wheat bran and not in cultures where perlite was used [97].

Although the substrate can have an influence on the aroma compounds produced during SSF, the aroma profile of fruiting bodies derived from different substrates remained unchanged for the delicious black poplar mushroom *Agrocybe aegerita* [99]. *A. aegerita* was cultivated on 100% wheat straw, 100% cocoa shells, as well as wheat straw supplemented with either cocoa shells (17%), citrus pellets (17%), carrot mesh (17%), or black tea pomace (17 and 45%). Straw-based substrates showed comparable growth of *A. aegerita*, whereas on 100% cocoa shells, only marginal mycelium growth and no fruiting bodies were observed. Fruiting bodies grown on 100% wheat straw and on wheat straw supplemented with black tea pomace (45%) were compared in regard to their aroma profile. After addition of methanol and water, homogenized fruiting bodies were extracted by means of LLE. The concentrated extracts were analyzed via GC-MS/MS-O. Eleven VOC were identified in the fruiting bodies, and the volatile composition of the two different SSF cultivations did not exhibit considerable differences. C8 compounds, including oct-1-en-3-ol, oct-1-en-3-one, and octan-3-one, contributed to the typical mushroom odor, whereas 2-phenylethanol added a rose-like note to the aroma profile.

2.3.2 Volatiles Produced During Fructification

In basidiomycetes, sexual reproduction consists of a complex, multipolar mating-type system, involving a haploid, monokaryotic stage [100]. Monokaryotic mycelium of matching mating types can fuse, resulting in a dikaryotic stage. Out of this stage, fruiting bodies derive to start a new reproduction cycle. Freihorst et al. [101] compared the volatile profile during SSF of two sexual compatible monokaryotic strains of *Schizophyllum commune* with the volatile composition of a dikaryon obtained from mating both analyzed monokaryons. All three strains were cultivated on solid complex medium for 7 days at 28°C. At the end of cultivation, volatiles were extracted using HS-SPME (DVB/CAR/PDMS) for 1 h and analyzed with a GC-MS system. Methyl 2-methylbutanoate was the dominant VOC in both monokaryotic cultures (80%) and in the dikaryotic samples (31%). Apart from that, the VOC profile of monokaryons and dikaryons differed tremendously. The volatilome, the aggregate of all VOC, of the monokaryons contained

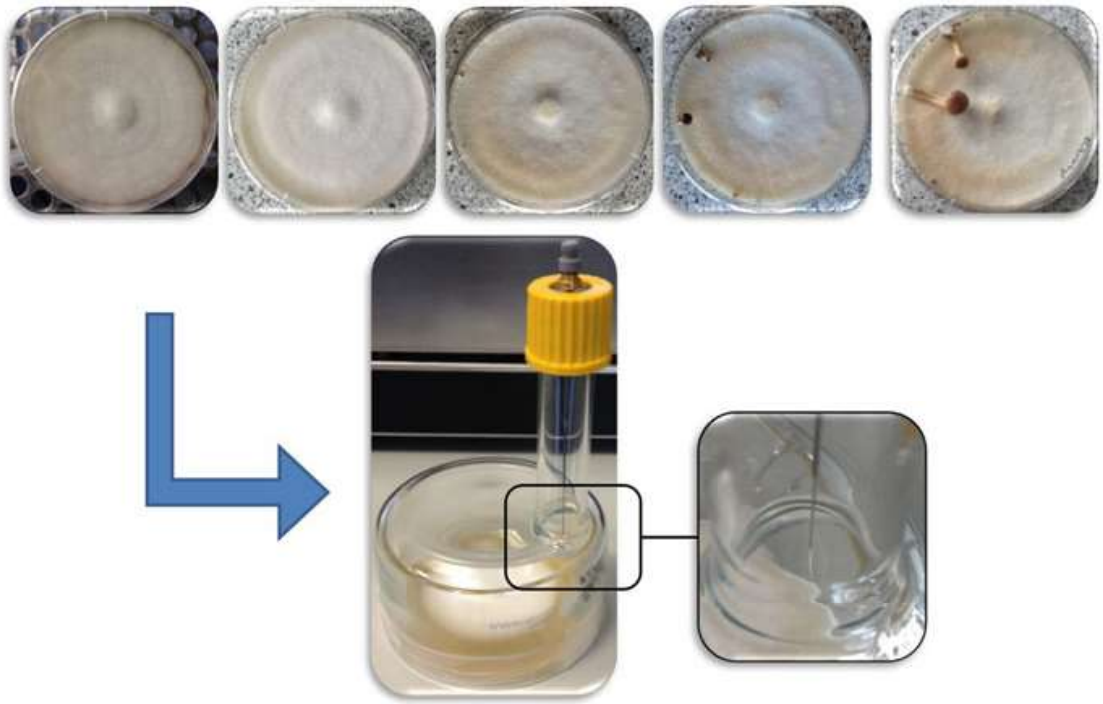

Fig. 6 Extraction of VOC with SPME during fructification of *A. aegerita* in SSF on malt extract agar using modified crystallizing dishes; photos kindly provided by Sabrina Herold

methyl 2-methylpropanoate, not found among the volatiles of the dikaryon. Vice versa, oct-1-en-3-ol, octan-3-one, *S*-methyl thioacetate, 3-methylbutan-1-ol, isobutyl acetate, and β-bisabolol were only detected in the HS of the dikaryon. Ethyl 2-methylbutanoate had a comparable ratio in the volatiles of all samples (monokaryons 1–4%, dikaryon 4%).

All these results demonstrate that cultivation phases as well as the genetic background of the analyzed specimens have a remarkable influence on the volatile composition of basidiomycetes during SSF. In a recent work of our research group (unpublished), we investigated the role of both factors on the volatilome of *A. aegerita* in SSF. Therefore, strains were cultivated on 1.5% MEA in modified crystallizing dishes (Fig. 6), allowing an efficient extraction of VOC by means of SPME. This system had the advantage to ensure aeration of the culture, necessary for the development of fruiting bodies. Furthermore, without harvesting the mushrooms, it was possible to analyze the changes of volatile composition in the HS of the same sample over the time, avoiding disturbance of the system and thus the formation of VOC artefacts due to disruption of cell compartments. Four monokaryotic strains, representing members of the "mycelium," "initials," "elongated," and "fruiter"-type, classified by Herzog et al. [102], and one dikaryotic strain were grown for 28 days.

Every second day, beginning with day 10 (agar plates were fully overgrown), volatiles were extracted in the HS using SPME (DVB/CAR/PDMS) and analyzed with GC-MS. The volatile profiles of all strains varied distinctively over the time. For the dikaryon, raised VOC concentrations were detected. In the HS of the dikaryotic

mycelium, mainly alcohols and ketones, like oct-1-en-3-ol, 2-methylbutan-1-ol, acetone, and cyclopentanone, were identified. The composition of the VOC changed significantly with the occurrence of fruiting bodies and during the sporulation phase. Here, sesquiterpenes, especially Δ^6-protoilludene, α-cubebene, and δ-cadinene, were the dominant substances. After sporulation, the amount of sesquiterpenes decreased, while additional VOC, mainly octan-3-one, appeared.

3 Conclusion

In addition to cultivation of mushrooms for food production, filamentous fungi are promising candidates for SSF applications in the aroma sector. They are able to grow on different substrates, which can result in a variable VOC profile, offering the still not fully exploited potential of gaining a whole range of valuable flavors. The diversity in these volatile profiles also depends on the developmental and reproductive stage of filamentous fungi, which facilitates the process control of SSF by observing the VOC production.

Acknowledgments We gratefully acknowledge the support by the Deutsche Forschungsgemeinschaft RU 2137/1 and by the excellence initiative LOEWE within the project "AROMAplus" financed by the Hessian Ministry of Science and Art.

References

1. Dunkel A, Steinhaus M, Kotthoff M et al (2014) Nature's chemical signatures in human olfaction: a foodborne perspective for future biotechnology. Angew Chem Int Ed Engl 53:7124–7143. https://doi.org/10.1002/anie.201309508
2. Grosch W (2001) Evaluation of the key odorants of foods by dilution experiments, aroma models and omission. Chem Senses 26:533–545. https://doi.org/10.1093/chemse/26.5.533
3. Biniecka M, Caroli S (2011) Analytical methods for the quantification of volatile aromatic compounds. Trends Anal Chem 30:1756–1770. https://doi.org/10.1016/j.trac.2011.06.015
4. Kleofas V, Popa F, Fraatz MA et al (2015) Aroma profile of the anise-like odour mushroom *Cortinarius odorifer*. Flavour Fragr J 30:381–386. https://doi.org/10.1002/ffj.3250
5. Wells MJM (2003) Principles of extraction and the extraction of semivolatile organics from liquids. In: Somenath M (ed) Sample preparation techniques in analytical chemistry. Wiley-VCH, Weinheim, pp 37–138
6. Engel W, Bahr W, Schieberle P (1999) Solvent assisted flavour evaporation – a new and versatile technique for the careful and direct isolation of aroma compounds from complex food matrices. Z Lebensm Unters Forsch 209:237–241. https://doi.org/10.1007/s002170050486
7. Zlatkis A, Lichtenstein HA, Tishbee A (1973) Concentration and analysis of trace volatile organics in gases and biological fluids with a new solid adsorbent. Chromatographia 6:67–70. https://doi.org/10.1007/BF02270540
8. Pillonel L, Bosset JO, Tabacchi R (2002) Rapid preconcentration and enrichment techniques for the analysis of food volatile. A review. LWT Food Sci Technol 35:1–14. https://doi.org/10.1006/fstl.2001.0804

9. Soria AC, García-Sarrió MJ, Sanz ML (2015) Volatile sampling by headspace techniques. TrAC Trends Anal Chem 71:85–99. https://doi.org/10.1016/j.trac.2015.04.015
10. Nawrath T, Dickschat JS, Kunze B et al (2010) The biosynthesis of branched dialkylpyrazines in myxobacteria. Chem Biodivers 7:2129–2144. https://doi.org/10.1002/cbdv.201000158
11. Grob K (1973) Organic substances in potable water and in its precursor. J Chromatogr A 84:255–273. https://doi.org/10.1016/S0021-9673(01)91705-4
12. Da Costa NC, Eri S (2009) Identification of aroma chemicals. In: Rowe DJ (ed) Chemistry and technology of flavors and fragrances. Blackwell, CRC Press, Oxford, pp 12–34
13. Slack GC, Snow NH, Kou D (2003) Extraction of volatile organic compounds from solids and liquids. In: Somenath M (ed) Sample preparation techniques in analytical chemistry. Wiley-VCH, Weinheim, pp 183–225
14. Sghaier L, Vial J, Sassiat P et al (2016) An overview of recent developments in volatile compounds analysis from edible oils: technique-oriented perspectives. Eur J Lipid Sci Technol 118:1853–1879. https://doi.org/10.1002/ejlt.201500508
15. Harper M (2000) Sorbent trapping of volatile organic compounds from air. J Chromatogr A 885:129–151. https://doi.org/10.1016/S0021-9673(00)00363-0
16. Helmig D, Vierling L (1995) Water adsorption capacity of the solid adsorbents Tenax TA, Tenax GR, Carbotrap, Carbotrap C, Carbosieve SIII, and Carboxen 569 and water management techniques for the atmospheric sampling of volatile organic trace gases. Anal Chem 67:4380–4386. https://doi.org/10.1021/ac00119a029
17. Bazemore R (2011) Sample preparation. In: Goodner K, Rousseff R (eds) Practical analysis of flavor and fragrance materials, vol 75. Wiley, Hoboken, pp 23–44
18. Bicchi C, Cordero C, Liberto E et al (2008) Headspace sampling of the volatile fraction of vegetable matrices. J Chromatogr A 1184:220–233. https://doi.org/10.1016/j.chroma.2007.06.019
19. Castro R, Natera R, Benitez P et al (2004) Comparative analysis of volatile compounds of 'fino' sherry wine by rotatory and continuous liquid–liquid extraction and solid-phase microextraction in conjunction with gas chromatography-mass spectrometry. Anal Chim Acta 513:141–150. https://doi.org/10.1016/j.aca.2004.02.002
20. Arthur CL, Pawliszyn J (1990) Solid phase microextraction with thermal desorption using fused silica optical fibers. Anal Chem 62:2145–2148. https://doi.org/10.1021/ac00218a019
21. Pawliszyn J (2003) Sample preparation: quo vadis? Anal Chem 75:2543–2558. https://doi.org/10.1021/ac034094h
22. Hou X, Wang L, Guo Y (2017) Recent developments in solid-phase microextraction coatings for environmental and biological analysis. Chem Lett 46:1444–1455. https://doi.org/10.1246/cl.170366
23. Azenha MA, Nogueira PJ, Silva AF (2006) Unbreakable solid-phase microextraction fibers obtained by sol-gel deposition on titanium wire. Anal Chem 78:2071–2074. https://doi.org/10.1021/ac0521246
24. Silva C, Cavaco C, Perestrelo R et al (2014) Microextraction by packed sorbent (MEPS) and solid-phase microextraction (SPME) as sample preparation procedures for the metabolomic profiling of urine. Metabolites 4:71–97. https://doi.org/10.3390/metabo4010071
25. Xu C-H, Chen G-S, Xiong Z-H et al (2016) Applications of solid-phase microextraction in food analysis. TrAC Trends Anal Chem 80:12–29. https://doi.org/10.1016/j.trac.2016.02.022
26. Lee LW, Cheong MW, Curran P et al (2016) Modulation of coffee aroma via the fermentation of green coffee beans with *Rhizopus oligosporus*: II. Effects of different roast levels. Food Chem 211:925–936. https://doi.org/10.1016/j.foodchem.2016.05.073
27. Zhang Q, Zhou L, Chen H et al (2016) Solid-phase microextraction technology for in vitro and in vivo metabolite analysis. Trends Anal Chem 80:57–65. https://doi.org/10.1016/j.trac.2016.02.017
28. Rutkowska M, Dubalska K, Konieczka P et al (2014) Microextraction techniques used in the procedures for determining organomercury and organotin compounds in environmental samples. Molecules 19:7581–7609. https://doi.org/10.3390/molecules19067581

29. Gómez-Ríos GA, Reyes-Garcés N, Bojko B et al (2016) Biocompatible solid-phase microextraction nanoelectrospray ionization: an unexploited tool in bioanalysis. Anal Chem 88:1259–1265. https://doi.org/10.1021/acs.analchem.5b03668
30. Boyacı E, Rodríguez-Lafuente Á, Gorynski K et al (2015) Sample preparation with solid phase microextraction and exhaustive extraction approaches: comparison for challenging cases. Anal Chim Acta 873:14–30. https://doi.org/10.1016/j.aca.2014.12.051
31. Zhang Z, Pawliszyn J (1993) Headspace solid-phase microextraction. Anal Chem 65:1843–1852. https://doi.org/10.1021/ac00062a008
32. Feng J, Qiu H, Liu X et al (2013) The development of solid-phase microextraction fibers with metal wires as supporting substrates. TrAC Trends Anal Chem 46:44–58. https://doi.org/10.1016/j.trac.2013.01.015
33. Baltussen E, Sandra P, David F et al (1999) Stir bar sorptive extraction (SBSE), a novel extraction technique for aqueous samples: theory and principles. J Microcolumn Sep 11:737–747. https://doi.org/10.1002/(SICI)1520-667X(1999)11:10<737:AID-MCS7>3.0.CO;2-4
34. Rykowska I, Wasiak W (2013) Advances in stir bar sorptive extraction coating: a review. Acta Chromatogr 25:27–46. https://doi.org/10.1556/AChrom.25.2013.1.13
35. Kawaguchi M, Ito R, Saito K et al (2006) Novel stir bar sorptive extraction methods for environmental and biomedical analysis. J Pharm Biomed Anal 40:500–508. https://doi.org/10.1016/j.jpba.2005.08.029
36. Merkle S, Kleeberg K, Fritsche J (2015) Recent developments and applications of solid phase microextraction (SPME) in food and environmental analysis – a review. Chromatography 2:293–381. https://doi.org/10.3390/chromatography2030293
37. Prieto A, Basauri O, Rodil R et al (2010) Stir-bar sorptive extraction: a view on method optimisation, novel applications, limitations and potential solutions. J Chromatogr A 1217:2642–2666. https://doi.org/10.1016/j.chroma.2009.12.051
38. Baltussen E, Cramers CA, Sandra PJF (2002) Sorptive sample preparation – a review. Anal Bioanal Chem 373:3–22. https://doi.org/10.1007/s00216-002-1266-2
39. Gilart N, Marcé RM, Borrull F et al (2014) New coatings for stir-bar sorptive extraction of polar emerging organic contaminants. TrAC Trends Anal Chem 54:11–23. https://doi.org/10.1016/j.trac.2013.10.010
40. Kabir A, Locatelli M, Ulusoy H (2017) Recent trends in microextraction techniques employed in analytical and bioanalytical sample preparation. Separations 4:36. https://doi.org/10.3390/separations4040036
41. Reineccius G (2010) Instrumental methods of analysis. In: Taylor AJ, Linforth RST (eds) Food flavour technology, 2nd edn. Blackwell, Ames, pp. 229–265
42. IOFI (2006) Statement on the identification in nature of flavouring substances, made by the working group on methods of analysis of the international organization of the flavour industry (IOFI). Flavour Fragr J 21:185. https://doi.org/10.1002/ffj.1721
43. Grosch W (2007) Gas chromatography – olfactometry of aroma compounds. In: Berger RG (ed) Flavours and fragrances: chemistry, bioprocessing and sustainability. Springer, Berlin, pp 363–378
44. van den Dool H, Kratz PD (1963) A generalization of the retention index system including linear temperature programmed gas – liquid partition chromatography. J Chromatogr A 11:463–471. https://doi.org/10.1016/S0021-9673(01)80947-X
45. Belitz H-D, Grosch W, Schieberle P (2009) Food chemistry, 4th edn. Springer, Berlin
46. Kleofas V, Popa F, Niedenthal E et al (2015) Analysis of the volatilome of *Calocybe gambosa*. Mycol Prog 14:93. https://doi.org/10.1007/s11557-015-1117-0
47. Trapp T, Jäger DA, Fraatz MA et al (2018) Development and validation of a novel method for aroma dilution analysis by means of stir bar sorptive extraction. Eur Food Res Technol 244:949–957. https://doi.org/10.1007/s00217-017-3003-2

48. Zhang Y, Fraatz MA, Horlamus F et al (2014) Identification of potent odorants in a novel nonalcoholic beverage produced by fermentation of wort with shiitake (*Lentinula edodes*). J Agric Food Chem 62:4195–4203. https://doi.org/10.1021/jf5005463
49. Zhu Y, Tramper J (2013) Koji – where east meets west in fermentation. Biotechnol Adv 31:1448–1457. https://doi.org/10.1016/j.biotechadv.2013.07.001
50. Ito K, Yoshida K, Ishikawa T et al (1990) Volatile compounds produced by the fungus *Aspergillus oryzae* in rice Koji and their changes during cultivation. J Ferment Bioeng 70:169–172. https://doi.org/10.1016/0922-338X(90)90178-Y
51. Kum S-J, Yang S-O, Lee SM et al (2015) Effects of *Aspergillus* species inoculation and their enzymatic activities on the formation of volatile components in fermented soybean paste (doenjang). J Agric Food Chem 63:1401–1418. https://doi.org/10.1021/jf5056002
52. Feng Y, Su G, Zhao H et al (2015) Characterisation of aroma profiles of commercial soy sauce by odour activity value and omission test. Food Chem 167:220–228. https://doi.org/10.1016/j.foodchem.2014.06.057
53. Jeleń H, Majcher M, Ginja A et al (2013) Determination of compounds responsible for tempeh aroma. Food Chem 141:459–465. https://doi.org/10.1016/j.foodchem.2013.03.047
54. Feng XM, Larsen TO, Schnürer J (2007) Production of volatile compounds by *Rhizopus oligosporus* during soybean and barley tempeh fermentation. Int J Food Microbiol 113:133–141. https://doi.org/10.1016/j.ijfoodmicro.2006.06.025
55. Hymery N, Vasseur V, Coton M et al (2014) Filamentous fungi and mycotoxins in cheese: a review. Compr Rev Food Sci Food Saf 13:437–456. https://doi.org/10.1111/1541-4337.12069
56. Vitova E, Loupancova B, Stoudkova H et al (2007) Application of SPME-GC method for analysis of the aroma of white surface mould cheeses. J Food Nutr Res 46:84–90
57. Kubíčková J, Grosch W (1997) Evaluation of potent odorants of camembert cheese by dilution and concentration techniques. Int Dairy J 7:65–70. https://doi.org/10.1016/S0958-6946(96)00044-1
58. Kubicková J, Grosch W (1998) Quantification of potent odorants in camembert cheese and calculation of their odour activity values. Int Dairy J 8:17–23. https://doi.org/10.1016/S0958-6946(98)00014-4
59. Karahadian C, Josephson DB, Lindsay RC (1985) Volatile compounds from Penicillium sp. contributing musty-earthy notes to brie and camembert cheese flavors. J Agric Food Chem 33:339–343. https://doi.org/10.1021/jf00063a005
60. Kinsella JE, Hwang D (1976) Biosynthesis of flavors by *Penicillium roqueforti*. Biotechnol Bioeng 18:927–938. https://doi.org/10.1002/bit.260180706
61. Gillot G, Jany J-L, Poirier E et al (2017) Functional diversity within the *Penicillium roqueforti* species. Int J Food Microbiol 241:141–150. https://doi.org/10.1016/j.ijfoodmicro.2016.10.001
62. Abbas A, Dobson ADW (2011) Yeasts and molds | *Penicillium roqueforti*. In: Fuquay JW (ed) Encyclopedia of dairy sciences, 2nd edn. Academic Press, Amsterdam, pp 772–775
63. Petrovio SE, Becarevic A, Banka L et al (1991) Effects of various carbon and nitrogen sources on the biosynthesis of extracellular acidic proteinases of *Penicillium roqueforti*. Biotechnol Lett 13:451–454. https://doi.org/10.1007/BF01031000
64. Martínez-Rodríguez Y, Acosta-Muñiz C, Olivas GI et al (2014) Effect of high hydrostatic pressure on mycelial development, spore viability and enzyme activity of *Penicillium roqueforti*. Int J Food Microbiol 168-169:42–46. https://doi.org/10.1016/j.ijfoodmicro.2013.10.012
65. McSweeney PLH, Sousa MJ (2000) Biochemical pathways for the production of flavour compounds in cheeses during ripening: a review. Lait 80:293–324. https://doi.org/10.1051/lait:2000127
66. Cao M, Fonseca LM, Schoenfuss TC et al (2014) Homogenization and lipase treatment of milk and resulting methyl ketone generation in blue cheese. J Agric Food Chem 62:5726–5733. https://doi.org/10.1021/jf4048786

67. Curioni PMG, Bosset JO (2002) Key odorants in various cheese types as determined by gas chromatography-olfactometry. Int Dairy J 12:959–984. https://doi.org/10.1016/S0958-6946(02)00124-3
68. Dartey CK, Kinsella JE (1971) Rate of formation of methyl ketones during blue cheese ripening. J Agric Food Chem 19:771–774. https://doi.org/10.1021/jf60176a029
69. Rossi SC, Vandenberghe LPS, Pereira BMP et al (2009) Improving fruity aroma production by fungi in SSF using citric pulp. Food Res Int 42:484–486. https://doi.org/10.1016/j.foodres.2009.01.016
70. Christen P, Meza JC, Revah S (1997) Fruity aroma production in solid state fermentation by *Ceratocystis fimbriata*: influence of the substrate type and the presence of precursors. Mycol Res 101:911–919. https://doi.org/10.1017/S0953756297003535
71. Hazelwood LA, Daran J-M, van Maris AJA et al (2008) The Ehrlich pathway for fusel alcohol production: a century of research on *Saccharomyces cerevisiae* metabolism. Appl Environ Microbiol 74:2259–2266. https://doi.org/10.1128/AEM.02625-07
72. Tai Y-S, Xiong M, Zhang K (2015) Engineered biosynthesis of medium-chain esters in *Escherichia coli*. Metab Eng 27:20–28. https://doi.org/10.1016/j.ymben.2014.10.004
73. Medeiros ABP, Christen P, Roussos S et al (2003) Coffee residues as substrates for aroma production by *Ceratocystis fimbriata* in solid state fermentation. Braz J Microbiol 34. https://doi.org/10.1590/S1517-83822003000300013
74. Kalyani A, Prapulla SG, Karanth NG (2000) Study on the production of 6-pentyl-alpha-pyrone using two methods of fermentation. Appl Microbiol Biotechnol 53:610–612
75. Sarhy-Bagnon V, Lozano P, Saucedo-Castañeda G et al (2000) Production of 6-pentyl-α-pyrone by *Trichoderma harzianum* in liquid and solid state cultures. Process Biochem 36:103–109. https://doi.org/10.1016/S0032-9592(00)00184-9
76. de Aráujo ÁA, Pastore GM, Berger RG (2002) Production of coconut aroma by fungi cultivation in solid-state fermentation. Appl Biochem Biotechnol 98:747–751. https://doi.org/10.1385/ABAB:98-100:1-9:747
77. Fadel HHM, Mahmoud MG, Asker MMS et al (2015) Characterization and evaluation of coconut aroma produced by *Trichoderma viride* EMCC-107 in solid state fermentation on sugarcane bagasse. Electron J Biotechnol 18:5–9. https://doi.org/10.1016/j.ejbt.2014.10.006
78. de Souza Ramos A, Fiaux SB, Leite SGF (2008) Production of 6-pentyl-α-pyrone by *Trichoderma harzianum* in solid-state fermentation. Braz J Microbiol 39:712–717. https://doi.org/10.1590/S1517-838220080004000022
79. Yamauchui H, Akita O, Obata T et al (1989) Production and application of a fruity odor in a solid-state culture of *Neurospora* sp. using pregelatinized polished rice. Agric Biol Chem 53:2881–2886. https://doi.org/10.1271/bbb1961.53.2881
80. Zhang Y, Zhu X, Li X et al (2017) The process-related dynamics of microbial community during a simulated fermentation of Chinese strong-flavored liquor. BMC Microbiol 17:196. https://doi.org/10.1186/s12866-017-1106-3
81. Aggelopoulos T, Katsieris K, Bekatorou A et al (2014) Solid state fermentation of food waste mixtures for single cell protein, aroma volatiles and fat production. Food Chem 145:710–716. https://doi.org/10.1016/j.foodchem.2013.07.105
82. Haidvogel W (2013) Pilzzucht und -verarbeitung. In: Hinker M, Seibert M (eds) Pilze in Innenräumen und am Arbeitsplatz, 1 Aufl. Springer, Wien, pp 51–62
83. Rühl M, Kües U (2007) Mushroom production. In: Kües U (ed) Wood production, wood technology, and biotechnological impacts. Universitätsverlag Göttingen, Göttingen, pp 555–586
84. Sánchez C (2010) Cultivation of *Pleurotus ostreatus* and other edible mushrooms. Appl Microbiol Biotechnol 85:1321–1337. https://doi.org/10.1007/s00253-009-2343-7
85. Pfaltzgraff LA, de Bruyn M, Cooper EC et al (2013) Food waste biomass: a resource for high-value chemicals. Green Chem 15:307. https://doi.org/10.1039/c2gc36978h

86. Rühl M, Zorn H (2016) Speisepilze – wertvolle Lebensmittel seit der Steinzeit: Nutritive und pharmakologische Eigenschaften, Kultivierung und Nutzen für die Entwicklung veganer Lebensmittel. Moderne Ernährung heute, vol 3
87. Fraatz MA, Zorn H (2010) Fungal flavours. In: Hofrichter M (ed) The mycota X: industrial applications, 2. Aufl. Springer, Berlin, pp S.249–264
88. Dickschat JS (2017) Fungal volatiles – a survey from edible mushrooms to moulds. Nat Prod Rep 34:310–328. https://doi.org/10.1039/c7np00003k
89. Gross B, Asther M (1989) Aromas from basidiomycetes: characteristics, analysis and production. Sci Aliment 9:427–454
90. Royse DJ, Bahler CC (1986) Effects of genotype, spawn run time, and substrate formulation on biological efficiency of shiitake. Appl Environ Microbiol 52:1425–1427
91. Kabbaj W, Breheret S, Guimberteau J et al (2002) Comparison of volatile compound production in fruit body and in mycelium of *Pleurotus ostreatus* identified by submerged and solid-state cultures. Appl Biochem Biotechnol 102:463–469. https://doi.org/10.1385/ABAB:102-103:1-6:463
92. Omarini A, Dambolena JS, Lucini E et al (2016) Biotransformation of 1,8-cineole by solid-state fermentation of Eucalyptus waste from the essential oil industry using *Pleurotus ostreatus* and *Favolus tenuiculus*. Folia Microbiol (Praha) 61:149–157. https://doi.org/10.1007/s12223-015-0422-y
93. Wu J, Wang C, Huang G et al (2016) Biotransformation of vine tea (*Ampelopsis grossedentata*) by solid-state fermentation using medicinal fungus *Poria cocos*. J Food Sci Technol 53:3225–3232. https://doi.org/10.1007/s13197-016-2297-6
94. Xia Y, Zhang B, Li W et al (2011) Changes in volatile compound composition of *Antrodia camphorata* during solid state fermentation. J Sci Food Agric 91:2463–2470. https://doi.org/10.1002/jsfa.4488
95. Ruiz-Dueñas FJ, Martínez AT (2009) Microbial degradation of lignin: how a bulky recalcitrant polymer is efficiently recycled in nature and how we can take advantage of this. Microb Biotechnol 2:164–177. https://doi.org/10.1111/j.1751-7915.2008.00078.x
96. Lapadatescu C, Ginies C, Le Quere JL et al (2000) Novel scheme for biosynthesis of aryl metabolites from L-phenylalanine in the fungus Bjerkandera adusta. Appl Environ Microbiol 66:1517–1522
97. Lapadatescu C, Bonnarme P (1999) Production of aryl metabolites in solid-state fermentations of the white-rot fungus *Bjerkandera adusta*. Biotechnol Lett 21:763–769. https://doi.org/10.1023/A:1005527205998
98. Lapadatescu C, Feron G, Vergoignan C et al (1997) Influence of cell immobilization on the production of benzaldehyde and benzyl alcohol by the white-rot fungi *Bjerkandera adusta*, *Ischnoderma benzoinum* and *Dichomitus squalens*. Appl Microbiol Biotechnol 47:708–714. https://doi.org/10.1007/s002530050999
99. Kleofas V, Sommer L, Fraatz MA et al (2014) Fruiting body production and aroma profile analysis of *Agrocybe aegerita* cultivated on different substrates. Nat Resour 5:233–240. https://doi.org/10.4236/nr.2014.56022
100. Kües U (2015) From two to many: multiple mating types in basidiomycetes. Fungal Biol Rev 29:126–166. https://doi.org/10.1016/j.fbr.2015.11.001
101. Freihorst D, Brunsch M, Wirth S et al (2018) Smelling the difference: transcriptome, proteome and volatilome changes after mating. Fungal Genet Biol 112:2–11. https://doi.org/10.1016/j.fgb.2016.08.007
102. Herzog R, Solovyeva I, Rühl M et al (2016) Dikaryotic fruiting body development in a single dikaryon of *Agrocybe aegerita* and the spectrum of monokaryotic fruiting types in its monokaryotic progeny. Mycol Prog 15:947–957. https://doi.org/10.1007/s11557-016-1221-9

Volatilomes of *Cyclocybe aegerita* during different stages of monokaryotic and dikaryotic fruiting.

Orban, A., Hennicke, F., and Rühl, M.

Biol. Chem. 2020, *401*, 995–1004.

DOI: 10.1515/hsz-2019-0392

Axel Orban, Florian Hennicke and Martin Rühl*

Volatilomes of *Cyclocybe aegerita* during different stages of monokaryotic and dikaryotic fruiting

https://doi.org/10.1515/hsz-2019-0392
Received October 10, 2019; accepted January 9, 2020

Abstract: Volatile organic compounds (VOC) are characteristic for different fungal species. However, little is known about VOC changes during development and their biological role. Therefore, we established a laboratory cultivation system in modified crystallizing dishes for analyzing VOC during fruiting body development of the dikaryotic strain *Cyclocybe aegerita* AAE-3 as well as four monokaryotic offspring siblings exhibiting different fruiting phenotypes. From these, VOC were extracted directly from the headspace (HS) and analyzed by means of gas chromatography-mass spectrometry (GC-MS). For all tested strains, alcohols and ketones, including oct-1-en-3-ol, 2-methylbutan-1-ol and cyclopentanone, were the dominant substances in the HS of early developmental stages. In the dikaryon, the composition of the VOC altered with ongoing fruiting body development and, even more drastically, during sporulation. At the latter stage, sesquiterpenes, especially Δ^6-protoilludene, α-cubebene and δ-cadinene, were the dominant substances. After sporulation, the amount of sesquiterpenes decreased, while additional VOC, mainly octan-3-one, appeared. In the HS of the monokaryons, less VOC were present of which all were detectable in the HS of the dikaryon *C. aegerita* AAE-3. The results of the present study show that the volatilome of *C. aegerita* changes considerably depending on the developmental stage of the fruiting body.

Keywords: Basidiomycota; fungi; mushroom aroma; sesquiterpenes; SPME-GC-MS; volatile organic compounds.

***Corresponding author: Martin Rühl,** Institute of Food Chemistry and Food Biotechnology, Justus Liebig University Giessen, D-35392 Giessen, Germany; and Institute for Molecular Biology and Applied Ecology IME Branch for Bioresources, D-35392 Giessen, Germany, e-mail: martin.ruehl@uni-giessen.de. https://orcid.org/0000-0001-8274-8175
Axel Orban: Institute of Food Chemistry and Food Biotechnology, Justus Liebig University Giessen, D-35392 Giessen, Germany
Florian Hennicke: Junior Research Group Genetics and Genomics of Fungi, Senckenberg Biodiversity and Climate Research Centre (SBiK-F), Senckenberg Gesellschaft für Naturforschung/Goethe University Frankfurt, D-60325 Frankfurt/Main, Germany

Introduction

The composition of aroma compounds is an essential quality characteristic of edible fungi. Various studies dealt with the aroma profile of fungi, which is often diverse and characteristic for each species (reviewed in Fraatz and Zorn, 2011; Dickschat, 2017). Depending on the substances contributing most to the overall flavor, fungi might be classified in three categories (Fraatz and Zorn, 2011). The first group is dominated by carbon-eight derivatives, such as oct-1-en-3-ol, octan-3-one and oct-1-en-3-one, perceived as 'typical' mushroom odors. Fungi with high amounts of terpenoid volatiles can be regarded as members of the second group and the last fraction consists of fungi rich in aroma active sulfur containing compounds. The white-rot fungus *Cyclocybe aegerita* is a member of the order Agaricales and inhabits mainly decaying wood, especially poplar and willow trees (Esser et al., 1974; Walther and Weiss, 2006). The volatile organic compounds (VOC) of *C. aegerita* fruiting bodies have been analyzed by means of solvent extraction (Rapior et al., 1998; Kleofas et al., 2014) and solid phase microextraction (SPME) (Costa et al., 2015). These studies revealed mushroom typical C8 alcohols and ketones like oct-1-en-3-ol, octan-3-ol, octan-1-ol, oct-1-en-3-one and octan-3-one as major substances in fruiting bodies, as well as benzaldehyde and 2-phenylethanol, contributing with almond and rose-like odors to the overall aroma impression. As in almost all studies on fungal VOC, these works were performed with fungal specimens derived solely from one developmental stage. Several studies investigated a time-dependent volatile profile of mushrooms after harvesting the corresponding fruiting bodies (Cruz et al., 1997; Mau et al., 1997; Wu et al., 2005; Cho et al., 2006; Zawirska-Wojtasiak et al., 2007; Zhang et al., 2008; Combet et al., 2009; Holighaus et al., 2014; Li et al., 2016; Tasaki et al., 2019). However, only one study analyzed different fruiting stages under nearly natural circumstances (Fäldt et al., 1999). Thus, a comprehensive analysis of the volatilome during different stages of fungal development in mushrooms is desirable, especially in light of the importance of VOC regarding fungal communication. In fact, several studies demonstrated

that C8 VOC have an influence on invertebrate behavior and might have an important function as 'infochemicals' (reviewed in Holighaus and Rohlfs, 2019). This includes the ability of some invertebrate species to distinguish between C8 enantiomers (Thakeow et al., 2008), preferring different VOC depending on sex (Thakeow et al., 2008) and life stage (Holighaus and Rohlfs, 2019) as well as the impact of VOC on predator-prey relationships (Steiner et al., 2007; Cevallos et al., 2017). VOC as fungal infochemicals probably play an important role in fungal survival, by repelling fungal predators or attracting insects for the purpose of spore dispersal (Holighaus and Rohlfs, 2019). Besides their role as infochemicals in interspecific communication, C8 VOC have been proven to have an influence on biological processes in fungi. Chitarra et al. (2005) reported inhibition of conidia germination by oct-1-en-3-ol in *Penicillium paneum*, whereas octan-3-one and less pronounced also octan-3-ol and oct-1-en-3-ol stimulated the conidiation in *Trichoderma* spp. (Nemčovič et al., 2008).

These different effects indicate that the fungal volatilome probably has to change during different developmental stages adapting to the altered requirements of the fungus. In this context, we analyzed all VOC emitted by *C. aegerita* during its life cycle under laboratory conditions, including dikaryotic fruiting body development as well as sporulation and its mating-independent fruiting mode, the monokaryotic fruiting *sensu stricto* (Herzog et al., 2019). Thus, we analyzed the volatilomes of the dikaryon *C. aegerita* AAE-3 and four monokaryons germinated from its basidiospores, which representatively show a full spectrum of monokaryotic fruiting phenotypes that can be exhibited by this fungal species. Phenotypes range from strains producing only monokaryotic initials, over others displaying elongated initials, to strains that can form differentiated monokaryotic mushrooms (Herzog et al., 2016). To clarify the potential role of VOC during different developmental stages of *C. aegerita*, the VOC produced during fruiting of *C. aegerita* AAE-3-derived monokaryons, each exhibiting a different monokaryotic fruiting phenotype, are compared to the VOC produced during fruiting of the dikaryon *C. aegerita* AAE-3. This comparison allows identifying certain VOC that are characteristic for a distinct developmental step in *C. aegerita* fruiting body development, such as VOC that are specific to sexual sporulation (involving meiosis). The latter only occurs in mushroom formation by the dikaryotic strain (Herzog et al., 2016). In addition, the analysis of the VOC will verify to what extent their production depends on a certain monokaryotic fruiting phenotype (monokaryons vs. monokaryons) or on the karyotype (monokaryons vs. dikaryons) of the specimens.

The clarification of the biological role of fungal VOC is not trivial, as already a non invasive monitoring of the VOC under natural circumstances can be challenging. Generally, a problematic aspect of studies on fungal VOC is the sample preparation. Fruiting bodies are damaged or chopped before extraction of the VOC. This procedure can create artefacts by disrupting cell structures and promote unwanted enzymatic reactions, which would naturally not occur (Fäldt et al., 1999; Combet et al., 2009). To overcome this problematic issue, we established a system to extract VOC in the headspace (HS) of *C. aegerita* cultures, allowing the analysis of VOC during all developmental stages without disturbing the fungal culture (Orban et al., 2019). Applying this system, the first comprehensive analysis of VOC produced during different developmental stages of dikaryotic and monokaryotic *C. aegerita* strains was conducted as a fundament to study the biological role of fungal VOC.

Results

Fruiting body development in *C. aegerita*

Cyclocybe aegerita AAE-3 was able to produce fruiting bodies and basidiospores under the chosen cultivation conditions (Figure 1). In all monokaryotic cultures, in agreement with a previous work (Herzog et al., 2016) no sexual sporulation, visible as spore print formation around the fruiting bodies, was observed (Figure 2). Among the monokaryons, *C. aegerita* AAE-3-40 and *C. aegerita* AAE-3-32 showed fruiting patterns comparable to previously reported ones (Herzog et al., 2016), whereas the fruiting phenotypes of *C. aegerita* AAE-3-37 and *C. aegerita* AAE-3-24 differed remarkably (for details see Supplementary Table S1). These differences may relate to the change in the cultivation conditions over the ones applied by Herzog et al. (2016), who discussed that a fruiter monokaryons' phenotype may vary depending on the cultivation setup, apparently also applies to non-fruiter phenotypes. The mycelium of the monokaryotic strains *C. aegerita* AAE-3-32 and *C. aegerita* AAE-3-24 exhibited growth rates similar to the dikaryotic strain *C. aegerita* AAE-3 whereas the monokaryons *C. aegerita* AAE-3-37 and *C. aegerita* AAE-3-40 grew slightly slower resulting in a not fully overgrown agar plate at day 10 (Figures 1 and 2).

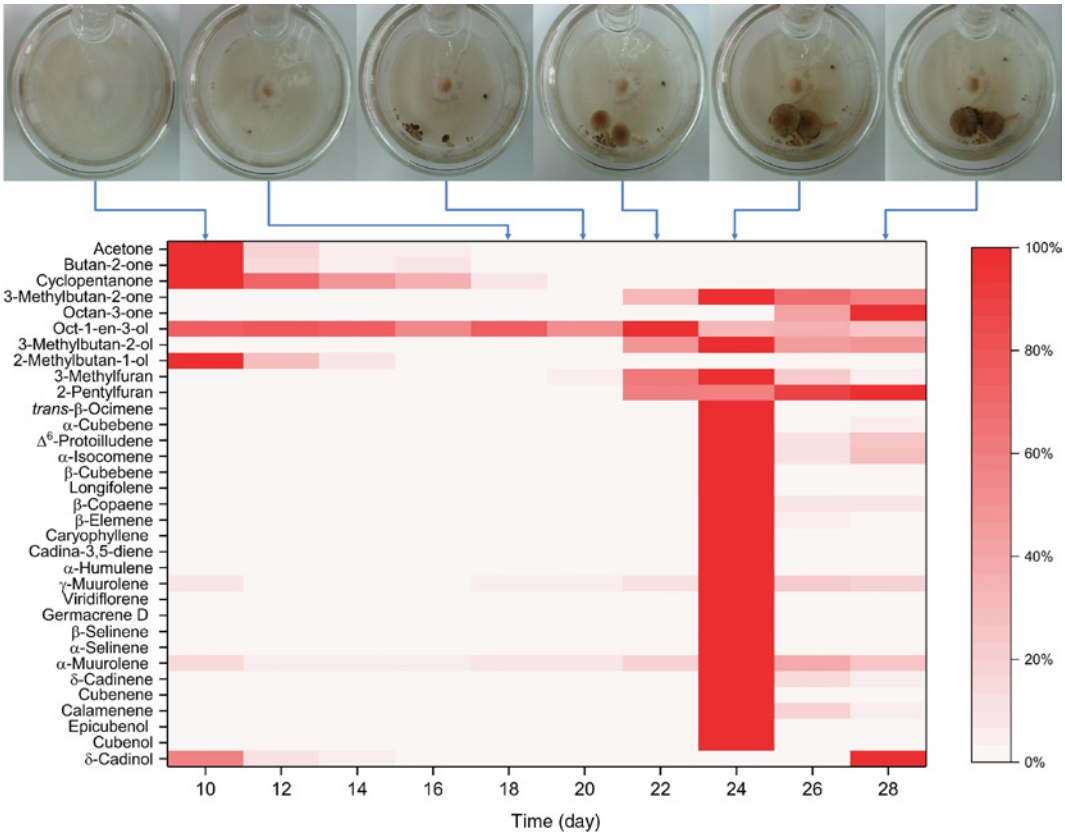

Figure 1: VOC of the dikaryotic strain *C. aegerita* AAE-3.
Shown is the development of the relative amount of volatiles between days 10 and 28 after inoculation. The percent disclosure refers to each substance and strain individually, meaning that 100% is related to the highest amount of the compound measured during the experiment. Samples were grown in triplicates at 24°C in the dark in modified crystallizing dishes containing 16 ml 1.5% MEA medium and sealed with Parafilm™. Ten days after inoculation, the Parafilm™ was removed, samples were transferred to a climate chamber (24°C, 95% RH, 12/12 h day/night rhythm) and cultured for further 18 days. VOC were collected by SPME from day 10 onwards: volatiles were absorbed directly from the HS of the crystallizing dishes for 14 h (7/7 h day/night) and analyzed by means of GC-MS.

VOC in the HS of *C. aegerita*

In total, about 150 substances were detected by means of gas chromatography-mass spectrometry (GC-MS) during cultivation in the HS of the tested strains. The fungal aroma compound oct-1-en-3-ol was present throughout the analyzed samples. Most substances occurred in the dikaryon *C. aegerita* AAE-3 at day 24 during its sporulation, with sesquiterpenes being the vast majority (Figure 3). Due to structural similarities of these substances, only a handful of them were identified using authentic standards and wood oils. In contrast to the dikaryotic strain, the tested monokaryotic siblings showed remarkably less VOC in the HS, all of them were also detected in dikaryotic samples (Table 1). In the HS of all tested strains, mostly alcohols and ketones, including 2-methylbutan-1-ol, acetone, butan-2-one and cyclopentanone, were the dominant substances at early developmental stages decreasing with ongoing cultivation.

VOC of the dikaryotic strain *C. aegerita* AAE-3

Regarding the HS of *C. aegerita* AAE-3, the development of fruiting bodies was accompanied by the appearance of 3-methylbutan-2-one, 3-methylbutan-2-ol, 3-methylfuran and 2-pentylfuran, all except the latter one with highest amounts at day 24 during sporulation and all only detected in the HS of the dikaryon (Figure 1, Table 1). Furthermore, at the time of sporulation, sesquiterpenes were the main volatiles in the HS of the dikaryon regarding the number of substances as well as the measured peak areas with Δ^6-protoilludene (about 50% of the total peak area), α-cubebene (about 12% of the total peak area) and δ-cadinene (about 7% of the total peak area) being the most dominant substances. Similar to the appearance of δ-cadinol, 2-pentylfuran and octan-3-one were most prominent at day 28, the latter VOC solely appearing after sporulation. It is worth mentioning that the rising amount

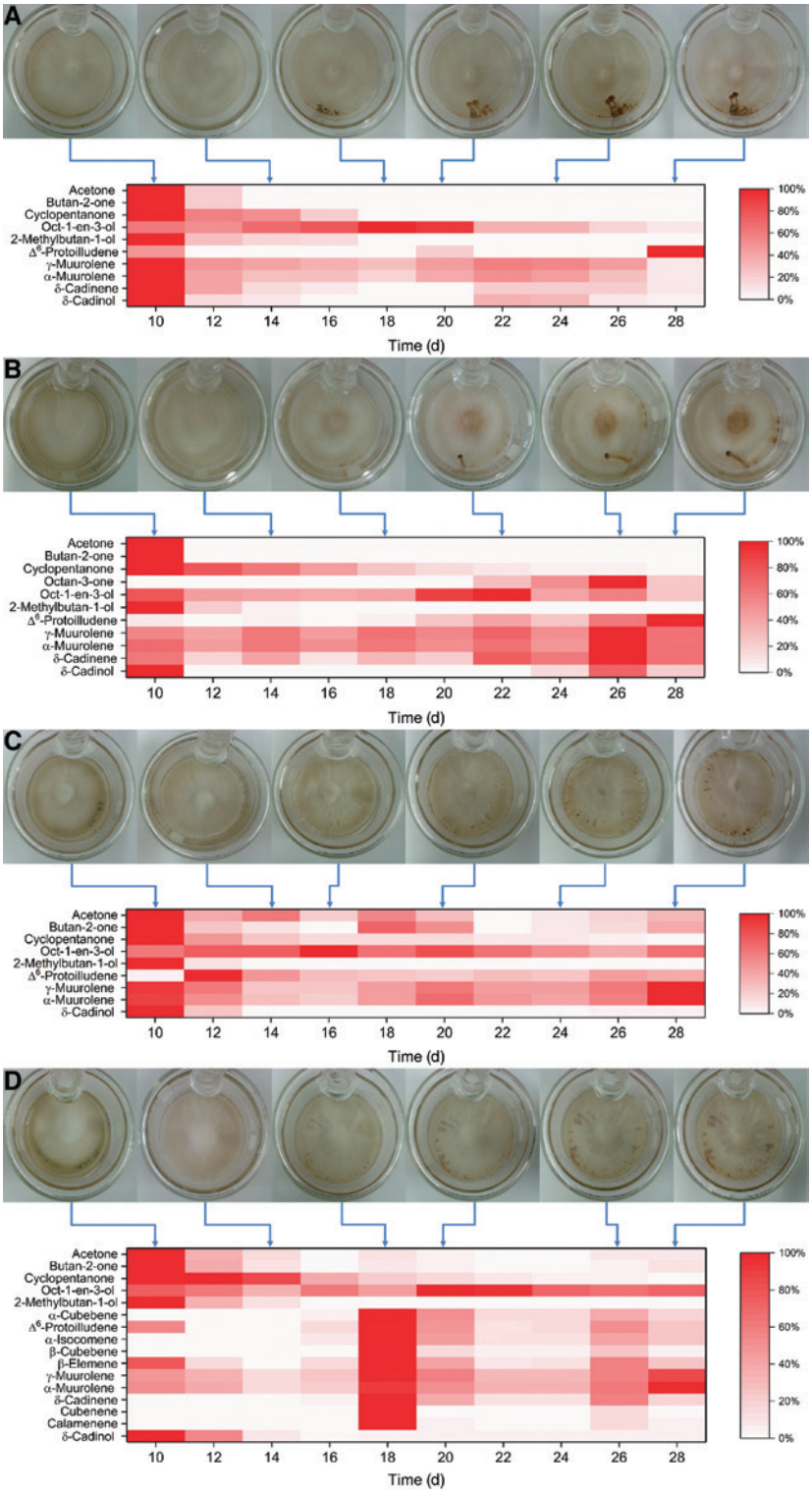

Figure 2: VOC of different monokaryotic *C. aegerita* strains.
(A) *C. aegerita* AAE-3-32, (B) *C. aegerita* AAE-3-24, (C) *C. aegerita* AAE-3-37 and (D) *C. aegerita* AAE-3-40. Shown is the development of the relative amount of volatiles between days 10 and 28 after inoculation. The percent disclosure refers to each substance and strain individually, meaning that 100% is related to the highest amount of the compound measured during the experiment. Strains were grown in triplicates at 24°C in the dark in modified crystallizing dishes containing 16 ml 1.5% MEA medium and sealed with Parafilm™. Ten days after inoculation, the Parafilm™ was removed, samples were transferred to a climate chamber (24°C, 95% rH, 12/12 h day/night rhythm) and cultured for further 18 days. VOC were collected by SPME from day 10 onwards: volatiles were absorbed directly from the HS of the crystallizing dishes for 14 h (7/7 h day/night) and analyzed by means of GC-MS.

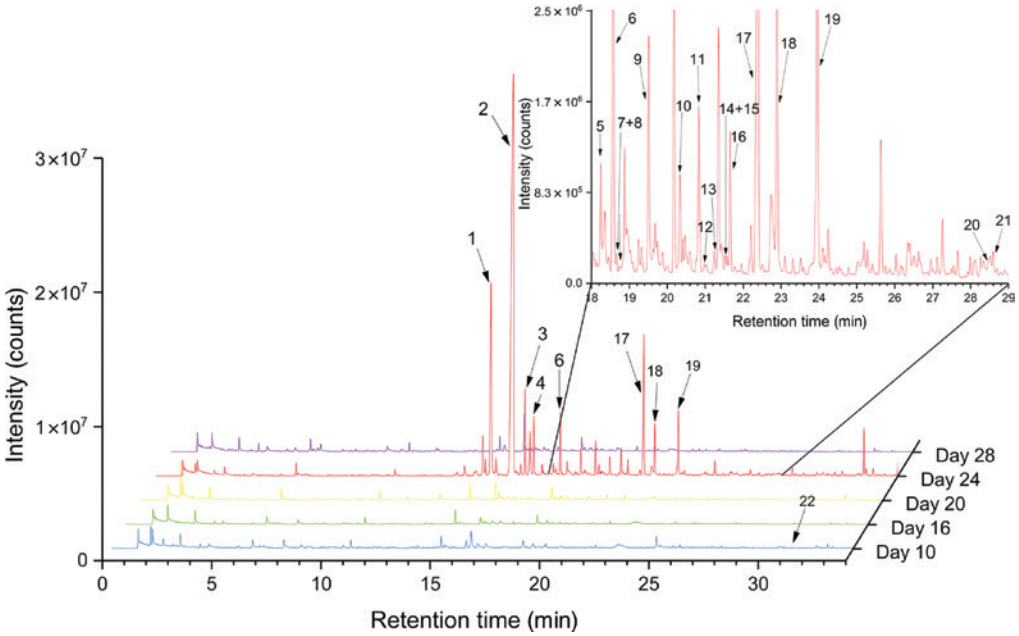

Figure 3: Comparison of GC-MS chromatograms of HS-SPME extracts of *C. aegerita* AAE-3 culture at day 10 (young mycelium), 16 (mycelium), 20 (young fruiting bodies), 24 (sporulation) and 28 (post sporulation).
With (1) α-cubebene, (2) Δ^6-protoilludene, (3) α-isocomene, (4) β-cubebene, (5) longifolene, (6) β-copaene, (7) β-elemene, (8) caryophyllene, (9) cadina-3,5-diene, (10) α-humulene, (11) γ-muurolene, (12) viridiflorene, (13) germacrene D, (14) β-selinene, (15) α-selinene, (16) α-muurolene, (17) δ-cadinene, (18) cubebene, (19) calamenene, (20) epicubenol, (21) cubenol and (22) δ-cadinol.

of octan-3-one after day 24 was accompanied by a decreasing concentration of oct-1-en-3-ol.

VOC of the monokaryotic *C. aegerita* strains

Generally, in the HS of all monokaryotic strains the peak areas of all sesquiterpenes, except for δ-cadinol, were lower in comparison to the dikaryotic strain *C. aegerita* AAE-3. For instance, the highest detected peak area of Δ^6-protoilludene in the latter strain with a value of $1.1\times10^8\pm0.9\times10^8$ was about 550 times, 325 times, 125 times and 15 times higher than in the monokaryotic strains *C. aegerita* AAE-3-32 ($2.0\times10^5\pm1.1\times10^5$), *C. aegerita* AAE-3-37 ($3.4\times10^5\pm1.0\times10^5$), *C. aegerita* AAE-3-24 ($8.9\times10^5\pm1.0\times10^5$) and *C. aegerita* AAE-3-40 ($8.1\times10^6\pm4.4\times10^6$), respectively. It is worth mentioning that, among all the tested strains, *C. aegerita* AAE-3-32 showed the lowest sesquiterpene peak areas. Interestingly, δ-cadinol, which shows the highest presence at day 10 of cultivation in all monokaryotic strains, re-occurred at later stages only in *C. aegerita* AAE-3-32 and *C. aegerita* AAE-3-24 strains after development of immature fruiting bodies (Figure 2A, B).

Similar to the dikaryotic strain *C. cinerea* AAE-3, two C8 VOC oct-1-en-3-ol and octan-3-one were detected with the monokaryotic siblings. Oct-1-en-3-ol was present in all analyzed strains throughout the cultivation period, whereas octan-3-one peaks where only evaluable in the HS of *C. aegerita* AAE-3-24 cultures. Here, octan-3-one could be detected after the formation of immature fruiting bodies at day 22 with an increasing concentration until immature fruiting bodies had formed at day 26 (Figure 2B). Interestingly, the amount of oct-1-en-3-ol peaked at day 22 and decreased, comparable with the VOC profile in the HS of the dikaryon, with the rising amount of octan-3-one. In the second monokaryon producing fruiting bodies, *C. aegerita* AAE-3-32, which, in contrast to *C. aegerita* AAE-3-24, also forms mushrooms with expanded caps (exhibiting impaired cap-opening in contrast to the dikaryotic fruiting bodies formed by *C. aegerita* AAE-3, see Herzog et al., 2016), small amounts of octan-3-one were detected from day 24 on. Nonetheless, the octan-3-one level was too small for an adequate identification and, thus, this compound is not represented in Table 1 and Figure 2A. In both other monokaryotic strains *C. aegerita* AAE-3-37 and *C. aegerita* AAE-3-40, no indication for an octan-3-one production was found. In *C. aegerita* AAE-3-37 oct-1-en-3-ol showed the highest amount at day 16 with the beginning development of small fruiting bodies, whereas in *C. aegerita* AAE-3-40 oct-1-en-3-ol was most prominent at day 20 and stayed at a comparably high level until the end of cultivation.

Table 1: Total number of VOC found in the HS of the *C. aegerita strains*.

VOC	AAE-3	AAE-3-32	AAE-3-24	AAE-3-37	AAE-3-40
Acetone	+	+	+	+	+
Butan-2-one	+	+	+	+	+
Cyclopentanone	+	+	+	+	+
3-Methylbutan-2-one	+	–	–	–	–
Octan-3-one	+	–	+	–	–
Oct-1-en-3-ol	+	+	+	+	+
3-Methylbutan-2-ol	+	–	–	–	–
2-Methylbutan-1-ol	+	+	+	+	+
3-Methylfuran	+	–	–	–	–
2-Pentylfuran	+	–	–	–	–
trans-β-Ocimene	+	–	–	–	–
α-Cubebene	+	–	–	–	+
Δ^6-Protoilludene	+	+	+	+	+
α-Isocomene	+	–	–	–	+
β-Cubebene	+	–	–	–	+
Longifolene	+	–	–	–	–
β-Copaene	+	–	–	–	–
β-Elemene	+	–	–	–	+
Caryophyllene	+	–	–	–	–
Cadina-3,5-diene	+	–	–	–	–
α-Humulene	+	–	–	–	–
γ-Muurolene	+	+	+	+	+
Viridiflorene	+	–	–	–	–
Germacrene D	+	–	–	–	–
β-Selinene	+	–	–	–	–
α-Selinene	+	–	–	–	–
α-Muurolene	+	+	+	+	+
δ-Cadinene	+	+	+	–	+
Cubenene	+	–	–	–	+
Calamenene	+	–	–	–	+
Epicubenol	+	–	–	–	–
Cubenol	+	–	–	–	–
δ-Cadinol	+	+	+	+	+

+, VOC detected in the HS; –, VOC not detected in the HS.

Discussion

In our study, the composition of VOC in the HS of *C. aegerita*, especially of the dikaryotic strain *C. aegerita* AAE-3, revealed remarkable changes during development. Of the ca. 150 VOC detected, the C8 compounds, such as oct-1-en-3-ol and octan-3-one, were minor compounds regarding the measured peak areas, especially compared to the sesquiterpenes, which appeared during sporulation. The fact that C8 VOC were more dominant in previous studies on *C. aegerita* fruiting bodies (Rapior et al., 1998; Kleofas et al., 2014; Costa et al., 2015) might be related to the applied sample preparation and extraction methods as disrupting the cell structure has a tremendous impact on VOC released by fungi. Combet et al. (2009) showed that slicing fruiting bodies of *Agaricus bisporus* resulted in approximately 10 times higher concentrations of oct-1-en-3-ol and octan-3-one compared to whole sporophores. More remarkable than the amount of C8 compounds was their alteration during different stages of fungal development, especially the rising amount of octan-3-one after sporulation in connection with the decreasing amount of oct-1-en-3-ol. Alternations of the C8 profile during maturation of fungi has been reported previously. Wu et al. (2005) compared the volatile compounds in young and mature fruiting bodies of *Polyporus* (*Laetiporus*) *sulfureus*. Young fruiting bodies offered a pleasant fungal odor with five key aroma compounds, among them oct-1-en-3-one and oct-1-en-3-ol. Aged specimens, on the other hand, revealed four characteristic odorous compounds, *inter alia* 2-methylpropanoic acid, contributing to a repelling scent and only traces of oct-1-en-3-ol were detected. Similar to *C. aegerita*, the oct-1-en-3-ol content in the oyster mushroom *Pleurotus ostreatus* decreased

from the mycelium stage to the primordium stage and increased thereafter (Tasaki et al., 2019). Comparable variations in the occurrence of oct-1-en-3-ol and octan-3-one were reported for *A. bisporus* (Cruz et al., 1997). It is worth mentioning that these studies dealt with the analysis of the aroma profile of mushrooms to determine the VOC in the context of food quality, thus VOC during sporulation or stages beyond were not determined. Our study revealed that developmental stages have a huge impact on the overall volatilome of *C. aegerita* which probably also applies to other fungi. Nevertheless, a comparison of aroma profiles of harvested fruiting bodies with our own results suggest that the change of C8 VOC profiles is species-specific and might vary strongly. The question remains as to why VOC profiles of *C. aegerita* strains and other fungi change during fungal development. In this context, a study of Holighaus et al. (2014) is of special interest as they investigated the changes in the C8 VOC composition of four different fruiting body development stages of the tinder fungus *Fomes fomentarius* and monitored the occurrence of fungivorous beetles at the same time. The study revealed changes in the C8 VOC profile during development accompanied by a clear alternation of the fungal beetle community. The specialist fungivore *Bolitophagus reticulatus* seemed to prefer the second stage with octan-3-one being the most prominent C8 compounds and avoided the first stage with comparable high amounts of oct-1-en-3-ol. The ability of *B. reticulatus* to distinguish between different C8 VOC was further confirmed by a behavioral study consisting of walking olfactometer preference tests revealing that *B. reticulatus* is attracted by octan-3-one and repelled by oct-1-en-3-ol (Holighaus et al., 2014). Taking this into account, the remarkable changes in the VOC composition displayed by *C. aegerita* at different stages might be part of a fungus survival strategy, ensuring an efficient reproduction by, for example, avoiding predation at early stages and enhancing spore-dispersal by fungivores after sporulation. Furthermore, Eastwood et al. (2013) showed that high levels of oct-1-en-3-ol in the HS of *A. bisporus* inhibited the formation of hyphal knots (very early fruiting body initials, i.e. aggregates of loosely intertwined hyphae). This is in good agreement with our results of the VOC in the HS of the dikaryon *C. aegerita* AAE-3 displaying the highest amounts of oct-1-en-3-ol at day 22, where mature fruiting bodies might suppress the development of adjoining fruiting structures. Alongside mature fruiting bodies, immature ones were observed, which did not develop further. Thus, the enhanced amount of oct-1-en-3-ol might contribute to the repression of further fruiting body development of immature fruiting bodies.

Compared to the C8 VOC, the sesquiterpenes in the HS of *C. aegerita* AAE-3 displayed a huge diversity and were especially during sporulation the most prominent substances. The most dominant sesquiterpene in the HS of *C. aegerita* AAE-3, Δ^6-protoilludene, was first described in the fungus *Fomitopsis insularis* (Nozoe et al., 1977) and was later found in several fungi such as *Fomitopsis pinicola* (Rösecke et al., 2000), *Ceratocystis piceae* (Hanssen et al., 1986) and *Fomes fomentarius* (Fäldt et al., 1999; Holighaus et al., 2014). Other sesquiterpenes identified in the HS of *C. aegerita* such as α-muurolene and β-cubebene were also discovered in other fungi (Hanssen, 1982; Rösecke et al., 2000). Despite the high amounts of sesquiterpenes detected in the HS of *C. aegerita* AAE-3, none of these VOC were found in previous studies dealing with volatiles from *C. aegerita*. This might be connected to the fact that sesquiterpenes in larger quantities only occurred in the HS of the dikaryon during a short time period around the event of sporulation, stages which were not sampled before. Such stage-specific production was also observed in the HS of the bracket fungi *Fomitopsis pinicola* and *Fomes fomentarius*, where an obvious increase of sesquiterpenes, *inter alia* Δ^6-protoilludene, was observed during sporulation (Fäldt et al., 1999). Also in the HS of *Coprinopsis cinerea* cultures, the concentration of sesquiterpenes such as β-himachalene and cuparene remarkably increased along with stipe elongation and autolysis (Thakeow, 2008; Chaisaena, 2009), during which most spores are released (Kües, 2000).

Despite the demonstrated connection between sporulation and the release of sesquiterpenes, their biological role in fungi is scarcely elucidated. It has been proven that sesquiterpenes exhibit antimicrobial activities and might therefore protect fungi against other fungi or bacteria (Ishikawa et al., 2001; Solís et al., 2004) and, comparable with C8 VOC, terpenes might function as infochemicals (Kües et al., 2018). Sesquiterpenes observed in *C. aegerita* might also function as precursors for different bioactive nonvolatile substances. The most prominent sesquiterpene in the HS of *C. aegerita*, Δ^6-protoilludene, can be processed into illudins with antimicrobial effects as well as melleolides and sterostrein A (Quin et al., 2014). Recently, the triterpenoid bovistol was found in *C. aegerita*, proposed to be derived from illudins originated from Δ^6-protoilludene (Surup et al., 2019).

In comparison to the dikaryon, monokaryons revealed remarkably less VOC in the HS. Interestingly, octan-3-one only appeared in the HS of *C. aegerita* strains with fruiting bodies. Unlike oct-1-en-3-ol, which was present in all strains and stages, octan-3-one seemed to be exclusively connected to the growth of fruiting bodies. Therefore, it

can be speculated that octan-3-one is produced in fruiting bodies rather than in the mycelium or, at least, that the presence of fruiting bodies is necessary for the biosynthesis. Overall, studies looking into volatiles of monokaryons and dikaryons are very rare. Omarini et al. (2014) investigated the biotransformation of valencene to nootkatone using *Pleurotus sapidus* and *Pleurotus florida*. The nootkatone production varied strongly among strains but seemed more dependent on the genetic qualities of the strains rather than the monokaryotic or dikaryotic state of the specimens. Freihorst et al. (2018) studied VOC released by *Schizophyllum commune* before and after mating. In good agreement with our study, monokaryons of *S. commune* displayed a less diverse volatilome than the dikaryon. Interestingly, the C8 VOC octan-3-one and oct-1-en-3-ol as well as the sesquiterpene β-bisabolol only occurred in the HS of the dikaryon. It is worth mentioning that only one stage was tested and the volatilome for monokaryons and dikaryons probably undergoes changes during development as observed for *C. aegerita*.

The present study elucidated the connection between fungal VOC and developmental stages of *C. aegerita*. Although the appearance and the amount of some VOC seemed to be linked to certain developmental stages, the mycelium rather than the fruiting bodies might be the origin of sesquiterpene synthesis. This would also explain the small but concise amounts of sesquiterpenes, which appeared in the HS of *C. aegerita* AAE-3 at early developmental stages during and shortly after vegetative growth. In addition, the occurrence of sesquiterpenes in the HS of the monokaryon *C. aegerita* AAE-3-40, which did not develop fruiting bodies, indicates a mycelium-based sesquiterpene production. In further studies, the knowledge about the tight connections between specific developmental stages and VOC production, combined with transcriptomics and proteomics approaches, should be addressed for the clarification of the scarcely understood biosynthesis of fungal VOC. Additionally, the remarkable changes in the volatilomes should be taken into account during further studies dealing with, for example, fungal intra- and interspecific VOC-based communication.

Materials and methods

Fungal strains and growth conditions

The tested dikaryotic strain *C. aegerita* AAE-3 and monokaryotic strains *C. aegerita* AAE-3-24, *C. aegerita* AAE-3-32, *C. aegerita* AAE-3-37 and *C. aegerita* AAE-3-40 were each grown in triplicates at 24°C in the dark in modified crystallizing dishes (lower dish: 70 mm in diameter, upper dish: 80 mm in diameter; glass pipe attached to the upper dish: outer diameter 16 mm, inner diameter 14 mm) with 16 ml 1.5% malt extract agar (MEA) (containing 15 g malt extract and 15 g agar per litre) and sealed with Parafilm™ (for a picture of the set up see Orban et al., 2019). Ten days after the inoculation, the Parafilm™ was removed and the samples were transferred to a climate chamber RUMED 3501 (Rubarth Apparate GmbH, Laatzen, Germany) (24°C, 95% relative humidity (RH), 12/12 h day/night rhythm) and cultured on glass plates for further 18 days.

Analysis of VOC by GC-MS

VOC were collected by SPME using a divinylbenzene-carboxen-polydimethylsiloxane (50/30 µm DVB/CAR/PDMS) fiber (Agilent Technologies, Santa Clara, CA, USA). Beginning with day 10 after inoculation, VOC were absorbed directly in the HS of the crystallizing dishes for 14 h (7/7 h day/night). This extraction was carried out every second day. For GC-MS analysis, an Agilent Technologies 7890A gas chromatograph equipped with Agilent VF-WAXms column (30 m × 0.25 mm, 0.25 µm) and connected to an Agilent 5975C MSD Triple-Axis mass spectrometer was used. Helium was used as a gas carrier, with a flow rate of 1.2 $ml \times min^{-1}$. Mass spectra were acquired in the mass range of 33–300 *m/z*. Ionization was performed by electron impact at 70 eV with an ion source temperature set at 230°C. The SPME fiber was inserted into the injector of the gas chromatograph for thermal desorption in splitless mode for 1 min, with the injector temperature held at 250°C. The GC oven temperature was programmed to ramp from 40°C (hold for 3 min) to 240°C (hold for 7 min) at $5°C \times min^{-1}$. VOC were identified initially by comparing obtained mass spectra with data from the NIST14 database (National Institute of Standards and Technology, Gaithersburg, MD, USA). Furthermore, Kovats retention indices of VOC were determined with a C7–C30 alkane mix and were compared to the published retention indices in literature or in the NIST database. Except for α-isocomene, longifolene, β-copaene, cadin-3,5-diene, β-selinene, α-selinene, cubenene and epicubenol, VOC structures were additionally verified by comparison of retention time and mass spectra with authentic standards or essential oils with known terpene compositions [Agger et al., 2009; Lopez-Gallego et al., 2010: cedrela woods oil (α-muurolene, δ-cadinene), cubeb oil (germacrene D, γ-muurolene, cubenol) and amyris wood oil (δ-cadinol)].

Data processing

The peak areas of identified substances were determined and used to calculate the relative amount of the respective VOC. Therefore, each substance of every sample was considered individually, meaning that 100% is related to the highest peak area of the compound measured in a sample during the experiment. The mean value of the relative VOC amounts of the triplicates was calculated for each substance (see Supplementary Table S2) and, afterwards, normalized to 100%. This approach enabled an appropriate overview about the connections between developmental stages and VOC patterns in the HS, whereas a direct comparison of the peak areas is generally difficult due to the lack of a reference quantity. The normalized data were used to generate the heatmaps using OriginPro (OriginLab Corporation, Northampton, MA, USA).

Acknowledgments: This study was financially supported by the Deutsche Forschungsgemeinschaft (DFG, German Research Foundation) – Funder Id: http://dx.doi.org/10.13039/501100001659, Grant Number: RU 2137/1-1. The support by LOEWE (State-Offensive for the Development of Scientific and Economic Excellence) is gratefully acknowledged. The authors thank the two anonymous reviewers for helpful comments and suggestions that helped to improve this paper.

References

Agger, S., Lopez-Gallego, F., and Schmidt-Dannert, C. (2009). Diversity of sesquiterpene synthases in the basidiomycete *Coprinus cinereus*. Mol. Microbiol. *72*, 1181–1195.

Cevallos, J.A., Okubo, R.P., Perlman, S.J., and Hallem, E.A. (2017). Olfactory preferences of the parasitic nematode *Howardula aoronymphium* and its insect host *Drosophila falleni*. J. Chem. Ecol. *43*, 362–373.

Chaisaena, W. (2009). Light Effects on Fruiting Body Development of Wildtype in Comparison to Light-insensitive Mutant Strains of the Basidiomycete *Coprinopsis cinerea*, Grazing of Mites (*Tyrophagus putrescentiae*) on the Strains and Production of Volatile Organic Compounds during Fruiting Body Development. PhD thesis (Göttingen, Germany: University of Göttingen).

Chitarra, G.S., Abee, T., Rombouts, F.M., and Dijksterhuis, J. (2005). 1-Octen-3-ol inhibits conidia germination of *Penicillium paneum* despite of mild effects on membrane permeability, respiration, intracellular pH, and changes the protein composition. FEMS Microbiol. Ecol. *54*, 67–75.

Cho, I.H., Choi, H.-K., and Kim, Y.-S. (2006). difference in the volatile composition of pine-mushrooms (*Tricholoma matsutake* Sing.) according to their grades. J. Agric. Food Chem. *54*, 4820–4825.

Combet, E., Henderson, J., Eastwood, D.C., and Burton, K.S. (2009). Influence of sporophore development, damage, storage, and tissue specificity on the enzymic formation of volatiles in mushrooms (*Agaricus bisporus*). J. Agric. Food Chem. *57*, 3709–3717.

Costa, R., De Grazia, S., Grasso, E., and Trozzi, A. (2015). Headspace-solid-phase microextraction-gas chromatography as analytical methodology for the determination of volatiles in wild mushrooms and evaluation of modifications occurring during storage. J. Anal. Methods Chem. *2015*, 951748.

Cruz, C., Noël-Suberville, C., and Montury, M. (1997). Fatty acid content and some flavor compound release in two strains of *Agaricus bisporus*, according to three stages of development. J. Agric. Food Chem. *45*, 64–67.

Dickschat, J.S. (2017). Fungal volatiles – a survey from edible mushrooms to moulds. Nat. Prod. Rep. *34*, 310–328.

Eastwood, D.C., Herman, B., Noble, R., Dobrovin-Pennington, A., Sreenivasaprasad, S., and Burton, K.S. (2013). Environmental regulation of reproductive phase change in *Agaricus bisporus* by 1-octen-3-ol, temperature and CO_2. Fungal Genet. Biol. *55*, 54–66.

Esser, K., Semerdžieva, M., and Stahl, U. (1974). Genetische Untersuchungen an dem Basidiomyceten *Agrocybe aegerita*. Theor. Appl. Genet. *45*, 77–85.

Fäldt, J., Jonsell, M., Nordlander, G., and Borg-Karlson, A.-K. (1999). Volatiles of bracket fungi *Fomitopsis pinicola* and *Fomes fomentarius* and their functions as insect attractants. J. Chem. Ecol. *25*, 567–590.

Fraatz, M.A. and Zorn, H. (2011). Fungal flavours. In: Industrial Applications, M. Hofrichter, ed. (Berlin, Heidelberg: Springer Berlin-Heidelberg), pp. 249–268.

Freihorst, D., Brunsch, M., Wirth, S., Krause, K., Kniemeyer, O., Linde, J., Kunert, M., Boland, W., and Kothe, E. (2018). Smelling the difference: transcriptome, proteome and volatilome changes after mating. Fungal Genet. Biol. *112*, 2–11.

Hanssen, H.-P. (1982). Sesquiterpene hydrocarbons from *Lentinus lepideus*. Phytochemistry *21*, 1159–1160.

Hanssen, H.-P., Sprecher, E., and Abraham, W.-R. (1986). 6-Protoilludene, the major volatile metabolite from *Ceratocystis piceae* liquid cultures. Phytochemistry *25*, 1979–1980.

Herzog, R., Solovyeva, I., Rühl, M., Thines, M., and Hennicke, F. (2016). Dikaryotic fruiting body development in a single dikaryon of *Agrocybe aegerita* and the spectrum of monokaryotic fruiting types in its monokaryotic progeny. Mycol. Prog. *15*, 947–957.

Herzog, R., Solovyeva, I., Bölker, M., Lugones, L.G., and Hennicke, F. (2019). Exploring molecular tools for transformation and gene expression in the cultivated edible mushroom *Agrocybe aegerita*. Mol. Genet. Genom. *296*, 663–677.

Holighaus, G. and Rohlfs, M. (2019). Volatile and non-volatile fungal oxylipins in fungus-invertebrate interactions. Fungal Ecol. *38*, 28–36.

Holighaus, G., Weißbecker, B., von Fragstein, M., and Schütz, S. (2014). Ubiquitous eight-carbon volatiles of fungi are infochemicals for a specialist fungivore. Chemoecology *24*, 57–66.

Ishikawa, N.K., Fukushi, Y., Yamaji, K., Tahara, S., and Takahashi, K. (2001). Antimicrobial cuparene-type sesquiterpenes, enokipodins C and D, from a mycelial culture of *Flammulina velutipes*. J. Nat. Prod. *64*, 932–934.

Kleofas, V., Sommer, L., Fraatz, M.A., Zorn, H., and Rühl, M. (2014). Fruiting body production and aroma profile analysis of *Agrocybe aegerita* cultivated on different substrates. Nat. Resour. *05*, 233.

Kües, U. (2000). Life history and developmental processes in the Basidiomycete *Coprinus cinereus*. Microbiol. Mol. Biol. Rev. *64*, 316–353.

Kües, U., Khonsuntia, W., Subba, S., and Dörnte, B. (2018). Volatiles in communication of agaricomycetes. In: Physiology and Genetics: Selected Basic and Applied Aspects, T. Anke, and A. Schüffler, eds. (Cham: Springer International Publishing), pp. 149–212.

Li, Q., Zhang, L., Li, W., Li, X., Huang, W., Yang, H., and Zheng, L. (2016). Chemical compositions and volatile compounds of *Tricholoma matsutake* from different geographical areas at different stages of maturity. Food Sci. Biotechnol. *25*, 71–77.

Lopez-Gallego, F., Agger, S.A., Abate-Pella, D., Distefano, M.D., and Schmidt-Dannert, C. (2010). Sesquiterpene synthases Cop4 and Cop6 from *Coprinus cinereus*: Catalytic promiscuity and cyclization of farnesyl pyrophosphate geometric isomers. ChemBioChem *11*, 1093–1106.

Mau, J.-L., Chyau, C.-C., Li, J.-Y., and Tseng, Y.-H. (1997). Flavor compounds in straw mushrooms *Volvariella volvacea* harvested at different stages of maturity. J. Agric. Food Chem. *45*, 4726–4729.

Nemčovič, M., Jakubíková, L., Víden, I., and Farkaš, V. (2008). Induction of conidiation by endogenous volatile compounds in *Trichoderma* spp. FEMS Microbiol. Lett. *284*, 231–236.

Nozoe, S., Kobayashi, H., Urano, S., and Furukawa, J. (1977). Isolation of D^6-protoilludene and the related alcohols. Tetrahedron Lett *18*, 1381–1384.

Omarini, A.B., Plagemann, I., Schimanski, S., Krings, U., and Berger, R.G. (2014). Crosses between monokaryons of *Pleurotus sapidus* or *Pleurotus florida* show an improved biotransformation of (+)-valencene to (+)-nootkatone. Bioresour. Technol. *171*, 113–119.

Orban, A., Fraatz, M.A., and Rühl, M. (2019). Aroma profile analyses of filamentous fungi cultivated on solid substrates. Adv. Biochem. Engin./Biotechnol. *169*, 85–107.

Quin, M.B., Flynn, C.M., and Schmidt-Dannert, C. (2014). Traversing the fungal terpenome. Nat. Prod. Rep. *31*, 1449–1473.

Rapior, S., Breheret, S., Talou, T., Pelissier, Y., Milhau, M., and Bessiere, J.M. (1998). Volatile components of fresh *Agrocybe aegerita* and *Tricholoma sulfureum*. Cryptogam. Mycol. *19*, 15–23.

Rösecke, J., Pietsch, M., and König, W.A. (2000). Volatile constituents of wood-rotting basidiomycetes. Phytochemistry *54*, 747–750.

Solís, C., Becerra, J., Flores, C., Robledo, J., and Silva, M. (2004). Antibacterial and antifungal terpenes from *Pilgerodendron uviferum* (D. Don) Florin. J. Chil. Chem. Soc. *49*, 157–161.

Steiner, S., Erdmann, D., Steidle, J.L., and Ruther, J. (2007). Host habitat assessment by a parasitoid using fungal volatiles. Front. Zool. *4*, 3.

Surup, F., Hennicke, F., Sella, N., Stroot, M., Bernecker, S., Pfütze, S., Stadler, M., and Rühl, M. (2019). New terpenoids from the fermentation broth of the edible mushroom *Cyclocybe aegerita*. Beilstein J. Org. Chem. *15*, 1000–1007.

Tasaki, Y., Kobayashi, D., Sato, R., Hayashi, S., and Joh, T. (2019). Variations in 1-octen-3-ol and lipoxygenase gene expression in the oyster mushroom *Pleurotus ostreatus* according to fruiting body development, tissue specificity, maturity, and postharvest storage. Mycoscience *60*, 170–176.

Thakeow, P. (2008). Development of a Basic Biosensor System for Wood Degradation using Volatile Organic Compounds. PhD thesis (Göttingen, Germany: University of Göttingen).

Thakeow, P., Angeli, S., Weißbecker, B., and Schütz, S. (2008). Antennal and behavioral responses of Cis boleti to fungal odor of *Trametes gibbosa*. Chem. Senses *33*, 379–387.

Walther, G. and Weiss, M. (2006). Anamorphs of the Bolbitiaceae (Basidiomycota, Agaricales). Mycologia *98*, 792–800.

Wu, S., Zorn, H., Krings, U., and Berger, R.G. (2005). Characteristic volatiles from young and aged fruiting bodies of wild *Polyporus sulfureus* (Bull.:Fr.) Fr. J. Agric. Food Chem. *53*, 4524–4528.

Zawirska-Wojtasiak, R., Siwulski, M., Wasowicz, E., and Sobieralski, K. (2007). Volatile compounds of importance in the aroma of cultivated mushrooms *Agaricus bisporus* at different conditions of cultivation. Pol. J. Food Nutr. Sci. *57*, 367–372.

Zhang, Z.-M., Wu, W.-W., and Li, G.-K. (2008). A GC-MS study of the volatile organic composition of straw and oyster mushrooms during maturity and its relation to antioxidant activity. J. Chromatogr. Sci. *46*, 690–696.

Supplementary Material: The online version of this article offers supplementary material (https://doi.org/10.1515/hsz-2019-0392).

Volatilomes of *Cyclocybe aegerita* during different stages of monokaryotic and dikaryotic fruiting.

Orban, A., Hennicke, F., and Rühl, M.

Biol. Chem. 2020, *401*, 995–1004.

DOI: 10.1515/hsz-2019-0392

----------Supporting Information----------

Table S1: Comparison of monokaryotic fruiting observed by Herzog et al. (2016) and in the current study.

Monokaryotic *C. aegerita* strain	Fruiting type observed by Herzog et al., 2016	Fruiting type observed in the current study
C. aegerita AAE-3-24	Mycelium	Immature fruiting bodies with elongated stipes and unexpanded caps
C. aegerita AAE-3-40	Fruiting body initials	Fruiting body initials
C. aegerita AAE-3-37	Elongated initials	Elongated initials and small fruiting bodies
C. aegerita AAE-3-32	Fruiter (expanded, opening-impaired caps)	Fruiter (expanded, opening-impaired caps)

Table S2.1: Relative amounts of VOCs in the HS of the dikaryotic strain *C. aegerita* AAE-3 between the days 10 and 28.

	Day 10		Day 12		Day 14		Day 16		Day 18		Day 20		Day 22		Day 24		Day 26		Day 28	
	Mean value	Standard deviation	Mean value	Standard deviation	Mean value	Standard deviation	Mean value	Standard deviation	Mean value	Standard deviation	Mean value	Standard deviation	Mean value	Standard deviation	Mean value	Standard deviation	Mean value	Standard deviation	Mean value	Standard deviation
Acetone	100	0	17	15	4	5	6	8	3	4	0	1	0	0	0	0	0	0	0	0
Butan-2-one	100	0	16	13	4	5	8	11	2	3	0	0	0	0	0	0	0	0	0	0
Cyclopentanone	100	0	73	13	49	6	34	15	10	8	3	4	0	0	0	0	0	0	0	0
3-Methylbutan-2-one	0	0	0	0	0	0	0	0	0	0	0	0	30	23	95	7	68	40	55	23
Octan-3-one	0	0	0	0	0	0	0	0	0	0	0	0	0	0	0	0	41	38	100	0
Oct-1-en-3-ol	74	19	76	20	73	19	54	24	74	29	49	27	97	3	32	12	36	19	25	15
3-Methylbutan-2-ol	0	0	0	0	0	0	0	0	0	0	0	0	48	34	100	0	45	37	49	38
2-Methylbutan-1-ol	67	47	19	15	6	5	2	3	0	0	0	0	0	0	0	0	0	0	0	0
3-Methylfuran	0	0	0	0	0	0	0	0	0	0	3	5	50	41	83	24	22	17	5	7
2-Pentylfuran	0	0	0	0	0	0	0	0	0	0	0	0	58	42	56	31	88	22	98	2
trans-β-Ocimene	0	0	0	0	0	0	0	0	0	0	0	0	0	0	100	0	0	6	0	0
α-Cubebene	0	0	0	0	0	0	0	0	0	0	0	0	0	0	100	0	0	0	6	7
Δ^6-Protoilludene	0	0	0	0	0	0	0	0	0	0	0	0	0	0	100	0	10	7	25	29
α-Isocomene	0	0	0	0	0	0	0	0	0	0	0	0	0	0	100	0	12	12	28	34
β-Cubebene	0	0	0	0	0	0	0	0	0	0	0	0	0	0	100	0	0	0	0	0
Longifolene	0	0	0	0	0	0	0	0	0	0	0	0	0	0	100	0	0	0	0	0
β-Copaene	0	0	0	0	0	0	0	0	0	0	0	0	2	3	100	0	9	8	7	10
β-Elemene	0	0	0	0	0	0	0	0	0	0	0	0	0	0	100	0	4	6	2	2
Caryophyllene	0	0	0	0	0	0	0	0	0	0	0	0	0	0	100	0	0	0	0	0
Cadina-3,5-diene	0	0	0	0	0	0	0	0	0	0	0	0	0	0	100	0	0	0	0	0
α-Humulene	0	0	0	0	0	0	0	0	0	0	0	0	0	0	100	0	0	0	0	0
γ-Muurolene	8	6	1	1	1	0	2	2	4	5	5	5	10	8	100	0	23	20	19	13
Viridiflorene	0	0	0	0	0	0	0	0	0	0	0	0	0	0	100	0	0	0	0	0
Germacrene D	0	0	0	0	0	0	0	0	0	0	0	0	0	0	100	0	0	0	0	0
β-Selinene	0	0	0	0	0	0	0	0	0	0	0	0	0	0	100	0	0	0	0	0
α-Selinene	0	0	0	0	0	0	0	0	0	0	0	0	0	0	100	0	0	0	0	0
α-Muurolene	16	9	5	4	4	4	5	5	9	10	9	9	19	17	100	0	40	34	24	18
δ-Cadinene	0	0	0	0	0	0	0	0	0	0	0	0	0	0	100	0	16	15	4	5
Cubenene	0	0	0	0	0	0	0	0	0	0	0	0	0	0	100	0	0	0	0	0
Calamenene	0	0	0	0	0	0	0	0	0	0	0	0	2	3	100	0	19	17	5	6
Epicubenol	0	0	0	0	0	0	0	0	0	0	0	0	0	0	100	0	0	0	0	0
Cubenol	0	0	0	0	0	0	0	0	0	0	0	0	0	0	100	0	0	0	0	0
δ-Cadinol	46	38	9	6	3	4	0	0	0	0	0	0	0	0	0	0	0	0	78	31

Table S2.2: Relative amounts of VOCs in the HS of the monokaryotic strain *C. aegerita* AAE-3-37 between the days 10 and 28.

	Day 10		Day 12		Day 14		Day 16		Day 18		Day 20		Day 22		Day 24		Day 26		Day 28	
	Mean value	Standard deviation	Mean value	Standard deviation	Mean value	Standard deviation	Mean value	Standard deviation	Mean value	Standard deviation	Mean value	Standard deviation	Mean value	Standard deviation	Mean value	Standard deviation	Mean value	Standard deviation	Mean value	Standard deviation
Acetone	97	5	38	10	60	16	21	19	55	34	28	18	0	0	9	12	18	25	31	33
Butan-2-one	90	14	24	17	10	14	0	0	66	30	46	23	0	0	8	11	14	19	34	31
Cyclopentanone	100	0	48	37	24	14	16	6	14	12	13	10	8	11	8	11	5	8	3	4
Oct-1-en-3-ol	58	17	70	19	70	5	94	8	63	10	76	1	61	11	48	9	35	2	61	28
2-Methylbutan-1-ol	100	0	10	15	0	0	0	0	0	0	0	0	0	0	0	0	0	0	0	0
Δ^6-Protoilludene	5	2	100	0	50	20	29	13	24	5	22	7	30	5	25	3	45	22	37	15
γ-Muurolene	75	22	51	18	21	20	21	20	37	12	50	15	37	15	36	18	49	20	81	28
α-Muurolene	72	24	43	20	23	25	18	20	37	16	56	23	38	17	35	13	47	20	81	26
δ-Cadinol	100	0	24	5	0	0	0	0	0	0	0	0	0	0	3	4	6	5	6	6

S2.3: Relative amounts of VOCs in the HS of the monokaryotic strain *C. aegerita* AAE-3-40 between the days 10 and 28.

	Day 10		Day 12		Day 14		Day 16		Day 18		Day 20		Day 22		Day 24		Day 26		Day 28	
	Mean value	Standard deviation	Mean value	Standard deviation	Mean value	Standard deviation	Mean value	Standard deviation	Mean value	Standard deviation	Mean value	Standard deviation	Mean value	Standard deviation	Mean value	Standard deviation	Mean value	Standard deviation	Mean value	Standard deviation
Acetone	100	0	36	17	14	11	0	0	10	8	6	5	0	0	0	0	7	5	7	10
Butan-2-one	100	0	38	8	11	11	0	0	8	12	5	7	0	0	0	0	5	7	12	17
Cyclopentanone	95	7	95	5	80	14	36	9	21	8	13	2	7	6	5	4	4	3	3	2
Oct-1-en-3-ol	75	13	61	13	34	10	62	30	43	2	98	1	95	6	71	13	63	2	70	7
2-Methylbutan-1-ol	100	0	34	10	10	8	0	0	0	0	0	0	0	0	0	0	0	0	0	0
α-Cubebene	0	0	0	0	0	0	5	7	100	0	53	7	14	5	13	10	39	43	18	15
Δ^6-Protoilludene	40	43	2	2	1	0	11	11	73	39	36	20	8	6	12	12	37	36	19	20
α-Isocomene	0	0	0	0	0	0	10	14	96	5	42	42	10	15	12	18	40	38	24	23
β-Cubebene	0	0	0	0	0	0	0	0	100	0	17	17	5	5	5	5	24	24	5	5
β-Elemene	52	37	10	8	2	1	11	11	65	35	28	20	6	5	8	8	37	45	16	12
γ-Muurolene	37	20	28	17	13	5	21	4	78	31	45	3	26	6	24	4	46	16	67	26
α-Muurolene	43	17	33	14	13	5	19	2	75	31	42	7	29	5	27	3	51	19	82	26
δ-Cadinene	1	1	0	0	0	0	3	3	95	5	35	10	11	4	12	2	54	46	16	6
Cubenene	0	0	0	0	0	0	0	0	100	0	3	3	0	0	0	0	15	15	2	2
Calamenene	0	0	0	0	0	0	1	1	100	0	5	8	1	2	3	5	16	19	4	5
δ-Cadinol	100	0	55	8	8	2	3	5	4	5	4	1	5	2	5	2	4	1	4	1

S2.4: Relative amounts of VOCs in the HS of the monokaryotic strain *C. aegerita* AAE-3-32 between the days 10 and 28.

	Day 10		Day 12		Day 14		Day 16		Day 18		Day 20		Day 22		Day 24		Day 26		Day 28	
	Mean value	Standard deviation	Mean value	Standard deviation	Mean value	Standard deviation	Mean value	Standard deviation	Mean value	Standard deviation	Mean value	Standard deviation	Mean value	Standard deviation	Mean value	Standard deviation	Mean value	Standard deviation	Mean value	Standard deviation
Acetone	100	0	20	15	0	0	0	0	0	0	0	0	0	0	0	0	0	0	0	0
Butan-2-one	100	0	21	15	0	0	0	0	0	0	0	0	0	0	0	0	0	0	0	0
Cyclopentanone	98	2	57	23	49	40	22	21	0	0	0	0	0	0	0	0	0	0	0	0
Oct-1-en-3-ol	53	15	44	13	61	10	67	17	87	17	81	27	31	11	30	23	17	3	8	6
2-Methylbutan-1-ol	100	0	29	8	19	18	16	20	0	0	0	0	0	0	0	0	0	0	0	0
Δ^6-Protoilludene	33	47	0	0	0	0	0	0	0	0	15	13	0	0	0	0	0	0	69	44
γ-Muurolene	98	3	49	4	40	13	34	25	27	23	43	18	57	42	52	26	43	33	9	12
α-Muurolene	95	7	38	3	27	6	27	21	18	13	37	11	50	41	43	14	28	21	7	9
δ-Cadinene	100	0	40	15	15	13	10	14	0	0	0	0	21	29	22	31	21	30	8	11
δ-Cadinol	100	0	15	4	7	2	1	1	1	1	0	0	34	13	33	15	8	6	5	5

S2.5: Relative amounts of VOCs in the HS of the monokaryotic strain *C. aegerita* AAE-3-24 between the days 10 and 28.

	Day 10		Day 12		Day 14		Day 16		Day 18		Day 20		Day 22		Day 24		Day 26		Day 28	
	Mean value	Standard deviation	Mean value	Standard deviation	Mean value	Standard deviation	Mean value	Standard deviation	Mean value	Standard deviation	Mean value	Standard deviation	Mean value	Standard deviation	Mean value	Standard deviation	Mean value	Standard deviation	Mean value	Standard deviation
Acetone	100	0	0	0	0	0	0	0	0	0	0	0	0	0	0	0	0	0	0	0
Butan-2-one	100	0	0	0	0	0	0	0	0	0	0	0	0	0	0	0	0	0	0	0
Cyclopentanone	100	0	80	14	62	16	45	19	24	11	16	8	7	7	6	5	4	4	2	2
Octan-3-one	0	0	0	0	0	0	0	0	0	0	0	0	27	38	46	41	91	12	22	9
Oct-1-en-3-ol	52	41	30	8	27	9	25	3	27	4	60	31	67	32	28	10	39	31	16	11
2-Methylbutan-1-ol	100	0	21	15	3	5	0	0	0	0	0	0	0	0	0	0	0	0	0	0
Δ^6-Protoilludene	6	6	2	1	3	4	1	1	4	2	20	18	33	25	20	13	49	37	77	33
γ-Muurolene	55	39	41	12	60	10	45	5	65	8	54	13	70	30	52	4	98	3	63	24
α-Muurolene	67	47	43	8	61	13	51	6	61	8	52	5	62	23	48	4	97	3	65	15
δ-Cadinene	53	38	17	15	37	3	10	14	27	21	18	13	66	47	53	16	87	18	56	8
δ-Cadinol	67	47	0	0	0	0	0	0	0	0	0	0	0	0	11	15	47	41	15	21

Transcriptome of different fruiting stages in the cultivated mushroom *Cyclocybe aegerita* suggests a complex regulation of fruiting and reveals enzymes putatively involved in fungal oxylipin biosynthesis.

Orban, A., Weber, A., Herzog, R., Hennicke, F., Rühl, M.

BMC Genomics 2021, *22*, 324

DOI: 10.1186/s12864-021-07648-5

Orban et al. BMC Genomics (2021) 22:324
https://doi.org/10.1186/s12864-021-07648-5

BMC Genomics

RESEARCH Open Access

Transcriptome of different fruiting stages in the cultivated mushroom *Cyclocybe aegerita* suggests a complex regulation of fruiting and reveals enzymes putatively involved in fungal oxylipin biosynthesis

Axel Orban[1], Annsophie Weber[1], Robert Herzog[2], Florian Hennicke[3*] and Martin Rühl[1,4*]

Abstract

Background: *Cyclocybe aegerita* (syn. *Agrocybe aegerita*) is a commercially cultivated mushroom. Its archetypal agaric morphology and its ability to undergo its whole life cycle under laboratory conditions makes this fungus a well-suited model for studying fruiting body (basidiome, basidiocarp) development. To elucidate the so far barely understood biosynthesis of fungal volatiles, alterations in the transcriptome during different developmental stages of *C. aegerita* were analyzed and combined with changes in the volatile profile during its different fruiting stages.

Results: A transcriptomic study at seven points in time during fruiting body development of *C. aegerita* with seven mycelial and five fruiting body stages was conducted. Differential gene expression was observed for genes involved in fungal fruiting body formation showing interesting transcriptional patterns and correlations of these fruiting-related genes with the developmental stages. Combining transcriptome and volatilome data, enzymes putatively involved in the biosynthesis of C8 oxylipins in *C. aegerita* including lipoxygenases (LOXs), dioxygenases (DOXs), hydroperoxide lyases (HPLs), alcohol dehydrogenases (ADHs) and ene-reductases could be identified. Furthermore, we were able to localize the mycelium as the main source for sesquiterpenes predominant during sporulation in the headspace of *C. aegerita* cultures. In contrast, changes in the C8 profile detected in late stages of development are probably due to the activity of enzymes located in the fruiting bodies.

Conclusions: In this study, the combination of volatilome and transcriptome data of *C. aegerita* revealed interesting candidates both for functional genetics-based analysis of fruiting-related genes and for prospective enzyme characterization studies to further elucidate the so far barely understood biosynthesis of fungal C8 oxylipins.

Keywords: Basidiomycota, C8 oxylipins, Global gene expression analysis, Volatilome, Developmental biology, Multicellular development, Carpophore, Mycelium, Black poplar mushroom, Pioppino, Sesquiterpenes, Dioxygenases

* Correspondence: florian.hennicke@rub.de; martin.ruehl@uni-giessen.de
[3]Project Group Genetics and Genomics of Fungi, Ruhr-University Bochum, Chair Evolution of Plants and Fungi, 44780 Bochum, North Rhine-Westphalia, Germany
[1]Institute of Food Chemistry and Food Biotechnology, Justus Liebig University Giessen, 35392 Giessen, Hesse, Germany
Full list of author information is available at the end of the article

Background

The formation of fruiting bodies (FBs, basidiomes, basidiocarps) that are in particular formed by species from the Basidiomycota class Agaricomycetes [1] is one of the most complex developmental processes in the fungal life cycle. Depending on the species, this development results in various FB shapes and features (e.g. nutritional mode or FB-specific natural products) the former of which has now been revealed as the major driver of diversification in mushrooms [2]. In a first step, hyphal knots develop as a result of enhanced hyphal branching in defined areas of the vegetative mycelium. The branches in the hyphal knots intertwine successively to initials, being for e.g. *Coprinopsis cinerea* about 1–2 mm in size [3, 4]. Usually, as in the model agaric *Cyclocybe aegerita* (V. Brig.) Vizzini (synonym: *Agrocybe aegerita* (V. Brig.) Singer) [5], cell differentiation takes place in these FB initials, which already becomes evident in late FB initials [6]. Progression of differentiation leads to the formation of bipolar primordia essentially comprising the different 'tissue' (more precisely referred to as plectenchyma or plectenchyme in fungi [6–8]) types observed in mature FBs. The subsequent development from differentiated primordia to FBs is mainly due to cell elongation rather than cell differentiation [4]. The formation and maturation of basidiospores and their subsequent release can be highly synchronized, as observed in species with an ephemeral life strategy producing short-lived, autolytic FBs such as the dung-dwelling well-studied model agaric *C. cinerea*. Other Agaricales ('agarics') species, representing the more typical case of how meiotic sporulation proceeds in these fungi, lack such a tight synchronization. Sampled FBs of such species contain e.g. spore-forming basidia in various developmental stages at the same time [9]. Asynchronous sporulation is exemplified in the long-lasting FBs of the bracket fungus *Schizophyllum commune*, another important Agaricales model system for mating and fruiting [7, 10–13], where older 'ripe' parts of the FB sporulate while younger FB parts still proliferate [3]. Environmental and physiological influences, such as nutrient availability, light and the occurrence of predators, have a great impact on the development of FBs (reviewed in [14]). High concentrations of CO_2, for example, can suppress fruiting or lead to malformed FBs [15–17]. Furthermore, oxylipins have proven to have an influence on developmental processes in fungi. Recently, Niu et al. demonstrated that 5,8-dihydroxyoctadecadienoic acid induces lateral hyphal branching in *Aspergillus* ssp. with G-protein coupled receptors being involved in the signal transduction [18]. Additionally, gene deletion experiments with inter alia *C. cinerea* and *S. commune* revealed a set of genes that are essential for the proper formation of FBs [7, 10–12, 19–30]. In *S. commune* for example, the deletion of the transcription factor *HOM2* was associated with an enhanced growth of vegetative mycelium unable to develop FBs whereas the deletion of *HOM1* and *GAT1* resulted in the formation of more but smaller FBs with an unusual morphology compared to the wild type [10, 12]. Furthermore, the blue light photoreceptor Wc-1 (also called Dst1 in *C. cinerea*) is essential for the photomorphogenesis of *C. cinerea* and *S. commune* [11, 12, 29]. Defects of this gene lead to suppressed primordium maturation with the pileus and stipe tissues at the upper part of the primordium remaining rudimentary [26]. Differential expression of several fruiting-related genes (FRGs) has been observed in different fungal species during FB development including the model agarics *S. commune* [13] and *C. cinerea* [26, 31] as well as the mushrooms *Agaricus bisporus* [32], *Armillaria ostoyae*, *Lentinus tigrinus*, *Phanerochaete chrysosporium*, *Rickenella mellea* [33], *Auriculariopsis ampla* [34], *Hypsizygus marmoreus* [35], *Ganoderma lucidum* [36], *Pleurotus eryngii* [37], *Hericium erinaceus* [38], *Lentinula edodes* [39] and *Flammulina filiformis* [40]. Besides morphological changes during FB development, the odor as a result of released volatile organic compounds (VOCs) is an important characteristic of different fungal species. Several studies revealed that the volatile profile of mushrooms differs depending on the developmental stage [41–49]. In this context, the function of VOCs as 'infochemicals' is of special interest since VOCs have proven to influence the behavior of invertebrates and play therefore probably an important role in the fungal life cycle by inter alia repelling fungal predators or attracting insects for the purpose of spore dispersal (reviewed in [50, 51]). Furthermore, C8 VOCs showed regulatory functions in fungi and influence on conidiation and conidia germination in *Penicillium paneum* and *Trichoderma* spp., respectively [52, 53]. Hence, the changes observed in volatilomes of fungi are probably due to the adaption of the organisms to the altering requirements during different developmental stages.

Recently, the changes of the volatilomes in the headspace (HS) of *Cyclocybe aegerita* (syn. *Agrocybe aegerita*), which is a commercially cultivated edible agaricomycete from Europe [5], during different fruiting stages of the dikaryon *C. aegerita* AAE-3 and a set of progeny monokaryons was monitored under nearly natural circumstances applying a non-invasive extraction method [54]. This study revealed drastic changes in the volatile profile across developmental stages. In early stages, alcohols and ketones, including oct-1-en-3-ol and cyclopentanone, were the main substances in the HS of the dikaryon. With ongoing FB development, the VOCs composition differed remarkably and particularly during sporulation. Sesquiterpenes, such as Δ^6-protoilludene, α-

cubebene and δ-cadinene, were the dominant substances detected in the HS at this stage. After sporulation, the amount of sesquiterpenes decreased, while the appearance of additional VOCs, especially octan-3-one, was observed. Despite the notable changes in VOCs profiles and the biological importance of fungal VOCs, overall little is known about the pathways leading to their formation. Even the biosynthesis of volatile C8 oxylipins, such as oct-1-en-3-ol, octan-3-one and oct-1-en-3-one, ubiquitously found in fungi and perceived as 'typical' mushroom odors, is so far scarcely understood. It has been proposed that volatile C8 oxylipins are derived from linoleic acid, probably involving lipoxygenases (LOXs), dioxygenases (DOXs) and hydroperoxide lyases (HPLs) in the formation process (reviewed in [51, 55]). However, enzymes clearly linked to volatile C8 oxylipin biosynthesis have been barely identified so far. To tap this hitherto neglected topic of fungal VOCs biosynthesis, we conducted a transcriptomic study with in total seven mycelium- and five FB development stages of *C. aegerita* AAE-3, chosen to be similar with stages sampled in the volatilome study of *C. aegerita* mentioned above [54]. Combining the volatilome and trancriptome data sets and comparing volatile profiles in the HS of *C. aegerita* with transcription patterns of selected genes, we were able to identify enzymes putatively involved in the formation of VOCs in fungi. Especially regarding C8 volatile pathways, we determine for the first time promising candidates responsible for the biosynthesis of fungal VOCs.

Results

Fruiting body development in *C. aegerita* in modified crystallizing dishes

The dikaryotic strain *C. aegerita* AAE-3 was able to produce FBs and basidiospores under the chosen cultivation conditions (Fig. 1). By day 18 post inoculation (p.i.), primordia emerged on fruiting-induced mycelium. Further on, they developed into FBs, typically sporulating at day 24 p.i. At the final stage sampled on day 28 p.i., these show first signs of aging, e.g. a moisture-soaked cap margin.

Differential gene expression during fruiting body development

To identify changes in the transcriptome during mushroom tissue formation and FB maturation in *C. aegerita*, RNA sequencing of different developmental stages of mycelium and FBs was conducted (Additional file 1). In total, transcripts representing 12,965 of the 14,115 annotated genes were identified (Additional file 2: Table S1, BioProject PRJNA677924, BioSamples 16,789,160 to 16,789,171). A principal component analysis (PCA) was performed for the transcriptomes of mycelium and FBs to highlight similar expression patterns of the different developmental stages (Fig. 2). For the mycelium samples, the first two principal components covered 36.2% of the data's original variation and developmental stages clustered roughly in three groups (Fig. 2a). The transcriptome of the young mycelium samples, which were taken prior to the day night shift all other samples have been

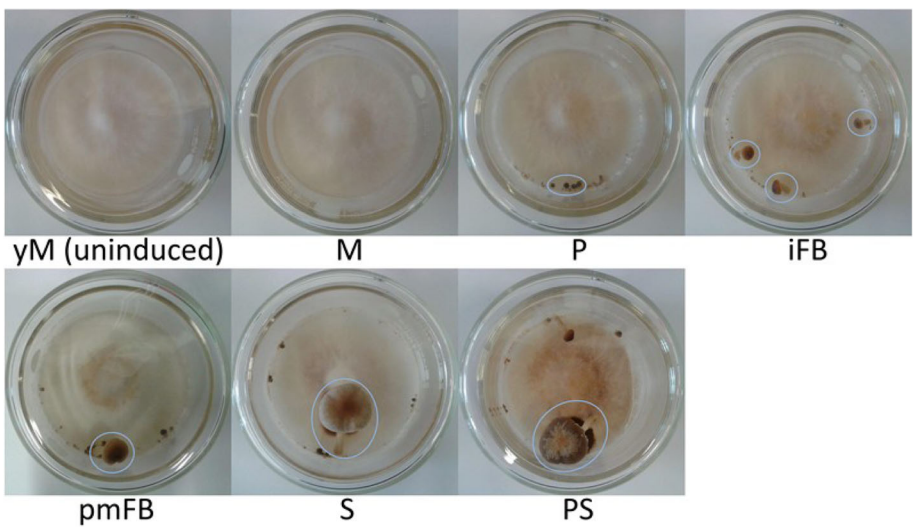

Fig. 1 Fruiting body development of *C. aegerita*. Samples were grown at 24 °C in the dark in crystallizing dishes containing 16 mL 1.5% MEA medium and were sealed with Parafilm™. Ten days after inoculation, the Parafilm™ was removed and samples were transferred to a climate chamber (24 °C, 95% rH, 12/12 h day/night rhythm) and cultured for further 18 days. Blue circles indicate examples of FB samples harvested at the designated stage. yM: young (uninduced) mycelium (day 10 post inoculation, p.i.); M: fruiting-primed mycelium (day 14 p.i.); P: primordia (day 18 p.i.); iFB: immature fruiting bodies (day 20 p.i.); pmFB: premature fruiting bodies (day 22 p.i.); S: sporulating mature FB (day 24 p.i.); PS: post sporulation (day 28 p.i.)

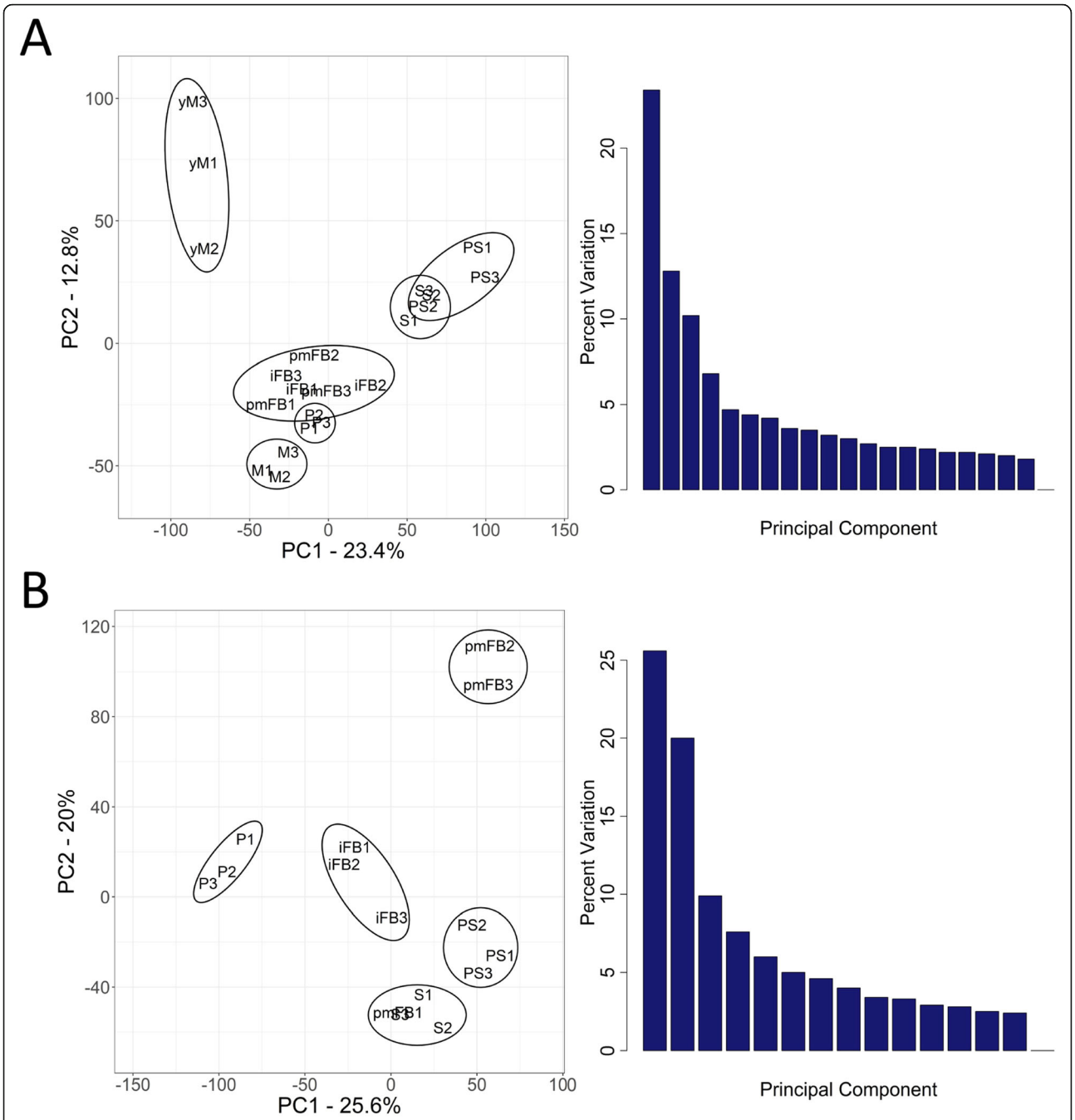

Fig. 2 Principal component analysis (PCA) (left) and scree plot (right) for transcriptome data of developmental stages of *C. aegerita*. **a** Transcriptome data of the mycelium samples. PC1 and PC2 covered 36.2% of the data's original variation. **b** Transcriptome data of the fruiting body samples. PC1 and PC2 covered 45.6% of the data's original variation. yM: young (uninduced) mycelium (day 10 post inoculation, p.i.); M: mycelium (day 14 p.i.); P: primordia (day 18 p.i.); iFB: immature fruiting bodies (day 20 p.i.); pmFB: premature fruiting bodies (day 22 p.i.); S: sporulation (day 24 p.i.); PS: post sporulation (day 28 p.i.)

exposed to, formed an individual cluster. The following four FB developmental stages (fruiting-primed mycelium to mature FBs) clustered together as well as the transcriptomes of the last two developmental stages (sporulation and post sporulation). The performed Friedman test revealed significant differences ($p = 5.448e^{-10}$) between the transcriptomes of the different developmental stages of the mycelium. The Wilcoxon-Nemenyi-McDonald-Thompson test, used as the post hoc analysis of the Friedman test, showed that transcriptomes of sporulation and post sporulation samples differed significantly ($p < 0.05$) from samples of all other stages, but

were similar to each other. Additionally, the transcriptome of young mycelium samples differed significantly from transcriptomes of fruiting-primed mycelium and primordia samples. For the FB samples, the first two principal components represented 45.6% of the data's original variation with all five developmental stages forming individual clusters (Fig. 2b). The performed Friedman test revealed significant differences ($p = 3.162e^{-13}$) between the transcriptomes of the different developmental stages of the FBs. The Wilcoxon-Nemenyi-McDonald-Thompson test displayed that primordia, immature FB and premature FB samples each showed significant differences ($p < 0.05$) regarding their transcriptomes compared to samples of the other stages, with pmFB1 being a striking exception sharing consistent features with sporulating FBs. Compared to the other premature FBs, pmFB1 samples were probably further developed but without showing visible signs of sporulation. Additionally, the sporulation and post sporulation stages did not differ significantly amongst themselves.

A highly interesting difference between two mycelial samples occurred during maturation of FBs. From day 22 to day 24 amongst genes having at least a read count of 100 in the mycelium samples, 66 genes showed a > 5-fold decrease (Additional file 2: Table S2) and 117 genes a > 5-fold increase (Additional file 2: Table S3). The deduced protein sequences of these regulated genes were analyzed by means of BLAST (tblastn) using characterized proteins present in the UniProt database. In total, 35 sequences of the downregulated and 75 sequences of the upregulated genes could be functionally allocated. Of these, most upregulated genes (15 of 75) are related to the mevalonate pathway and the sesquiterpenoid clusters, whereas the down-regulated genes mainly code for six putative hydrophobins and other fruiting-related genes (FRGs). Thus, we focus on the FRGs as well as on genes that are involved in the biosynthesis of volatile compounds mainly produced during fructification and sporulation.

Transcription of fruiting-related genes (FRGs)

In the genome sequence of *C. aegerita*, Gupta et al. [56] identified an array of putative homologs of genes confirmed to play a role in fruiting of model agarics. The transcription levels of these FRGs were analyzed, whereby only genes were considered showing maximum transcription levels higher than 25 normalized read counts (NRC) (Fig. 3). Structurally according to Gupta et al. [56], these FRGs can be grouped into three major groups. The largest group of putative *C. aegerita* FRGs encodes for the transcription factors Bri1, Bwc2, C2H2, Exp1, Fst3, Fst4, Gat1, Hom1, Hom2 and Pcc1, which had been described from *S. commune* and *Coprinopsis cinerea* [10, 12, 20, 28, 29], originally. A second group of FRGs annotated to the *C. aegerita* AAE-3 genome sequence [56] includes the genes *CFS1*, *DST1*, *DST2*, *ELN3* and *ICH1*, encoding for proteins with diverse functions, e.g. blue light perception or a putative role in cell wall carbohydrate production, all derived from putatively orthologous genes of *C. cinerea* [21, 25–27, 30]. A third group consists of four previously annotated genes [56], *PRI1* to *PRI4*, proven to be transcriptionally upregulated in primordia of the wild type strain *C. aegerita* SM51 also known as WT-1 [19, 22–24].

Regarding their expression patterns during fruiting, these very different FRGs were clustered according to the developmental phase and hyphal context when and where they were mainly expressed (Fig. 3). In total, four larger cohorts can be distinguished from another: two in the mycelium and two in the mushroom tissue. In the mycelium, a first cohort comprises genes reaching expression maxima already early in mycelial stages until primordia developed. It includes the genes *ELN3–2*, *ELN3–3*, *FST3*, *BWC2*, *PRI2*, *DST1*, *CFS1*, *ICH1*, *EXP1*, *PRI3–1*, *HOM1*, *PRI4–4* and *PRI1–1*. Four of them, namely *ELN3–3*, *CFS1*, *PRI1* and *PRI2,* have elevated expression levels spanning multiple stages (Fig. 3a). The second group consists of genes whose expression peaked in mycelium during the formation of post-primordial fruiting stages: *PRI3–2*, *PRI4–3*, *PRI3–6*, *PRI3–4*, *FST4*, *BRI1* and *PCC1*.

In FBs, the first cohort comprises genes which reached an expression maximum in early fruiting stages. The genes *BRI1*, *PRI2*, *ELN3–1*, *ICH1*, *BWC2*, *DST2*, *DST1*, *PRI4–4*, *FST4* and *PRI3–1* revealed expression maxima in *C. aegerita* primordia, some of them such as *DST1*, *FST4* and *PRI3–1* showed a continuously high expression in subsequent FB stages (Fig. 3b). Other genes in this group, including *PRI4–3*, *PRI4–2*, *ELN3–2*, *PRI3–4*, *PRI3–2*, *PRI4–1* and *PRI1–1*, displayed highest expression in immature FBs with *PRI4–3*, *PRI3–2* and *PRI1–1* revealing remarkably high expression in previous and subsequent stages. The second gene cohort is formed by the genes *EXP1*, *ELN3–3*, *PCC1*, *FST3 and HOM1* revealing high expression in late fruiting stages. All genes in this cohort showed expression maxima within FB tissue samples which only span two stages, except for *FST3* which revealed constantly elevated transcription in FB tissue until reaching the post-sporulation stage (Fig. 3b). Moreover, correlations between the expression of individual FRGs in FB tissue and mycelium samples were investigated. Generally, formation of clusters of strongly positive correlated genes was more apparent in FRGs expressed in FB samples (Additional file 3: Figures S2 and S3).

RT-qPCR-based confirmation of expression values of selected candidate genes

Expression of four predicted *C. aegerita* orthologs of known transcription factor-encoding FRGs from *S.*

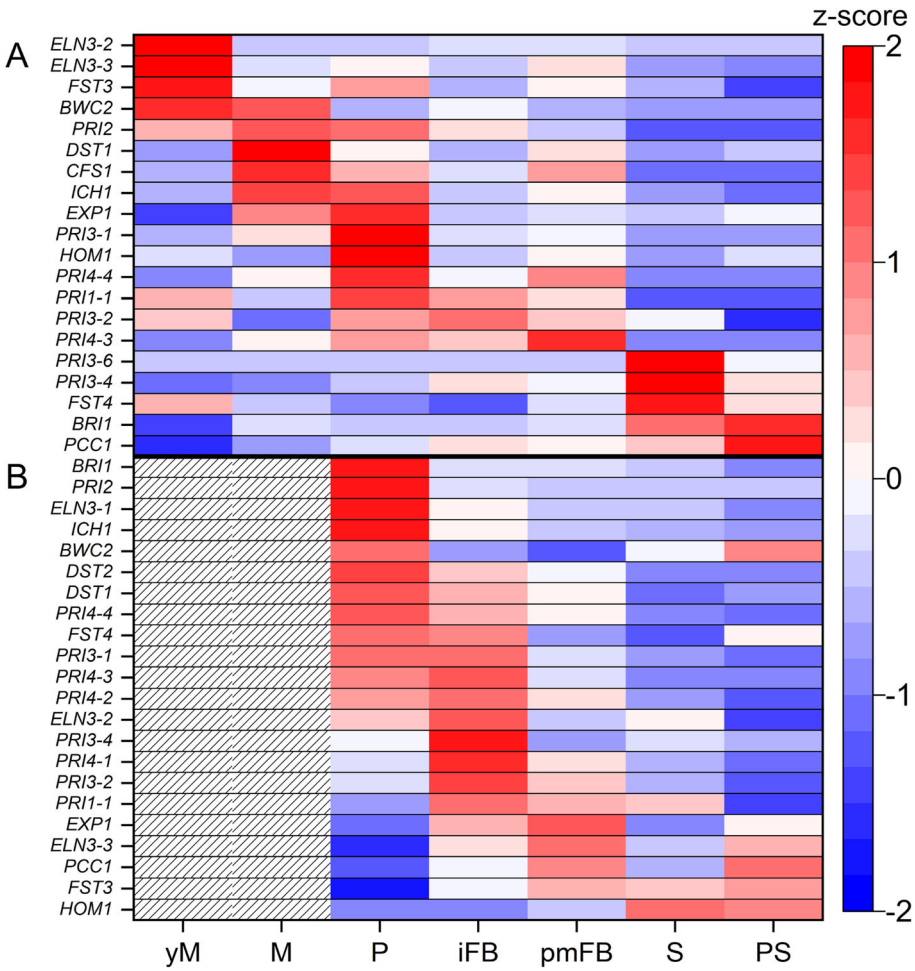

Fig. 3 Transcription of putative *C. aegerita* homologs of fruiting-related genes (FRGs) in mycelium (**a**) and in mushroom tissue (**b**) during different developmental stages. NRC per gene were transformed to z-score values (respective scale to the right) whereby only genes were considered showing maximum transcription levels higher than 25 NRC. Red colors indicate transcriptional upregulation while blue colors represent downregulation. White colors indicate a z-score of zero and hatched areas show an absence of sampling due the non-applicability. yM: young (uninduced) mycelium (day 10 post inoculation, p.i.); M: mycelium (day 14 p.i.); P: primordia (day 18 p.i.); iFB: immature fruiting bodies (day 20 p.i.); pmFB: premature fruiting bodies (day 22 p.i.); S: sporulation (day 24 p.i.); PS: post sporulation (day 28 p.i.). FRGs (in order of appearance in the panels **a** and **b**): *ELN3–2* (AAE3_06792), *ELN3–3* (AAE3_13318), *FST3* (AAE3_09009), *BWC2* (AAE3_13841), *PRI2* (AAE3_02445), *DST1* (AAE3_10538), *CFS1* (AAE3_01819), *ICH1* (AAE3_04768), *EXP1* (AAE3_02324), *PRI3–1* (AAE3_14114), *HOM1* (AAE3_03904), *PRI4–4* (AAE3_04667), *PRI1–1* (AAE3_04306), *PRI3–2* (AAE3_14115), *PRI4–3* (AAE3_04665), *PRI3–6* (AAE3_13216), *PRI3–4* (AAE3_14116), *FST4* (AAE3_11357), *BRI1* (AAE3_08826), *PCC1* (AAE3_01481), *ELN3–1* (AAE3_00364), *DST2* (AAE3_02725), *PRI4–2* (AAE3_04675), *PRI4–1* (AAE3_04684)

commune and *C. cinerea* was additionally monitored via quantitative real-time reverse transcription-PCR (RT-qPCR) (Additional file 3: Figure S4; 2-fold expression change as cut-off) to get a further hint in how far a predicted ortholog might work in the same way during fruiting of *C. aegerita*. The RT-qPCR-monitored expression pattern of *HOM1* (Additional file 3: Figure S4A) showed a transcriptional induction from the FB initial stage through the primordium and immature FB stage which confirmed its expression pattern detected within the RNA-seq analysis (see Fig. 3), at least for the congruently assessed development stages. The expression profile of *GAT1* monitored by RT-qPCR (Additional file 3: Figure S4B) proved that this FRG is indeed differentially expressed during fruiting of *C. aegerita* AAE-3, despite its sub-threshold expression values in the RNA-seq analysis above. The transcriptional induction of *DST1* in primordia and immature FB cap tissue over its expression in young mycelium (Additional file 3: Figure S4C) was congruent with its high expression in primordia and immature FBs over young mycelium detected by the RNA-seq analysis (see Fig. 3). Eventually, the RT-qPCR-monitored expression pattern of *BWC2* (Additional file 3: Figure S4D) generally confirmed the transcriptional induction of this gene during fruiting (from the primordium stage on) compared to its expression in mycelial

stages, at least for the assessed development stages compared to the ones assessed by the RNA-seq analysis (see Fig. 3).

Elucidation of aroma related biosynthesis pathways during development of *C. aegerita*

To take up results of a recently published work on VOCs produced by *C. aegerita* during different developmental stages [54], this transcriptome study should help to elucidate biosynthesis pathways of VOCs such as sesquiterpenoids and oxylipins in *C. aegerita*. The large diversity of sesquiterpenes and other terpenes is derived from only two precursors, dimethylallyl diphosphate and isopentenyl diphosphate, which in fungi are produced from acetyl-CoA by means of the mevalonate pathway [57]. Genes coding for enzymes of the mevalonate pathway were identified in the *C. aegerita* genome by means of BLAST search using amino acid sequences of already characterized fungal analogs. Generally, the expression of enzymes involved in the mevalonate pathway were upregulated in the mycelium during sporulation and post sporulation, whereas in FBs, the transcription of these enzymes was rather higher in early stages of development (Additional file 4: Figure S5). This scenario is especially true for the farnesyl pyrophosphate synthase gene. Its corresponding enzyme provides farnesyl pyrophosphate, which is cyclized by sesquiterpene synthases (STSs) into a wide range of sesquiterpenes [58]. The genome of *C. aegerita* contains 11 genes coding for STSs [59]. Of these, nine gave rise to one or more sesquiterpenes after transformation into *E. coli* [59] (Additional file 4: Figure S5). The comparison of the transcription levels of the different STSs revealed remarkable differences, also strongly depending on sample type and developmental stage (Fig. 4, Additional file 4: Figure S6). Generally, the maximum transcription levels of the STSs were noticeably lower in the examined FB stages than in the mycelial samples, never exceeding 50 NRC in the FB samples. When comparing the occurrence of Δ^6-protoilludene, the most dominant VOC in the HS of *C. aegerita* AAE-3 during sporulation at day 24 p.i [54]. (Fig. 4), with the gene expression values of the two known Δ^6-protoilludene synthases Agr6 and Agr7 [59], the transcription pattern of *AGR6* (AAE3_04120) in the mycelium perfectly reflects the occurrence of Δ^6-protoilludene. In contrast, *AGR7* (AAE3_10454) showed the highest transcription levels in the mycelium after sporulation at day 28 p.i. when Δ^6-protoilludene production already decreased. *AGR2* (AAE3_12839), which is associated with the production of viridiflorene [59], peaked simultaneously with the highest amount of viridiflorene at day 24 p.i. during sporulation revealing a 200-fold expression upregulation compared to day 22. In contrast, AAE3_13291, the gene coding for Agr5, showed the highest transcription level later on at day 28 p.i. It is worth mentioning that *AGR3* (AAE3_13190), which codes for a promiscuous STS involved in the biosynthesis of α-muurolene, δ-cadinene, γ-muurolene and δ-cadinol, was the only examined STS having its maximum transcription level at an early developmental stage at day 10 p.i., where some of its possible products also showed a slight maximum (Fig. 4). Nevertheless, throughout the peak maxima of α-muurolene, δ-cadinene, γ-muurolene and δ-cadinol during sporulation *AGR3* transcripts stayed at a low level. In contrast to the STSs mentioned above, genes coding for Agr1, Agr4, Agr8 and Agr9 were barely expressed in *C. aegerita* under the applied experimental conditions, neither in the mycelium nor in the FB samples (Additional file 4: Figure S6).

In addition to the sesquiterpenes, the biosynthesis of oxylipins in fungi is of special interest. Biosynthesis of volatile fungal oxylipins, including the typical mushroom C8 aroma compounds such as oct-1-en-3-ol, octan-3-one and octan-3-ol, but also other oxylipins like 2-pentylfuran, ubiquitously found in fungi, is yet barely understood. Oxylipins derive from oxidized fatty acids or substances originating therefrom [60]. Linoleic acid, a product of the fatty acid synthesis and further processing steps (see Additional file 5), serves as a precursor for fungal (volatile) oxylipins, involving presumably lipoxygenases (LOXs), dioxygenases (DOXs), hydroperoxide lyases (HPLs), alcohol dehydrogenases (ADHs) and enereductases in the formation process [49, 61–65] (Additional file 6: Figure S8). Interestingly, the composition of the three volatile oxylipins detected in the HS of *C. aegerita* AAE-3 varied remarkably depending on the developmental stages [54] (Fig. 5). Taking these variations into account, identification of unknown enzymes involved in fungal volatile oxylipin formation by analyzing correlation patterns would be a favorable approach. Therefore, transcriptome and volatilome data analysis were performed in R, revealing high correlations between the expression patterns of certain genes and the occurrence of oxylipins. Nonetheless, even the application of a stringent Spearman's rank correlation coefficient threshold ($\rho = 0.7$) resulted in too many hits for an efficient identification of genes putatively involved in volatile oxylipin biosynthesis (e.g. for oct-1-en-3-ol about 1000 genes with a matching expression profile were found in the FB samples) illustrating that a correlation does not necessarily means that a causal relation exists. Accordingly, BLAST searches were performed (for details see Methods) to reduce the number of genes coding for enzymes putatively involved in volatile oxylipin biosynthesis. For the most promising candidates, gene expression patterns were matched to the volatile oxylipin profiles to reveal putatively relevant connections.

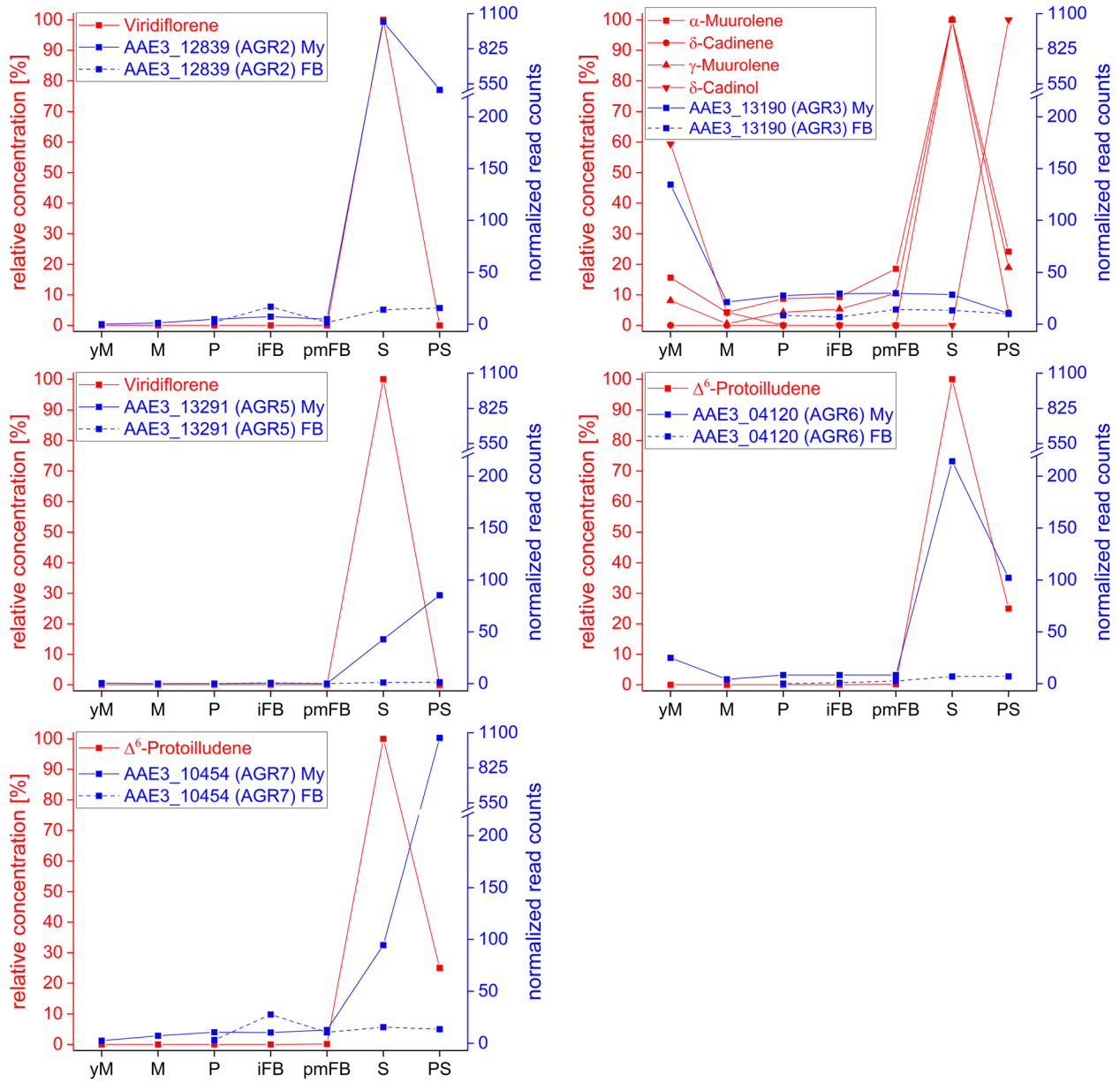

Fig. 4 Transcription levels of genes coding for the sesquiterpene synthases (STSs) Agr2, Agr3, Agr5, Agr6 and Agr7 (blue) in the mycelium (My) and in fruiting bodies (FB) during different developmental stages of *C. aegerita* as well as the relative concentrations of the corresponding sesquiterpenes (red) in the HS of *C. aegerita* [54]. yM: young (uninduced) mycelium (day 10 post inoculation, p.i.); M: mycelium (day 14 p.i.); P: primordia (day 18 p.i.); iFB: immature fruiting bodies (day 20 p.i.); pmFB: premature fruiting bodies (day 22 p.i.); S: sporulation (day 24 p.i.); PS: post sporulation (day 28 p.i.)

The first step towards oxylipins is the oxygenation of fatty acids, mainly linoleic acids, by LOXs. The maximum transcription levels of the LOX genes in *C. aegerita* were noticeably higher in FBs than in the mycelium (Fig. 5), except for *LOX2* (AAE3_01552) and *LOX3* (AAE3_09652), of which the latter was barely expressed. The by far highest transcription level amongst all LOX genes was detected for *LOX4* (AAE3_04864) showing a successively upregulation in FB stages during development and peaking during sporulation at day 24 p.i. that lead to a 62-fold upregulation compared to the primordia stage. In contrast, in the mycelium the transcription of *LOX4* (Fig. 5) was remarkably less pronounced showing 135-fold less expression during sporulation compared to FBs. In mature FBs, *LOX5* (AAE3_07753) displayed the second highest transcription level of all LOX genes showing a transcription pattern quite similar to the occurrence of oct-1-en-3-ol in

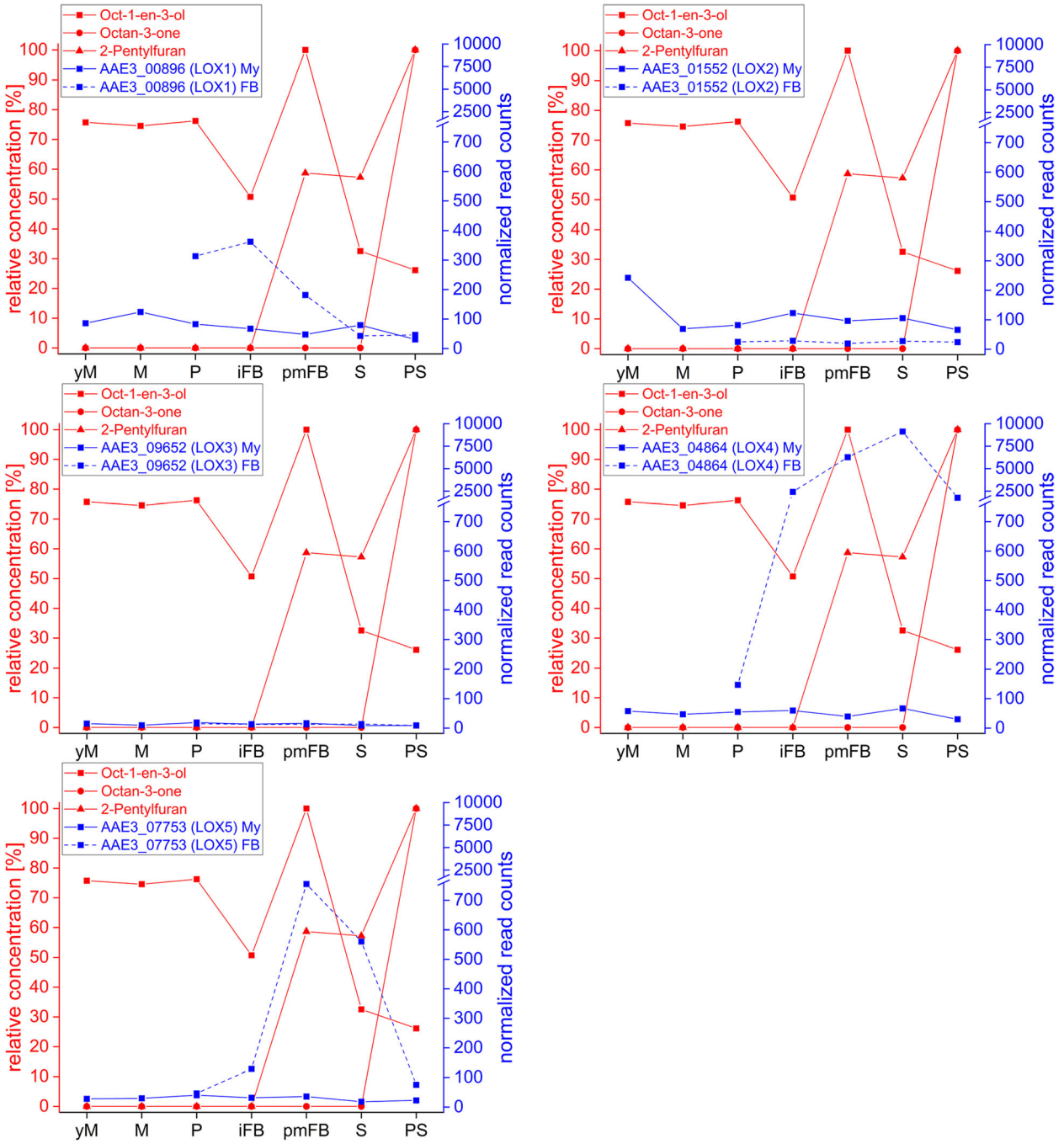

Fig. 5 Transcription levels of the lipoxygenases *LOX1–5* (blue) in the mycelium (My) and in fruiting bodies (FB) during different developmental stages of *C. aegerita* as well as the relative concentrations of volatile oxylipins (red) in the HS of *C. aegerita* [54]. yM: young (uninduced) mycelium (day 10 post inoculation, p.i.); M: mycelium (day 14 p.i.); P: primordia (day 18 p.i.); iFB: immature fruiting bodies (day 20 p.i.); pmFB: premature fruiting bodies (day 22 p.i.); S: sporulation (day 24 p.i.); PS: post sporulation (day 28 p.i.)

the HS of *C. aegerita*. Conversely, *LOX1* (AAE3_00896) revealed its highest transcription levels in early FB stages, peaking in immature FBs and decreasing afterwards.

In contrast to all other LOX genes, *LOX2* (AAE3_01552) displayed a remarkably higher transcription level in the mycelium revealing a 10-fold higher maximum expression at day 10 p.i. compared to the quite constant transcription levels in FB stages.

Besides the activity of LOXs on linoleic acid, DOXs might also play a crucial role in the formation of fungal volatile oxylipins [49] (Additional file 6: Figure S8). Two

putative DOXs genes were found in the genome of *C. aegerita* by means of BLAST search using amino acid sequences of already characterized ascomyceteous DOXs. Interestingly, the transcription of the putative DOX gene AAE3_00407 was upregulated in the mycelium of early fruiting stages (2-fold change), whereas the transcription in the FBs remained comparably low (Fig. 6). In contrast, the expression of the putative DOX gene AAE3_13098 was high in young fruiting stages, peaking with nearly 4500 NRC in immature FBs, thereafter showing a 2.5-fold transcription decrease, along with the dropping amount of oct-1-en-3-ol in the HS, towards late FB stages (Fig. 6). It is worth mentioning that AAE3_13098 revealed also high expression (about 2000 NRC) in young mycelium stages as well as in later mycelium stages with an almost constant expression level of slightly above 1000 NRC.

It is likely that, analogous to plants, fungi have HPLs catalyzing the cleavage of hydroperoxide molecules into a C8 body that is subsequently converted by oxidoreductases into different VOCs (Additional file 6: Figure S8). The most prominent expression of a putative HPL was revealed by its encoding gene AAE3_05330 (3500 NRC) in late FB stages with a 2.3-fold increase of the transcription level compared to primordia stages and with high expression in the mycelium (1000 NRC at day 14 p.i.) (Additional file 6: Figure S9). For AAE3_09203, the highest expression was observed in immature FBs (2000 NRC), whereas in the mycelium the transcription of AAE3_09203 was remarkably lower revealing 16-fold less expression at this stage. Interestingly, in FB stages as well as in the mycelium, the course of expression of AAE3_09203 was comparable to the transcription of the putative DOX AAE3_13098. AAE3_09218 showed high expression in primordia (1500 NRC) with a 3-fold expression downregulation towards later stages. In the mycelium, the highest transcriptions were observed for AAE3_12835 (2000 NRC) and AAE3_04119 (1600 NRC) during sporulation but both with comparable low expression (17-fold and 58-fold less expression, respectively) in FB stages. In contrast, AAE3_06380 revealed quite constant transcription levels (about 1000 NRC) in the mycelium as well as in FB stages.

In addition to the oxygenation of linoleic acid by means of LOXs or DOXs and the subsequent cleavage to C8 oxylipins by means of HPLs, the enzymatic conversion of mentioned C8 oxylipins might play an important role in the formation of C8 VOCs in fungi. In this context, ADHs and ene-reductases might play an important role, explaining the observed decrease of oct-1-en-3-ol during sporulation and, thereafter, the increase of octan-3-one in the HS of *C. aegerita* [54]. Putative ADHs and ene-reductases were identified in the genome of *C. aegerita* by means of BLAST search using amino acid sequences of characterized ADHs and ene-reductases. The transcription levels of putative ADHs and ene-reductases were analyzed in the mycelium and in FB stages (Additional file 6: Figures S10 and S11). In general, most genes coding for putative ADHs showed transcription levels under 500 NRC in the mycelium and in FB tissue samples. Interestingly, the expression of AAE3_00054, AAE3_10620 and AAE3_12451 successively increased in FB stages, showing during sporulation high transcription levels with a 30-fold, 4-fold and 72-fold expression upregulation, respectively, compared to primordia stages and peaking concurrently with a low level of oct-1-en-3-ol content in the HS of *C. aegerita*. Comparable transcription, with over 2500 NRC during

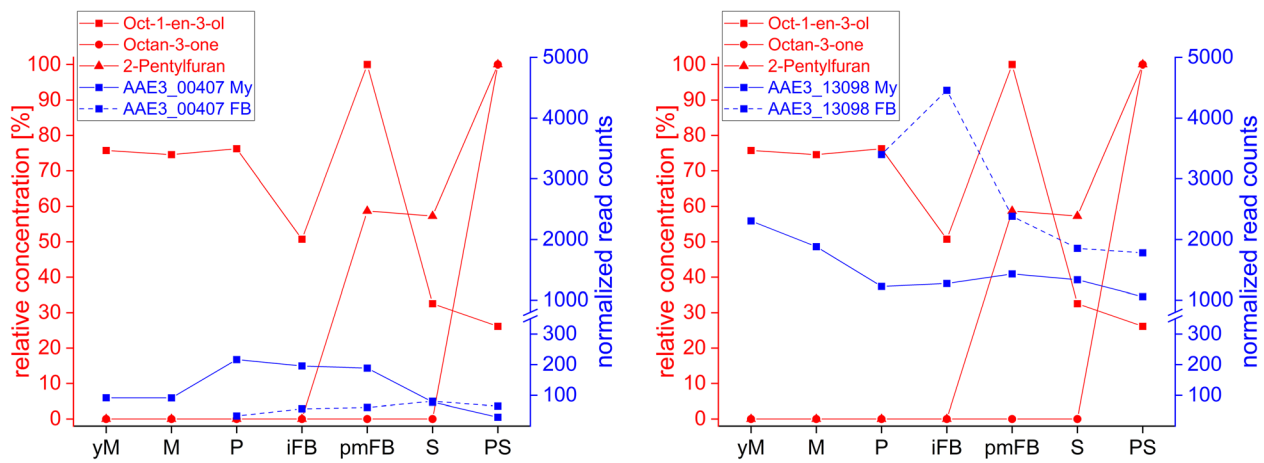

Fig. 6 Transcription levels of the putative dioxygenase (DOX) genes AAE3_00407 and AAE3_13098 (blue) in the mycelium (My) and in fruiting bodies (FB) during different developmental stages of *C. aegerita* as well as the relative concentrations of volatile oxylipins (red) in the HS of *C. aegerita* [54]. yM: young (uninduced) mycelium (day 10 post inoculation, p.i.); M: mycelium (day 14 p.i.); P: primordia (day 18 p.i.); iFB: immature fruiting bodies (day 20 p.i.); pmFB: premature fruiting bodies (day 22 p.i.); S: sporulation (day 24 p.i.); PS: post sporulation (day 28 p.i.)

sporulation, was observed for AAE3_05375 in the mycelium, already displaying a high expression (900 NRC) in the young mycelium at day 10 p.i. Remarkably, the expression of AAE3_02583 reached, with nearly 3000 NRC, a high transcription level after sporulation at day 28 p.i., displaying, compared to expression during sporulation, a 23-fold upregulation concomitant with the appearance of octan-3-one in the HS of *C. aegerita*.

The genome of *C. aegerita* revealed some interesting putative ene-reductases (Additional file 6: Figure S11). The by far highest expression was revealed by AAE3_13549 in mature FBs (3300 NRC) as well as in FBs during sporulation (7900 NRC) and after sporulation (4750 NRC), representing a 34-fold upregulation during sporulation compared to primordia stages. Interestingly, the expression pattern of AAE3_13549 showed remarkable similarity with the transcription of the highly expressed putative ADHs AAE3_00054, AAE3_10620 and AAE3_12451 in FB stages. In contrast, the maximum transcription level of AAE3_13549 in the mycelium during sporulation was quite low, showing, compared to FBs, 24-fold less expression. In contrast to AAE3_13549, other putative ene-reductases were only slightly upregulated during late fruiting stages compared to early developmental stages. Such was observed during sporulation inter alia for AAE3_00194, with a 2-fold higher transcription level in the mycelium and a 1.5-fold expression upregulation in FB stages, or for AAE3_02355, with a 5-fold higher expression in the mycelium. It is worth mentioning that of the putative ene-reductases belonging to the OYE (old yellow enzyme) family only AAE3_09471 showed a maximum expression higher than 300 NRC, with about 400 NRC in sporulating FBs.

Discussion

In this study, we conducted the first comparative transcriptome analysis of *C. aegerita* comprising the most important life stages of *C. aegerita* after successful mating and dikaryotization including seven mycelium and five FB developmental stages, for the first time also considering samples of the mycelium during fructification. A previous study dealing with the transcriptome of *C. aegerita* based on a de novo assembly of expressed sequences tags only compared one mycelium developmental stage with one fruiting stage without specifying the time of sampling [66]. Our transcriptomic data are in good agreement with results of other transcriptome studies on different developmental stages of other fungi of the phylum Basidiomycota regarding number of transcripts and differentially expressed genes (DEGs) [33, 37, 67–69]. For instance, Song et al. found 11,675 unique transcripts [70] of 13,028 predicted genes [71] by RNA-Seq analysis of mycelium and mature FBs of *Lentinula edodes*.

The differences of the transcription pattern between the FB stages in *C. aegerita* was expected (Fig. 2b). However, the differences within the fungal mycelium samples was astonishing (Fig. 2a). The beginning of the day/night shift from day 10 onwards explains the extreme alteration in the transcriptome between day 10 and day 14, but not the variation in the transcripts within the mycelial samples occurring during sporulation of the FBs (Fig. 2). Multiple genes are responsible for this alteration that can be assigned as e.g. FRGs or as genes involved in biosynthetic pathways of VOCs.

Fruiting-related genes (FRGs)

Among the genes that are known to be crucial for the initiation of fruiting, Pcc1 from *C. cinerea* is supposed to be either a repressor or an interaction partner of the heterodimer of homeodomain proteins HD1 and HD2 that triggers mating locus *A*-regulated development including fruiting [20]. Accordingly, its putative *C. aegerita* ortholog *PCC1* is highly expressed already from the beginning of the *C. aegerita* fruiting process. *PCC1* shows a high expression already in uninduced young mycelium (> 2000 normalized reads), which permanently increases to > 6000 NRC after sporulation, and also exhibits high expression values in FB tissue samples of different fruiting stages (Fig. 7). Of the differentially expressed genes relevant to fruiting initiation in the related agaric *S. commune* [10, 12], the transcription factor-encoding genes *BRI1* and *FST4* [56] showed a clear transcriptional induction in primordia and, in the case of the latter gene, also in immature FBs of *C. aegerita* AAE-3. Induction of both genes in primordia is in agreement with the findings by Ohm et al. [10] and Pelkmans et al. [12]. They showed that the Δ*fst4* mutant is not able to form FB initials ('aggregates') as it triggers the transition from vegetative growth to fruiting. On the other hand, Pelkmans et al. [12] showed that the Δ*bri1* mutant is delayed in fruiting, chiefly due to a reduced growth speed that may be explained by downregulation of crucial cellular processes. Our observation that *BRI1* and *FST4* also get strongly induced during the sporulation/post-sporulation stage in the mycelium might relate to the phenomenon that *C. aegerita* fruits in consecutive flushes ([5], Fig. 7) once the fruiting process has been triggered by environmental cues. In the present study, the induction of genes like *PCC1*, *BRI1* and *FST4*, induced at early developmental stages in *S. commune* [10, 12, 34], at the sporulation/post-sporulation stage may be characteristic of species that fruit in consecutive flushes like *C. aegerita*. If not revealed by future analysis of mycelium close to elder first flush FBs of *S. commune* that another increase in expression of such FRGs may just happen much later there, the expression maximum of *C. aegerita PCC1*, *BRI1* and *FST4* at the (post-)sporulation stage might

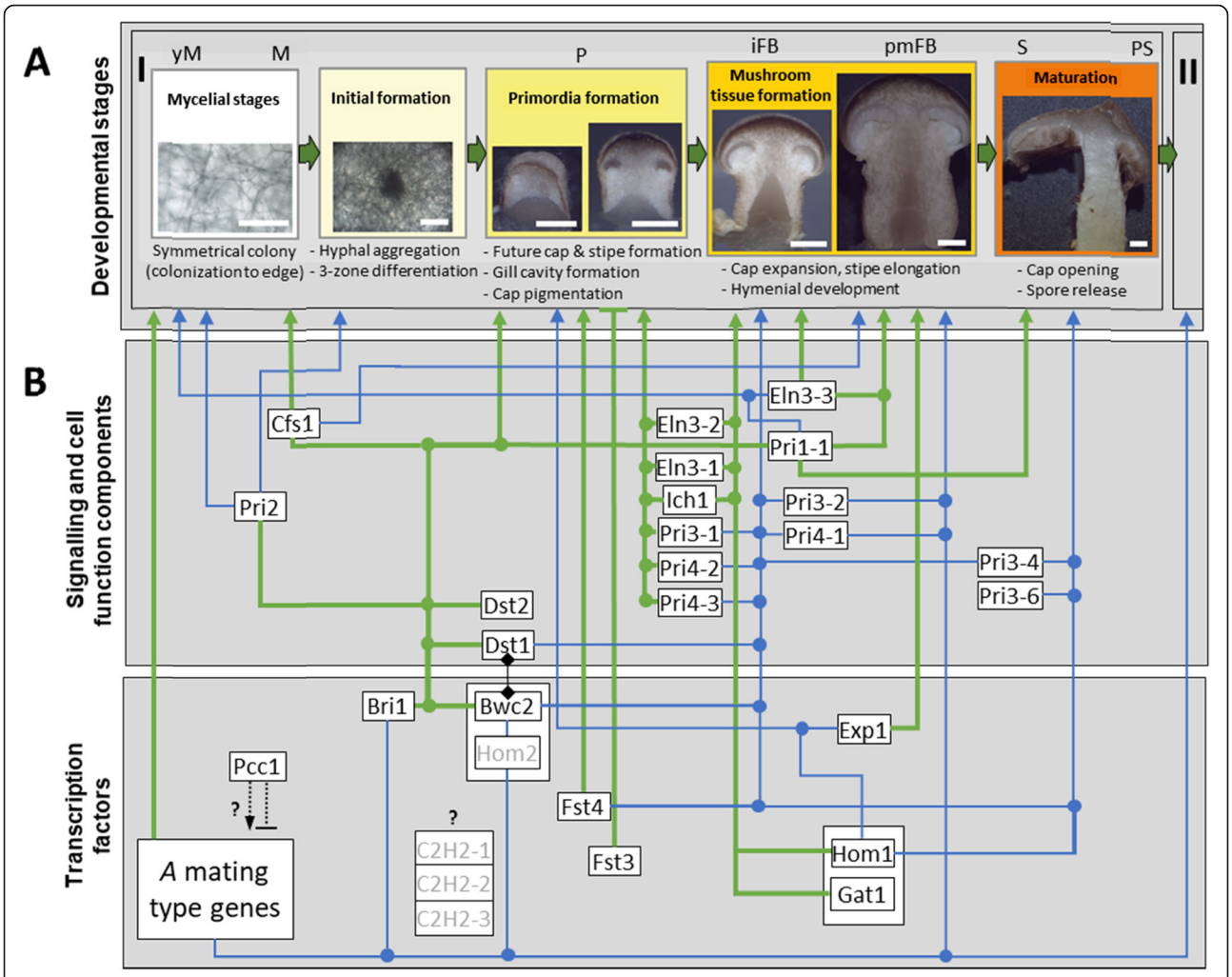

Fig. 7 Hypothetic roles of *C. aegerita* orthologs of "classic" model agaric fruiting-related genes (FRGs) from *S. commune*, *C. cinerea* and *C. aegerita* SM51 in FB development of *C. aegerita* AAE-3. **a** Landmarks during fruiting of *C. aegerita* AAE-3 in the fruiting regime of Herzog et al. [6] as monitored by handcuts. The five stages of this process are shown in white to orange boxes. Scale bars represent 100 µm (white box), 400 µm (light yellow box), 0.5 mm (yellow box), 1 mm (dark yellow box) and 2 mm (orange box). **b** Model for the regulation of *C. aegerita* AAE-3 FB development. Indices I and II symbolize consecutive fruiting flushes that are typical for *C. aegerita* fructification. Green lines represent a presumed functional role in a certain stage by the respective putative *C. aegerita* AAE-3 orthologs of proteins with experimentally ascertained function from *S. commune* and *C. cinerea*. These presumptions are necessarily also based on the differential expression data of the corresponding *C. aegerita*-FRG from the present study. For the sake of simplicity this categorization also extends to the *C. aegerita* AAE-3 counterparts of the *PRI1* to *PRI4* genes of *C. aegerita* SM51 where functions were presumed based on transcription profiling and in silico analyses. Putative interaction between Dst1 and Bwc2 is symbolized by a thin line ending in a diamond on each side. Blue lines represent hypothetical roles within *C. aegerita* AAE-3 fruiting body development solely based on the expression data recorded within the present study. Dotted lines represent conjectured (in) direct transcriptional activation/repression of target genes based on publications on putative counterparts from another mushroom. Grayed-out genes did not show differential expression in the present study in the respective developmental stage(s) of *C. aegerita* AAE-3 but have previously been shown to trigger relevant fruiting body developmental processes in the model mushroom *S. commune* [10, 12]

mark a big difference to species producing even more long-lasting FBs. In contrast to *C. aegerita* FBs, *S. commune* FBs are characterized by an extremely long persistence (> 50 years, [72]), releasing spores whenever conditions are favorable [7]. Alternatively, the here observed post-sporulation induction could also be a hint that transcription factors like Bri1 may not exclusively govern the expression of genes that are involved in the generation of FB structures. Possibly, transcriptional induction of genes involved in fruiting-associated processes could be regulated, too, by such a factor. Such could be volatile production for spore disperser attraction or fungivore repellency. As a gene triggering the formation of light-induced FB initials, which also seems to play a role in subsequent fruiting stages [27] (Fig. 7), *CFS1* showed an expression profile that peaked in

fruiting-induced mycelium and markedly decreased in later mycelium stages.

Induction in fruiting-induced mycelium in contrast to vegetative mycelium correlates well with the expression data of the *C. cinerea* ortholog in mycelial stages [27]. Still, there may be a difference between this FRG's expression in both fungi, since it shows an expression maximum in primordia of *C. cinerea* implying a role also for later stages of FB development in the plectenchyma of *C. cinerea* [27], while in *C aegerita* expression remains high in mycelium to a considerable amount until the premature FB stage but not in primordia of *C. aegerita*. This, of course neither rules out a putative indirect action of Cfs1 on *C. aegerita* FB stages forming on the fruiting-induced mycelium connected to them nor that a putative role of Cfs1 in later stages of development might potentially be mediated post-transcriptionally.

Being required for proper primordia development in response to illumination [26, 29, 30], the expression patterns of *BWC2* and *DST1* mostly match the expression patterns of their *C. cinerea* counterparts (Fig. 7). In addition, our quantitative PCR data are chiefly in agreement with the transcriptomic data on *BWC2* and *DST1* expression (see Fig. 3 and Additional file 3: Fig. S4), even though standard deviation in the sample from stipes of immature fruiting bodies was too high to confirm differential expression of *DST1* and *BWC2* there. Both genes are upregulated from the primordium stage onwards, interestingly also in the cap of developing FBs, implying a possible function in FB tissue generation there (Fig. 7). As a future experimental directive, it might be worth to test, e.g. by transcript profiling, whether a potential cap differentiation-associated tissue specificity of Dst1 expression might apply, which would corroborate the hypothesis that Dst1 may even have a function in the induction of cap formation. Such a cap tissue-specific expression localization, potentially from the primordial stage on, was also presumed for ageritin expression [72]. Moreover, transcriptomic data indicates upregulation of *DST1* in fruiting-induced mycelium, indicating a hypothetical role of *DST1* in the transition of FB initials to primordia that would need verification by functional analyses. Similar to *DST1*, *DST2* was also upregulated in primordia and developing FBs, as expected compared to its *C. cinerea* counterpart [29, 30] (Fig. 7).

According to Ohm et al. [10], the expression values of *FST3* in developing and maturating FBs in *C. aegerita* might restrict the extent of additional primordia formation ensuring that some FBs can fully develop assuming limited resources for sexual reproduction [10]. The paralogized *C2H2*, which is relevant to the transition from FB initials to primordia in the related agaric *S. commune* [10, 12], showed very low expression values. This leaves it open to future work how these paralogs might be involved in fruiting and whether they might be subject to post-transcriptional regulation. The same applies for *HOM2*, which also displayed less than 25 NRC (Fig. 7).

Among the cohort of genes associated with proper primordial development, the putative *C. cinerea* counterpart of *ICH1* had been characterized by a remarkable primordium malformation phenotype in the case of a recessive mutation of its DNA sequence [21]. Exhibiting an expression pattern that aligns very well with its *C. cinerea* counterpart, it can be presumed that *ICH1* should be similarly essential to proper primodium development (Fig. 7). In another *C. aegerita* wild type strain [19, 22–24], four genes were reported as transcriptionally induced during primordium development. In the genome sequence of *C. aegerita* AAE-3 [56], paralogization (commonly also referred to as gene duplication(s)/gene multiplication) for three of them can be detected. In the case of *PRI1*, the difference between the expressions of the paralogs during fruiting is similarly striking as it has been recently observed with the basidiome defense genes *AGT1* and *AGT2* of which only the former is transcriptionally induced during fruiting although both genes encode a functional ribotoxin [72, 73] and are located directly adjacent to each other on the chromosome. Both, *PRI1–1* and *PRI1–2* are supposed to encode a hemolysin. In the case of Pri1–1, a hemolytic activity has been proven at least for its putative *Pleurotus ostreatus* ortholog pleurotolysin [74]. Thus, the here-observed extraordinary high expression of *PRI1–1* during fruiting may go well together with a potential defense function of this protein to protect *C. aegerita* from predation during FB formation (Fig. 7). Supported by comparably high transcription levels especially in fruiting-induced mycelium and in primordia, and by the fact that *PRI2* should encode a hydrophobin, one may speculate whether Pri2 play an essential role for FB initial formation (Fig. 7). Making this point, Ohm et al. [10] discuss phenotypes and expression profiles, e.g. of the Δ*fst4* mutant which cannot form FB initials and displays a severely affected expression of dikaryon-specific hydrophobins. The scarcity of sequence motif annotation of hydrophobin genes [56] makes it very difficult to speculate about their possible functions, even for the highly expressed paralogs of *PRI3* (AAE3_14114 and AAE3_14115) and *PRI4* (AAE3_04665). Potential functions of *PRI3* and *PRI4* for the development of primordia into immature FBs or FB maturation-associated processes, as tentatively adumbrated by Fig. 7, may only be revealed to the point once gene knockout methodology is established for *C. aegerita*.

In *C. cinerea*, the gene encoding the Exp1 protein has been attributed a role in the basidiome maturation associated process of cap expansion [28]. *EXP1* has its expression maximum when cap expansion takes place in

premature fruiting bodies implying a conserved function with its *C. cinerea* counterpart. Besides this, it is also upregulated in induced mycelium at the beginning of the fruiting process. Since a faint upregulation of the *C. cinerea* gene has been observed already in primordia [28], it may not be unexpected that the HMG-box transcription factor Exp1 could also regulate genes outside FB maturation (Fig. 7). Being involved in the FB maturation-associated process of stipe elongation in *C. cinerea*, the paralogs of *ELN3* exhibited diverging expression patterns during fruiting. Only *ELN3–1* (AAE3_00364) was exclusively upregulated in FB tissue. Displaying its maximum transcription in primordia, and to a lesser extent in maturing FBs, its function may extend also to a role in primordial plectenchyma formation. In contrast, *ELN3–2* (AAE3_06792) and ELN3–*3* (AAE3_13318) had their expression maxima in uninduced mycelium with lesser expression maxima in developing FBs or primordia (only *ELN3–2*). Compared to other model agarics, as anticipated by Gupta et al. [56], the here-recorded differential gene expression of *EXP1* and the *ELN3* paralogs implies a more complex genetic regulation of basidiome maturation in *C. aegerita* (Fig. 7). This, of course, needs verification by functional genetics analyses in future studies.

In *S. commune*, the Gat1- and the Hom1-encoding gene get transcriptionally induced mainly during development of FBs although a slight expression is detectable for *HOM1* already during aggregate and primordia formation [10, 12]. Functional analyses revealed both transcription factors to be important for plectenchyma formation in developing FBs of this species [10, 12]. Also, despite a possible (partial) shift in function during fruiting, both transcription factors are conserved also among other Agaricales members [34]. Differential expression of *HOM1* and *GAT1* in *C. aegerita* is chiefly congruent with the expression pattern of their *S. commune* counterparts [12]. This provides evidence to hypothesize that their functions should be conserved in *C. aegerita* (Fig. 7).

The cluster analysis on FRGs expressed in FB tissue samples (Additional file 3: Figure S2) resulted in clear groups of strongly positively correlated genes. This cluster formation is also chiefly in agreement with the assignment of genes into the expression maxima cohorts established within Fig. 3, particularly for genes that have early or late expression maxima in FB tissue. In contrast, the cluster analysis of the mycelium samples showed much less comprehensive cluster formation. Accordingly, the general overlap between the clusters from the cluster analysis and the gene cohorts revealing early or late expression maxima in mycelial stages (Fig. 3, Additional file 3: Figure S3) was also much less comprehensive. This underlines that a cluster analysis can be very useful to time-efficiently identify strongly positive correlated genes with common differential expression patterns.

VOC related biosynthesis pathways

Sesquiterpene synthases from fungi have proven to often have a high catalytic promiscuity, leading to a highly diverse number of sesquiterpenes despite low variety of enzymes [75–78]. Furthermore, modifications of terpenes catalyzed by cytochrome P450 monooxygenases, oxidoreductases and different group transferases [79] might also contribute to the high diversity of sesquiterpenes observed in the HS of *C. aegerita* [54]. Most sesquiterpenes produced by the recombinant *E. coli* clones were also present during sporulation in the HS of *C. aegerita* [59]. Interestingly, genes of the mevalonate pathway as well as of the STSs showed generally higher expression levels in the mycelium than in FB samples during the late phase of the fruiting process. This indicates that the mycelium rather than the FB tissue is the origin of the high amounts of sesquiterpenes observed in the HS of *C. aegerita* during sporulation [54]. This would also explain the occurrence of sesquiterpenes in the HS of the monokaryon AAE-3-40, which do not develop FBs [54], and why these substances were not detected in previous studies on VOCs in FBs of *C. aegerita* [80–82]. In this context the question remains, if sporulation triggers the release of sesquiterpenes or if sesquiterpenes are somehow associated with the release of spores. Nonetheless, it seems that sesquiterpenes are involved in a so far barely understood communication between mycelium and FBs.

In addition to the sesquiterpenes, the biosynthesis of oxylipins in fungi is of special interest. The pathways leading to volatile fungal oxylipins, including the typical mushroom C8 VOCs such as oct-1-en-3-ol, octan-3-one and octan-3-ol, but also other oxylipins, like 2-pentylfuran, are still scarcely known despite their ubiquitous occurrence in fungi. Fungal volatile oxylipins are derived from linoleic acid and are therefore connected to the biosynthesis of fatty acids [60]. Generally, we observed a higher expression of genes involved in the fatty acid synthesis and further processing to linoleic acid in FB stages than in mycelial stages. Comparable data was obtained by Wang et al. investigating one mycelium and one FB developmental stage of *C. aegerita* and showing an upregulation of genes involved in fatty acid metabolism in FBs [66]. A similar upregulation was observed in *S. commune* during FB development [13]. In fact, a recently published comprehensive transcriptomic study dealing with six different Agaricomycetes species and the gene expression during various developmental stages

revealed as well a higher expression of genes involved in lipid biosynthesis in fruiting stages throughout all investigated species [33]. This might indicate that this pattern is quite common among mushroom-forming fungi.

It is widely accepted that LOXs and DOXs are involved in fungal oxylipin biosynthesis using linoleic acid as precursor, although little is known about the exact formation processes [60]. Despite the prominent role of LOXs in the fungal oxylipin synthesis, only three LOXs in Basidiomycota are functionally characterized so far [83–85]. Among them, the *C. aegerita* Lox4, a 13-LOX exclusively producing 13-hydroperoxy-9,11-octadecadienoic acid (13-HPOD) [85] whereas LOXs from *Pleurotus ostreatus* [83] and *Pleurotus sapidus* [84] produce, along with the main product 13-HPOD, also minor amounts of 9-hydroperoxy-10,12-octadecadienoic acid (9-HPOD). The role of 13-HPOD in the formation processes of fungal VOCs is still largely unknown. It seems that the biosynthesis of n-hexanal is associated with 13-HPOD [86]. However, it was also proposed that 13-HPOD is involved in the synthesis of oct-1-en-3-one, which is subsequently reduced to oct-1-en-3-ol or octan-3-one by so far unknown ADHs or ene-reductases, respectively (Fig. 8). In parallel, it is assumed that oct-1-en-3-ol emerges from 10-hydroperox-8,12-octadecadienoic acid (10-HPOD) as precursor [49, 87]. Nonetheless, several studies excluded 13-HPOD from being a precursor of oct-1-en-3-ol [63, 86, 88]. Recently, Tasaki et al. determined the transcription levels of *PoLOX1* and *PoLOX2* along with the oct-1-en-3-ol content and LOX activity in mycelium, primordia, young FBs and mature FBs of *P. ostreatus* [49]. In agreement with our results, LOX genes were mostly expressed in FB developmental stages with *PoLOX1* mainly in primordia and *PoLOX2* primarily in fully developed FBs. Tasaki et al. reported a correlation between LOX activity and *PoLOX1* expression in FB developmental stages. However, no LOX activity was detected in the mycelium, excluding LOXs as a source for oct-1-en-3-ol present in the mycelium [49]. Our transcriptomic data indicates similar with only little pronounced expression of LOX genes in the mycelium despite the presence of oct-1-en-3-ol during all mycelial stages [54].

Thus, a DOX might be responsible for the oct-1-en-ol production. In contrast to the quite well understood DOXs from Ascomycota [89], to our knowledge, no DOXs from Basidiomycota are characterized so far. Recently, Oliw analyzed reaction products of *Rhizoctonia solani* mycelium after addition of linoleic acid and observed substances probably derived from 9*S*-DOX-AOS (allene oxide synthase), 8*S*-DOX-8,9-ODS (oleate diol synthase) and 8*R*-DOX activity [90]. The biosynthesis of 8*S*-HPOME, 8*S*,9*S*-DiHOME and 8*R*-HPODE were linked to the proteins KEP54849 or KEP46854. This is due to the presence of a NXXQ motif in the I-helix of the CYP (cytochrome P450) domains, proven to be involved in the hydroperoxide isomerase activities of 7,8- and 5,8-LDS (linoleate diol synthase) [91], and the occurrence of the YRWH sequence. Whereas KEP52552,

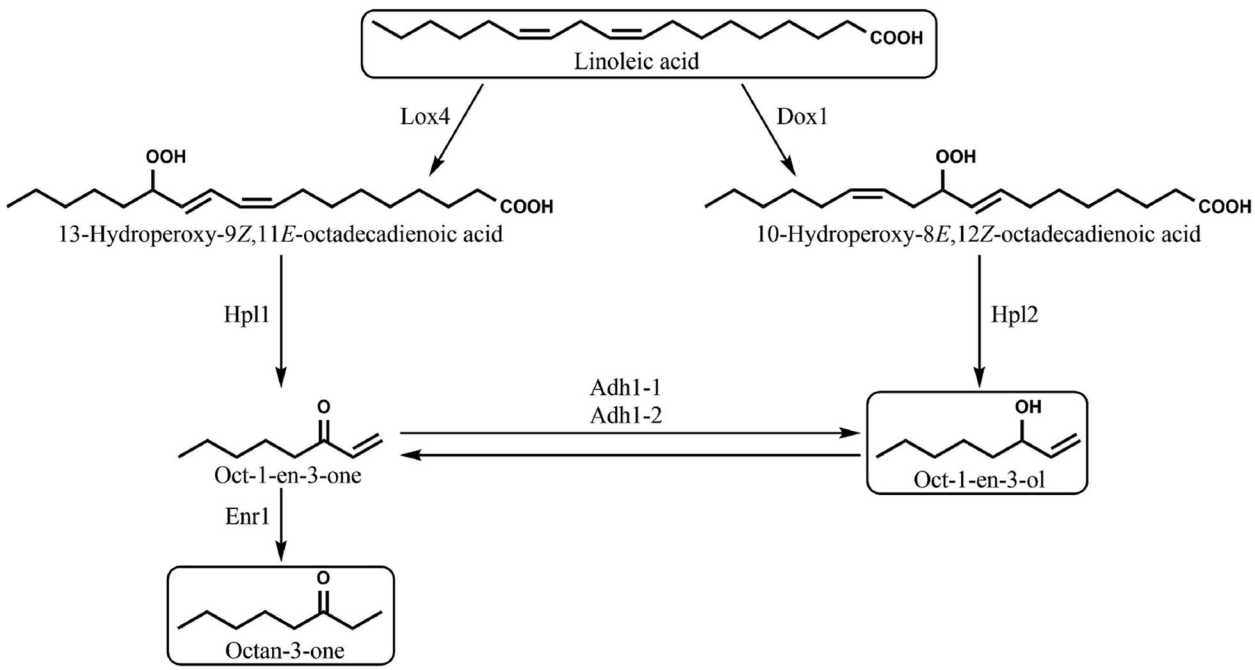

Fig. 8 Putative pathways for the enzymatic formation of oxylipins derived from linoleic acid in *C. aegerita*. Lox4 (AAE3_04864), Dox1 (AAE3_13098), Hpl1 (AAE3_05330), Hpl2 (AAE3_09203), Adh1–1 (AAE3_00054), Adh1–2 (AAE3_06559), Enr1 (AAE3_13549)

lacking the NXXQ motif and revealing an uncommon YHWH sequence, was connected to the 9*S*-DOX-AOS activity [90]. On basis of amino acid sequences of characterized DOXs from ascomycetes and putative DOXs of the basidiomycete fungus *R. solani*, two putative DOXs of *C. aegerita* show highest similarities with the ones from *R. solani* (AAE3_00407 with KEP52552 and AAE_13098 with KEP54849) (Additional file 7: Figure S12), which might indicate similar reaction products of these DOXs. Nonetheless, the putative DOXs in *C. aegerita* reveal remarkable differences to the two putative DOXs KEP52552 and KEP54849 from *R. solani* regarding leucine and valine residues in the DOX domain (AAE3_13098: Val-403, Leu-407; AAE3_00407: Phe-331, Leu-335) (Additional file 7: Figure S13A). These are confirmed to be crucial for the oxygenation at C^{-10} and C^{-8} of linoleic acid [92, 93]. In this context, it is worth mentioning that the putative DOX KEP46854, which shows overall less amino acid sequence similarity with the two putative DOXs from *C. aegerita* (Additional file 7: Figure S12), possesses a VXXXL residue. The same applies to AAE3_13098. Additionally, both putative DOXs from *C. aegerita* harbor, unlike KEP52552, the YRWH motif, commonly found in the DOX domains of 8- and 10-DOXs, whereas the corresponding sequence in 9*S*-DOX-AOS, 9*R*-DOX-AOS and 9*R*-DOX enzymes is normally YRFH (Additional file 7: Figure S13A). In the C-terminal CYP domains of AAE3_13098 and AAE3_00407, the NXXQ motif is absent. This motif is commonly found in 10*R*-DOX-EAS (epoxy alcohol synthase), 5,8- and 7,8-LDS, but not in 9*S*-DOX-AOS, 9*R*-DOX-AOS, 10*R*-DOX-CYP and 9*R*-DOX enzymes, the latter lacking a CYP domain and consequently also this motif [94] (Additional file 7: Figure S13B). Furthermore, like 10*R*-DOX-CYPs, both putative DOXs are missing a conserved cysteine residue in the CYP domain which serves as the fifth iron ligand in P450 enzymes and is essential for the function [93] (Additional file 7: Figure S13B). Therefore, it is likely that the CYP domains of DOXs from *C. aegerita* are, comparable to 10*R*-DOX-CYPs, not functional [93]. Hence, the putative DOXs from *C. aegerita* and 10*R*-DOX-CYPs have some structural features in common, even though the important leucine and valine residues mentioned above as part of a conserved LRTIV motif in 10*R*-DOX-CYPs differ from residues observed in AAE3_13098 and AAE3_00407 (Additional file 7: Figure S13A). Interestingly, 10*R*-DOX-CYPs of the fungal phylum of Ascomycota reveal the potential to form volatile C8 compounds since they produce inter alia 10-HPOD, which serves as a precursor for oct-1-en-ol [55, 63]. Moreover, addition of linoleic acid to an extract of *E. coli* containing a recombinant 10*R*-DOX-CYP from *A. nidulans* resulted in the production of oct-1-en-3-ol, oct-2-en-1-ol, oct-2-enal and octan-3-one [93]. Taking these aspects into account, it is possible that DOXs from *C. aegerita* might constitute a novel DOX subfamily with so far unknown products. In this context, the putative DOX AAE3_13098, which also shows comparably high transcription in the mycelium and similarities of its expression course to the oct-1-en-3-ol pattern in the HS of *C. aegerita*, seems to be an interesting candidate for future characterization studies. This way, one may become able to tap the so far neglected topic of DOXs in Basidiomycota and their potential role in (volatile) oxylipin formation (Fig. 8).

In plants, the cleavage of fatty acid hydroperoxides by HPLs is well known and HPLs can be divided into 9-HPLs, 13-HPLs and 9/13-HPLs responsible for the synthesis of C6- and C9-aldehydes which have, along with their derivatives, various functions in plants [95, 96]. In contrast, there is only scarce information about fungal HPLs. In an early study, Wurzenberger and Grosch incubated 9-, 10-, 12- and 13-HPOD with a protein fraction isolated from an extract obtained from the button mushroom *Agaricus bisporus* [63]. They observed that only addition of 10-HPOD resulted in the formation of oct-1-en-3-ol and 10-oxo-*trans*-8-decenoic acid probably due to the presence of a 10-HPOD specific HPL. Despite the fact that other studies suggest the existence of such an enzyme as well [86, 88], to our knowledge no fungal HPL has been isolated and characterized so far. Phylogenetic analysis revealed that putative HPLs encoded by AAE3_09218, AAE3_09203, AAE3_06699 and AAE3_11433 were closer related to characterized plant HPLs and AOS than the other putative HPLs we found in the genome of *C. aegerita* (Additional file 7: Figure S14). In FB samples as well as in the mycelial stages, the course of expression of the putative HPL gene AAE3_09203 was comparable to the transcription of the putative DOX gene AAE3_13098. Both genes showed similarities to the oct-1-en-3-ol pattern in the HS of *C. aegerita* (Additional file 7: Figure S15), making AAE3_09203 an interesting candidate for characterization studies. It is worth mentioning that AAE3_05330, identified as a putative HPL by means of BLAST search using a 13-HPL protein sequence of *A. thaliana*, shared similarities in the expression pattern with the gene coding for the characterized Lox4. Both genes were highly transcribed in late fruiting stages along with the appearance of octan-3-one, which might indicate an involvement of both enzymes in the formation of this C8 VOC (Fig. 8, Additional file 7: Figure S16).

In addition to the oxygenation of linoleic acid by LOXs/DOXs and the subsequent cleavage into C8 compounds, further enzymes are necessary to provide a plentitude of C8 VOCs in fungi. It has been demonstrated that in *A. bisporus* oct-1-en-3-one can be converted to oct-1-en-3-ol as well as to octan-3-one,

probably by means of two different enzymes [64]. These results were confirmed by Wanner and Tressl using a crude enzyme extract of *Saccharomyces cerevisiae* [65]. Furthermore, they were able to isolate two reductases capable to convert oct-1-en-3-one to octan-3-one [65]. In this context, ADHs and ene-reductases might play an important role, explaining the observed decrease of oct-1-en-3-ol during sporulation and, thereafter, the increase of octan-3-one in the HS of *C. aegerita* [54]. A heterologously expressed ADH from the fungus *Neurospora crassa* was able to oxidize octan-1-ol [97]. Using the amino acid sequence of this ADH (Q9P6C8), we identified putative ADHs in the genome of *C. aegerita* by means of BLAST search which might be able to oxidize oct-1-en-3-ol to oct-1-en-3-one (Fig. 8, Additional file 6: Figure S10). Of those genes, the putative ADH gene AAE3_00054 showed highest expression of all putative ADH genes in FB development stages. This high expression came along with a decreasing amount of oct-1-en-3-ol and an increasing amount of octan-3-one in the HS of *C. aegerita*. In addition, phylogenetic analysis showed that AAE3_00054 and AAE3_06559 are closer related to the ADH of *N. crassa* than the other putative ADHs (Additional file 7: Figure S17).

The gene AAE3_13549 coding for a putative ene-reductase showed the highest transcription levels of all putative ene-reductases in late stages of FB development. Interestingly, amino acid sequence alignment revealed notable similarity (54%) between the putative *C. aegerita* ene-reductase encoded by AAE_13549 and the characterized plant ene-reductase from *N. tabacum* (Q9SLN8) known to be able to reduce oct-1-en-3-one (Fig. 8, Additional file 7: Figure S18). Additionally, in FB development stages, resemblance between the transcription of AAE3_13549 and the putative ADHs AAE3_00054, which codes for a putative ADH, along with the decreasing amount of oct-1-en-3-ol and the increasing amount of octan-3-one (Additional file 7: Figure S19) supports the proposed transformation of oct-1-en-3-ol via oct-1-en-3-one to octan-3-one [49, 64].

Overall, it seems that the first occurrence of octan-3-one in the HS of *C. aegerita* in late FB developmental stages is probably due to enzymatic activities in the FB tissue and not in the mycelium. This assumption bases on the fact that the transcription levels of genes coding for enzymes putatively related to the formation processes of C8 VOCs, such as enzymes involved in the fatty acid synthesis, LOXs, putative DOXs, putative HPLs, putative ADHs and putative ene-reductases, in FB stages showed transcription patterns that were matchable to the octan-3-one production. This would also explain why octan-3-one was not observed in the HS of *C. aegerita* monokaryotic strains unable to develop FBs [54]. In contrast, the transcriptome data suggest that the origin of the sesquiterpenes appearing in the HS of *C. aegerita* during the sporulation is the mycelium instead of the FBs. This is highly interesting as the sesquiterpene production occurs during sexual sporulation. The formation of various VOCs in different morphological parts of *C. aegerita* might be, along with the changing volatilome during different developmental stages [54], an important part in fungal communication which involves several VOCs as infochemicals with numerous functions (reviewed in [50, 51]). This is an aspect, which should be kept in mind during further studies dealing with e.g. fungal intra- and interspecific VOC based communication. In total, the combination of volatilome and transcriptome data proved to be a powerful tool to elucidate coherences regarding the VOC biosynthesis pathways in fungi.

Conclusions

In this work, we investigated the changes in the transcriptome of *C. aegerita* during different points in time of FB development including seven mycelial and five plectenchymatic samples. On the one hand, the transcriptomic data generated here gave first insights into how the network of known FRGs may direct the complex process of FB development in *C. aegerita*. The here-observed differential expression patterns of partially highly paralogized FRGs during fruiting in contrast to the situation in the other model agarics *C. cinerea* or *S. commune* suggests a seemingly more complex regulation of fruiting in *C. aegerita*. On the other hand, by comparing the transcriptome with volatilome data of a recently conducted study [54], we were able to identify enzymes potentially involved in the biosynthesis of C8 oxylipins. Despite ubiquitously found in fungi and contributing to the typical mushroom odor, little is known about pathways leading to C8 based VOCs. To further elucidate this topic, enzymes of interest identified in this study, including LOXs, DOXs, HPLs, ADHs and ene-reductases, are valuable candidates for further studies. Additionally, we were able to localize the mycelium as the presumable main source of observed sesquiterpenes, whereas the in late stages detected changes in the C8 compound profile is most likely due to the activity of enzymes located in the FB tissue.

Methods

Fungal materials

The tested dikaryotic strain *C. aegerita* AAE-3 was grown at 24 °C in the dark in crystallizing dishes (lower dish: 70 mm in diameter, upper dish: 80 mm in diameter) with 16 mL 1.5% MEA (containing 15 g malt extract and 15 g agar per L) and sealed with Parafilm™. Ten days after the inoculation, the Parafilm™ was removed and the samples were transferred to a climate chamber

(24 °C, 95%rH, 12/12 h day/night rhythm) and cultured on glass plates for further 18 days. Seven developmental stages of *C. aegerita* AAE-3 were tested, consisting of young mycelium (day 10 post inculation, p.i.), mycelium (day 14 p.i.), primordia (day 18 p.i.), immature FBs (day 20 p.i.), premature FBs (day 22 p.i.), sporulation (day 24 p.i.) and post sporulation (day 28 p.i.). Accordingly, seven mycelium and five FB stages were sampled. FB stages were collected by means of a scalpel used to carefully separate the FB samples from the mycelium. From a single agar plate only FB samples of a certain stage were sampled using the whole FB for RNA extraction and discarding younger stages (for details see Fig. 1). Mycelium samples were obtained using a spatula to gently remove the mycelium from the agar plate and thereby avoiding to collect possible FB stages. All samples were stored in RNAlater (Quiagen, Venlo, Netherlands) at − 20 °C. Each stage was grown in six replications of which two comparable samples were pooled prior to RNA extraction resulting in 36 RNA samples for sequencing. Accordingly, transcriptomic data presented are the mean values of RNA sample triplicates.

RNA isolation and sequencing

For the RNA extraction, RNAlater was removed and samples were frozen in liquid nitrogen and ground into powder using mortar and pestle. Total RNA was extracted using TRIzol® (Life Technologies, Carlsberg, California, USA) according to the manufacturer's instructions. Obtained RNA was solved in DEPC treated water and quantity as well as quality was assessed by means of photometric analysis (Pearl nanophotometer, Implen, Munich, Germany) and agarose gel electrophoresis (Peqlab electrophoresis chamber, VWR Life Science, Radnor, Pennsylvania, USA). RNA samples were stored at − 80 °C. For sequencing, RNA samples were send on dry ice to Lexogen (Lexogen GmbH, Vienna, Austria). The quality of the RNA samples was verified by Lexogen using a capillary gel electrophoresis system (Bioanalyzer, Agilent, Waldbronn, Germany). The complete sequencing procedure was offered as a Lexogen QuantSeq FWD SR5 service, including RNA quality control, RNA quantification, QuantSeq FWD library preparation for Illumina sequencing, NextSeq 75cyc high output sequencing, read trimming, mapping and quantification. Cutadapt version 1.16 [98] was used to trim the reads by removing trailing poly(A) and poly(G) as well as adapter sequences. STAR aligner version 2.5.3a (for details see: https://github.com/alexdobin/STAR/blob/master/doc/STARmanual.pdf) was used to align the trimmed reads on the *C. aegerita* reference genome [56] (version 2.2 of the genome has been used and can be downloaded via the respective genome browser (http://www.thines-lab.senckenberg.de/agrocybe_genome/). Quantification of the aligned reads was performed by featureCounts version 1.6.2. The QuantSeq 3′ mRNA sequencing method generates for each transcript only one fragment so the number of reads can be linked directly to the number of transcripts and is therefore proportional to the gene expression [99]. The average number of reads over all samples used for the alignment was 14.4 million reads per sample of which 93.1% resulted in a unique alignment to the reference genome and 1.4% were mapped to multiple loci. About 0.1% of the reads were discarded since the mapping resulted in too many loci and around 5.4% of the reads were too short for an adequate alignment.

Transcriptome analysis and bioinformatics

Transcriptome data analysis were performed and implemented in R (version 3.6.0) [100]. Different R packages were applied as parts of scripts used for the transcriptome analysis. DEG analysis was accomplished by means of the R package "ImpulseDE2" (version 1.8.0) displaying not only permanent but also transient changes at the level of transcription [101, 102]. Accordingly, DEGs can be classified into four groups: transition up for monotonous upregulated genes, transition down for monotonous downregulated genes, transient up for transiently upregulated genes and transient down for transiently downregulated genes (for details see Fisher et al. [101]). The "ggplot2" R package (version 3.1.1) is part of the "tidyverse" collection and a powerful and versatile tool for graphical visualization [103]. This package was applied to generate the PCA plots. The subsequent used Friedman test and the Wilcoxon-Nemenyi-McDonald-Thompson test were originally implemented by Galili [104] and internally based on the R packages "coin" and "multcomp". The R package "ComplexHeatmap" (version 2.0.0) were used to visualize the correlation matrices. For the correlation analysis Spearman rank correlation was applied. All R scripts used within this publication are deposited at https://github.com/AnnsophieWeber/ComparisonOfMetabolomeAndTranscriptomeData.

Identification of proteins in *C. aegerita*

Generally, proteins were identified in the genome of *C. aegerita* using BLAST search (Geneious version 11.1.5, Biomatters, New Zealand) using amino acid sequences of mainly characterized proteins against the UniProt database [105]. Generally, a blastp E-value threshold of 1e-10 was applied and hits with the lowest E-values and highest identity were blasted (blastp) against the UniProt database to verify the results. Multiple hits were compared by alignment of the protein sequences and a phylogenetic analysis. Phylogenetic analyzes were performed by means of Phylogeny.fr (http://www.phylogeny.fr/) using default parameters [106].

Alignments were carried out by using Clustal Omega (https://www.ebi.ac.uk/Tools/msa/clustalo/) with default parameters [107].

Protein IDs for FRGs in *C. aegerita* were obtained from Gupta et al. [56] with exception of a second putative homolog of *AaPRI1* from *C. aegerita* SM51 within the *C. aegerita* AAE-3 genome sequence represented by the ID AAE3_04306. For LOXs in *C. aegerita*, protein IDs were used which were published by Karrer and Rühl [85]. STS protein IDs were obtained from Zhang et al. [59]. For identification of enzymes involved in the mevalonate pathway analogues in *S. cerevisiae* were used: acetoacetyl-CoA synthase (P41338), 3-hydroxy-3-methylglutaryl-CoA synthase (P54839), 3-hydroxy-3-methylglutaryl-CoA reductase (P12683, P12684), phosphomevalonate kinase (P24521), diphosphomevalonate decarboxylase (P32377), isopentenyl-diphosphate delta isomerase (P15496), dimethylallyltransferase/farnesyl pyrophosphate synthase (P08524). For enzymes putatively involved in the fatty acid synthesis, analogs from different fungi were used: acetyl-CoA carboxylase (*Laccaria bicolor*, B0CUD8), fatty acid synthase (*Omphalotus olearius*, B3GN11), β-ketoacyl-CoA synthase (*S. cerevisiae*, P25358), Δ^9-fatty acid desaturase (*L. edodes*, Q76C19), Δ^{12}-fatty acid desaturase (Q65YX3, *L. edodes*). Putative DOXs were identified in the genome of *C. aegerita* using protein sequences of characterized DOXs from Ascomycetes including a 8R-DOX-7,8-LDS (*Gaeumannomyces graminis*, AAD49559), a 9R-DOX (*Fusarium oxysporum*, EGU79548) and a 10R-DOX-CYP (*Aspergillus fumigatus*, ABV21633). Putative HPLs of *C. aegerita* were identified by means of BLAST search using protein sequences of characterized members of the CYP74 family in plants including a 13-HPL (*Arabidopsis thaliana*, Q9ZSY9), a 9-HPL (*Prunus dulcis*, Q7XB42), a 9/13-HPL (*Cucumis sativus,* Q9M5J2) and a 13-AOS (*A. thaliana*, Q96242). Considering the features of known CYP74 proteins in plants, we chose for each of the four proteins mentioned above the top 10 matches revealing sequence lengths between 300 and 700 amino acids. Additionally, to reduce the number of putative HPLs to the essentials, only genes were considered showing maximum transcription levels higher than 300 NRC. Putative ADHs were identified using an ADH of the fungus *Neurospora crassa* (Q9P6C8) proven to be able to oxidize octan-1-ol [97]. To reduce the number of putative ADHs to the essentials, only genes were considered showing maximum transcription levels higher than 300 NRC. Putative ene-reductases were identified in the genome of *C. aegerita* using sequences of characterized non-FMN ene-reductases of plants accepting inter alia non-2-enal and oct-1-en-3-one as substrates [108, 109] (*Nicotiana tabacum*, Q9SLN8; *A. thaliana*, Q39172) and a fungal non-FMN ene-reductase (*Sporidiobolus salmonicolor*, A0A0D6ERK8). In addition, sequences of fungal FMN depending OYE ene-reductases were used proven to be able to reduce amongst others citral (geranial) which shows some structural similarities with non-2-enal and oct-1-en-3-one [110, 111] (*Pichia stipites*, A3LT82; *Meyerozyma guilliermondii*, A5DR62). To reduce the number of putative ene-reductases to the essentials, only genes were considered showing maximum transcription levels higher than 300 NRC.

RT-qPCR based confirmation of expression values of selected candidate genes

To exemplarily validate our transcriptomic data on FB development of *C. aegerita* AAE-3 via RT-qPCR, an optimal combination of two reference genes (gene IDs AAE3_02268 and AAE3_07769) with high expression stability during vegetative growth and fruiting of *C. aegerita* was identified recently by Hennicke et al. and Tayyrov et al. [72, 73]. Primers for the reference genes and general RT-qPCR conditions are identical to the ones employed by Hennicke et al. and Tayyrov et al. [72, 73], while primers for the genes *HOM1*, *GAT1*, *BWC2* and *DST1* (Additional file 3: Table S4) were designed here, applying the same criteria. Mycelial and fruiting stage samples were obtained, extracted and RNA quality assessed as performed by Hennicke et al. and Tayyrov et al. [72, 73], from developmental stages/plectenchymatic samples of *C. aegerita* AAE-3 chiefly congruent to the ones of the RNA-seq analysis in the present study, deviating only by these: fruiting body initials (FBi) at day 15 to 16 post inoculation (p.i.); fruiting body primordia (P) at day 17 to the morning of day 19 p.i.; immature FBs separately sampled into stipe (iFBs) and cap (iFBc) at day 19 to the morning of day 21 p.i. Samples of the stages premature FBs (day 22 p.i.), sporulation (day 24 p.i.), and post sporulation (day 28 p.i.) were not assessed here.

Abbreviations

ADHs: Alcohol dehydrogenases; AOS: Allene-oxide synthase; CYP: Cytochrome P450; DEGs: Differentially expressed genes; DOXs: Dioxygenases; EAS: Epoxy alcohol synthase; FBs: Fruiting bodies; FRGs: Fruiting-related genes; HPLs: Hydroperoxide lyases; 9-HPOD: 9-Hydroperoxy-10,12-octadecadienoic acid; 10-HPOD: 10-Hydroperoxy-8,12-octadecadienoic acid; 13-HPOD: 13-Hydroperoxy-9,11-octadecadienoic acid; HS: Headspace; LDS: Linoleate diol synthase; LOXs: Lipoxygenases; NRC: Normalized read counts; ODS: Oleate diol synthase; OYE: Old yellow enzyme; PCA: Principal component analysis; p.i: Post inoculation; RT-qPCR: Real-time reverse transcription quantitative polymerase chain reaction; STSs: Sesquiterpene synthases; VOCs: Volatile organic compounds

Supplementary Information

The online version contains supplementary material available at https://doi.org/10.1186/s12864-021-07648-5 .

Additional file 1: Differential gene expression during fruiting body development. **Figure S1.** Heatmap of DEGs in mycelium and FB samples.

Additional file 2: Table S1. Read counts of all sequenced genes. **Table S2.** Genes showing a > 5 fold decrease between day 22 and day 22 in the mycelium. **Table S3.** Genes showing a > 5 fold increase between day 22 and day 22 in the mycelium.

Additional file 3: Transcription of fruiting-related genes (FRGs). **Figure S2.** Correlation of the expression of putative *C. aegerita* homologs of FRGs in plectenchymatic samples (FB 'tissue') during the fructification process. **Figure S3.** Correlation of the expression of putative *C. aegerita* homologs of FRGs in mycelium samples. **Figure S4.** RT-qPCR-based expression level assessment with *C. aegerita* orthologs of four well-known fruiting-related genes (FRGs) during fruiting of *C. aegerita*. **Table S4:** RT-qPCR primers for the FRGs *HOM1*, *GAT1*, *BWC2* and *DST1*.

Additional file 4: Terpenoid biosynthesis. **Figure S5.** Expression of genes involved in the mevalonate pathway and of the sesquiterpene synthases Agr1 to Agr9 in *C. aegerita*. **Figure S6.** Transcription levels of the sesquiterpene synthases Agr1, Agr4, Agr8 and Agr9.

Additional file 5: The fatty acid metabolism. **Figure S7.** Expression of genes putatively involved in the fatty acid biosynthesis of *C. aegerita*.

Additional file 6: Figure S8. Proposed pathways for the enzymatic formation of fungal oxylipins. **Figure S9.** Transcription levels of putative HPLs as well as the relative concentrations of volatile oxylipins in the headspace of *C. aegerita*. **Figure S10.** Transcription levels of putative ADHs as well as the relative concentrations of volatile oxylipins in the headspace of *C. aegerita*. **Figure S11.** Transcription levels of putative ene-reductases as well as the relative concentrations of volatile oxylipins in the headspace of *C. aegerita*.

Additional file 7: Revealing putative enzymes of the oxylipin pathway in *C. aegerita*. **Figure S12.** Phylogenetic analysis of different DOXs. **Figure S13.** Partial amino acid sequence alignment of different DOXs. **Figure S14.** Phylogenetic analysis of different CYP74 proteins. **Figure S15.** Transcription levels of the putative DOX AAE3_13098 and the putative HPL AAE3_09203. **Figure S16.** Transcription levels of AAE3_04864 (*LOX4*) and the putative HPL AAE3_05330. **Figure S17.** Phylogenetic analysis of putative ADHs. **Figure S18.** Amino acid sequence alignment of ene-reductases. **Figure S19.** Transcription levels of the putative ADHs AAE3_00054 and AAE3_06559 as well as the putative ene-reductase AAE3_13549.

Acknowledgements
The authors thank the three anonymous reviewers for their elaborated comments and suggestions that helped to improve this paper.

Authors' contributions
MR conceived the study; AO, FH, MR and RH performed experiments and analyzed data. AW developed the used R scripts; AO, FH and MR drafted the manuscript. All of the authors read and improved the final manuscript. The author(s) read and approved the final manuscript.

Funding
This study was financially supported by the Deutsche Forschungsgemeinschaft (DFG, German Research Foundation) – Funder Id: https://doi.org/10.13039/501100001659, Grant Number: RU 2137/1–1. FH acknowledges funding from the DFG under grant HE 7849/3–1. Open Access funding enabled and organized by Projekt DEAL.

Availability of data and materials
Data are available within the NCBI BioProject PRJNA677924 under the BioSample numbers 16789160 to 16789171.

Declarations

Ethics approval and consent to participate
Not applicable.

Consent for publication
Not applicable.

Competing interests
The authors declare that they have no competing interests.

Author details
[1]Institute of Food Chemistry and Food Biotechnology, Justus Liebig University Giessen, 35392 Giessen, Hesse, Germany. [2]International Institute Zittau, Technical University Dresden, 02763 Zittau, Saxony, Germany. [3]Project Group Genetics and Genomics of Fungi, Ruhr-University Bochum, Chair Evolution of Plants and Fungi, 44780 Bochum, North Rhine-Westphalia, Germany. [4]Fraunhofer Institute for Molecular Biology and Applied Ecology IME Branch for Bioresources, 35392 Giessen, Hesse, Germany.

Received: 11 December 2020 Accepted: 19 April 2021
Published online: 04 May 2021

References
1. Sandargo B, Chepkirui C, Cheng T, Chaverra-Muñoz L, Thongbai B, Stadler M, et al. Biological and chemical diversity go hand in hand: Basidiomycota as source of new pharmaceuticals and agrochemicals. Biotechnol Adv. 2019; 37(6):107344. https://doi.org/10.1016/j.biotechadv.2019.01.011.
2. Sánchez-García M, Ryberg M, Khan FK, Varga T, Nagy LG, Hibbett DS. Fruiting body form, not nutritional mode, is the major driver of diversification in mushroom-forming fungi. Proc Natl Acad Sci. 2020;117(51): 32528–34. https://doi.org/10.1073/pnas.1922539117.
3. Kües U, Liu Y. Fruiting body production in basidiomycetes. Appl Microbiol Biotechnol. 2000;54(2):141–52. https://doi.org/10.1007/s002530000396.
4. Kües U. Life history and developmental processes in the basidiomycete *Coprinus cinereus*. Microbiol Mol Biol Rev MMBR. 2000;64(2):316–53. https://doi.org/10.1128/MMBR.64.2.316-353.2000.
5. Frings RA, Maciá-Vicente JG, Buße S, Čmoková A, Kellner H, Hofrichter M, et al. Multilocus phylogeny- and fruiting feature-assisted delimitation of European *Cyclocybe aegerita* from a new Asian species complex and related species. Mycol Prog. 2020;19(10):1001–16. https://doi.org/10.1007/s11557-020-01599-z.
6. Herzog R, Solovyeva I, Rühl M, Thines M, Hennicke F. Dikaryotic fruiting body development in a single dikaryon of *Agrocybe aegerita* and the spectrum of monokaryotic fruiting types in its monokaryotic progeny. Mycol Prog. 2016;15(9):947–57. https://doi.org/10.1007/s11557-016-1221-9.
7. Knabe N, Jung E-M, Freihorst D, Hennicke F, Horton JS, Kothe E. A central role for Ras1 in morphogenesis of the Basidiomycete *Schizophyllum commune*. Eukaryot Cell. 2013;12(6):941–52. https://doi.org/10.1128/EC.00355-12.
8. Gube M. The gleba development of *Langermannia gigantea* (Batsch: Pers.) Rostk. (Basidiomycetes) compared to other Lycoperdaceae, and some systematic implications. Mycologia. 2007;99:396–405.
9. Clémençon H. Anatomy of the Hymenomycetes: an introduction to the cytology and plectology of crust fungi, bracket fungi, club fungi, chanterelles, agarics and boletes (in German). Teufen: Kommissionsverlag F. Flück-Wirth; 1997.
10. Ohm RA, de Jong JF, de Bekker C, Wösten HAB, Lugones LG. Transcription factor genes of *Schizophyllum commune* involved in regulation of mushroom formation. Mol Microbiol. 2011;81(6):1433–45. https://doi.org/10.1111/j.1365-2958.2011.07776.x.
11. Ohm RA, Aerts D, Wösten HAB, Lugones LG. The blue light receptor complex WC-1/2 of *Schizophyllum commune* is involved in mushroom formation and protection against phototoxicity. Environ Microbiol. 2013; 15(3):943–55. https://doi.org/10.1111/j.1462-2920.2012.02878.x.
12. Pelkmans JF, Patil MB, Gehrmann T, Reinders MJT, Wösten HAB, Lugones LG. Transcription factors of *Schizophyllum commune* involved in mushroom formation and modulation of vegetative growth. Sci Rep. 2017;7(1):310. https://doi.org/10.1038/s41598-017-00483-3.
13. Ohm RA, de Jong JF, Lugones LG, Aerts A, Kothe E, Stajich JE, et al. Genome sequence of the model mushroom *Schizophyllum commune*. Nat Biotechnol. 2010;28(9):957–63. https://doi.org/10.1038/nbt.1643.
14. Kües U, Navarro-González M. How do Agaricomycetes shape their fruiting bodies? 1. Morphological aspects of development. Fungal Biol Rev. 2015; 29(2):63–97. https://doi.org/10.1016/j.fbr.2015.05.001.
15. Turner EM. Development of excised sporocarps of *Agaricus bisporus* and its control by CO2. Trans Br Mycol Soc. 1977;69(2):183–6. https://doi.org/10.1016/S0007-1536(77)80035-1.
16. Wessels JGH. Fruiting in the higher fungi. In: Rose AH, editor. Advances in microbial physiology: Academic; 1993. p. 147–202. https://doi.org/10.1016/S0065-2911(08)60029-6.

17. Kinugawa K, Suzuki A, Takamatsu Y, Kato M, Tanaka K. Effects of concentrated carbon dioxide on the fruiting of several cultivated basidiomycetes (II). Mycoscience. 1994;35(4):345–52. https://doi.org/10.1007/BF02268504.
18. Niu M, Steffan BN, Fischer GJ, Venkatesh N, Raffa NL, Wettstein MA, et al. Fungal oxylipins direct programmed developmental switches in filamentous fungi. Nat Commun. 2020;11(1):5158. https://doi.org/10.1038/s41467-020-18999-0.
19. Fernandez Espinar M-T, Labarère J. Cloning and sequencing of the Aa-Pri1 gene specifically expressed during fruiting initiation in the edible mushroom *Agrocybe aegerita*, and analysis of the predicted amino-acid sequence. Curr Genet. 1997;32(6):420–4. https://doi.org/10.1007/s002940050297.
20. Murata Y, Fujii M, Zolan ME, Kamada T. Molecular analysis of pcc1, a gene that leads to A-regulated sexual morphogenesis in *Coprinus cinereus*. Genetics. 1998;149:1753–61.
21. Muraguchi H, Kamada T. The ich1 gene of the mushroom *Coprinus cinereus* is essential for pileus formation in fruiting. Development. 1998;125(16):3133–41.
22. Santos C, Labarère J. Aa-Pri2, a single-copy gene from *Agrocybe aegerita*, specifically expressed during fruiting initiation, encodes a hydrophobin with a leucine-zipper domain. Curr Genet. 1999;35(5):564–70. https://doi.org/10.1007/s002940050454.
23. Sirand-Pugnet P, Labarère J. Molecular characterization of the Pri3 gene encoding a cysteine-rich protein, specifically expressed during fruiting initiation within the *Agrocybe aegerita* complex. Curr Genet. 2002;41(1):31–42. https://doi.org/10.1007/s00294-002-0277-z.
24. Sirand-Pugnet P, Santos C, Labarère J. The Aa-Pri4 gene, specifically expressed during fruiting initiation in the *Agrocybe aegerita* complex, contains an unusual CT-rich leader intron within the 5′ uncoding region. Curr Genet. 2003;44(3):124–31. https://doi.org/10.1007/s00294-003-0435-y.
25. Arima T, Yamamoto M, Hirata A, Kawano S, Kamada T. The eln3 gene involved in fruiting body morphogenesis of *Coprinus cinereus* encodes a putative membrane protein with a general glycosyltransferase domain. Fungal Genet Biol. 2004;41(8):805–12. https://doi.org/10.1016/j.fgb.2004.04.003.
26. Terashima K, Yuki K, Muraguchi H, Akiyama M, Kamada T. The dst1 gene involved in mushroom Photomorphogenesis of *Coprinus cinereus* encodes a putative photoreceptor for blue light. Genetics. 2005;171(1):101–8. https://doi.org/10.1534/genetics.104.040048.
27. Liu Y, Srivilai P, Loos S, Aebi M, Kües U. An essential gene for fruiting body initiation in the Basidiomycete *Coprinopsis cinerea* is homologous to bacterial Cyclopropane fatty acid synthase genes. Genetics. 2006;172(2):873–84. https://doi.org/10.1534/genetics.105.045542.
28. Muraguchi H, Fujita T, Kishibe Y, Konno K, Ueda N, Nakahori K, et al. The exp1 gene essential for pileus expansion and autolysis of the inky cap mushroom *Coprinopsis cinerea* (*Coprinus cinereus*) encodes an HMG protein. Fungal Genet Biol. 2008;45(6):890–6. https://doi.org/10.1016/j.fgb.2007.11.004.
29. Kamada T, Sano H, Nakazawa T, Nakahori K. Regulation of fruiting body photomorphogenesis in *Coprinopsis cinerea*. Fungal Genet Biol. 2010;47(11):917–21. https://doi.org/10.1016/j.fgb.2010.05.003.
30. Kuratani M, Tanaka K, Terashima K, Muraguchi H, Nakazawa T, Nakahori K, et al. The dst2 gene essential for photomorphogenesis of *Coprinopsis cinerea* encodes a protein with a putative FAD-binding-4 domain. Fungal Genet Biol. 2010;47(2):152–8. https://doi.org/10.1016/j.fgb.2009.10.006.
31. Plaza DF, Lin C-W, van der Velden NSJ, Aebi M, Künzler M. Comparative transcriptomics of the model mushroom *Coprinopsis cinerea* reveals tissue-specific armories and a conserved circuitry for sexual development. BMC Genomics. 2014;15(1):492. https://doi.org/10.1186/1471-2164-15-492.
32. Gehrmann T, Pelkmans JF, Ohm RA, Vos AM, Sonnenberg ASM, Baars JJP, et al. Nucleus-specific expression in the multinuclear mushroom-forming fungus *Agaricus bisporus* reveals different nuclear regulatory programs. Proc Natl Acad Sci. 2018;115(17):4429–34. https://doi.org/10.1073/pnas.1721381115.
33. Krizsán K, Almási É, Merényi Z, Sahu N, Virágh M, Kószó T, et al. Transcriptomic atlas of mushroom development reveals conserved genes behind complex multicellularity in fungi. Proc Natl Acad Sci. 2019;116(15):7409–18. https://doi.org/10.1073/pnas.1817822116.
34. Almási É, Sahu N, Krizsán K, Bálint B, Kovács GM, Kiss B, et al. Comparative genomics reveals unique wood-decay strategies and fruiting body development in the Schizophyllaceae. New Phytol. 2019;224(2):902–15. https://doi.org/10.1111/nph.16032.
35. Zhang J, Ren A, Chen H, Zhao M, Shi L, Chen M, et al. Transcriptome analysis and its application in identifying genes associated with fruiting body development in Basidiomycete *Hypsizygus marmoreus*. PLoS One. 2015;10(4):e0123025. https://doi.org/10.1371/journal.pone.0123025.
36. Yu G, Wang M, Huang J, Yin Y-L, Chen Y-J, Jiang S, et al. Deep insight into the *Ganoderma lucidum* by comprehensive analysis of its transcriptome. PLoS One. 2012;7(8):e44031. https://doi.org/10.1371/journal.pone.0044031.
37. Xie C, Gong W, Zhu Z, Yan L, Hu Z, Peng Y. Comparative transcriptomics of *Pleurotus eryngii* reveals blue-light regulation of carbohydrate-active enzymes (CAZymes) expression at primordium differentiated into fruiting body stage. Genomics. 2018;110(3):201–9. https://doi.org/10.1016/j.ygeno.2017.09.012.
38. Chen J, Zeng X, Yang Y, Xing Y, Zhang Q, Li J, et al. Genomic and transcriptomic analyses reveal differential regulation of diverse terpenoid and polyketides secondary metabolites in *Hericium erinaceus*. Sci Rep. 2017;7(1):10151.
39. Yoo S, Lee H-Y, Markkandan K, Moon S, Ahn YJ, Ji S, et al. Comparative transcriptome analysis identified candidate genes involved in mycelium browning in *Lentinula edodes*. BMC Genomics. 2019;20(1):121. https://doi.org/10.1186/s12864-019-5509-4.
40. Liu X-B, Xia E-H, Li M, Cui Y-Y, Wang P-M, Zhang J-X, et al. Transcriptome data reveal conserved patterns of fruiting body development and response to heat stress in the mushroom-forming fungus *Flammulina filiformis*. PLoS One. 2020;15(10):e0239890. https://doi.org/10.1371/journal.pone.0239890.
41. Cruz C, Noël-Suberville C, Montury M. Fatty acid content and some flavor compound release in two strains of *Agaricus bisporus*, according to three stages of development. J Agric Food Chem. 1997;45(1):64–7. https://doi.org/10.1021/jf960300t.
42. Mau J-L, Chyau C-C, Li J-Y, Tseng Y-H. Flavor compounds in straw mushrooms *Volvariella volvacea* harvested at different stages of maturity. J Agric Food Chem. 1997;45(12):4726–9. https://doi.org/10.1021/jf9703314.
43. Fäldt J, Jonsell M, Nordlander G, Borg-Karlson A-K. Volatiles of bracket Fungi *Fomitopsis pinicola* and *Fomes fomentarius* and their functions as insect attractants. J Chem Ecol. 1999;25(3):567–90. https://doi.org/10.1023/A:1020958005023.
44. Wu S, Zorn H, Krings U, Berger RG. Characteristic volatiles from young and aged fruiting bodies of wild *Polyporus sulfureus* (Bull.:Fr.) Fr. J Agric Food Chem. 2005;53:4524–8.
45. Cho IH, Choi H-K, Kim Y-S. Difference in the volatile composition of pine-mushrooms (*Tricholoma matsutake* sing.) according to their grades. J Agric Food Chem. 2006;54(13):4820–5. https://doi.org/10.1021/jf0601416.
46. Zawirska-Wojtasiak R, Siwulski M, Wasowicz E, Sobieralski K. Volatile compounds of importance in the aroma of cultivated mushrooms *Agaricus bisporus* at different conditions of cultivation. Pol J Food Nutr Sci. 2007;57:367–72.
47. Combet E, Henderson J, Eastwood DC, Burton KS. Influence of Sporophore development, damage, storage, and tissue specificity on the enzymic formation of volatiles in mushrooms (*Agaricus bisporus*). J Agric Food Chem. 2009;57(9):3709–17. https://doi.org/10.1021/jf8036209.
48. Holighaus G, Weißbecker B, von Fragstein M, Schütz S. Ubiquitous eight-carbon volatiles of fungi are infochemicals for a specialist fungivore. Chemoecology. 2014;24(2):57–66. https://doi.org/10.1007/s00049-014-0151-8.
49. Tasaki Y, Kobayashi D, Sato R, Hayashi S, Joh T. Variations in 1-octen-3-ol and lipoxygenase gene expression in the oyster mushroom *Pleurotus ostreatus* according to fruiting body development, tissue specificity, maturity, and postharvest storage. 2019. https://pubag.nal.usda.gov/catalog/6341911. Accessed 6 Aug 2019.
50. Holighaus G, Rohlfs M. Volatile and non-volatile fungal oxylipins in fungus-invertebrate interactions. Fungal Ecol. 2019;38:28–36. https://doi.org/10.1016/j.funeco.2018.09.005.
51. Kües U, Khonsuntia W, Subba S, Dörnte B. Volatiles in communication of Agaricomycetes. In: Anke T, Schüffler A, editors. Physiology and genetics: selected basic and applied aspects. Cham: Springer International Publishing; 2018. p. 149–212. https://doi.org/10.1007/978-3-319-71740-1_6.
52. Chitarra GS, Abee T, Rombouts FM, Dijksterhuis J. 1-Octen-3-ol inhibits conidia germination of *Penicillium paneum* despite of mild effects on membrane permeability, respiration, intracellular pH, and changes the protein composition. FEMS Microbiol Ecol. 2005;54(1):67–75. https://doi.org/10.1016/j.femsec.2005.02.013.
53. Nemčovič M, Jakubíková L, Víden I, Farkaš V. Induction of conidiation by endogenous volatile compounds in *Trichoderma* spp. FEMS Microbiol Lett. 2008;284(2):231–6. https://doi.org/10.1111/j.1574-6968.2008.01202.x.

54. Orban A, Hennicke F, Rühl M. Volatilomes of *Cyclocybe aegerita* during different stages of monokaryotic and dikaryotic fruiting. Biol Chem. 2020; 401(8):995–1004. https://doi.org/10.1515/hsz-2019-0392.
55. Combet E, Eastwood DC, Burton KS, Combet E, Henderson J, Henderson J, et al. Eight-carbon volatiles in mushrooms and fungi: properties, analysis, and biosynthesis. Mycoscience. 2006;47(6):317–26. https://doi.org/10.1007/S10267-006-0318-4.
56. Gupta DK, Rühl M, Mishra B, Kleofas V, Hofrichter M, Herzog R, et al. The genome sequence of the commercially cultivated mushroom *Agrocybe aegerita* reveals a conserved repertoire of fruiting-related genes and a versatile suite of biopolymer-degrading enzymes. BMC Genomics. 2018; 19(1):48. https://doi.org/10.1186/s12864-017-4430-y.
57. Miziorko HM. Enzymes of the mevalonate pathway of isoprenoid biosynthesis. Arch Biochem Biophys. 2011;505(2):131–43. https://doi.org/10.1016/j.abb.2010.09.028.
58. Christianson DW. Structural biology and chemistry of the terpenoid cyclases. Chem Rev. 2006;106(8):3412–42. https://doi.org/10.1021/cr050286w.
59. Zhang C, Chen X, Orban A, Shukal S, Birk F, Too H-P, et al. *Agrocybe aegerita* serves as a gateway for identifying Sesquiterpene biosynthetic enzymes in higher Fungi. ACS Chem Biol. 2020;15(5):1268–77. https://doi.org/10.1021/acschembio.0c00155.
60. Brodhun F, Feussner I. Oxylipins in fungi. FEBS J. 2011;278(7):1047–63. https://doi.org/10.1111/j.1742-4658.2011.08027.x.
61. Heddergott C, Calvo AM, Latgé JP. The Volatome of *Aspergillus fumigatus*. Eukaryot Cell. 2014;13(8):1014–25. https://doi.org/10.1128/EC.00074-14.
62. Wurzenberger M, Grosch W. Stereochemistry of the cleavage of the 10-hydroperoxide isomer of linoleic acid to 1-octen-3-ol by a hydroperoxide lyase from mushrooms (*Psalliota bispora*). Biochim Biophys Acta BBA - Lipids Lipid Metab. 1984;795(1):163–5. https://doi.org/10.1016/0005-2760(84)90117-6.
63. Wurzenberger M, Grosch W. The formation of 1-octen-3-ol from the 10-hydroperoxide isomer of linoleic acid by a hydroperoxide lyase in mushrooms (*Psalliota bispora*). Biochim Biophys Acta BBA - Lipids Lipid Metab. 1984;794(1):25–30. https://doi.org/10.1016/0005-2760(84)90293-5.
64. Chen CC, Wu CM. Studies on the enzymic reduction of 1-octen-3-one in mushroom (*Agaricus bisporus*). J Agric Food Chem. 1984;32(6):1342–4. https://doi.org/10.1021/jf00126a030.
65. Wanner P, Tressl R. Purification and characterization of two enone reductases from *Saccharomyces cerevisiae*. Eur J Biochem. 1998;255(1):271–8. https://doi.org/10.1046/j.1432-1327.1998.2550271.x.
66. Wang M, Gu B, Huang J, Jiang S, Chen Y, Yin Y, et al. Transcriptome and proteome exploration to provide a resource for the study of *Agrocybe aegerita*. PLoS One. 2013;8(2):e56686. https://doi.org/10.1371/journal.pone.0056686.
67. Muraguchi H, Umezawa K, Niikura M, Yoshida M, Kozaki T, Ishii K, et al. Strand-specific RNA-Seq analyses of fruiting body development in *Coprinopsis cinerea*. PLoS One. 2015;10(10):e0141586. https://doi.org/10.1371/journal.pone.0141586.
68. Wu B, Xu Z, Knudson A, Carlson A, Chen N, Kovaka S, et al. Genomics and development of *Lentinus tigrinus*: a white-rot wood-decaying mushroom with dimorphic fruiting bodies. Genome Biol Evol. 2018;10(12):3250–61. https://doi.org/10.1093/gbe/evy246.
69. Sipos G, Prasanna AN, Walter MC, O'Connor E, Bálint B, Krizsán K, et al. Genome expansion and lineage-specific genetic innovations in the forest pathogenic fungi *Armillaria*. Nat Ecol Evol. 2017;1(12):1931–41. https://doi.org/10.1038/s41559-017-0347-8.
70. Song H-Y, Kim D-H, Kim J-M. Comparative transcriptome analysis of dikaryotic mycelia and mature fruiting bodies in the edible mushroom *Lentinula edodes*. Sci Rep. 2018;8:1–15.
71. Shim D, Park S-G, Kim K, Bae W, Lee GW, Ha B-S, et al. Whole genome de novo sequencing and genome annotation of the world popular cultivated edible mushroom, *Lentinula edodes*. J Biotechnol. 2016;223:24–5. https://doi.org/10.1016/j.jbiotec.2016.02.032.
72. Tayyrov A, Azevedo S, Herzog R, Vogt E, Arzt S, Lüthy P, et al. Heterologous production and functional characterization of Ageritin, a novel type of Ribotoxin highly expressed during fruiting of the edible mushroom *Agrocybe aegerita*. Appl Environ Microbiol. 2019;85(21). https://doi.org/10.1128/AEM.01549-19.
73. Hennicke F, Künzler M, Tayyrov A, Lüthy P. Ageritin as bioinsecticide and methods of generating and using it. European Patent 3670527. 2020.
74. Tomita T, Noguchi K, Mimuro H, Ukaji F, Ito K, Sugawara-Tomita N, et al. Pleurotolysin, a novel sphingomyelin-specific two-component cytolysin from the edible mushroom *Pleurotus ostreatus*, assembles into a transmembrane pore complex. J Biol Chem. 2004;279(26):26975–82. https://doi.org/10.1074/jbc.M402676200.
75. Agger S, Lopez-Gallego F, Schmidt-Dannert C. Diversity of sesquiterpene synthases in the basidiomycete *Coprinus cinereus*. Mol Microbiol. 2009;72(5): 1181–95. https://doi.org/10.1111/j.1365-2958.2009.06717.x.
76. Lopez-Gallego F, Agger SA, Pella DA, Distefano MD, Schmidt-Dannert C. Sesquiterpene synthases Cop4 and Cop6 from *Coprinus cinereus*: catalytic promiscuity and cyclization of farnesyl pyrophosphate geometrical isomers. Chembiochem Eur J Chem Biol. 2010; 11(8):1093–106. https://doi.org/10.1002/cbic.200900671.
77. Wawrzyn GT, Quin MB, Choudhary S, López-Gallego F, Schmidt-Dannert C. Draft genome of *Omphalotus olearius* provides a predictive framework for sesquiterpenoid natural product biosynthesis in Basidiomycota. Chem Biol. 2012;19(6):772–83. https://doi.org/10.1016/j.chembiol.2012.05.012.
78. Quin MB, Flynn CM, Wawrzyn GT, Choudhary S, Schmidt-Dannert C. Mushroom hunting using bioinformatics: application of a predictive framework facilitates the selective identification of sesquiterpene synthases in Basidiomycota. Chembiochem Eur J Chem Biol. 2013;14(18):2480–91. https://doi.org/10.1002/cbic.201300349.
79. Quin MB, Flynn CM, Schmidt-Dannert C. Traversing the fungal terpenome. Nat Prod Rep. 2014;31(10):1449–73. https://doi.org/10.1039/C4NP00075G.
80. Rapior S, Breheret S, Talou T, Pelissier Y, Milhau M, Bessiere JM. Volatile components of fresh *Agrocybe aegerita* and Tricholoma sulfureum. Cryptogam Mycol. 1998;19:15–23.
81. Kleofas V, Sommer L, Fraatz MA, Zorn H, Rühl M. Fruiting body production and aroma profile analysis of *Agrocybe aegerita* cultivated on different substrates. Nat Resour. 2014;05:233.
82. Costa R, De Grazia S, Grasso E, Trozzi A. Headspace-solid-phase microextraction-gas chromatography as analytical methodology for the determination of volatiles in wild mushrooms and evaluation of modifications occurring during storage. J Anal Methods Chem. 2015;2015:1–10. https://doi.org/10.1155/2015/951748.
83. Kuribayashi T, Kaise H, Uno C, Hara T, Hayakawa T, Joh T. Purification and characterization of Lipoxygenase from *Pleurotus ostreatus*. J Agric Food Chem. 2002;50(5):1247–53. https://doi.org/10.1021/jf0112217.
84. Plagemann I, Zelena K, Arendt P, Ringel PD, Krings U, Berger RG. LOXPsa1, the first recombinant lipoxygenase from a basidiomycete fungus. J Mol Catal B Enzym. 2013;87:99–104. https://doi.org/10.1016/j.molcatb.2012.11.004.
85. Karrer D, Rühl M. A new lipoxygenase from the agaric fungus *Agrocybe aegerita*: biochemical characterization and kinetic properties. PLoS One. 2019;14(6):e0218625. https://doi.org/10.1371/journal.pone.0218625.
86. Matsui K, Sasahara S, Akakabe Y, Kajiwara T. Linoleic acid 10-Hydroperoxide as an intermediate during formation of 1-Octen-3-ol from linoleic acid in *Lentinus decadetes*. Biosci Biotechnol Biochem. 2003;67(10):2280–2. https://doi.org/10.1271/bbb.67.2280.
87. Joh T, Kudo T, Tasaki Y, Hara T. Mushroom flavor compounds and the biosynthesis mechanism (in Japanese). Aroma Res. 2012;13:26–30.
88. Assaf S, Hadar Y, Dosoretz CG. 1-Octen-3-ol and 13-hydroperoxylinoleate are products of distinct pathways in the oxidative breakdown of linoleic acid by *Pleurotus pulmonarius*. Enzym Microb Technol. 1997;21(7):484–90. https://doi.org/10.1016/S0141-0229(97)00019-7.
89. Oliw EH. Product specificity of fungal 8R- and 9S-dioxygenases of the peroxidase-cyclooxygenase superfamily with amino acid derivatized polyenoic fatty acids. Arch Biochem Biophys. 2018;640:93–101. https://doi.org/10.1016/j.abb.2017.12.018.
90. Oliw EH. Biosynthesis of Oxylipins by *Rhizoctonia solani* with Allene oxide and Oleate 8S,9S-Diol synthase activities. Lipids. 2018;53(5):527–37. https://doi.org/10.1002/lipd.12051.
91. Hoffmann I, Oliw EH. 7,8- and 5,8-linoleate diol synthases support the heterolytic scission of oxygen–oxygen bonds by different amide residues. Arch Biochem Biophys. 2013;539(1):87–91. https://doi.org/10.1016/j.abb.2013.09.010.
92. Garscha U, Oliw EH. Leucine/Valine residues direct oxygenation of linoleic acid by (10R)- and (8R)-dioxygenases: expression and site-directed mutagenesis of (10R)-dioxygenase with epoxyalcohol synthase activity. J Biol Chem. 2009;284(20):13755–65. https://doi.org/10.1074/jbc.M808665200.
93. Brodhun F, Schneider S, Göbel C, Hornung E, Feussner I. PpoC from *Aspergillus nidulans* is a fusion protein with only one active haem. Biochem J. 2010;425(3):553–65. https://doi.org/10.1042/BJ20091096 .
94. Sooman L, Oliw EH. Discovery of a novel linoleate dioxygenase of *Fusarium oxysporum* and Linoleate Diol synthase of *Colletotrichum graminicola*. Lipids. 2015;50(12):1243–52. https://doi.org/10.1007/s11745-015-4078-9.

95. Stolterfoht H, Rinnofner C, Winkler M, Pichler H. Recombinant lipoxygenases and hydroperoxide lyases for the synthesis of green leaf volatiles. J Agric Food Chem. 2019;67(49):13367–92. https://doi.org/10.1021/acs.jafc.9b02690.
96. ul Hassan MN, Zainal Z, Ismail I. Green leaf volatiles: biosynthesis, biological functions and their applications in biotechnology. Plant Biotechnol J. 2015; 13(6):727–39. https://doi.org/10.1111/pbi.12368.
97. Park Y-C, San K-Y, Bennett GN. Characterization of alcohol dehydrogenase 1 and 3 from *Neurospora crassa* FGSC2489. Appl Microbiol Biotechnol. 2007; 76(2):349–56. https://doi.org/10.1007/s00253-007-0998-5.
98. Martin M. Cutadapt removes adapter sequences from high-throughput sequencing reads. EMBnet.journal. 2011;17(1):10–2. https://doi.org/10.14806/ej.17.1.200.
99. Moll P, Ante M, Seitz A, Reda T. QuantSeq 3′ mRNA sequencing for RNA quantification. Nat Methods. 2014;11:i–iii.
100. R Core Team. R: a language and environment for statistical computing. Vienna: R Foundation for Statistical Computing; 2019. URL https://www.R-project.org/
101. Fischer DS, Theis FJ, Yosef N. Impulse model-based differential expression analysis of time course sequencing data. Nucleic Acids Res. 2018;46:e119.
102. Spies D, Renz PF, Beyer TA, Ciaudo C. Comparative analysis of differential gene expression tools for RNA sequencing time course data. Brief Bioinform. 2019;20(1):288–98. https://doi.org/10.1093/bib/bbx115.
103. Wickham H. ggplot2: elegant graphics for data analysis. 2nd ed: Springer International Publishing; 2016. https://doi.org/10.1007/978-3-319-24277-4.
104. Galili, T. Post hoc analysis for Friedman's Test (r code). 2010. Blog. Retrieved May 28, 2019, from https://www.r-statistics.com/2010/02/post-hoc-analysis-for-friedmanstest-r-code/.
105. The UniProt Consortium. UniProt: a worldwide hub of protein knowledge. Nucleic Acids Res. 2019;47(D1):D506–15.
106. Dereeper A, Guignon V, Blanc G, Audic S, Buffet S, Chevenet F, et al. Phylogeny.fr: robust phylogenetic analysis for the non-specialist. Nucleic Acids Res. 2008;36(Web Server issue):W465–9.
107. Goujon M, McWilliam H, Li W, Valentin F, Squizzato S, Paern J, et al. A new bioinformatics analysis tools framework at EMBL–EBI. Nucleic Acids Res. 2010;38(suppl_2):W695–9.
108. Mansell DJ, Toogood HS, Waller J, Hughes JMX, Levy CW, Gardiner JM, et al. Biocatalytic asymmetric alkene reduction: crystal structure and characterization of a double bond Reductase from *Nicotiana tabacum*. ACS Catal. 2013;3(3):370–9. https://doi.org/10.1021/cs300709m.
109. Mano J, Torii Y, Hayashi S, Takimoto K, Matsui K, Nakamura K, et al. The NADPH:Quinone Oxidoreductase P1-ζ-crystallin in *Arabidopsis* catalyzes the α,β-Hydrogenation of 2-Alkenals: detoxication of the lipid peroxide-derived reactive aldehydes. Plant Cell Physiol. 2002;43(12):1445–55. https://doi.org/10.1093/pcp/pcf187.
110. Zhang B, Zheng L, Lin J, Wei D. Characterization of an ene-reductase from *Meyerozyma guilliermondii* for asymmetric bioreduction of α,β-unsaturated compounds. Biotechnol Lett. 2016;38(9):1527–34. https://doi.org/10.1007/s10529-016-2124-1.
111. Bougioukou DJ, Walton AZ, Stewart JD. Towards preparative-scale, biocatalytic alkene reductions. Chem Commun. 2010;46(45):8558–60. https://doi.org/10.1039/c0cc03119d.

Publisher's Note

Transcriptome of different fruiting stages in the cultivated mushroom *Cyclocybe aegerita* suggests a complex regulation of fruiting and reveals enzymes putatively involved in fungal oxylipin biosynthesis.

Orban, A., Weber, A., Herzog, R., Hennicke, F., Rühl, M.

BMC Genomics 2021, *22*, 324

DOI: 10.1186/s12864-021-07648-5

----------Supporting Information----------

Differential gene expression during fruiting body development

In the mycelium, as a result of the comparison of the different developmental stages, 129 genes were classified as transient down, 152 genes as transient up, 1,553 genes as transition down and 1,784 genes as transition up (Figure S1A), whereas for fruiting bodies, no genes were identified as transient down, 2 genes as transient up, 758 genes as transition down and 912 genes as transition up (Figure S1B). In total, both transcriptome data sets revealed 4,632 differentially expressed genes (DEGs) of which 2,960 genes were uniquely differentially expressed in the mycelium and 1,014 genes were only differentially expressed in fruiting bodies, leaving 658 DEGs both life stages had in common (Figure S1).

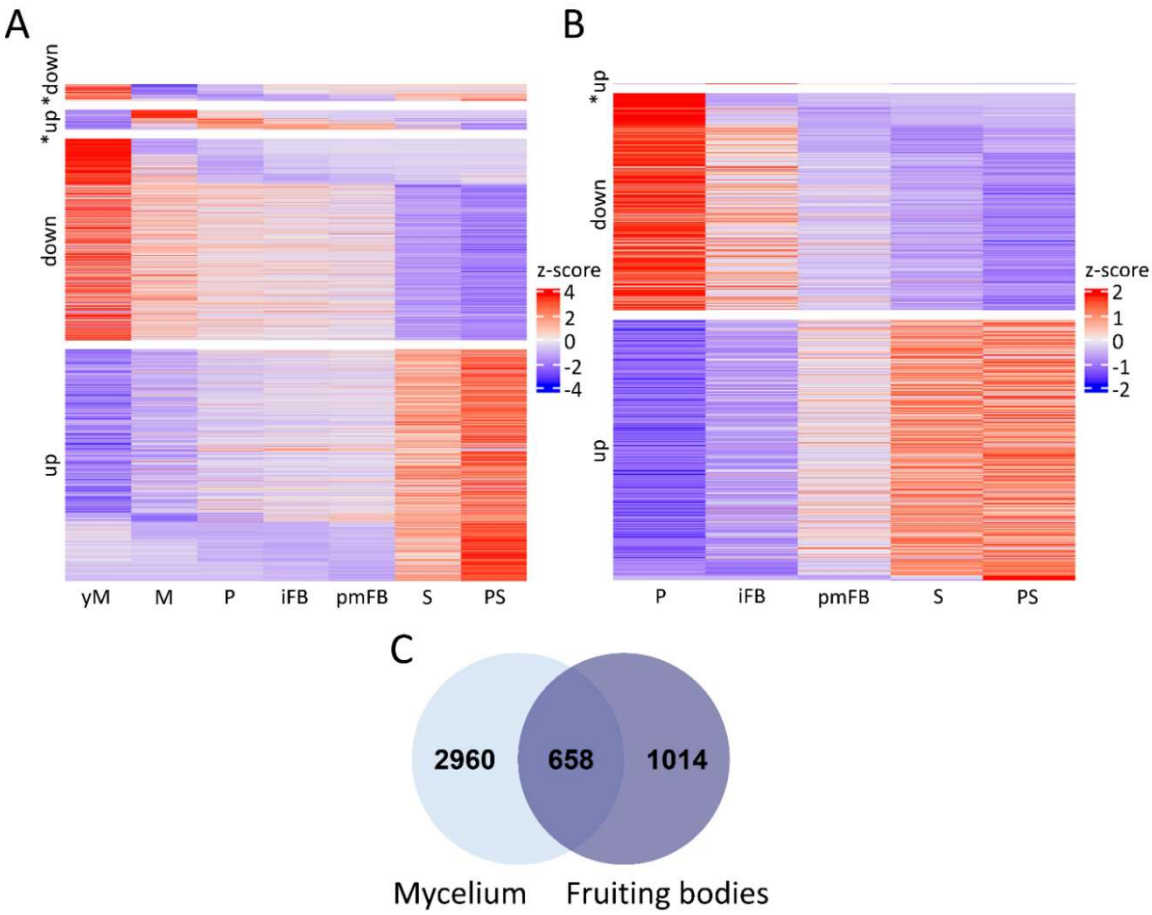

Figure S1: Differential gene expression during fruiting body development in C. aegerita. A) Differential expressed genes (DEGs) in the mycelium. B) DEGs in fruiting bodies. Each heatmap block represents one differential gene expression class:*down: transient down; *up: transient up; down: transition down; up: transition up. Normalized read counts were transformed to z-score values (respective scale to the right). Red colors indicate transcriptional upregulation while blue colors represent downregulation. yM: young (uninduced) mycelium (day 10 post inoculation, p.i.); M: mycelium (day 14 p.i.); P: primordia (day 18 p.i.); iFB: immature fruiting bodies (day 20 p.i.); pmFB: premature fruiting bodies (day 22 p.i.); S: sporulation (day 24 p.i.); PS: post sporulation (day 28 p.i.). C) Venn diagram presenting the overlap of DEGs among mycelium and fruiting bodies, as well as the number of DEGs only present in one sample type.

Transcription of fruiting-related genes (FRGs)

In FB samples, expression of all four *PRI4* paralogs, the *PRI3* paralogs *PRI3-1* and *-2*, *PRI2*, *BRI1*, *DST1* and *-2*, *ELN3-1* and *-2*, and *ICH1* strongly correlated with each other in a first cluster, the expression of *BWC2*, *PRI3-6* and *CFS1* strongly correlated with each other in a second one, and the expression of *EXP1*, *ELN3-3*, *PCC1* and *FST3* strongly correlated with each other in a third one (Figure S2). Among the *PRI3* paralogs, a strong correlation was also visible for the expression of *PRI3-1* and *-4*, whereas the expression of *PRI3-4* correlated with the one of *PRI3-6* in a fairly positive manner. Individual positive correlation was also detected between the expression of *FST4* versus *BWC2*, *DST1* and *-2*, *ELN3-1* and *-2*, *ICH1*, *PRI2*, *PRI3-1*, *-4* and *-6*, and *PRI4-2* to *-4*, as well as between the one of *HOM1* versus *FST3* and *CFS1* (Figure S2).

Some of these correlations were also observed in the mycelium samples where cluster formation was less comprehensive. Clusters of expression-wise strongly positive correlated genes were recognized, first, with all four *PRI4* paralogs, *DST1*, and *EXP1* (Figure S3; with *PRI4-2* and *DST1* revealing the weakest correlation among them) aligning with the correlation among *PRI4-1* to *-4* and *DST1* in the fruiting body samples (Figure S2). A second cluster was apparent between *PRI3-1*, *ICH1*, *CFS1*, *DST2* and *PRI2* (Figure S3) mirroring the correlation between *ICH1* and *DST2* observed in the fruiting body samples (Figure S2). A third cluster was recognized with *ELN3-3*, *FST3* and *BWC2* (Figure S3) comparable with the correlation between *ELN3-3* and *FST3* in the fruiting body samples (Figure S2). Two last clusters were evident in mycelium samples with *PRI3-4* and *-6*, *BRI1* and *PCC1* on the one hand, and with *ELN3-1* and *-2* on the other hand (Figure S3). There, *ELN3-1* and *-2* also showed a strongly positive correlation of their expression in plectenchyme samples (Figure S2). Furthermore, the positive expression-wise correlation between the *PRI3* paralogs *PRI3-1* and *-2* in plectenchyme samples aligned with the one in the mycelium samples, while the fairly positive correlation of the expression of *PRI3-4* and *-6* in the plectenchyme samples was complemented by a strongly positive correlation within the mycelium samples (Figure S3).

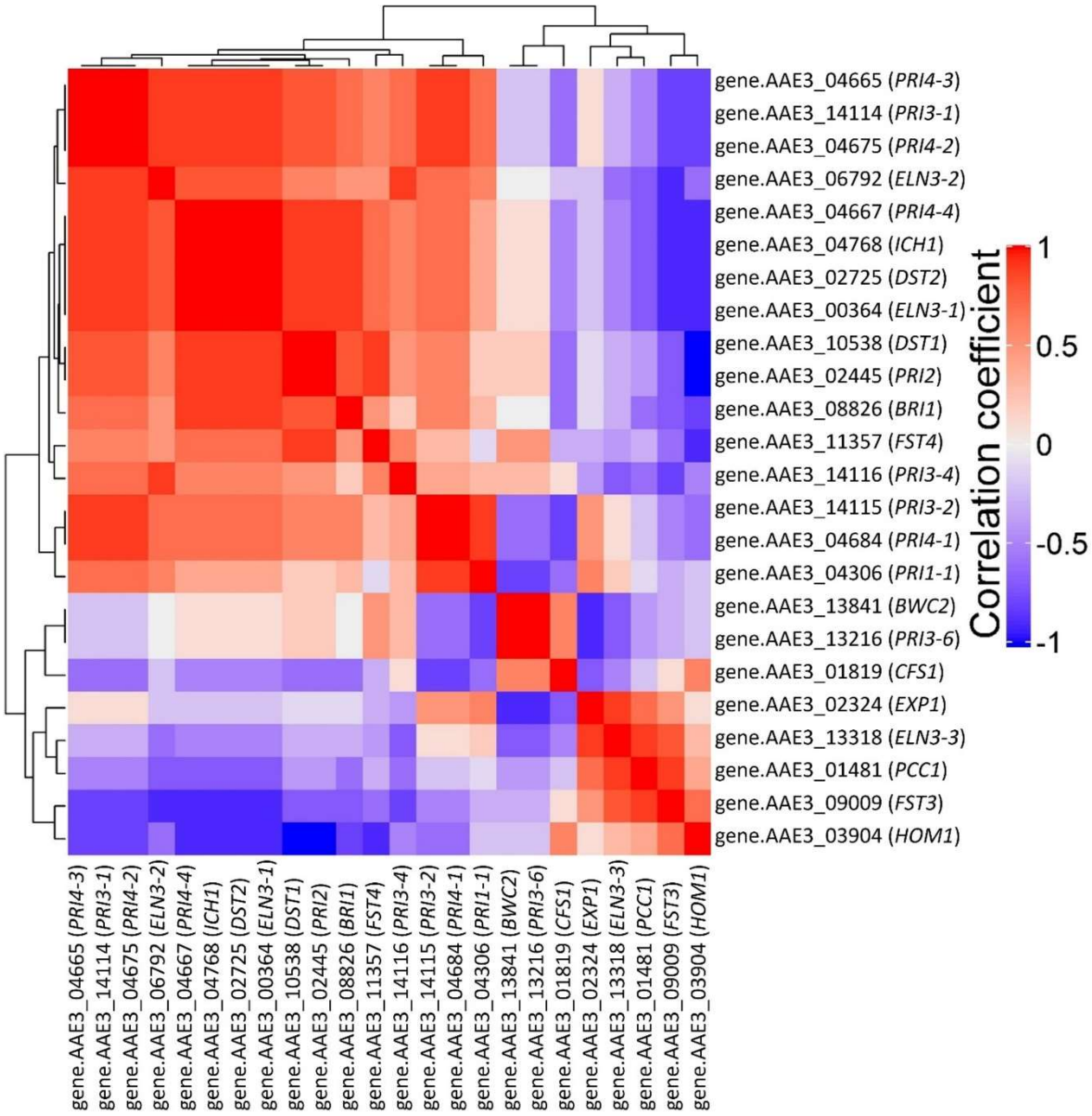

Figure S2: Correlation of the expression of putative *C. aegerita* homologs of fruiting-related genes (FRGs) in plectenchymatic samples (fruiting body 'tissue') during the fructification process. Only genes were considered showing maximum transcription levels higher than 25 normalized read counts. Red colors represent positive correlation, blue colors represent negative correlation and grey/light colors represent no/weak correlation between the selected genes.

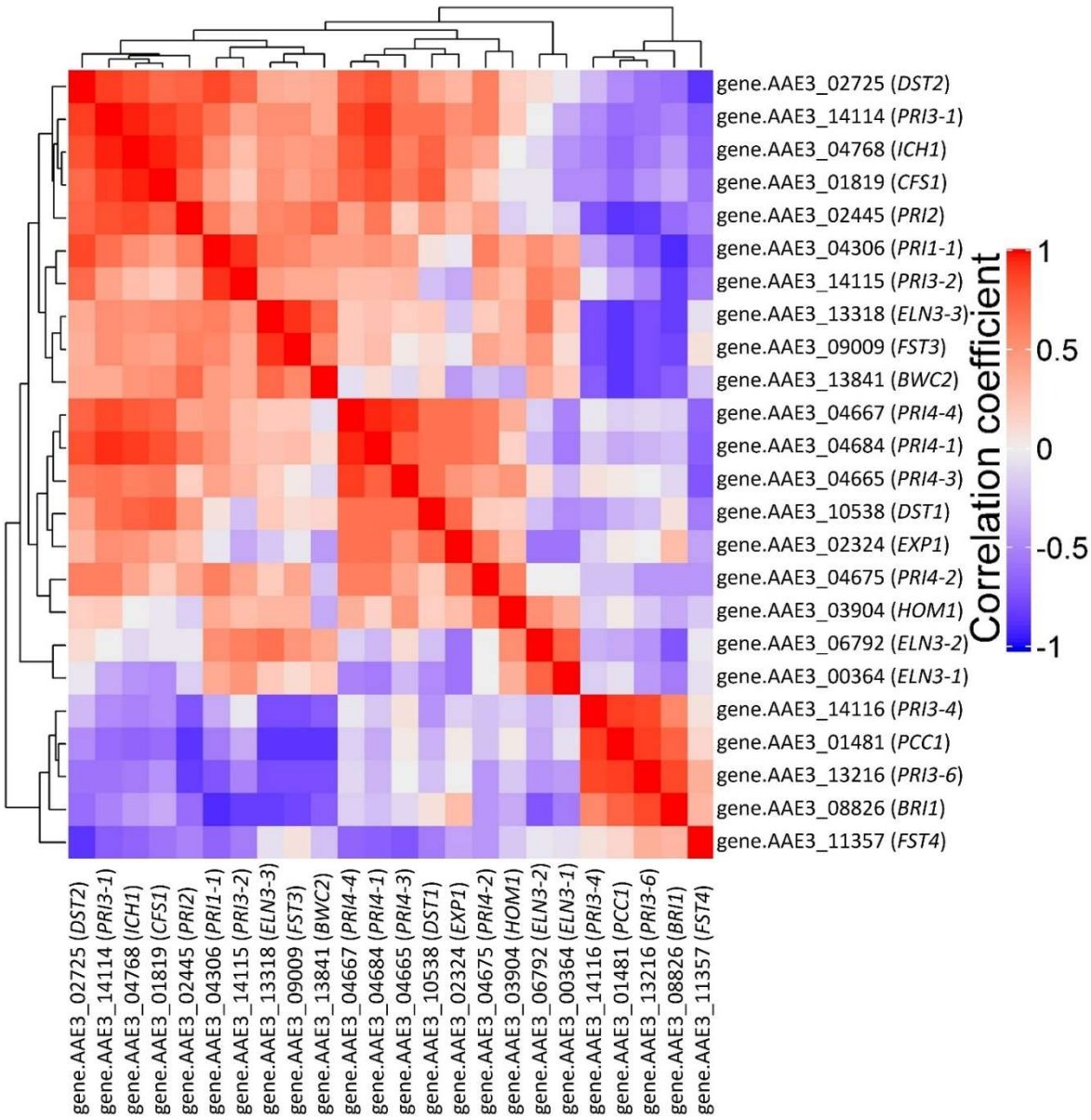

Figure S3: Correlation of the expression of putative *C. aegerita* homologs of fruiting-related genes (FRGs) in mycelium samples. Only genes were considered showing maximum transcription levels higher than 25 normalized read counts. Red colors represent positive correlation, blue colors represent negative correlation and grey/light colors represent no/weak correlation between the selected genes.

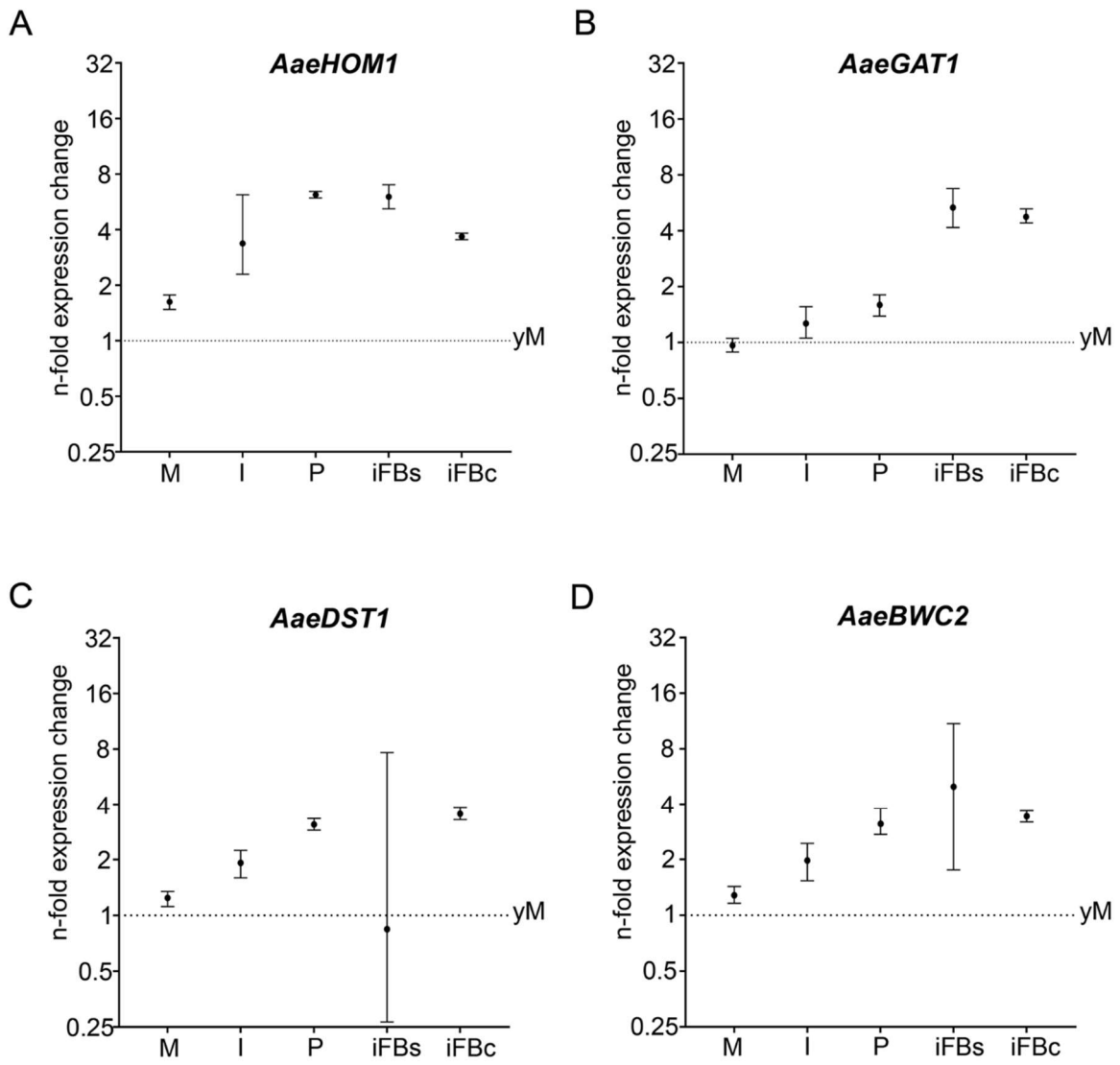

Figure S4: Relative qRT-PCR based expression level assessment with *C. aegerita* orthologs of four well-known fruiting-related genes (FRGs) during fruiting of *C. aegerita*. Expression changes are shown on a log 2 scale. The error bars represent the standard deviation of three biological replicates. For initials and primordia each replicate was a separate RNA extraction of pooled individuals, each collected from sets of 2–3 plates (for initials) or 1 plate (for primordia) with no overlap between plates/sample pools. The dotted horizontal line represents the expression level of the respective gene in young (uninduced) mycelium (yM) as the reference expression. Sampled *C. aegerita* AAE-3 materials: M, fruiting-primed mycelium 24 h to 48 h before emergence of fruiting body (FB) initials; I, FB initials; P, primordia; iFBs, immature FB stipe; iFBc, immature FB cap. A-B Expression of AaeHOM1 (gene ID AAE3_03904) and AaeGAT1 (gene ID AAE3_00943). C-D Expression of AaeDST1 (gene ID AAE3_10538) and AaeBWC2 (gene ID AAE3_13841).

Terpenoid biosynthesis

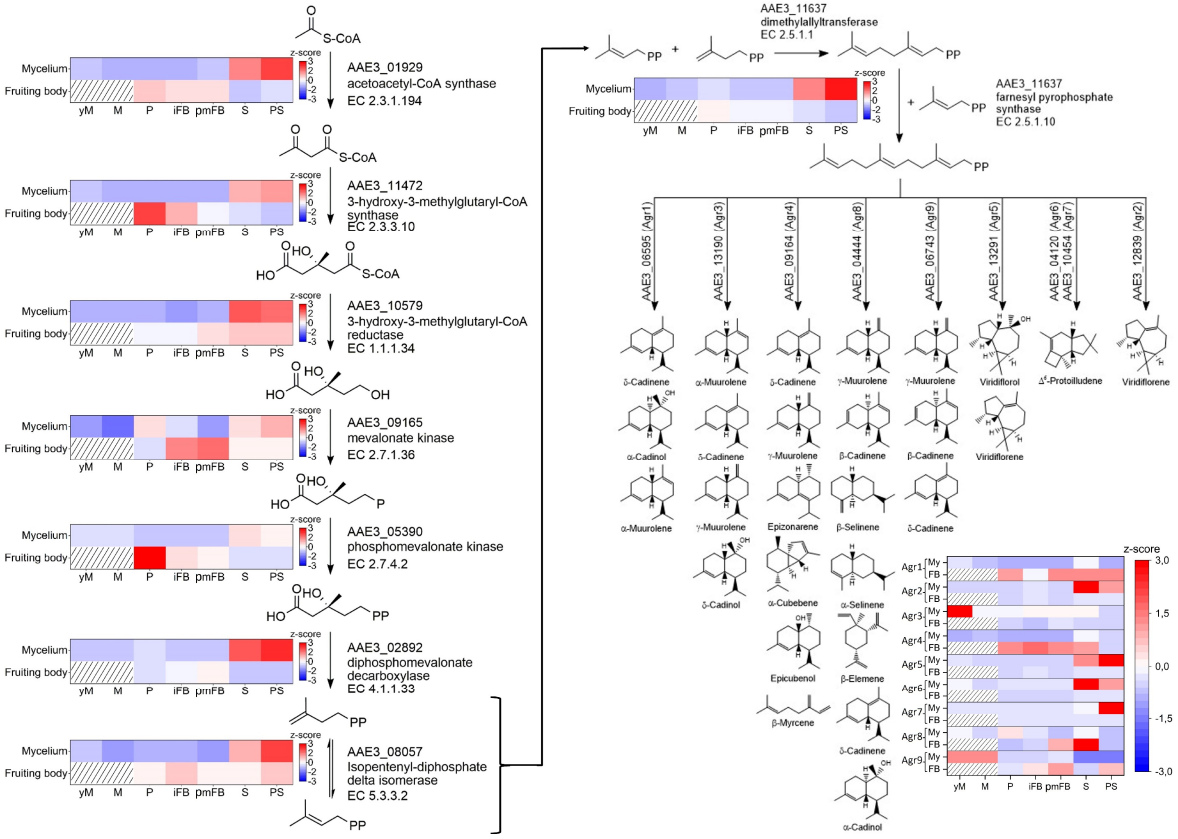

Figure S5: Expression of genes involved in the mevalonate pathway and of the sesquiterpene synthases (STSs) Agr1 to Agr9 in the mycelium and fruiting bodies of *C. aegerita*. Normalized read counts per gene were transformed to z-score values (respective scale to the right). Red colors indicate transcriptional upregulation while blue colors represent downregulation. White colors indicate a z-score of zero and hatched areas show an absence of sampling due the non-applicability. Interestingly, the transcription levels of genes involved in the mevalonate pathway were typically higher in the mycelium than in the fruiting bodies, except for the 3-hydroxy-3-methylglutaryl-CoA synthase gene (AAE3_11472), the mevalonate kinase gene (AAE3_09165) and the phosphomevalonate kinase gene (AAE3_05390). The farnesyl pyrophosphate synthase gene (AAE3_11637), responsible for the biosynthesis of the precursor of sesquiterpenes, was in both sample types highly expressed, especially in mycelium during late developmental stages (over 7,000 normalized read counts) and in primordia (over 2,900 normalized read counts). yM: young (uninduced) mycelium (day 10 post inoculation, p.i.); M: fruiting-primed mycelium (day 14 p.i.); P: primordia (day 18 p.i.); iFB: immature fruiting bodies (day 20 p.i.); pmFB: premature fruiting bodies (day 22 p.i.); S: sporulation (day 24 p.i.); PS: post sporulation (day 28 p.i.).

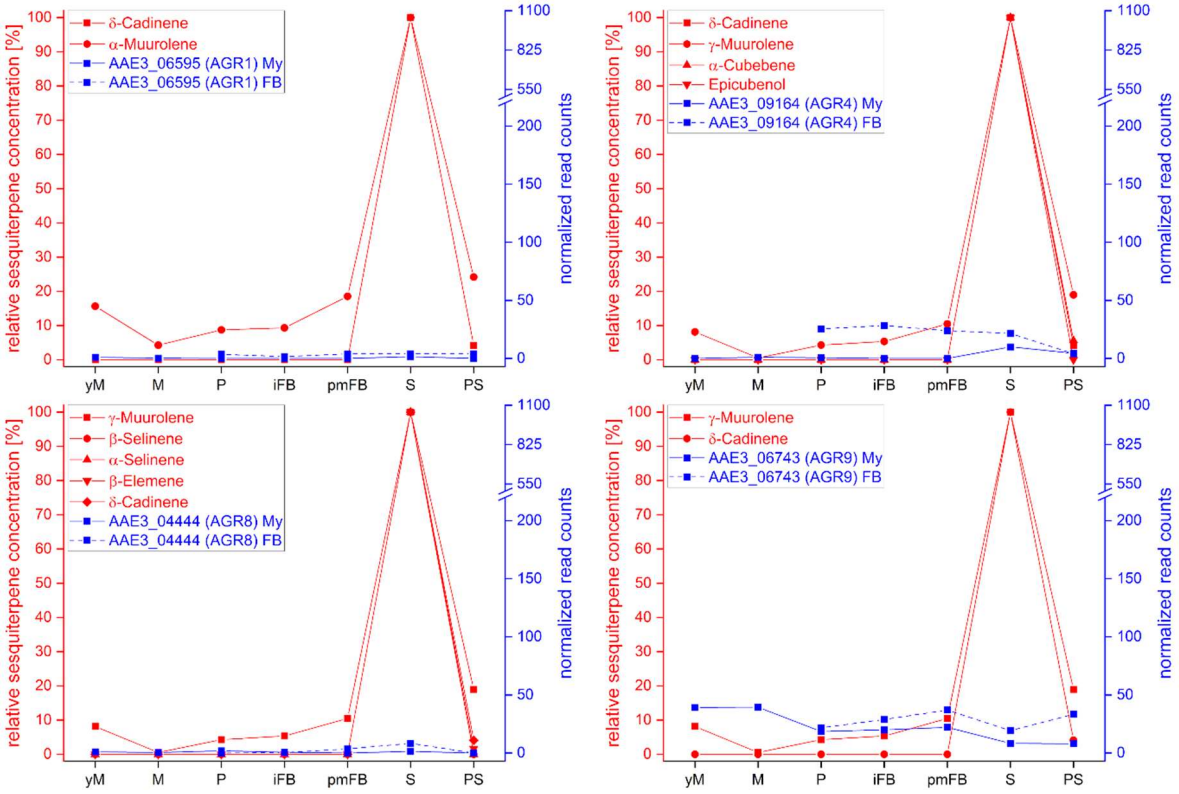

Figure S6: Transcription levels of the genes coding for the sesquiterpene synthases (STSs) Agr1, Agr4, Agr8 and Agr9 (blue) in the mycelium (My) and in fruiting bodies (FB) during different developmental stages of *C. aegerita* as well as the relative concentrations of the corresponding sesquiterpenes (red) in the HS of *C. aegerita*. Interestingly, compared to the STSs Agr2, Agr3, Agr5, Agr6 and Agr7, Agr9 coded by the gene AAE3_06743, involved in the synthesis of γ-muurolene and δ-cadinene, displayed in the mycelium as well as in FB quite constant transcription levels, ranging between 8 and 40 normalized read counts. This also applied for the transcription level of AAE3_09164 (*AGR4*) in FB whereas in the mycelium the highest transcription level was with 10 normalized read counts during sporulation quite low. Of all STS investigated in *C. aegerita* AAE-3, AAE3_06595 (*AGR1*) and AAE3_04444 (*AGR8*) showed the lowest transcription levels, not exceeding 9 normalized read counts in the examined developmental stages, neither in the mycelium nor in the plectenchmyatic samples of the different fruiting body stages. yM: young (uninduced) mycelium (day 10 post inoculation, p.i.); M: fruiting-primed mycelium (day 14 p.i.); P: primordia (day 18 p.i.); iFB: immature fruiting bodies (day 20 p.i.); pmFB: premature fruiting bodies (day 22 p.i.); S: sporulation (day 24 p.i.); PS: post sporulation (day 28 p.i.).

The fatty acid metabolism

The fatty acid synthase (FAS) is a multifunctional enzyme playing a key role in the cytosolic fatty acid synthesis. In fungi, the FAS complex normally consists of eight enzyme domains including an acetyltransferase (AT), an enoyl reductase, a dehydratase (DH), malonyl/palmitoyltransferase (MPT), an acyl carrier protein (ACP), a ketoreductase (KR), a ketosynthase (KS) and a phosphopantetheinyl transferase (PPT) [1, 2]. The FAS complex differs among fungi. In Basidiomycota, it tends to be a monomeric FAS protein encoded by a single gene whereas in Ascomycota the FAS complex is a $\alpha_6\beta_6$ oligomer with the eight domains encoded in two genes [3–5]. The cytosolic fatty acid synthesis is initialized by the binding of acetyl-CoA to a phosphopantetheinyl linker of ACP catalyzed by AT and the binding of a malonyl-CoA elongation unit by means of MPT followed by condensation, accompanied by a decarboxylation step, to β-ketoacyl-SACP derivatives catalyzed by the KS domain [2] (Figure S7). Malonyl-CoA is provided by an acetyl-CoA carboxylase catalyzing the carboxylation of acetyl-CoA. Subsequently, multiple reduction steps involving KR, DH and ER occur, lead to the corresponding acyl-SACP. Repetitions of this cycle and reversed loading reaction catalyzed by MPT result in the release of palmitoyl and stearoyl-CoA which can be further elongated catalyzed by β-ketoacyl-CoA synthases (elongases). Stearyl-CoA can be transformed successively into the polyunsaturated fatty acid linoleic acid by means of desaturases [6] (Figure S7). Genes coding for enzymes involved in fatty acid synthesis and processing were identified in the *C. aegerita* genome by means of BLAST search using amino acid sequences of already characterized fungal analogues. Generally, these enzymes were higher expressed in plectenchymatic samples (fruiting body stages) than in the mycelium with exception of the putative Δ^9-fatty acid desaturase AAE3_10709 and the putative Δ^{12}-fatty acid desaturase AAE3_00256 (Figure S7). Interestingly, many genes revealed the highest transcription levels in primordia and/or late fruiting body development stages including the putative acetyl-CoA carboxylase AAE3_00446, the putative FAS AAE3_09085, the putative elongase AAE3_08045, the putative Δ^9-fatty acid desaturases AAE3_00260, AAE3_10708 (homolog of *Le*-FAD1 [7]) and AAE3_07049 as well as the putative Δ^{12}-fatty acid desaturases AAE3_00132, AAE3_00257, AAE3_03586 (homolog of *Le*-FAD2 [8]) and AAE3_12354.

Nonetheless, in our study, most genes involved in fatty acid biosynthesis and processing also showed a decent transcription over 100 normalized read counts in the mycelium. An enhanced biosynthesis of fatty acid in younger mycelium stages and subsequent storage is quite likely taking the comparably high fat content in the mycelium of various fungi into account [9, 10]. A crucial step in the biosynthesis of fungal volatile oxylipins is the formation of unsaturated fatty acids, especially linoleic acid, from saturated fatty acids catalyzed by desaturases [3] (Figure S7). Sakai et al. characterized a Δ^9-fatty acid desaturase (FAD1) [7] and a Δ^{12}-fatty acid desaturase (FAD2) [8] from *L. edodes* and compared the levels of expression in mycelium, primordia and mature fruiting bodies. Depending on the cultivation conditions, *FAD1* showed an increase in transcription by 4.1 and 6.0-fold and *FAD2* by 3.5 and 4.2-fold in primordia and fruiting bodies compared to the mycelium [7, 8] which is in good agreement with our results. Additionally, Wang et al. reported for *L. edodes* a high and quite constant expression of *FAD2* in three different developmental stages of fruiting bodies [11] counting as well for young fruiting stages of *C. aegerita*, nonetheless it is worth to mention that in primordia, a developmental stage not investigated by Wang et al., we observed remarkably higher transcription of AAE3_10708 (putative homolog of *Le*-FAD1) and especially of AAE3_03586 (putative homolog of *Le*-FAD2) than in all other developmental stages.

References

1. Schweizer E, Hofmann J. Microbial Type I Fatty Acid Synthases (FAS): Major Players in a Network of Cellular FAS Systems. Microbiol Mol Biol Rev. 2004;68:501–17.

2. Dickschat JS. Fungal volatiles – a survey from edible mushrooms to moulds. Nat Prod Rep. 2017;34:310–28.

3. Reich M, Göbel C, Kohler A, Buée M, Martin F, Feussner I, et al. Fatty acid metabolism in the ectomycorrhizal fungus *Laccaria bicolor*. New Phytol. 2009;182:950–64.

4. Antelo L, Schlipp A, Hof C, Eisfeld K, Berg H, Hornbogen T, et al. The Fatty Acid Synthase of the Basidiomycete *Omphalotus olearius* is a Single Polypeptide. Z Für Naturforschung C. 2014;64:244–250.

5. Jenni S, Leibundgut M, Maier T, Ban N. Architecture of a Fungal Fatty Acid Synthase at 5 Å Resolution. Science. 2006;311:1263–7.

6. Beccaccioli M, Reverberi M, Scala V. Fungal lipids: biosynthesis and signalling during plant-pathogen interaction. Front Biosci Landmark Ed. 2019;24:172–85.

7. Sakai H, Kajiwara S. A stearoyl-CoA-specific Delta 9 fatty acid desaturase from the basidiomycete *Lentinula edodes*. Biosci Biotechnol Biochem. 2003;67:2431–7.

8. Sakai H, Kajiwara S. Cloning and functional characterization of a Δ12 fatty acid desaturase gene from the basidiomycete *Lentinula edodes*. Mol Genet Genomics. 2005;273:336–41.

9. Sumner JL. The fatty acid composition of basidiomycetes. N Z J Bot. 1973;11:435–42.

10. Cohen N, Cohen J, Asatiani M, Varshney V, Yu H-T, Yang Y-C, et al. Chemical Composition and Nutritional and Medicinal Value of Fruit Bodies and Submerged Cultured Mycelia of Culinary-Medicinal Higher Basidiomycetes Mushrooms. Int J Med Mushrooms. 2014;16:273–91.

11. Wang Y, Zeng X, Liu W. De novo transcriptomic analysis during *Lentinula edodes* fruiting body growth. Gene. 2018;641:326–34.

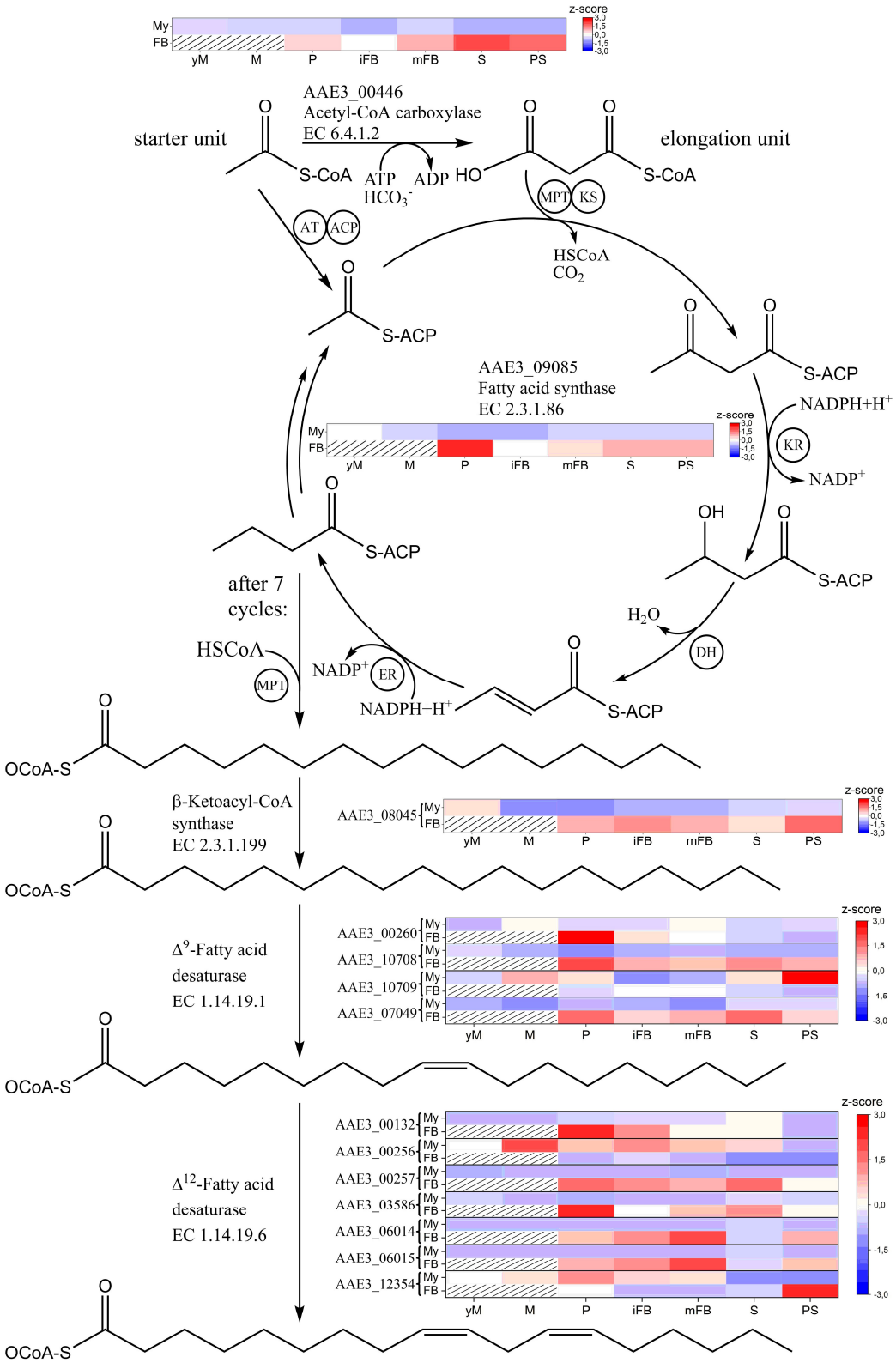

Figure S7: Expression of genes putatively involved in the fatty acid biosynthesis in the mycelium (My) and in fruiting bodies (FB) of *C. aegerita*. Normalized read counts were transformed to z-score values (respective scale to the right) whereby only genes were considered showing maximum transcription levels higher than 25 normalized read counts. Red colors indicate transcriptional upregulation while blue colors represent downregulation. White colors indicate a z-score of zero and hatched areas show an absence of sampling due the non-applicability. yM: young (uninduced) mycelium (day 10 post inoculation, p.i.); M: mycelium (day 14 p.i.); P: primordia (day 18 p.i.); iFB: immature fruiting bodies (day 20 p.i.); pmFB: premature fruiting bodies (day 22 p.i.); S: sporulation (day 24 p.i.); PS: post sporulation (day 28 p.i.).

Enzymes acting on C8 oxylipins

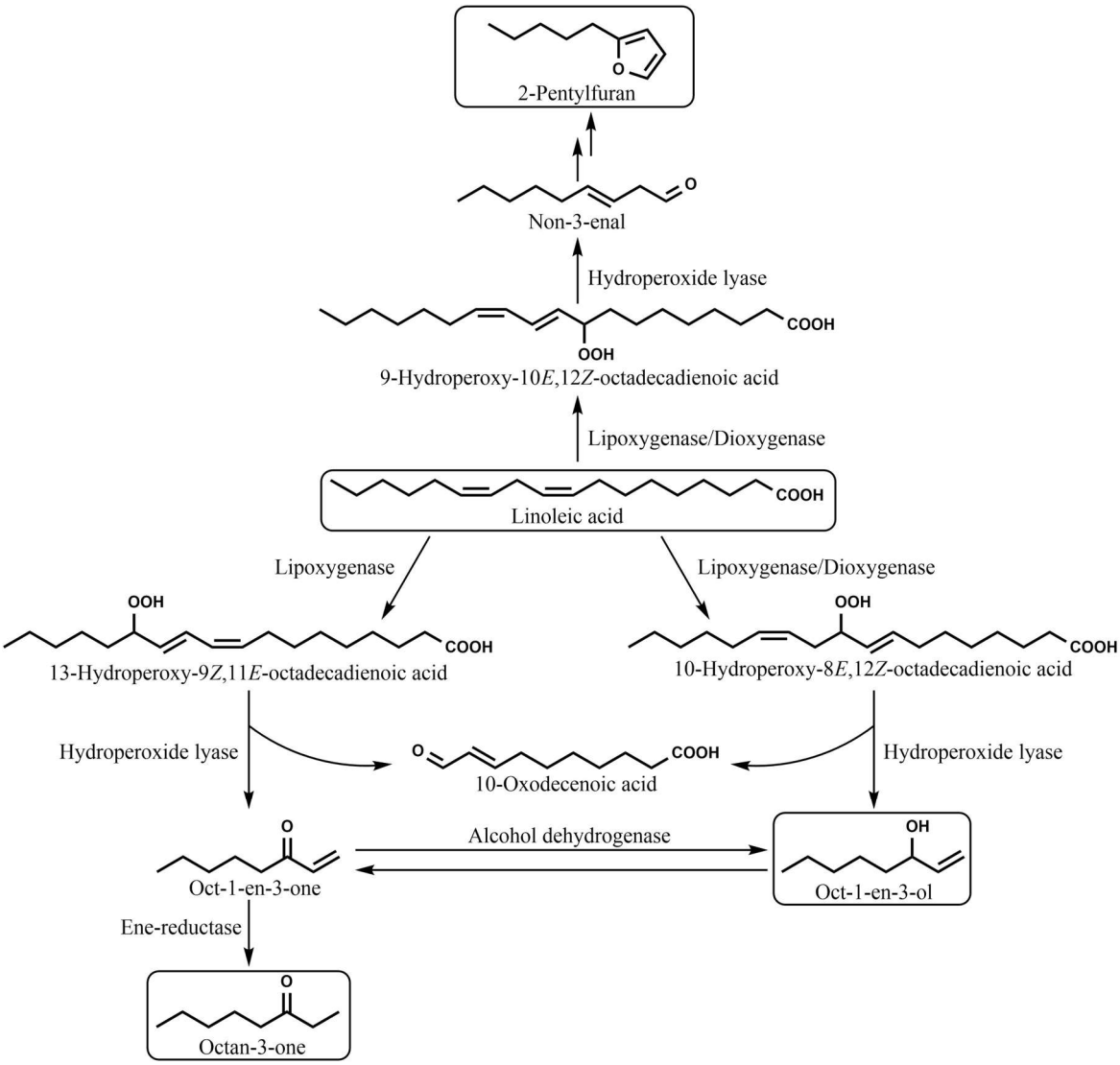

Figure S8: Proposed pathways for the enzymatic formation of fungal oxylipins.

Putative HPLs of *C. aegerita* were identified by means of BLAST search using protein sequences of characterized members of the CYP74 family in plants (Figure S9). Putative ADHs were identified using an ADH of the fungus *N. crassa* (Q9P6C8)) proven to be able to oxidize octan-1-ol [1]. To reduce the number of putative ADHs to the essentials, only genes were considered showing maximum transcription levels higher than 300 normalized read counts. Analogously, putative ene-reductases were analyzed by means of BLAST search using sequences of characterized non-FMN ene-reductases of plants accepting *inter alia*

non-2-enal and oct-1-en-3-one as substrates [2, 3] (*Nicotiana tabacum*, Q9SLN8; *Arabidopsis thaliana*, Q39172) and a fungal non-FMN ene-reductase (*Sporidiobolus salmonicolor*, A0A0D6ERK8). Additionally, sequences of fungal FMN depending old yellow enzyme (OYE) ene-reductases were used proven to be able to reduce amongst others citral (geranial) which shows some structural similarities with non-2-enal and oct-1-en-3-one [4, 5] (*Pichia stipites*, A3LT82), *Meyerozyma guilliermondii*, A5DR62). To reduce the number of putative ene-reductases to the essentials, only genes were considered showing maximum transcription levels higher than 300 normalized read counts (Figure S11). It is worth to mention that the putative OYE ene-reductases generally showed, compared to the putative non-FMN ene-reductases, low expression.

References

1. Park Y-C, San K-Y, Bennett GN. Characterization of alcohol dehydrogenase 1 and 3 from *Neurospora crassa* FGSC2489. Appl Microbiol Biotechnol. 2007;76:349–56.

2. Mansell DJ, Toogood HS, Waller J, Hughes JMX, Levy CW, Gardiner JM, et al. Biocatalytic Asymmetric Alkene Reduction: Crystal Structure and Characterization of a Double Bond Reductase from *Nicotiana tabacum*. ACS Catal. 2013;3:370–9.

3. Mano J, Torii Y, Hayashi S, Takimoto K, Matsui K, Nakamura K, et al. The NADPH:Quinone Oxidoreductase P1-ζ-crystallin in *Arabidopsis* Catalyzes the α,β-Hydrogenation of 2-Alkenals: Detoxication of the Lipid Peroxide-Derived Reactive Aldehydes. Plant Cell Physiol. 2002;43:1445–55.

4. Zhang B, Zheng L, Lin J, Wei D. Characterization of an ene-reductase from *Meyerozyma guilliermondii* for asymmetric bioreduction of α,β-unsaturated compounds. Biotechnol Lett. 2016;38:1527–34.

5. Bougioukou DJ, Walton AZ, Stewart JD. Towards preparative-scale, biocatalytic alkene reductions. Chem Commun. 2010;46:8558–60.

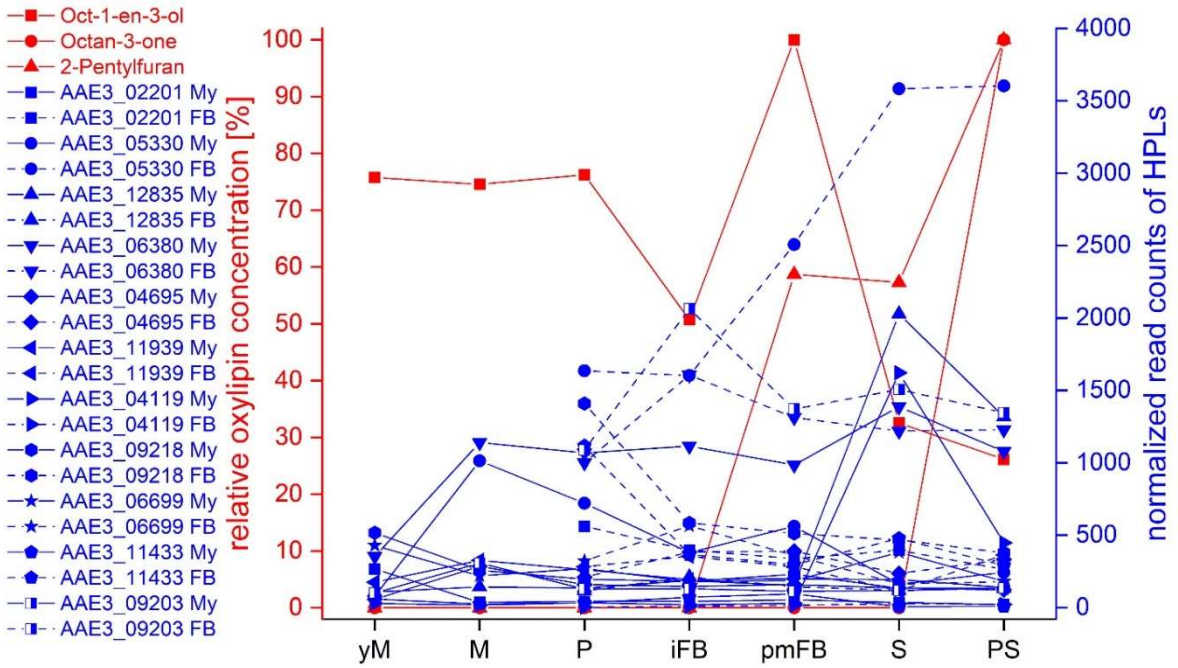

Figure S9: Transcription levels of genes coding for putative HPLs (blue) in the mycelium (My) and in fruiting bodies (FB) during different developmental stages of *C. aegerita* as well as the relative concentrations of volatile oxylipins (red) in the HS of *C. aegerita*. Only genes were considered showing maximum transcription levels higher than 300 normalized read counts. yM: young (uninduced) mycelium (day 10 post inoculation, p.i.); M: mycelium (day 14 p.i.); P: primordia (day 18 p.i.); iFB: immature fruiting bodies (day 20 p.i.); pmFB: premature fruiting bodies (day 22 p.i.); S: sporulation (day 24 p.i.); PS: post sporulation (day 28 p.i.).

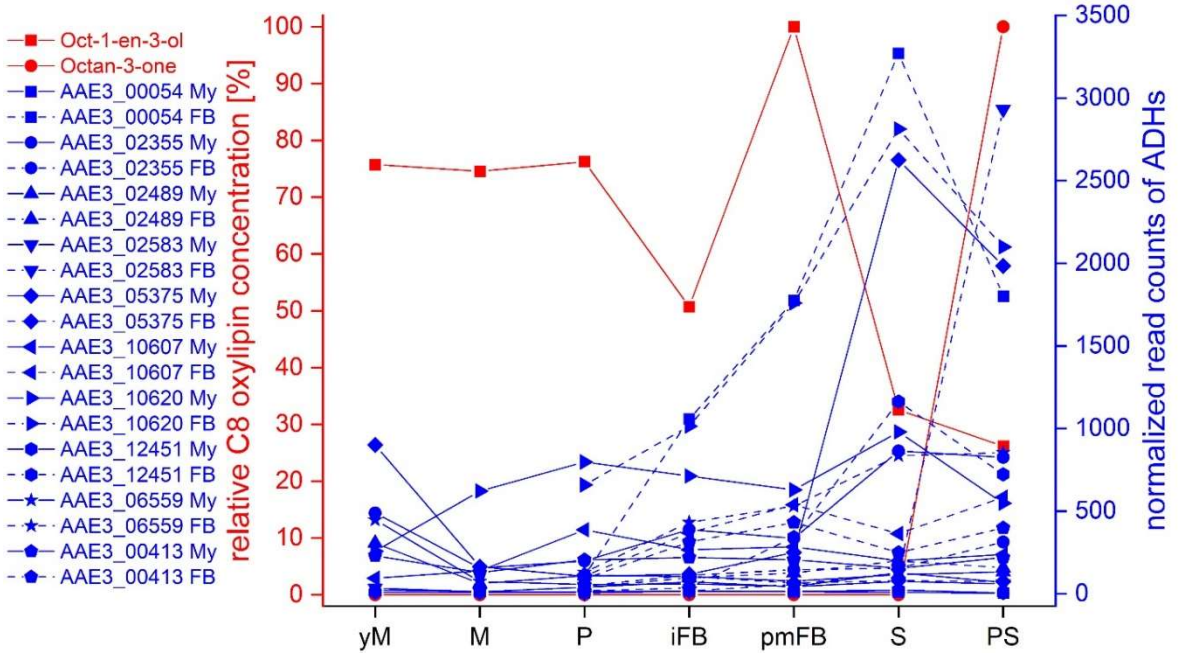

Figure S10: Transcription levels of genes coding for putative ADHs (blue) in the mycelium (My) and in fruiting bodies (FB) during different developmental stages of *C. aegerita* as well as the relative concentrations of volatile C8 oxylipins (red) in the HS of *C. aegerita*. Only genes were considered showing maximum transcription levels higher than 300 normalized read counts. yM: young (uninduced) mycelium (day 10 post inoculation, p.i.); M: mycelium (day 14 p.i.); P: primordia (day 18 p.i.); iFB: immature fruiting bodies (day 20 p.i.); pmFB: premature fruiting bodies (day 22 p.i.); S: sporulation (day 24 p.i.); PS: post sporulation (day 28 p.i.).

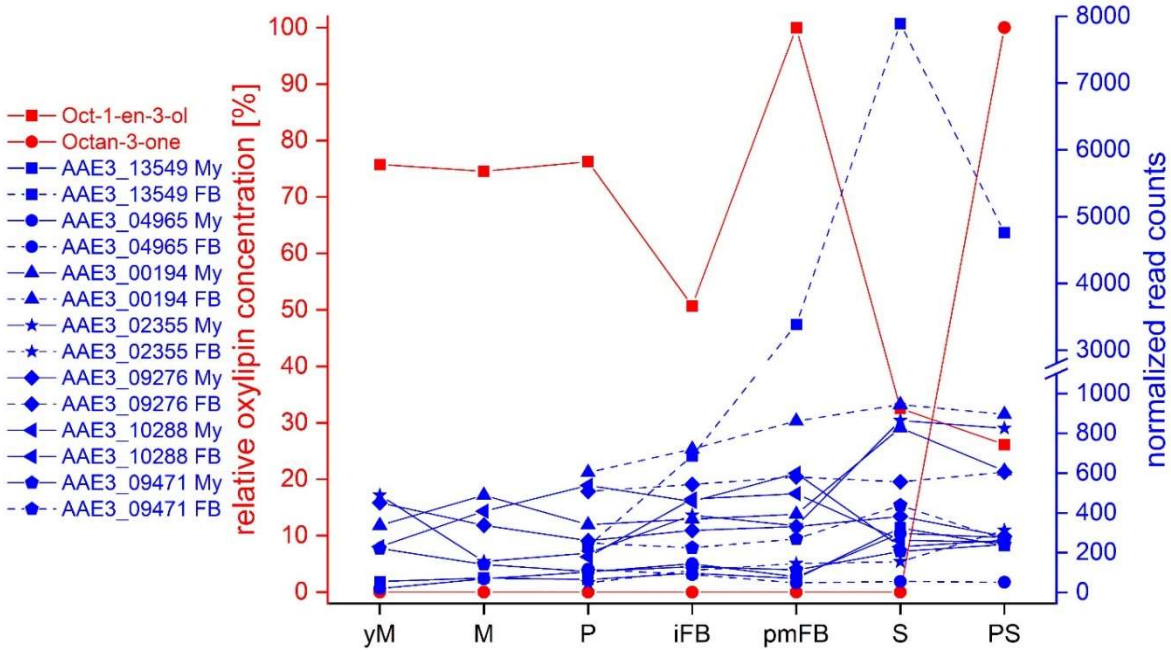

Figure S11: Transcription levels of genes coding for putative ene-reductases (blue) in the mycelium (My) and in fruiting bodies (FB) during different developmental stages of *C. aegerita* as well as the relative concentrations of volatile C8 oxylipins (red) in the HS of *C. aegerita*. Only genes were considered showing maximum transcription levels higher than 300 normalized read counts. yM: young (uninduced) mycelium (day 10 post inoculation, p.i.); M: mycelium (day 14 p.i.); P: primordia (day 18 p.i.); iFB: immature fruiting bodies (day 20 p.i.); pmFB: premature fruiting bodies (day 22 p.i.); S: sporulation (day 24 p.i.); PS: post sporulation (day 28 p.i.).

Revealing putative enzymes of the oxylipin pathway in *C. aegerita*

Putative DOXs were identified in the genome of *C. aegerita* by means of BLAST search using protein sequences of characterized DOXs from Ascomycetes including a 8R-DOX-7,8-LDS (linoleate diol synthase) (*Gaeumannomyces graminis*, AAD49559), a 9R-DOX (*Fusarium oxysporum*, EGU79548) and a 10R-DOX-CYP (cytochrome P450) (*Aspergillus fumigatus*, ABV21633). This way, two putative DOXs (AAE3_00407 and AAE3_13098) were found, being, as reported for other fungal 8-, 9- and 10-DOXs, fused to CYPs, which are usually catalytically functional [1]. Fungal DOX-CYPs consist of several subfamilies including *inter alia* 5,8- and 7,8-LDS, 10*R*-DOX-EAS (epoxy alcohol synthase), 9*S*- and 9*R*-DOX-AOS (allene oxide synthase), 8*S*- and 8*R*-DOX-AOS and 10*R*-DOX-CYP enzymes, the latter lacking the heme-thiolate ligand in the CYP domain. Therefore, this domain is proposed to be not functional [2, 3]. All DOX fusion proteins harbor the dioxygenase domain at the N-terminus whereas the P450 domain, responsible for the rearrangement of the N-terminally formed hydroperoxide fatty acid, is located at the C-terminus [4]. Phylogenetic analysis revealed that fungal DOXs cluster in different groups, with the two putative DOXs from *C. aegerita* assembling with putative DOXs of the basidiomycete fungus *Rhizoctonia solani* indicating sequence and potentially functional difference between DOXs from Basidiomycota and the so far characterized DOXs from Ascomycota (Supplementary Figure S12).

References

1. Oliw EH. Polyunsaturated C-18 fatty acids derivatized with Gly and Ile as an additional tool for studies of the catalytic evolution of fungal 8-and 9-dioxygenases. Biochim Biophys Acta-Mol Cell Biol Lipids. 2018;1863:1378–87.

2. Oliw EH. Biosynthesis of Oxylipins by *Rhizoctonia solani* with Allene Oxide and Oleate 8S,9S-Diol Synthase Activities. Lipids. 2018;53:527–37.

3. Brodhun F, Schneider S, Göbel C, Hornung E, Feussner I. PpoC from *Aspergillus nidulans* is a fusion protein with only one active haem. Biochem J. 2010;425:553–65.

4. Hoffmann I, Oliw EH. Discovery of a linoleate 9S-dioxygenase and an allene oxide synthase in a fusion protein of *Fusarium oxysporum*. J Lipid Res. 2013;54:3471–80.

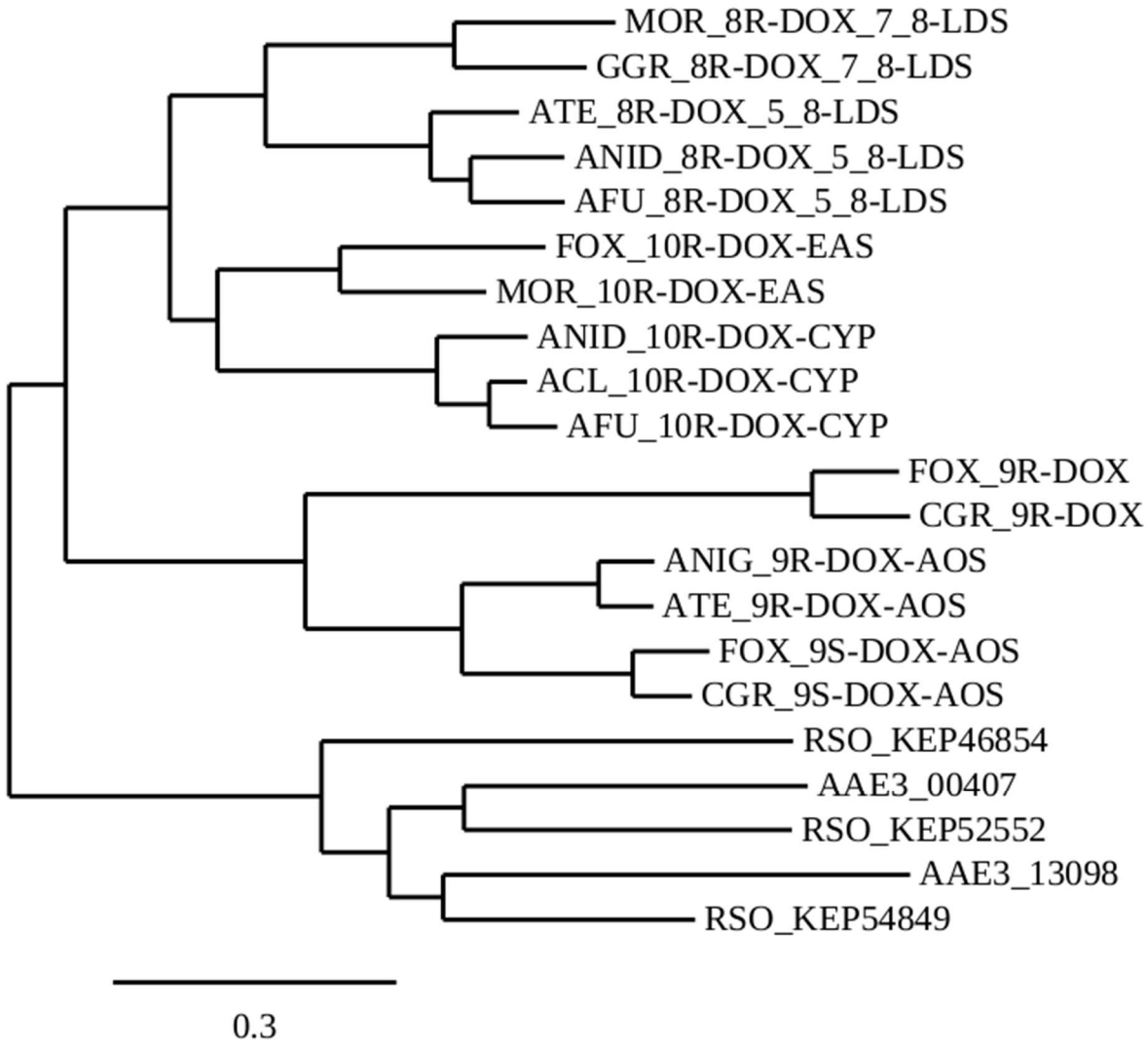

Figure S12: Phylogenetic analysis of different DOXs from Ascomycota and putative DOXs from the Basidiomycota *C. aegerita* and *Rhizoctonia solani*. MOR: *Magnaporthe oryzae*, GGR: *Gaeumannomyces graminis*, ATE: *Aspergillus terreus*, ANID: *Aspergillus nidulans*, AFU: *Aspergillus fumigatus*, FOX: *Fusarium oxysporum*, ANIG; *Aspergillus niger*, ACL: *Aspergillus clavatus*, CGR: *Colletotrichum graminicola*, RSO: *Rhizoctonia solani*. MOR_8R-DOX_7_8-LDS (EHA52010), GGR_8R-DOX_7_8-LDS (AAD49559), ATE_8R-DOX_5_8-LDS (AGA95448), ANID_8R-DOX_5_8-LDS (EAA65132), AFU_8R-DOX_5_8-LDS (EDP50447), FOX_10R-DOX-EAS (EGU86021), MOR_10R-DOX-EAS (EHA53428), ANID_10R-DOX-CYP (AY613780), ACL_10R-DOX-CYP (EAW09782), AFU_10R-DOX-CYP (ABV21633), FOX_9R-DOX (EGU79548, FOXB_09952), CGR_9R-DOX (EFQ36675, GLRG_11821), ANIG_9R-DOX-AOS (EHA25900), ATE_9R-DOX-AOS (AGH14485), FOX_9S-DOX-AOS (EGU88194), CGR_9S-DOX-AOS (EFQ27323).

```
A)
FOX_9R-DOX              DLFDKLMAREE--GGRESQSGLSAMLIYHATIIIHDIFRTNDNDKNISDSSSYLDLSPLYGYTTEMQRKVRDDKYKLGLLKPDTFAEDRLLRQPPGVCIMLVMYNRYHNYAARQLLRINE      291
CGR_9R-DOX              VLFDRLMAREN--GGRQSQSGLSSMLLYHATIIIHDIFRTNDNDKNLSDSSSYLDLSPLYGYTEEMVRKVRDNKYKLGLLKPDTFAEDRLLRQPPGVCIMLVMYNRYHNYAARQLLQINE      287
AAE3_13098              LVFDTLLKRDK---FEKHPAGISALFFAFADLVIHSIFNTNHTDWTINDASSYLDLSILYGSSDQEVDSIRKKD-GSGALYEDVFADKRLLMMPPASCALLVLLSRNHNFIAQRIRDINE      362
AAE3_00407              LIFDTLLRRQG---FKKHPGGLSSLMFSFATLVIHSVFRTSHRDWSINETSSYVDLAPLYGNNQKEQDRLRIRD-GRGLLYPDVFSEDRLLLLPPAVCTLLVLFSRNHNYIAKKLLEINE      282
RSO_KEP52552            LVFECLLKRDK---VTPHPAGLSAMFFSFATLVIHTCFRTNHRDVTINETSSYVDLAPLYGNNQEDQDSVRRWD-GTGRLKEDVFTENRLLFLPPAVCTLLVLFCRNHNFIARKLYLINE      297
RSO_KEP54849            LIFDTLLRRDT-PGGKEHPAGVSSLLFSFAVLIIHSLFRTAPSSMYINDTSSYLDLSPLYGHSFEAQMKVRRND-GTGRLYEDVFAENRLLLMPPAVSALLIMFSRNHNYIATKLLQINE      348
RSO_KEP46854            MVVDELLTASSSTPRDLHPGGNSSLTFAFASLVTHSLFRTDPSDWGKNNTSSYLDLSPLYGSNQAEQDLVRVKD-GRGLLHPDTFSEGRLVFLPPAAAALLVMWNRNHNFIANNILKINE      239
ANIG_9R-DOX-AOS         LLFDLLMARDD-TTFRENPAGISSVLFYHASIIIHDVFCTNRRDPNISDTSSYLDLAPLYGSSYEDQLRVRTMQ--RGMLKPDTFHEKRLLGQPPGVNVILVMYNRFHNYVADVLLKINE      348
ATE_9R-DOX-AOS          LLFDLLMARDD-STFKENPAGISSMLFYHASIIIHDIFRTNRRDPNISDTSSYLDLAPLYGSSLEDQLKVRTME--KGMLKPDTFHEKRLLGQPAGVNVILVMYSRFHNYVADMLLKINE      348
FOX_9S-DOX-AOS          LLFDLLMARDE-TTFQENPAGISSMLFYHAAIIIHDIFRTNRTDMNKSDTSSYLDLAPLYGSSLKDQHEIRTMK--EGKLKPDTFHEKRLLGQPAGVNVMLVLYSRFHNYVADILLKINE      319
CGR_9S-DOX-AOS          LLFDLLMARDD-STFKENPAGISSMLFYHASIIIHDIFRTNRTDMNKSDTSSYLDLAPLYGSSLKDQLEIRTMK--EGMLKPDTFHERRLLGQPAGVNAMLVLYNRFHNYVCDILLKINE      319
MOR_8R-DOX(7,8-LDS)     TIFDTLMARDP-AKFRPHPNQISSVLFYFATIITHDIFQTSSRDPSINLTSSYLDLSPLYGRNLEEQLSVRAMK--DGLLKPDTFCSKRVHGFPPGVGVLLIMFNRFHNYVVTSLAKINE      296
GGR_8R-DOX(7,8-LDS)     TIFDTLMVRDP-AKFRPHPNKISSMLFYLATIITHDIFQTSPRDFNINLTSSYLDLSPLYGRNHDEQMAVRTGK--DGLLKPDTFSSKRVIGFPPGVGAFLIMFNRFHNYVVTQLAKINE      286
ANID_10R-DOX-CYP        LVFDTLFAR---QKFTPHPNKVSSLFFDWASLIIHDIFQTDYRDYNKNKTSAYLDLAILYGDVQEEQDLVRTHK--DGKLKPDSFSEPRLQAFPAACCVLLVMLNRFHNYVVEELAAINE      337
ACL_10R-DOX-CYP         LVFDTLFAR---QSFKPHPNNVSSLFFDWASLIIHDIFQTDYRNPHVNKTSGYLDLSILYGDVQEEQNLIRTFE--GGRLKTDSFSEPRLQAFPAACCVLLVMLNRFHNHVVEQLAAINE      332
AFU_10R-DOX-CYP         LVFDTLFAR---QTFKPHPNKVSSVFFYWASLIIHDIFQTDYKNPNMNKTSGYLDLSILYGDVQEEQNLIRTFK--DGKLKPDSFSEPRLQAFPATCCVLMVMLNRFHNYAVEQLAAINE      336
ATE_8R-DOX(5,8-LDS)     ALFDSLLAR---KDFKEHPNKISSVLFYIASIIHDLFQTDHRDSSINRTSSYLDLSPLYGNNQDEQYLMRTFK--DGKLKPDCFSSKRILGFPPGVGVLLIMFNRFHNYVVEQLAAVNE      276
ANID_8R-DOX(5,8-LDS)    TIFDCLLRR---KEYREHPNKISSVLFYLASIIHDLFQTDPKDNSVSKTSSYLDLSPLYGNNQDEQNLVRTFK--DGKLKPDCFATKRVLGFPPGVGVLLIMFNRFHNYVVDQLAAINE      285
AFU_8R-DOX(5,8-LDS)     TLFDCLLAR---KEYKEHPNKISSVLFYIASIIHDLFETDRKDPAISLTSSYLDLSPLYGNNQQEQDLIRTFK--DGKLKPDCFSTKRVLGFPPDVGVVLIMFNRFHNYVVEKLAMINE      285
FOX_10R-DOX-EAS         AIFESVFAR---DAFRKNPNNVSSILWYWATIIIHDLFWTNLQDPNQNDSSSYLDLAPLYGSTEKDRDSIRTFK--DGQLKPDCFADKRLIGNPPGVPILLIMFNRFHNHVATNLADINE      310
MOR_10R-DOX-EAS         LIFDSIMGRTP-NSYRKHPNNVSSILWYWATIIIHDIFWTDPRDINTNKSSSYLDLAPLYGNSQEMQDSIRTFK--DGRMKPDCYADKRLAGMPPGVSVLLIMFNRFHNHVAENLALINE      359
                         :.: ::               *::    * :: *  * *   .   . :*.*:**: ***        :*  .   * :  * :   *:   *     .:::  * **.    :  :**
FOX_9R-DOX              TLKLKDHDHQAAKDFEAACDEFKDAWEAAWNKQDDDLFNTARLITCGMYIQISVHDYLRALMGFHQFDTNFTLDPRADFDQKK-----TSRGIGNQVTVEFNLLYRFHCAISRKDEAYTE      525
CGR_9R-DOX              GQKLERESPALLKSFENNCKDFKIAWQAACDKQDDDLFNTARLITQGMYVNISVHDYLRALMGFHQFDTNFTLDPRKDFDQKK-----TTRGIGNQVTVEFNLLYRFHCAISLRDEKYVE      522
AAE3_13098              ------------------------------MLQDDEIFHRARLVNCGYFMQIILGDYVGAILGLVRDETDWRLNPLMTMRELD--HDFAPTGEGNVCSVEFNLLYRWHATLSEPDTEWIT      463
AAE3_00407              -----------------------DPISKAKLVEQEEDIFQTARLINCGWFGMVVFSDYFSSILGLVRDGSSWSLTPFDEMRKED--HSLFERGKGNVCSVEFNCLYRWHATTSREDEQWTH      391
RSO_KEP52552            -----------------------RR------KQQDHVLFNTARLINVGFFVSIVLGDYLASILGIVREGSDWSLNPFQDIVQSE--RNHVPRGDGNSVSVEFNLLYHWHSTTSALDEEWTE      400
RSO_KEP54849            GTASTAYTTPAGSRFLGLDNQASRKARTPLEEQDHVIFNTARLINCGFFMHIIISDYIGAILGLTREGSSYSLNPLEEIRGSD--HQLVGRGEGNSCSVEFNLLYRWHATLSAADEKWTE      529
RSO_KEP46854            --------------------------PEKCARQDKEIFETARLINCGSFMSVVFGDYVAGFLGLSREGSSWGMQPFDPIQGSE--G-EVGRGQGNHCSVEFNLLYRWHAVTSEADEKWTD      341
ANIG_9R-DOX-AOS         -----------------------EDAKRKALAKQDEDLFQVTRLIVNGLYVNISLHDYLRGLTNTHHSASDWTLDPRVAVSRAFD-ADGVPRGVGNQVSAEFNLLYRFHSVISRRDEQWTN      456
ATE_9R-DOX-AOS          -----------------------EEARKKALAKQDEDLFQVARLVVNGLYVNISLHDYLRGLTNTHHSASDWTLDPRIAVGRTFD-PDGVPRGIGNQISAEFNLLYRFHSVISRRDEKWTN      456
FOX_9S-DOX-AOS          -----------------------EEDKAKAIAKQDHDLFNVARLITGGLYINICLHDYLRAITNTHHSASDWTLDPRVAIDKQFD-GDGVPRGVGNQVSVEFNLLYRFHSCISKRDEKWIN      429
CGR_9S-DOX-AOS          -----------------------PEDRAKAVAKQDHDLFNTARLIVGGLYINISLHDYLRAITNTHHSKSDWTLDPRVEIGKQFD-GEGVPRGVGNQVSVEFNLLYRFHSCISKKDERWID      429
MOR_8R-DOX(7,8-LDS)     ------------------------DDTAAWEKYDNDLFQTGRLITCGLYVNIVLVDYVRTILNLNRVDSSWILDPRTEEGKSLL-SKPTPEAVGNQVSVEFNLIYRWHCGMSQRDDKWTT      400
GGR_8R-DOX(7,8-LDS)     ------------------------PDDTAGWETYDNSLFQTGRLITCGLYINIVLGDYVRTILNLNRANTTWNLDPRTKEGKSLL-SKPTPEAVGNQVSVEFNLIYRWHCTISERDDKWTT      391
ANID_10R-DOX-CYP        -----------------------EEQAKKAWAKYDEDLFQTGRLITCGLFINITLYDYLRTIVNLNRVNSTWCLDPRAQMEGSA-----TPAGLGNQCSVEFNLAYRWHSAISANDEKWTE      442
ACL_10R-DOX-CYP         -----------------------EDQAKKAWEKYDEDLFQTGRLITCGLYINITLYDYLRTIVNLNRTNSTWCLDPRAQMEGNN----TTPSGLGNQCSVEFNLAYRWHSAISANDEKWTE      438
AFU_10R-DOX-CYP         -----------------------EEEAKKAWAKYDEDLFQTGRLITCGLYINITLYDYLRTIVNLNRTNSTWCLDPRAQMEGSH----TAPSGLGNQCSVEFNLAYRWHSATSATDEKWTE      442
ATE_8R-DOX(5,8-LDS)     ------------------------SNDKEYAKYDNNLFQTGRLVTCGLYINIILKDYVRTILNINRTNSTWSLDPRMDMKDGLL-GDAAPLATGNQVSAEFNLIYRWHSCISQRDEKWTT      380
ANID_8R-DOX(5,8-LDS)    ------------------------SNVDEYAKYDNNLFQTGRLVTCGLYANIILKDYVRTILNINRTDSTWSLDPRMEMKDGLL-GEAAAMATGNQVSAEFNVVYRWHACISKRDEKWTE      389
AFU_8R-DOX(5,8-LDS)     ------------------------SDTAAYAKYDNDLFQTGRLVTCGLYVNIILKDYVRTILNINRTDSIWSLDPRSEMKDGLL-GRAAAQATGNQVAAEFNLVYRWHSCISQRDQKWTE      389
FOX_10R-DOX-EAS         -----------------------PEAADAAWKKRDTELFETARLVTSGLYINITLIDYVRNIINLNRVDTTWTLDPRQEMGVSVGTKDLSESGTGNVVSAEFNLCYRWHSCLSEMDDKWVQ      420
MOR_10R-DOX-EAS         -----------------------GEAREAAWKKYDNDLFQVARLVTSGLYINITLVDYVRNIVNLNRVDTTWTLDPRQDAGAHVGTADGAERGTGNAVSAEFNLCYRWHSCISEKDSKFVE      469
                                                                  :  :*.  **:  * :  : . **.  : .  :  : : : *               . **  :.***  *::*.  *  *  :
```

B)

```
FOX_9R-DOX              GVFVAKQVLA-YEKDQSK--AA-AILLLVCLDFAYNAVVSFTATLDGYMRDLYAAADGRP  1106
CGR_9R-DOX              GVFVARQVLK-HEPNRVR--AA-AILLLISLDFAYNAVVSFSATLDGFMEDLCQVANGDN  1134
AAE3_13098              SHMFLKKLWHKLGKNYTRTEFTAQ-VFAAVIPTVALYSQAVAHIVDFYLDQ---------  987
AAE3_00407              YHDIVKRLY-ELGE--STDQLANT-ILALMVTAGTELVITITNALNVYLGS---------  898
RSO_KEP52552            SFDFMRRLH-KSGK--SKDQLCNA-VLAAIVA-SFEFIPALINVVNFYLET---------  904
RSO_KEP54849            AQAFLTNLY-ANKGDLTVEQLSYN-VFGCMIASVSNYAQAATQVVDFYLDD---------  1050
RSO_KEP46854            SDAFHTALL-ASKK--PINDLVAM-ICGMLVSSTVNFAQATSHMVDFYMDE---------  861
ANIG_9R-DOX-AOS         GNNVVKQMME---MDMTAAETAEVCW-LTAVGGVGAPVGLVADVLQYYLRP---------  973
ATE_9R-DOX-AOS          GNNVAKEMME---MGMSAEEVADICW-LTAIGGVGTPSGVVANVLQYYFRY---------  972
FOX_9S-DOX-AOS          GLKLVEELLA---QGNNVDQVTDNLW-LTAFGGIGVPVTAFYEVLSFFLRP---------  954
CGR_9S-DOX-AOS          GHKLVEELLA---QGNSAEQVVDNMW-LTAFGGIGAPVTAFYEVLEYFLRR---------  955
MOR_8R-DOX(7,8-LDS)     GDLMLRRMIEAYGEGKSVKEAVYGQIMPSIAAGTANQTQIMAQCLDYYMSD---------  961
GGR_8R-DOX(7,8-LDS)     GDQLLQRMLSQ--DGRSIEETVSGTILPVVMAGTANQTQLLAQCLDYYLG----------  952
ANID_10R-DOX-CYP        GDQLIKRLAE---GGLSVSDITYGQILPTAVELVHGQAQMFTRVVEYYLN----------  935
ACL_10R-DOX-CYP         GAHMTKQLLE---NGLGASEITWSQILPTVIAMVPSQAQAFTQIIDFYLSK---------  947
AFU_10R-DOX-CYP         GVHLTKQLLE---NGLGAHEIAWAQFLPTVIAMVPAQAQAFTQIVDFYLSK---------  951
ATE_8R-DOX(5,8-LDS)     GIHMIQRLLA---SGLPASEIVWTHLLPTAGGMVANQGQLFSQCLDYYLSE---------  893
ANID_8R-DOX(5,8-LDS)    GIHMIQRLLD---SGLPATEIVWTHILPTAGGMVANQAQLFSQCLDYYLSE---------  902
AFU_8R-DOX(5,8-LDS)     GVHMIQRLLD---SGMPAPEIVWTHVLPTAGGMVANQAQLFSQSLDYYLSE---------  902
FOX_10R-DOX-EAS         GENMAKGLKK---AGLSTEDIVWSQILPTAGAMVPNQAQVFAQTLDWYLSP---------  929
MOR_10R-DOX-EAS         GKTMIKGLKA---HGLSDYDIAWSHVVPTSGAMVPNQAQVFAQAVDYYLSP---------  980
```

```
FOX_9R-DOX              QVLM---SQLSIADK----F----GVFAPRRVATISLTSMIKFVAQMKNPRRGHDAQGKL        1251
CGR_9R-DOX              EFLT---LQLSIADK----Y----AVFSPRRFTPLSQAQMIKFIALTRNTRRGPAAQGEL        1272
AAE3_13098              -------DYLRAASNPGLASFIGETGLLTSEFFQSTVPGVLAAIFKLKDLQRGPGLSGSF        1126
AAE3_00407              SLTRPAKDRLSADGAFNY-LGEGLTVKVKLSF-------------DMLPAVT---DNAPL        1015
RSO_KEP52552            DPRRPVNNY-------TL-MGDGLHRCFTDDFVHSTMACAIRAVFQLKNVRRGPGKSGHL        1039
RSO_KEP54849            NPDRPREAY-------NL-FGFGLHKCMGDQFTERTMPAVIKSIFKLKNVRRAPGESGKL        1188
RSO_KEP46854            DPRRPKEHY-------AI-QAIGAHGCPGLDATEQCMAMILREIFKLKNIRRAPGVLGQL        1001
ANI_9R-DOX-AOS          KLDRPSNAY--------IHFGYGAHECLGKEIGLTFAVSMLRVLAGLKYLRPAPGDMGML        1108
ATE_9R-DOX-AOS          RLDRPASAY--------IQWGYGAHECLGKEIAITFAVSMIRILAGLKYLRPAPGEMGVL        1106
FOX_9S-DOX-AOS          NPQRKKEDV--------SAFSYGQHECIAKDVALAFVTGLIKLVADLKELRPAPGQMGTV        1084
CGR_9S-DOX-AOS          DAKRKTDPV--------SAFSYGQHECLAKDIATTFIVGLVKLVADLKQLRPAPGQMGLV        1085
MOR_8R-DOX(7,8-LDS)     RLDRDLDSY--------TFFGLGPHRCAGDKVVRITMTAVFKVLLQLDGLRRAEGGRGVF        1122
GGR_8R-DOX(7,8-LDS)     RLDRPLESY--------VHFGLGPHRCAGEPISQIALSSVMKVLLQLDGLRRAAGPRGEI        1113
ANI_10R-DOX-CYP         RLDRPDESY--------LNYGIGSQIGLGKDATLTAVTAMVRAAFSLEGLRPAPGVQGVL        1072
ACL_10R-DOX-CYP         RLDRPLDAY--------INHSLGPHGFLSKETSQIALTAMLRAVGRLNNLRRAPGAQGEV        1084
AFU_10R-DOX-CYP         RLDRPMNSY--------INPTLGPHGFLSKETSHIALTAMLRAVGRLNNLRVAPGVQGQL        1088
ATE_8R-DOX(5,8-LDS)     RLDRDMDLY--------VHFGSGPHKCLGFGLCKLGLTTMLKVVGGLDNLRRAPGPQGQL        1030
ANI_8R-DOX(5,8-LDS)     KLDRDMNLY--------AHFGFGPHKCLGLDLCKTGLSTMLKVLGRLDNLRRAPGAQGQL        1039
AFU_8R-DOX(5,8-LDS)     KLDRDMNLY--------AHFGFGPHQCLGLGLCKTALTTMLKVIGRLDNLRRAPGGQGKL        1039
FOX_10R-DOX-EAS         DPKRPLDKY--------IHYGVGPHACLGRDISQVALTELFRAVFRKKGVRRVPGAQGEL        1068
MOR_10R-DOX-EAS         NPRRPAKKY--------IHYGVGPHACLGRDASQIAITEMFRCLFRRRNVRRVPGPQGEL        1119
```

Figure S13: Partial amino acid sequence alignment of different DOXs from Ascomycota and putative DOXs from the Basidiomycota *C. aegerita* and *Rhizoctonia solani*. A) N-terminal DOX domain containing histidine heme ligands residues as well as the catalytic tyrosine residue shown on a black background, latter being part of the YRWH motif (dark grey background). Leucine and valine residues responsible for the oxygenation at C-10 and C-8 of linoleic acid are underlined with light grey background. B) C-terminal P450 domain containing the NXXQ motif (dark grey background) and the cysteine residue responsible for the coordination of heme iron (black background). Alignment was carried out by using Clustal Omega with default parameters. MOR: *Magnaporthe oryzae*, GGR: *Gaeumannomyces graminis*, ATE: *Aspergillus terreus*, ANID: *Aspergillus nidulans*, AFU: *Aspergillus fumigatus*, FOX: *Fusarium oxysporum*, ANIG; *Aspergillus niger*, ACL: *Aspergillus clavatus*, CGR: *Colletotrichum graminicola*, RSO: *Rhizoctonia solani*. MOR_8R-DOX_7_8-LDS (EHA52010), GGR_8R-DOX_7_8-LDS (AAD49559), ATE_8R-DOX_5_8-LDS (AGA95448), ANID_8R-DOX_5_8-LDS (EAA65132), AFU_8R-DOX_5_8-LDS (EDP50447), FOX_10R-DOX-EAS (EGU86021), MOR_10R-DOX-EAS (EHA53428), ANID_10R-DOX-CYP (AY613780), ACL_10R-DOX-CYP (EAW09782), AFU_10R-DOX-CYP (ABV21633), FOX_9R-DOX (EGU79548, FOXB_09952), CGR_9R-DOX (EFQ36675, GLRG_11821), ANIG_9R-DOX-AOS (EHA25900), ATE_9R-DOX-AOS (AGH14485), FOX_9S-DOX-AOS (EGU88194), CGR_9S-DOX-AOS (EFQ27323).

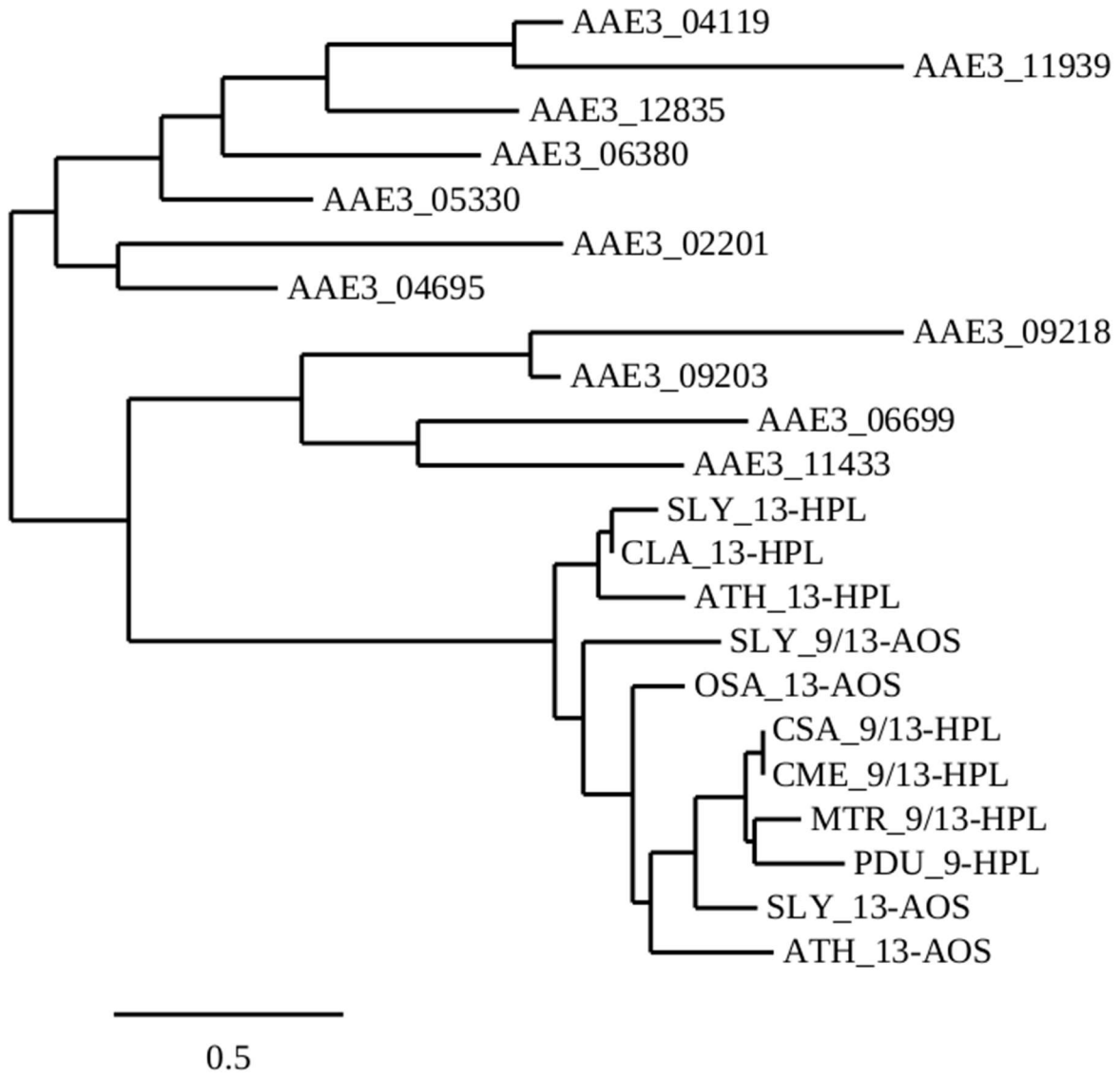

Figure S14: Phylogenetic analysis of different CYP74 proteins of plant and putative HPLs from *C. aegerita*. SLY: *Solanum lycopersicum*, CLA: *Citrullus lanatus*, ATH: *Arabidopsis thaliana*, OSA: *Oryza sativa*, CSA: *Cucumis sativus*, CME: *Cucumis melo*, MTR: *Medicago truncatula*, PDU: *Prunus dulcis*. SLY_13-HPL (K4CF70), CLA_13-HPL (Q66UT1), ATH_13-HPL (Q9ZSY9), SLY_9/13-AOS (Q9LLB0), OSA_13-AOS (Q7XYS3), CSA_9/13-HPL (Q9M5J2, AF229811), CME_9/13-HPL (Q93XR3), MTR_9/13-HPL (Q7X9B3), PDU_9-HPL (Q7XB42, AJ578748), SLY_13-AOS (Q9LLB0), ATH_13-AOS (Q96242).

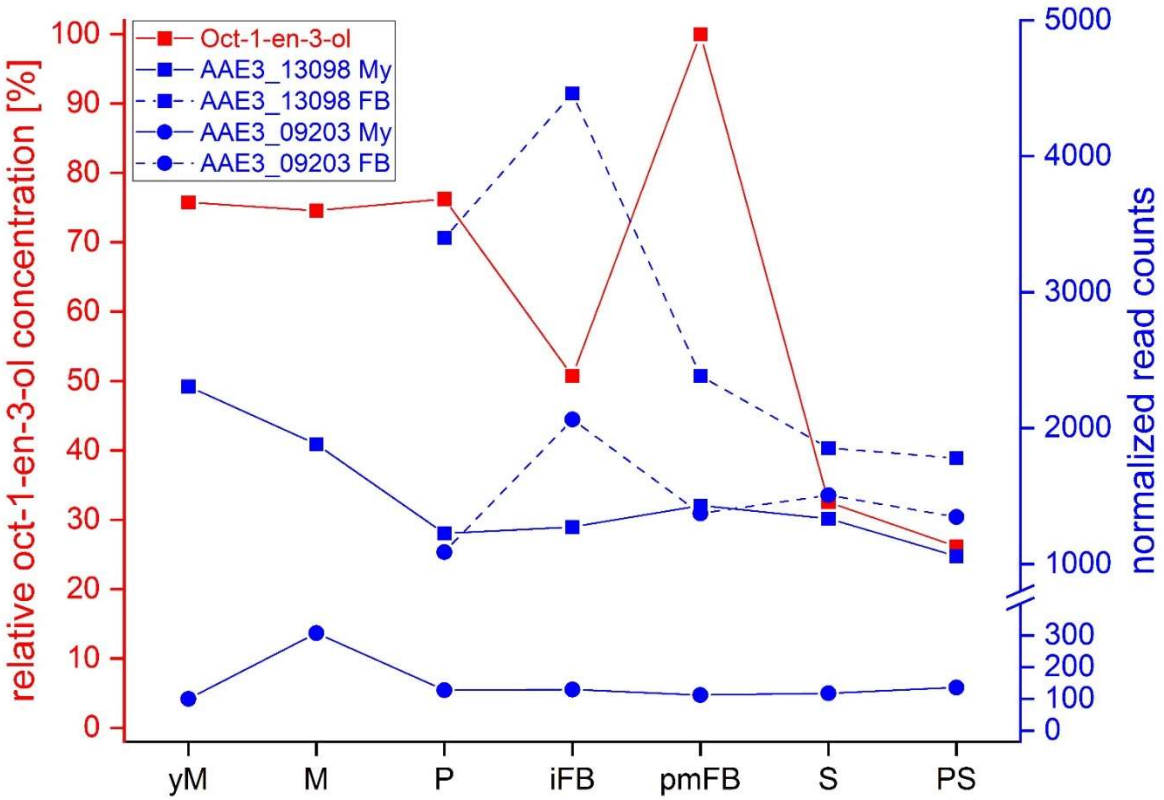

Figure S15: Transcription levels of the putative DOX AAE3_13098 and the putative HPL AAE3_09203 (blue) in the mycelium (My) and in fruiting bodies (FB) during different developmental stages of *C. aegerita* as well as the relative concentration of oct-1-en-3-ol (red) in the HS of *C. aegerita.* yM: young (uninduced) mycelium (day 10 post inoculation, p.i.); M: mycelium (day 14 p.i.); P: primordia (day 18 p.i.); iFB: immature fruiting bodies (day 20 p.i.); pmFB: premature fruiting bodies (day 22 p.i.); S: sporulation (day 24 p.i.); PS: post sporulation (day 28 p.i.).

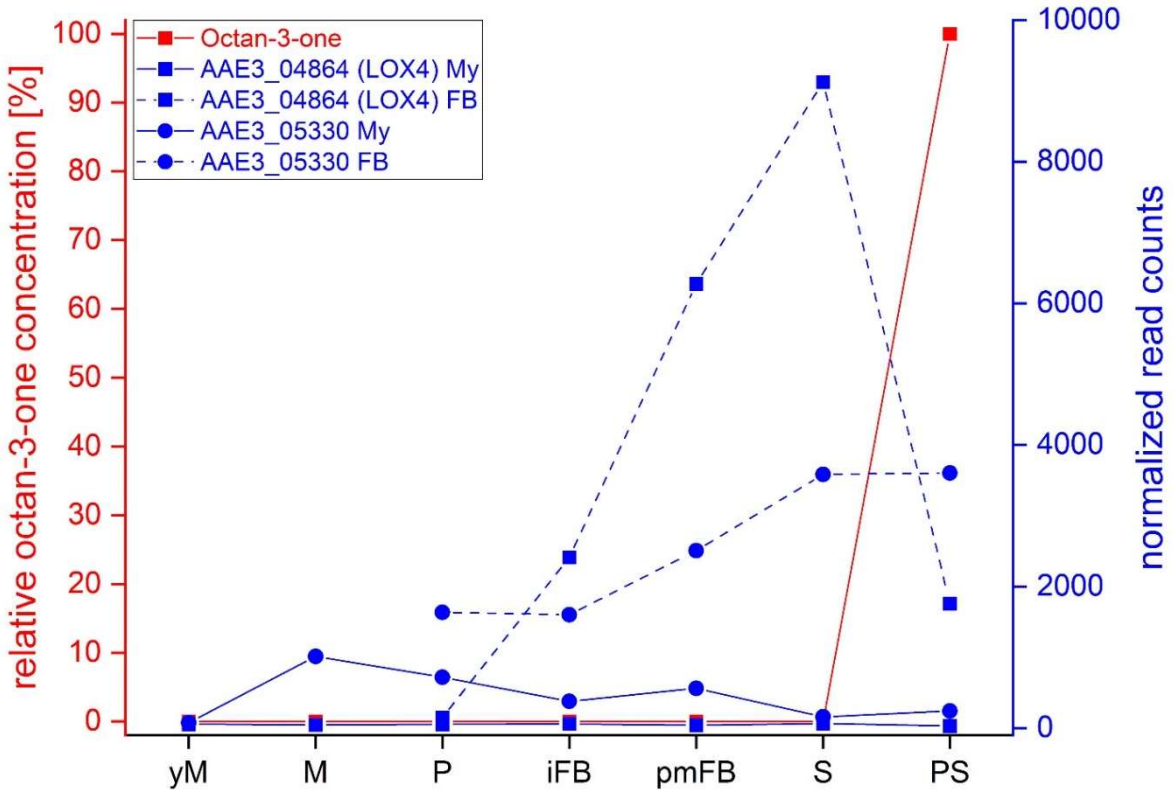

Figure S16: Transcription levels of AAE3_04864 (*LOX4*) and the putative HPL AAE3_05330 (blue) in the mycelium (My) and in fruiting bodies (FB) during different developmental stages of *C. aegerita* as well as the relative concentration of octan-3-one (red) in the HS of *C. aegerita.* yM: young (uninduced) mycelium (day 10 post inoculation, p.i.); M: mycelium (day 14 p.i.); P: primordia (day 18 p.i.); iFB: immature fruiting bodies (day 20 p.i.); pmFB: premature fruiting bodies (day 22 p.i.); S: sporulation (day 24 p.i.); PS: post sporulation (day 28 p.i.).

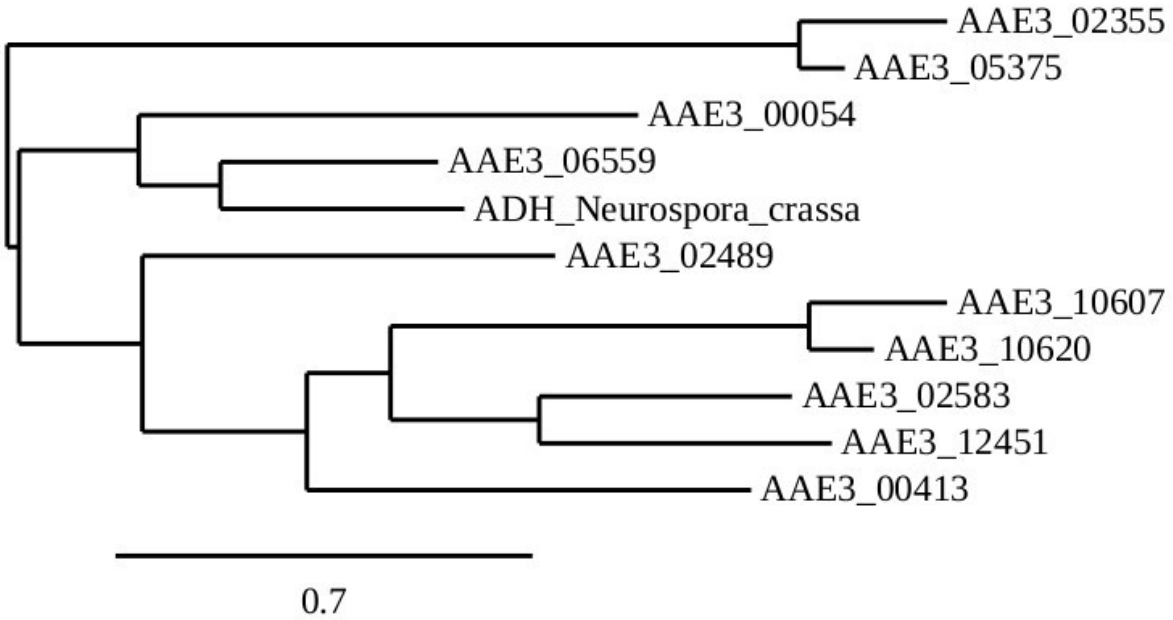

Figure S17: Phylogenetic analysis of putative ADHs from *C. aegerita* and an ADH from *Neurospora crassa* (Q9P6C8).

```
Sporidiobolus_salmonicolor      ------------------------------------------------------------ 0
AAE3_13549                      -MAPVTNGRIIFNSIPTGFPVPGETTIYDTTETIDLDTAPLDGGFLLKTLELSVDPYMRG 59
Nicotiana_tabacum               MAEEVSNKQVILKNYVTGYPKESDMEIKN--VTIKLKVPEGSNDVVVKNLYLSCDPYMRS 58
Arabidopsis_thaliana            --MTATNKQVILKDYVSGFPTESDFDFTT--TTVELRVPEGTNSVLVKNLYLSCDPYMRI 56


Sporidiobolus_salmonicolor      ----RPAGTKSYVPPFELGQPIANFGTGEARPVPHLSPDDRQLTALSPQVLKSANASIKQ 56
AAE3_13549                      GMRAPEK--KSYSAPFTLGQPLRGYGVGV--------------------VLRSENPQVKA 97
Nicotiana_tabacum               RMRKIEG---SYVESFAPGSPITGYGVAK--------------------VLESGDPKFQK 95
Arabidopsis_thaliana            RMGKPDPSTAALAQAYTPGQPIQGYGVSR--------------------IIESGHPDYKK 96
                                          :    :  *.*: .:*..                     ::.* . . :

Sporidiobolus_salmonicolor      GQHVYGSFPFAEYNVFSKEEASRLRILENKEGLPWTTWVGAAGMPGQTAWHGLRAIGKPQ 116
AAE3_13549                      GDHLYGFFEHTHYSIRKDL--TGLQAIENAYNLPWSVFIGVIGMPGKTAYMAWKEYAHPK 155
Nicotiana_tabacum               GDLVWGMTGWEEYSIITPT---QTLFKIHDKDVPLSYYTGILGMPGMTAYAGFHEVCSPK 152
Arabidopsis_thaliana            GDLLWGIVAWEEYSVITPM--THAHFKIQHTDVPLSYYTGLLGMPGMTAYAGFYEVCSPK 154
                                *: ::*     .*.: .           :  .:* : : *  **** **: .      *:

Sporidiobolus_salmonicolor      KGETIFVSGAMGAVGQMVISIAHKLGLKVIASAGSDEKVELLKKEFKVEVAFNYKTVDTE 176
AAE3_13549                      QGETVFVSTGAGPVGSFVIQLAKADGLKVIASAGSEEKVQFMK-EVGADVAFNYKTTNTA 214
Nicotiana_tabacum               KGETVFVSAASGAVGQLVGQFAKMLGCYVVGSAGSKEKVDLLKSKFGFDEAFNYKEEQDL 212
Arabidopsis_thaliana            EGETVYVSAASGAVGQLVGQLAKMMGCYVVGSAGSKEKVDLLKTKFGFDDAFNYKEESDL 214
                                :***::** . * **.:* .:*:  *  *:.****.***:::* :.  : *****  .

Sporidiobolus_salmonicolor      KIL----SENPFQIYWDNVAGPTFEAVLNTIEPRGRIIGCVAKQHSNDYNGQPYGIKNIF 232
AAE3_13549                      EVLE---KEGPIDIYWDNVGGETLEAALNAANVNARFIECGMISGYN--SGG-APVRNIF 268
Nicotiana_tabacum               SAALKRYFPDGIDIYFENVGGKMLDAVLVNMKLYGRIAVCGMISQYN--LEQTEGVHNLF 270
Arabidopsis_thaliana            TAALKRCFPNGIDIYFENVGGKMLDAVLVNMNMHGRIAVCGMISQYN--LENQEGVHNLS 272
                                         . ::**::**.*  ::*.*   :  .*:  *   .  *        ::*:

Sporidiobolus_salmonicolor      QVVSKELLYQGFIVLNHP---IEAFYDEVPKWIASGEVTKPKEHIYKGLDN-GESFNDLF 288
AAE3_13549                      HVIGKSITMTGFIVSRIEPKYSAEFYKEVPAKVASGELKY-REHVYNGLEKLGDVILAVQ 327
Nicotiana_tabacum               CLITKRIRMEGFLVFDYYHLYPK-YLEMVIPQIKAGKVVY-VEDVAHGLESAPTALVGLF 328
Arabidopsis_thaliana            NIIYKRIRIQGFVVSDFYDKYSK-FLEFVLPHIREGKITY-VEDVADGLEKAPEALVGLF 330
                                 :: * :   **:*          : . *   :  *::    *.: .**:.    :  :

Sporidiobolus_salmonicolor      TGANFGKAVISLE--    301
AAE3_13549                      KGENKAKAVVHVADD    342
Nicotiana_tabacum               SGRNIGKQVVMVSRE    343
Arabidopsis_thaliana            HGKNVGKQVVVVARE    345
                                 * * .* *: :
```

Figure S18: Amino acid sequence alignment of ene-reductases from plants, the fungus *Sporidiobolus salmonicolor,* and the putative ene-reductase AAE3_13549 from *C. aegerita*. *Nicotiana tabacum* (Q9SLN8), *Arabidopsis thaliana* (Q39172), *Sporidiobolus salmonicolor* (A0A0D6ERK8).

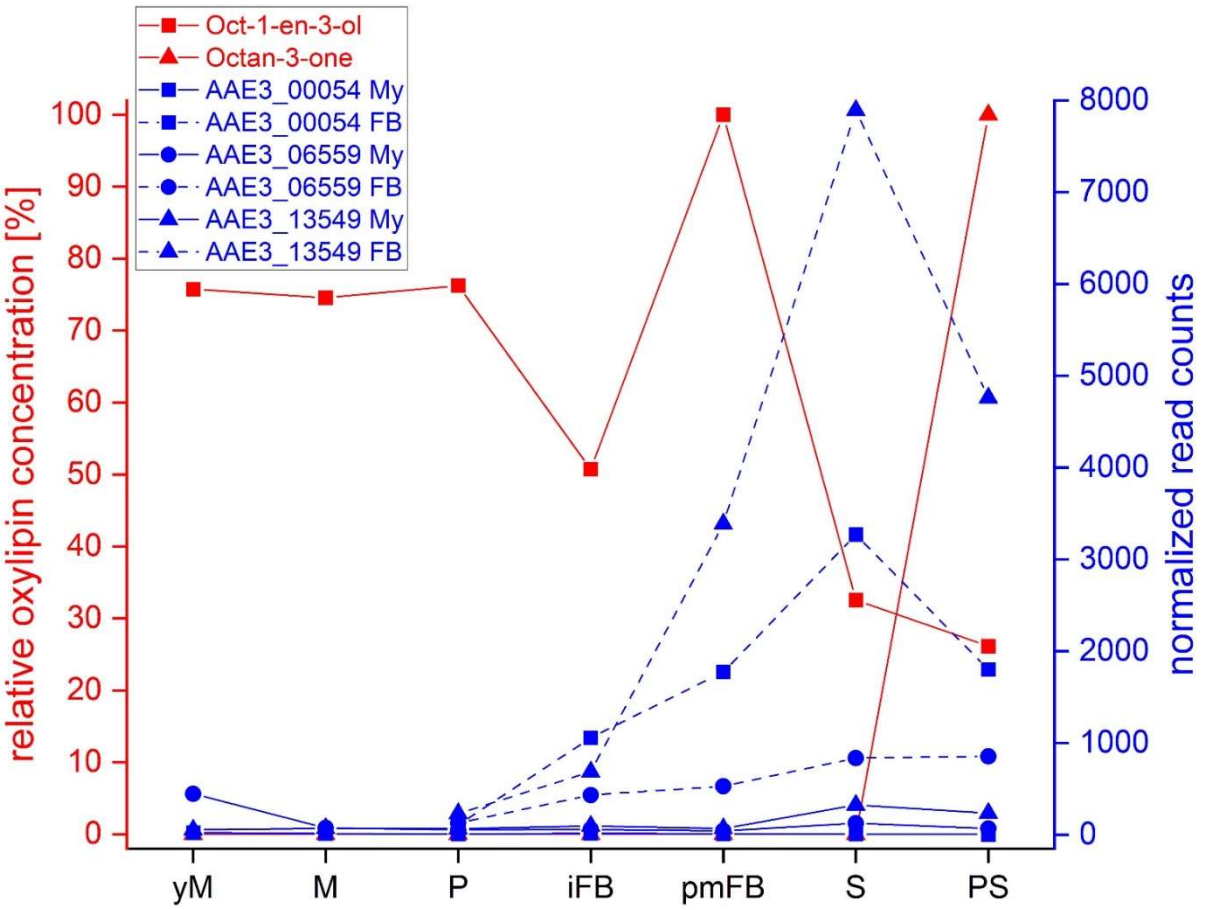

Figure S19: Transcription levels of the putative ADHs AAE3_00054 and AAE3_06559 as well as the putative ene-reductase AAE3_13549 (blue) in the mycelium (My) and in fruiting bodies (FB) during different developmental stages of *C. aegerita* as well as the relative concentrations of C8 oxylipins (red) in the HS of *C. aegerita.* yM: young (uninduced) mycelium (day 10 post inoculation, p.i.); M: mycelium (day 14 p.i.); P: primordia (day 18 p.i.); iFB: immature fruiting bodies (day 20 p.i.); pmFB: premature fruiting bodies (day 22 p.i.); S: sporulation (day 24 p.i.); PS: post sporulation (day 28 p.i.).